

HOUSTON-GALVESTON-BRAZORIA AREA
EXCEPTIONAL EVENT DEMONSTRATION FOR OZONE
ON
JUNE 20, SEPTEMBER 13, SEPTEMBER 21, and OCTOBER 8, 2022



TEXAS COMMISSION ON ENVIRONMENTAL QUALITY
P.O. BOX 13087
AUSTIN, TEXAS 78711-3087

MAY 24, 2023 PUBLIC COMMENT DOCUMENT

THIS PAGE INTENTIONALLY LEFT BLANK

EXECUTIVE SUMMARY

On June 20, September 13, September 21, and October 8, 2022, the Houston Bayland Park monitoring site measured maximum daily average eight-hour (MDA8) ozone concentrations of 82, 89, 92, and 87 parts per billion (ppb), respectively. The Houston Harvard Street monitoring site measured MDA8 ozone concentrations of 97 and 88 ppb on June 20 and September 21, 2022, respectively. These maximum daily averages cause the Houston-Galveston-Brazoria (HGB) area to violate the 2008 eight-hour ozone National Ambient Air Quality Standard (NAAQS). This demonstration provides support for the influence of emissions from exceptional or natural events (wildfires) that adversely influenced ozone measurements at the sites.

Based on an initial analysis, the Texas Commission on Environmental Quality (TCEQ) entered a preliminary flag and notified the United States Environmental Protection Agency (EPA) of its intent to submit an exceptional event demonstration for the dates above as required by the [Exceptional Events Rule \(exceptional_events_rule_revisions_2060-as02_final.pdf \(epa.gov\)\)](#). The TCEQ submits this exceptional event demonstration in support of the determination that the HGB area air quality was influenced by exceptional events on June 20, September 13, September 21, and October 8, 2022. These events caused exceedances of the 2008 eight-hour ozone NAAQS. The TCEQ requests that the EPA concur with this technical demonstration and enter an exceptional event flag for the appropriate Air Quality System data records for the Houston Bayland Park Continuous Air Monitoring Station (CAMS) 53 ozone measurements on June 20, September 13, September 21, and October 8, 2022, and Houston Harvard Street CAMS 417 ozone measurements on June 20 and September 21, 2022.

The TCEQ's determination is supported through the accumulated weight of evidence documented in this package. Specifically, this demonstration shows:

- analyses of National Oceanic and Atmospheric Administration Hazard Mapping System fire and smoke product showing evidence of smoke plumes over the HGB area on June 20, September 13, September 21, and October 8, 2022;
- analyses of High-Resolution Rapid Refresh Near-Surface Smoke Modeling showing evidence of smoke near the surface from wildfires in Louisiana, Alabama, Texas, and Mississippi over the HGB area on June 20, September 13, September 21, and October 8, 2022;
- trajectory analyses and satellite imagery evidence of emissions transport from wildfires in Louisiana, Alabama, Mississippi, and Texas to the Bayland Park and Harvard Street monitors;
- analyses of historical ozone measurements showing that wildfire emissions affected ozone concentrations over a large portion of the HGB area on June 20, September 13, September 21, and October 8, 2022;
- analyses of satellite imagery detailing elevated Atmospheric Optical Depth measurements on June 20, September 13, September 21, and October 8, 2022;
- evidence of volatile organic compound to nitrogen oxides ratios greater than 25 at the surrounding monitoring sites in the HGB area on June 20, September 13, September 21, and October 8, 2022, supporting the hypothesis of wildfire emissions influencing air quality in the HGB area;

- analyses of carbon monoxide data showing unusually high levels on September 13, September 21, and October 8, 2022, suggesting wildfire influence on air quality in the HGB area;
- analyses of benzene to toluene ratios, with ratios near 1.5, which is consistent with ratios found in the wildfire plumes on June 20, September 13, September 21, and October 8, 2022;
- analyses of hourly fine particulate matter data showing high level across a wide regional area on days with recognizable smoke plumes on June 20, September 13, September 21, and October 8, 2022, supporting the hypothesis that wildfire emissions have influenced air quality;
- analyses of speciated fine particulate matter data showing moderate to high levels of potassium and organic carbon on September 13, September 21, and October 8, 2022, supporting that the air quality was influenced by biomass burning;
- coinciding values of hourly ozone and fine particulate matter on the time series analyses suggesting that these values were related and caused by wildfires;
- analyses of Black and Brown Carbon Network data showing evidence of biomass burning on select sites on September 13, September 21, and October 8, 2022;
- matching day analyses showing that, when controlled for the presence of smoke, meteorologically similar days would not have experienced the ozone exceedances observed on June 20, September 13, September 21, and October 8, 2022; and
- a statistical regression model analysis that shows wildfire contribution to ozone in the HGB area on June 20, September 13, September 21, and October 8, 2022.

TABLE OF CONTENTS

Executive Summary

Table of Contents

List of Acronyms

List of Tables

List of Figures

List of Appendices

Chapter 1: Introduction

1.1 The Houston Bayland Park and Houston Harvard Street Monitors

1.2 Comparison of Historical Ozone Data

1.3 Narrative Conceptual Model

1.3.1 Characteristics of a Typical High Ozone Event

1.3.2 Characteristics of the June 20, 2022 High Ozone Event

1.3.3 Characteristics of the September 13, 2022 High Ozone Event

1.3.4 Characteristics of the September 21, 2022 High Ozone Event

1.3.5 Characteristics of the October 8, 2022 High Ozone Event

1.4 Fires Influencing Exceedances in the HGB Area

Chapter 2: Exceptional Event Requirements For States

2.1 Relevant Regulatory Documents

2.2 Requirements for an Exceptional Event

2.3 The Event is Not Reasonably Controllable or Preventable

2.4 The Event is Not Likely to Recur or is Natural

2.5 The TCEQ Followed the Public Comment Process

2.6 Mitigation Requirements Of 40 CFR §51.930

2.6.1 Prompt Public Notification

2.6.2 Public Education

2.6.3 Implementation of Measures to Protect Public Health

Chapter 3: Causal Relationship

3.1 Period of Analysis

3.2 Tiered Analysis

3.3 Hazard Mapping System Plume

3.4 True Color Satellite Imagery Shows Transport to HGB Monitors

3.5 Aerosol Optical Depth Measurements

3.6 Wildfire Emissions Transported to Bayland Park and Harvard Street Monitors

3.7 Analysis of Measured Pollutants

3.7.1 The Regional Effect of Wildfire Emissions

- 3.7.2 Analysis of Ground Based Monitoring Data
 - 3.7.2.1 VOC to NO_x Ratios
 - 3.7.2.2 High Sensitivity CO Measurements
 - 3.7.2.3 Benzene to Toluene Ratios
 - 3.7.2.4 Hourly Particulate Matter (PM) Measurements
 - 3.7.2.5 Speciated PM_{2.5} Measurements
 - 3.7.2.6 Ozone and PM_{2.5} Time Series
 - 3.7.2.7 Biomass Burning Indicator
- 3.8 Matching Day Analysis
 - 3.8.1 June 20, 2022
 - 3.8.2 September 13, 2022
 - 3.8.3 September 21, 2022
 - 3.8.4 October 8, 2022
- 3.9 Generalized Additive Model Analysis
- 3.10 Causal Relationship Conclusion
- Chapter 4: Public Comment
- Chapter 5: References
- APPENDIX A: Public Comments

LIST OF ACRONYMS

AAE	Absorption Angström exponent
AOD	Aerosol Optical Depth
AQI	Air Quality Index
AQS	Air Quality System
ARL	Air Resource Laboratory
Auto-GC	Automated Gas Chromatograph
BB	Biomass Burning
BC2	Black and Brown Carbon
CAMS	Continuous Air Monitoring Station
CDT	Central Daylight Time
CFR	Code of Federal Regulations
CO	Carbon Monoxide
CRS	Cubic Regression Splines
CST	Central Standard Time
DFW	Dallas-Fort Worth
EER	Exceptional Events Rule
EPA	Environment Protection Agency
GAM	Generalized Additive Models
GLM	Generalized Linear Models
HGB	Houston-Galveston-Brazoria
HMS	Hazard Mapping System
hpa	Hectopascals
HRRR	High-Resolution Rapid Refresh
km	Kilometers
LEADS	Leading Environmental Analysis and Display System
MAIAC	Multi-Angle Implementation of Atmospheric Correction
mb	Millibar
MDA8	Maximum Daily Average Eight-hour
MODIS	Moderate Resolution Imaging Spectroradiometer
mph	Miles Per Hour
NAAQS	National Ambient Air Quality Standards
NAM	North American Mesoscale Forecast System
NASA	National Aeronautics and Space Administration
NER	Normalized Enhancement Ratio
NOAA	National Oceanic and Atmospheric Administration
NO _x	Nitrogen Oxides
NO _y	Reactive Oxides of Nitrogen
PAMS	Photochemical Assessment Monitoring Station
PM ₁₀	Particulate Matter less than or equal to 10 microns in diameter
PM _{2.5}	Fine Particulate Matter less than or equal to 2.5 microns in diameter
ppb	Parts Per Billion
SAE	Scattering Angström exponent
SIP	State Implementation Plan
Suomi-NPP	Suomi National Polar-orbiting Partnership
TCEQ	Texas Commission on Environmental Quality
UTC	Universal Coordinated Time
VIIRS	Visible Infrared Imaging Radiometer Suite

VOC Volatile Organic Compound

LIST OF TABLES

Table 1-1: Background Information for the Bayland Park and Harvard Street Monitors
Table 1-2: Wildfires That Impacted HGB Area
Table 2-1: 40 CFR §50.14(c)(3) Exceptional Event Demonstration Requirements
Table 2-2: 40 CFR §51.930 Exceptional Event Demonstration Requirements
Table 3-1: HYSPLIT Model Information
Table 3-2: Monitoring Sites Above the 95th Percentile
Table 3-3: Biomass Burning Events at Each BC2 Site in Houston ± 1 Day of Event Days
Table 3-4: Meteorological Matching Parameters for June 20, 2022
Table 3-5: Meteorological Matching Parameters for September 13, 2022
Table 3-6: Meteorological Matching Parameters for September 21, 2022
Table 3-7: Meteorological Matching Parameters for October 8, 2022
Table 3-8: Meteorological Parameters Used for Houston Bayland Park GAMs
Table 3-9: Houston Bayland Park Ozone GAM Performance
Table 3-10: GAM Results for 2022 Ozone Exceedance Days at Houston Bayland Park
Table 3-11: Determination of Wildfire Contribution to Ozone at Houston Bayland Park in 2022

LIST OF FIGURES

- Figure 1-1: Location of Bayland Park and Harvard Street Monitors
- Figure 1-2: Comparison of Historical MDA8 at Bayland Park
- Figure 1-3: Comparison of Historical MDA8 at Harvard Street
- Figure 1-4: HGB and Bayland Park Ozone Trends 2000 through 2022
- Figure 1-5: Drought Conditions on June 21, 2022
- Figure 1-6: NOAA HMS Fire and Smoke Product on June 20, 2022
- Figure 1-7: HRRR Near-Surface Smoke Modeling on June 20, 2022, 06:00 UTC
- Figure 1-8: HRRR Near-Surface Smoke Modeling on June 20, 2022, 16:00 UTC
- Figure 1-9: NOAA 500 mb Height and Wind Analysis at 7:00 PM CDT June 20, 2022
- Figure 1-10: NOAA Surface Analysis at 7:00 PM CDT June 20, 2022
- Figure 1-11: NOAA-20 VIIRS True Color Satellite Imagery on June 20, 2022
- Figure 1-12: Drought Conditions on September 13, 2022
- Figure 1-13: NOAA HMS Fire and Smoke Product on September 13, 2022
- Figure 1-14: HRRR Near-Surface Smoke Modeling on September 13, 2022, 01:00 UTC
- Figure 1-15: HRRR Near-Surface Smoke Modeling on September 13, 2022, 13:00 UTC
- Figure 1-16: NOAA 500 mb Height and Wind Analysis at 7:00 PM CDT September 13, 2022
- Figure 1-17: NOAA Surface Analysis at 7:00 PM CDT September 13, 2022
- Figure 1-18: NOAA-20 VIIRS True Color Satellite Imagery on September 13, 2022
- Figure 1-19: Drought Conditions on September 21, 2022
- Figure 1-20: NOAA HMS Fire and Smoke Product on September 21, 2022
- Figure 1-21: HRRR Near-Surface Smoke Modeling on September 20, 2022, 11:00 UTC
- Figure 1-22: HRRR Near-Surface Smoke Modeling on September 21, 2022, 00:00 UTC
- Figure 1-23: HRRR Near-Surface Smoke Modeling on September 21, 2022, 19:00 UTC
- Figure 1-24: NOAA 500 mb Height and Wind Analysis at 7:00 PM CDT September 21, 2022
- Figure 1-25: NOAA Surface Analysis at 7:00 PM CDT September 21, 2022
- Figure 1-26: NOAA-20 VIIRS True Color Satellite Imagery on September 21, 2022
- Figure 1-27: Drought Conditions on October 11, 2022
- Figure 1-28: NOAA HMS Fire and Smoke Product on October 8, 2022
- Figure 1-29: HRRR Near-Surface Smoke Modeling on October 7, 2022, 13:00 UTC
- Figure 1-30: HRRR Near-Surface Smoke Modeling on October 7, 2022, 07:00 UTC
- Figure 1-31: HRRR Near-Surface Smoke Modeling on October 8, 2022, 17:00 UTC
- Figure 1-32: NOAA 500 mb Height and Wind Analysis at 7:00 PM CDT October 8, 2022
- Figure 1-33: NOAA Surface Analysis at 7:00 PM CDT October 8, 2022
- Figure 1-34: NOAA-20 VIIRS True Color Satellite Imagery on October 8, 2022

Figure 1-35: Location of Fire That Impacted HGB on June 20, 2022
Figure 1-36: Location of Fires That Impacted HGB on September 13, 2022
Figure 1-37: Location of Fires That Impacted HGB on September 21, 2022
Figure 1-38: Location of Fires That Impacted HGB on October 8, 2022
Figure 3-1: NOAA HMS Plume Map for June 20, 2022
Figure 3-2: NOAA HMS Plume Map for September 13, 2022
Figure 3-3: NOAA HMS Plume Map for September 21, 2022
Figure 3-4: NOAA HMS Plume Map for October 8, 2022
Figure 3-5: Terra Modis True Color Imagery on June 20, 2022
Figure 3-6: Terra Modis True Color Imagery on September 13, 2022
Figure 3-7: Terra Modis True Color Imagery on September 21, 2022
Figure 3-8: Terra Modis True Color Imagery on October 8, 2022
Figure 3-9: MAIAC Combined AOD on June 20, 2022
Figure 3-10: MAIAC Combined AOD on September 13, 2022
Figure 3-11: MAIAC Combined AOD on September 21, 2022
Figure 3-12: MAIAC Combined AOD on October 8, 2022
Figure 3-13: Backward HYSPLIT Trajectories on June 20, 2022
Figure 3-14: Backward HYSPLIT Trajectories on September 13, 2022
Figure 3-15: Backward HYSPLIT Trajectories on September 21, 2022
Figure 3-16: Backward HYSPLIT Trajectories on October 8, 2022
Figure 3-17: Backward HYSPLIT Trajectories on June 20, 2022
Figure 3-18: Backward HYSPLIT Trajectories on September 21, 2022
Figure 3-19: Monitoring Sites Above Their 95th Percentile on June 20, 2022
Figure 3-20: Monitoring Sites Above Their 95th Percentile on September 13, 2022
Figure 3-21: Monitoring Sites Above Their 95th Percentile on September 21, 2022
Figure 3-22: Monitoring Sites Above Their 95th Percentile on October 8, 2022
Figure 3-23: VOC/NO_x Ratios at Channelview Monitoring Site on June 20, 2022
Figure 3-24: VOC/NO_x Ratios at Clinton Monitoring Site on June 20, 2022
Figure 3-25: VOC/NO_x Ratios at Oyster Creek Monitoring Site on June 20, 2022
Figure 3-26: VOC/NO_x Ratios at Texas City 34th Street Monitoring Site on June 20, 2022
Figure 3-27: VOC/NO_x Ratios at Wallisville Monitoring Site on June 20, 2022
Figure 3-28: VOC/NO_x Ratios at Oyster Creek Monitoring Site on September 13, 2022
Figure 3-29: VOC/NO_x Ratios at Wallisville Road Monitoring Site on September 13, 2022
Figure 3-30: VOC/NO_x Ratios at Clinton Monitoring Site on September 21, 2022
Figure 3-31: VOC/NO_x Ratios at Oyster Creek Monitoring Site on September 21, 2022
Figure 3-32: VOC/NO_x Ratios at Oyster Creek Monitoring Site on October 8, 2022
Figure 3-33: CO Measurements at Clinton Monitoring Site on September 13, 2022
Figure 3-34: CO Measurements at Clinton Monitoring Site on September 21, 2022

Figure 3-35: CO Measurements at Clinton Monitoring Site on October 8, 2022

Figure 3-36: Benzene to Toluene Ratios at the Cesar Chavez Monitoring Site on June 20, 2022

Figure 3-37: Benzene to Toluene Ratios at the Channelview Monitoring Site on June 20, 2022

Figure 3-38: Benzene to Toluene Ratios at the Clinton Monitoring Site on June 20, 2022

Figure 3-39: Benzene to Toluene Ratios at the Oyster Creek Monitoring Site on June 20, 2022

Figure 3-40: Benzene to Toluene Ratios at the Texas City 34th Street Monitoring Site on June 20, 2022

Figure 3-41: Benzene to Toluene Ratios at the Cesar Chavez Monitoring Site on September 13, 2022

Figure 3-42: Benzene to Toluene Ratios at the Channelview Monitoring Site on September 13, 2022

Figure 3-43: Benzene to Toluene Ratios at the Clinton Monitoring Site on September 13, 2022

Figure 3-44: Benzene to Toluene Ratios at the Oyster Creek Monitoring Site on September 13, 2022

Figure 3-45: Benzene to Toluene Ratios at the Texas City 34th Street Monitoring Site on September 13, 2022

Figure 3-46: Benzene to Toluene Ratios at the Wallisville Road Monitoring Site on September 13, 2022

Figure 3-47: Benzene to Toluene Ratios at the Cesar Chavez Monitoring Site on September 21, 2022

Figure 3-48: Benzene to Toluene Ratios at the Channelview Monitoring Site on September 21, 2022

Figure 3-49: Benzene to Toluene Ratios at the Clinton Monitoring Site on September 21, 2022

Figure 3-50: Benzene to Toluene Ratios at the Oyster Creek Monitoring Site on September 21, 2022

Figure 3-51: Benzene to Toluene Ratios at the Texas City 34th Street Monitoring Site on September 21, 2022

Figure 3-52: Benzene to Toluene Ratios at the Wallisville Road Monitoring Site on September 21, 2022

Figure 3-53: Benzene to Toluene Ratios at the Cesar Chavez Monitoring Site on October 8, 2022

Figure 3-54: Benzene to Toluene Ratios at the Channelview Monitoring Site on October 8, 2022

Figure 3-55: Benzene to Toluene Ratios at the Clinton Monitoring Site on October 8, 2022

Figure 3-56: Benzene to Toluene Ratios at the Oyster Creek Monitoring Site on October 8, 2022

Figure 3-57: Benzene to Toluene Ratios at the Texas City 34th Street Monitoring Site on October 8, 2022

Figure 3-58: PM_{2.5} Levels at the Bayland Park Monitoring Site on June 20, 2022

Figure 3-59: PM_{2.5} Levels at the Aldine Monitoring Site on June 20, 2022

Figure 3-60: PM_{2.5} Levels at the Baytown Monitoring Site on June 20, 2022

Figure 3-61: PM_{2.5} Levels at the Clinton Monitoring Site on June 20, 2022

Figure 3-62: PM_{2.5} Levels at the Conroe-Relocated Monitoring Site on June 20, 2022

Figure 3-63: PM_{2.5} Levels at the Galveston 99th Street Monitoring Site on June 20, 2022

Figure 3-64: PM_{2.5} Levels at the Oyster Creek Monitoring Site on June 20, 2022

Figure 3-65: PM_{2.5} Levels at the Seabrook Friendship Park Monitoring Site on June 20, 2022

Figure 3-66: PM_{2.5} Levels at the Westhollow Monitoring Site on June 20, 2022

Figure 3-67: PM_{2.5} Levels at the Bayland Park Monitoring Site on September 13, 2022

Figure 3-68: PM_{2.5} Levels at the Aldine Monitoring Site on September 13, 2022

Figure 3-69: PM_{2.5} Levels at the Clinton Monitoring Site on September 13, 2022

Figure 3-70: PM_{2.5} Levels at the Conroe-Relocated Monitoring Site on September 13, 2022

Figure 3-71: PM_{2.5} Levels at the Westhollow Monitoring Site on September 13, 2022

Figure 3-72: PM_{2.5} Levels at the Bayland Park Monitoring Site on September 21, 2022

Figure 3-73: PM_{2.5} Levels at the Baytown Monitoring Site on September 21, 2022

Figure 3-74: PM_{2.5} Levels at the Clinton Monitoring Site on September 21, 2022

Figure 3-75: PM_{2.5} Levels at the Conroe-Relocated Monitoring Site on September 21, 2022

Figure 3-76: PM_{2.5} Levels at the Galveston 99th Street Monitoring Site on September 21, 2022

Figure 3-77: PM_{2.5} Levels at the Seabrook Friendship Park Monitoring Site on September 21, 2022

Figure 3-78: PM_{2.5} Levels at the Westhollow Monitoring Site on September 21, 2022

Figure 3-79: PM_{2.5} Levels at the Bayland Park Monitoring Site on October 8, 2022

Figure 3-80: PM_{2.5} Levels at the Aldine Monitoring Site on October 8, 2022

Figure 3-81: PM_{2.5} Levels at the Baytown Monitoring Site on October 8, 2022

Figure 3-82: PM_{2.5} Levels at the Galveston 99th Street Monitoring Site on October 8, 2022

Figure 3-83: PM_{2.5} Levels at the Oyster Creek Monitoring Site on October 8, 2022

Figure 3-84: PM_{2.5} Levels at the Seabrook Friendship Park Monitoring Site on October 8, 2022

Figure 3-85: Speciated PM_{2.5} Data at the North Wayside Monitoring Site

Figure 3-86: Speciated PM_{2.5} Measurements at the Clinton Monitoring Site

Figure 3-87: Bayland Park Ozone and PM_{2.5} Time Series for June 20, 2022

Figure 3-88: Bayland Park Ozone and PM_{2.5} Time Series for September 13, 2022

Figure 3-89: Bayland Park Ozone and PM_{2.5} Time Series for September 21, 2022

Figure 3-90: Bayland Park Ozone and PM_{2.5} Time Series for October 8, 2022

Figure 3-91: Harvard Street Ozone Time Series for June 20, 2022

Figure 3-92: Harvard Street Ozone Time Series for September 21, 2022

Figure 3-93: Time Series of Aerosol Optical Properties at Aldine around September 13, 2022

Figure 3-94: Time Series of Aerosol Optical Properties at Liberty around September 13, 2022

Figure 3-95: Time Series of Aerosol Optical Properties at Galveston around September 13, 2022

Figure 3-96: HMS and Back Trajectories on September 13, 2022

Figure 3-97: Time Series of Aerosol Optical Properties at Aldine around September 21, 2022

Figure 3-98: Time Series of Aerosol Optical Properties at Liberty around September 21, 2022

Figure 3-99: Time series of Aerosol Optical Properties at Galveston around September 21, 2022

Figure 3-100: HMS and Back Trajectories on September 21, 2022

Figure 3-101: Time Series of Aerosol Optical Properties at Aldine around October 8, 2022

Figure 3-102: Time Series of Aerosol Optical Properties at Liberty around October 8, 2022

Figure 3-103: Time Series of Aerosol Optical Properties at Galveston around October 8, 2022

Figure 3-104: HMS and Back Trajectories on October 8, 2022

Figure 3-105: Backward Trajectories from the Bayland Park Monitor on June 20, 2022 and June 5, 2020

Figure 3-106: Weather Chart for June 20, 2022

Figure 3-107: Surface Weather Chart for June 5, 2020

Figure 3-108: 500-mb Weather Chart for June 20, 2022

Figure 3-109: 500-mb Weather Chart for June 5, 2020

Figure 3-110: Backward Trajectories from the Bayland Park Monitor on September 13, 2022, and September 23, 2021

Figure 3-111: Surface Weather Chart for September 13, 2022

Figure 3-112: Surface Weather Chart for September 23, 2021

Figure 3-113: 500-mb Weather Chart for September 13, 2022

Figure 3-114: 500-mb Weather Chart for September 23, 2021

Figure 3-115: Backward Trajectories from the Bayland Park Monitor on September 21, 2022 and August 12, 2017

Figure 3-116: Surface Weather Chart for September 21, 2022

Figure 3-117: Surface Weather Chart for August 12, 2017

Figure 3-118: 500-mb Weather Chart for September 21, 2022

Figure 3-119: 500-mb Weather Chart for August 12, 2017

Figure 3-120: Backward Trajectories from the Bayland Park Monitor on October 8, 2022 and October 18, 2021

Figure 3-121: Surface Weather Chart for October 8, 2022

Figure 3-122: Surface Weather Chart for October 18, 2021

Figure 3-123: 500-Millibar Weather Chart for October 8, 2022

Figure 3-124: 500-Millibar Weather Chart for October 18, 2021

Figure 3-125: Training Model Results Compared to Observed Ozone

Figure 3-126: 2022 Model Predictions Compared to Observed Ozone

Figure 3-127: Comparison of 2022 Predictions with Results from Training Model

Figure 3-128: GAM Residuals for Training and Validation Dataset

Figure 3-129: Time Series of Observed and Predicted Maximum Daily Ozone for June 2022

Figure 3-130: Time Series of Observed and Predicted Maximum Daily Ozone for September 2022

Figure 3-131: Time Series of Observed and Predicted Maximum Daily Ozone for October 2022

Figure 3-132: Predicted and Observed Ozone with 95th Percentile of Positive Residuals

LIST OF APPENDICES

Appendix A Public Comments

CHAPTER 1: INTRODUCTION

On June 20, September 13, September 21, and October 8, 2022, the Houston Bayland Park monitoring site measured maximum daily average eight-hour (MDA8) ozone concentrations of 82, 89, 92, and 87 parts per billion (ppb), respectively. The Houston Harvard Street monitoring site measured MDA8 ozone concentrations of 97 and 88 ppb on June 20 and September 21, 2022, respectively. The measured MDA8 ozone averages were influenced by emissions from wildfires burning in Texas, Louisiana, Alabama, and Mississippi. Smoke from these fires coalesced into plumes, ozone and particulates formed in the wildfire plumes, and the plumes covered much of the central United States (U.S.), ultimately influencing the air quality in the Houston-Galveston-Brazoria (HGB) area.

The federal Clean Air Act (§319) allows the U.S. Environmental Protection Agency (EPA) to exclude monitoring data influenced by exceptional events such as wildfires when making certain regulatory determinations relating to the National Ambient Air Quality Standards (NAAQS). The Texas Commission on Environmental Quality (TCEQ) has determined that the ozone concentrations exceeding the NAAQS on June 20, September 13, September 21, and October 8, 2022 qualify as exceptional events under 40 Code of Federal Regulations §50.14, the revised [Exceptional Events Rule \(EER\) \(exceptional_events_rule_revisions_2060-as02_final.pdf \(epa.gov\)\)](#). This document provides technical support to demonstrate that the wildfires caused the measured exceedances at the Bayland Park and Harvard Street monitors on these dates. The TCEQ requests that the EPA concur with this finding and exclude the MDA8 taken at the Bayland Park and Harvard Street monitors on these days from design value calculations. Without any exclusions, Bayland Park's 2022 fourth highest MDA8 is 84 ppb and the monitor's 2020 through 2022 ozone design value is 78 ppb. The Harvard Street monitor has been active since 2021 with only two years of readings. The projected 2023 design value with average fourth highest MDA8 is 78 ppb. The EPA's concurrence that these four days were influenced by exceptional events would lower Bayland Park's fourth highest daily ozone MDA8 to 73 ppb and its 2020 through 2022 ozone design value to 75 ppb. A 2020 through 2022 ozone design value of 75 ppb brings Bayland Park and the entire HGB nonattainment area into attainment of the 2008 eight-hour ozone NAAQS.

The EPA has adopted a weight-of-evidence approach to evaluating exceptional event demonstrations (U.S. EPA, 2016a, p. 3). The TCEQ prepared analyses documenting the causal relationship between wildfire emissions and the measured high levels of ozone at the Bayland Park and Harvard Street monitors.

1.1 THE HOUSTON BAYLAND PARK AND HOUSTON HARVARD STREET MONITORS

The Bayland Park monitor (Continuous Air Monitoring Station (CAMS) 53) is located in Bayland Park, which is situated three miles outside of the southwest end of the Inner Loop 610. The Harvard Street monitor (CAMS 417) is located about 2 blocks south of I-10 on Harvard Street (See Figure 1-1: *Location of Bayland Park and Harvard Street Monitors*). The Bayland Park monitor has been active since March 24, 1998 and the Harvard Street monitor since January 25, 2021.

Siting and instrumentation information for these two monitors are shown in Table 1-1: *Background Information for the Bayland Park and Harvard Street Monitors*. The Bayland Park monitor is the design value setting monitor for the HGB area after the 2022 ozone season.

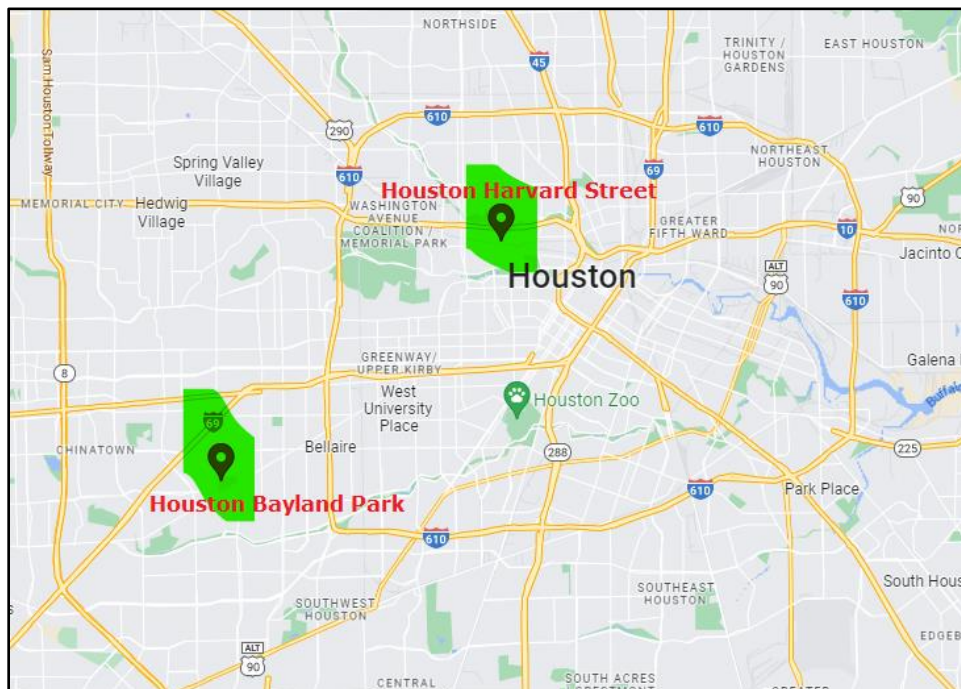


Figure 1-1: Location of Bayland Park and Harvard Street Monitors

Table 1-1: Background Information for the Bayland Park and Harvard Street Monitors

Monitor Detail	Bayland Park	Harvard Street
Air Quality System (AQS) Number	482010055 (CAMS53)	482010417 (CAMS417)
Activation Date	March 24, 1998	January 25, 2021
Address	6400 Bissonnet Street, Houston, TX 77074	160 Harvard Street, Houston, TX 77007
Latitude/Longitude	N 29.6957470° / W 95.4992224°	N 29.7728604° / W 95.3958580°
Elevation	19.5 Meters	Unknown
Pollutant Instrumentation	Ozone, Nitrogen Oxides (NO _x), Fine Particulate Matter (PM _{2.5}), and Volatile Organic Compound (VOC) Canister	Ozone and NO _x
Meteorological Instrumentation	Winds, Solar Radiation, and Outdoor Temperature	-

1.2 COMPARISON OF HISTORICAL OZONE DATA

As required by the EER, the TCEQ compared MDA8 ozone of the influenced days to all MDA8 ozone from January 1, 2018 through December 31, 2022. MDA8 ozone values were estimated in accordance with EPA procedures for determining ozone design values.

Based on data for calendar years 2018-2022, the 99th percentile of MDA8 for Bayland Park was determined to be 79.125 ppb. Based on data for calendar years 2021-2022, the 99th percentile of MDA8 for Harvard Street was determined to be 78.630 ppb. Figure 1-2: *Comparison of Historical MDA8 at Bayland Park* shows that all four influenced days (in red) lie above the 99th percentile line. Figure 1-3: *Comparison of Historical MDA8 at Harvard Street* shows that two of the influenced days (in red) lie above the 99th percentile line.

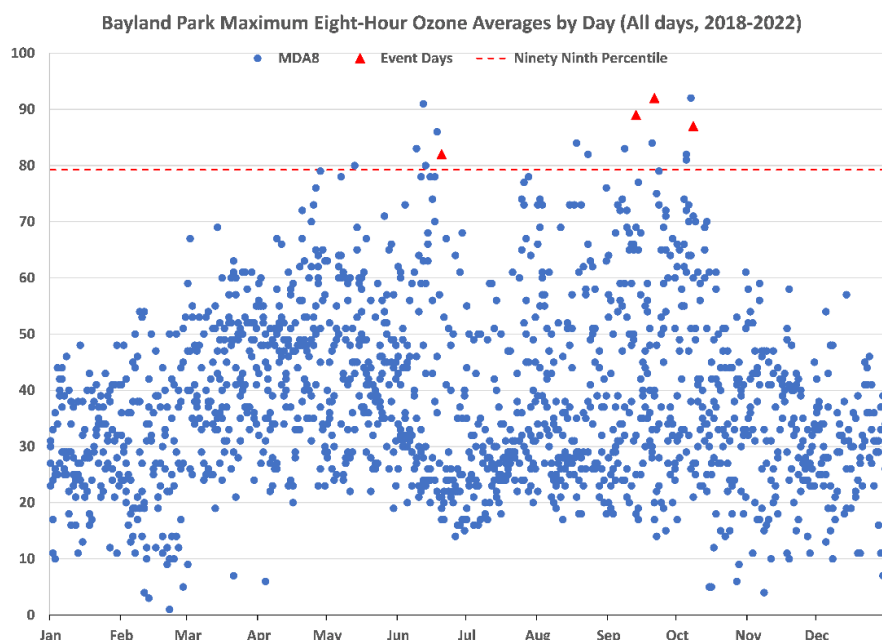


Figure 1-2: Comparison of Historical MDA8 at Bayland Park

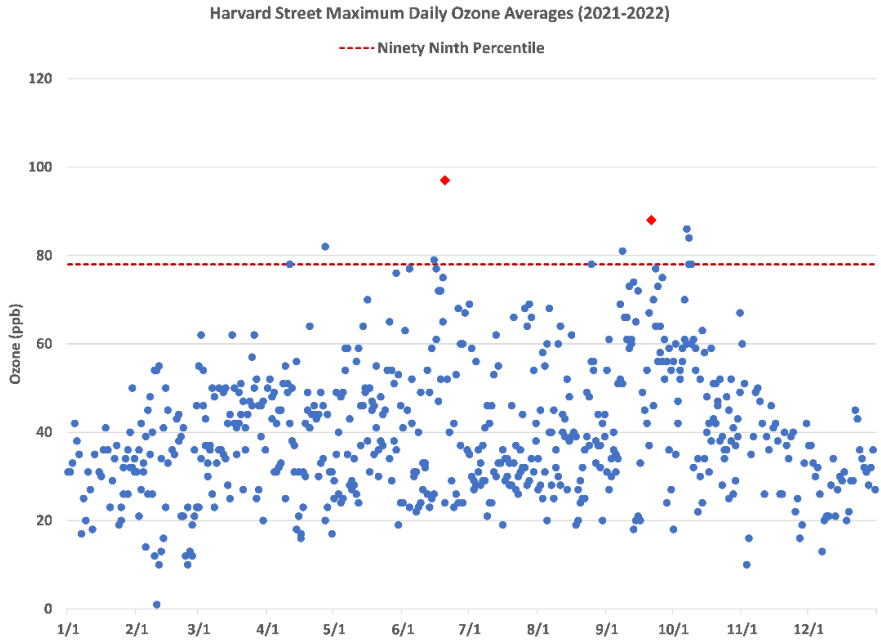


Figure 1-3: Comparison of Historical MDA8 at Harvard Street

1.3 NARRATIVE CONCEPTUAL MODEL

The HGB metropolitan area covers roughly 10,000 square miles and is home to over 7 million residents according to the U.S. Census Bureau (2020). Despite population increases, the area has steadily improved its ozone air quality. Figure 1-4: *HGB and Bayland Park Ozone Trends 2000 through 2022* shows that HGB’s ozone design value has dropped from 112 ppb in 2000 to 78 ppb in 2022. This represents an approximately 30% decrease over that period.

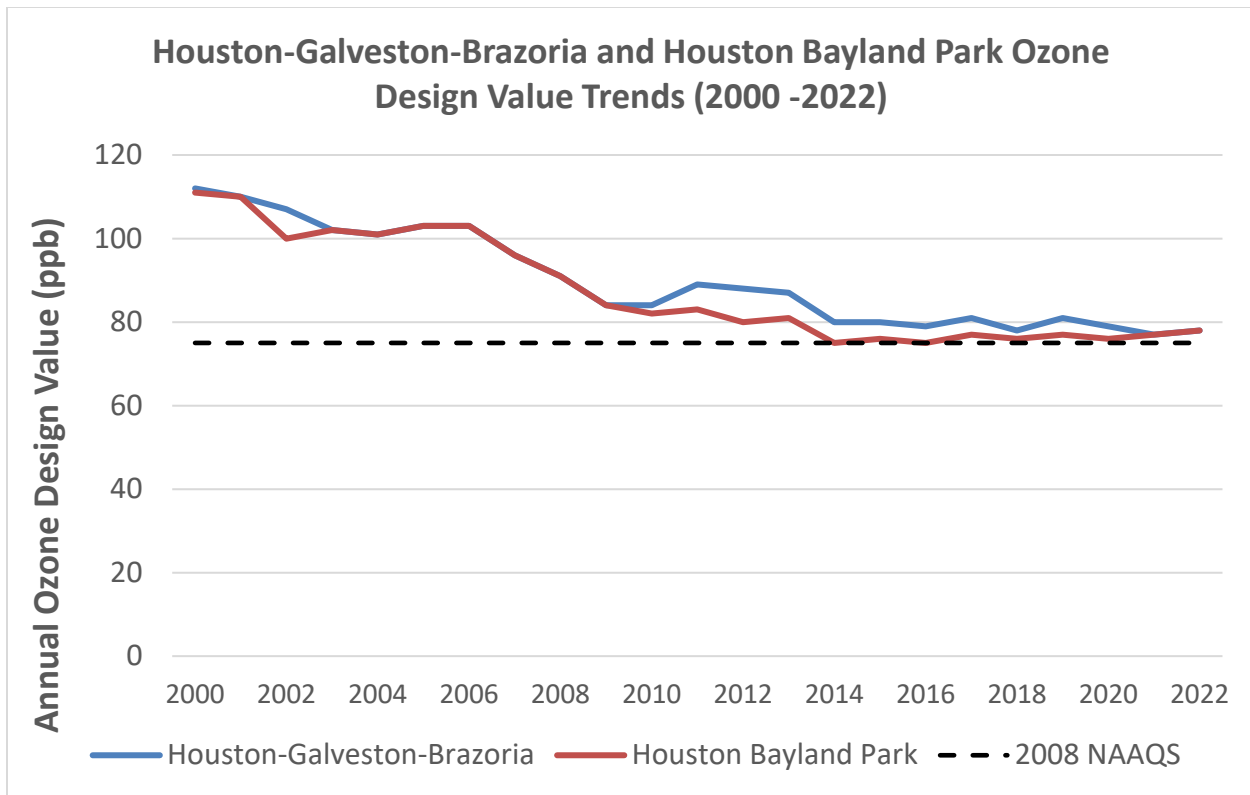


Figure 1-4: HGB and Bayland Park Ozone Trends 2000 through 2022

1.3.1 Characteristics of a Typical High Ozone Event

Meteorological conditions linked to high ozone in the HGB area include high temperatures, low relative humidity, and slow recirculating winds. Surface winds tend to be extremely slow on high ozone days, and typically originate in the direction of the Houston Ship Channel before moving across the urban area to downwind monitors. This causes the location of the highest ozone to change from year to year.

The highest ozone concentrations occur with the slowest upper-level wind speeds and under conditions that contain a wind flow reversal, which allows for increased accumulation of pollutants in the area. Although these days with the slowest wind speeds observe the highest ozone concentrations, the area can also get high ozone with continental air masses transported into the area.

High ozone is not likely when low pressure systems are over the area. Cloudy weather and precipitation associated with these systems inhibit the formation of ozone. High ozone is also not likely when there are strong pressure gradients, which are associated with higher winds. This allows for dispersion of ozone and ozone precursors.

1.3.2 Characteristics of the June 20, 2022 High Ozone Event

Extremely warm and dry conditions, particularly along the Texas Gulf Coast (see Figure 1-5: *Drought Conditions on June 21, 2022*), were present before and during the event. These conditions are conducive to wildfire development, which created areas of smoke, as seen in National Oceanic and Atmospheric (NOAA) Hazard Mapping System (HMS),

that later influenced the HGB area (see Figure 1-6: *NOAA HMS Fire and Smoke Product on June 20, 2022*).

Early on June 20, 2022, a fire started between Galveston Bay and Beaumont-Port Arthur as seen in Figure 1-7: *HRRR Near-Surface Smoke Modeling on June 20, 2022, 06:00 UTC*. Smoke then lofted into the HGB area in the morning as conditions in the area typically become highly conducive to ozone formation (see Figure 1-8: *HRRR Near-Surface Smoke Modeling on June 20, 2022, 16:00 UTC*). This movement is consistent with the flow seen in the 500 millibar (mb) weather charts (See Figure 1-9: *NOAA 500 mb Height and Wind Analysis at 7:00 PM CDT June 20, 2022*).

Figure 1-10: *NOAA Surface Analysis at 7:00 PM CDT June 20, 2022* shows evidence of strong high pressure controlling the atmosphere over Southeast Texas. High pressure systems are often associated with wide scale subsidence, which can mix air from aloft down to ground level. Isolated convective clouds over the HGB area are present on the NOAA-20 Visible Infrared Imaging Radiometer Suite (VIIRS) satellite (see Figure 1-11: *NOAA-20 VIIRS True Color Satellite Imagery on June 20, 2022*). These clouds are likely due to convective updrafts associated with on shore flow during the afternoon of June 20, 2022. Downdrafts associated with this convection may have resulted in peak wind gusts at the Bayland Park monitor of 20 miles per hour (mph). The presence of these downdrafts may also have contributed to mixing air from aloft down to ground level.

U.S. Drought Monitor

June 21, 2022

(Released Thursday, Jun. 23, 2022)

Valid 8 a.m. EDT

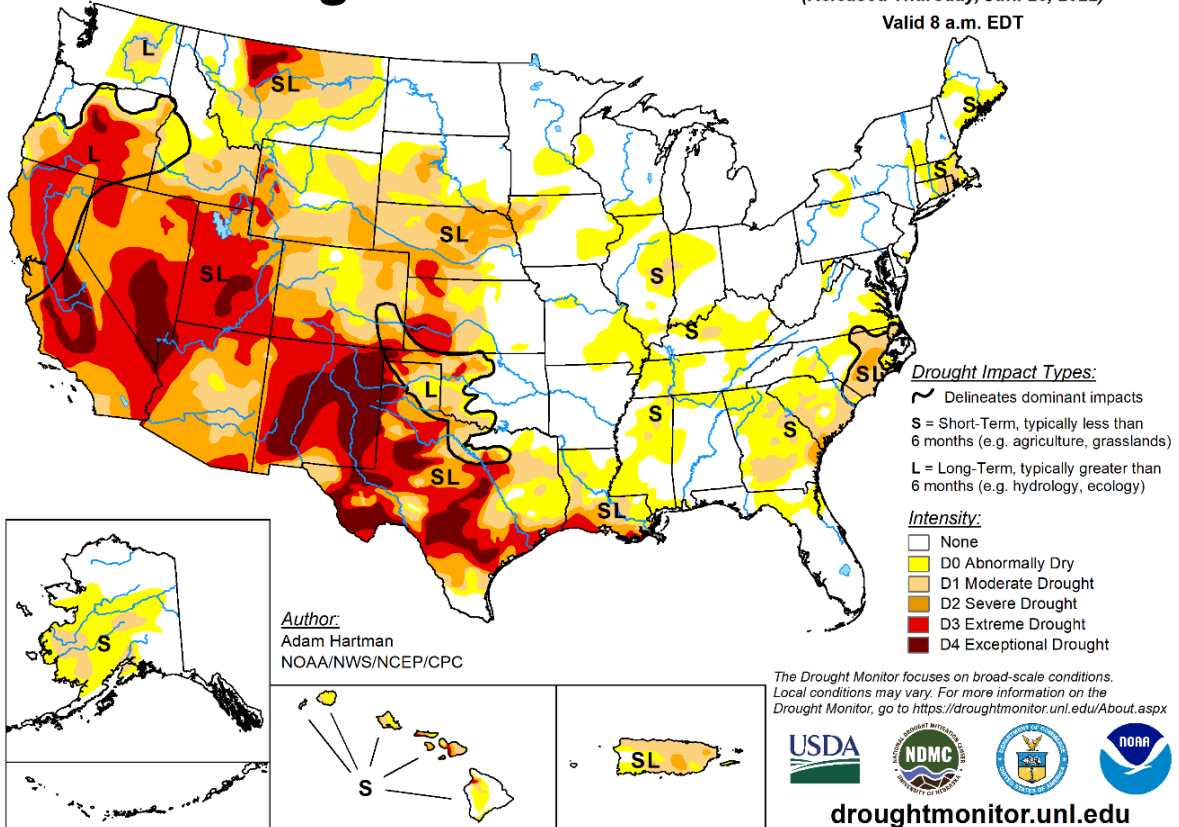


Figure 1-5: Drought Conditions on June 21, 2022

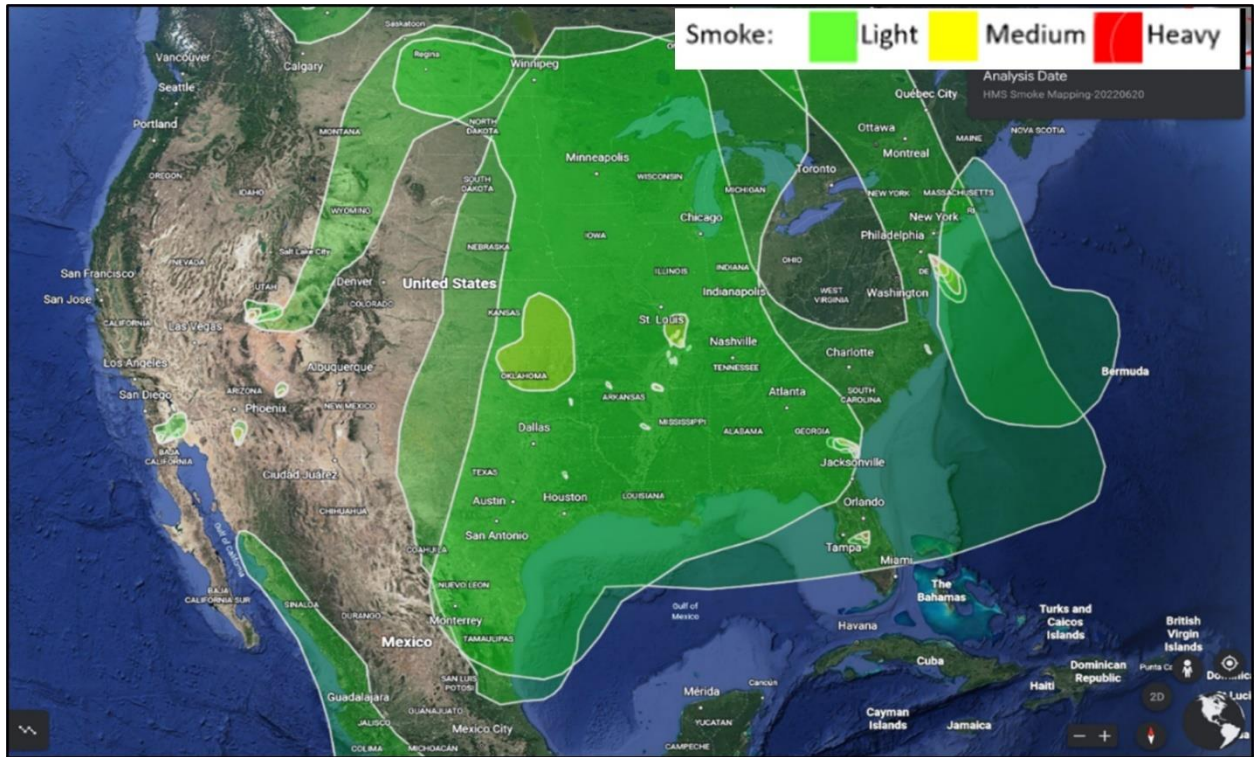


Figure 1-6: NOAA HMS Fire and Smoke Product on June 20, 2022

HRRR-NCEP 06/20/2022 (06:00) 0h fcst Valid 06/20/2022 06:00 UTC
Near-Surface Smoke ($\mu\text{g}/\text{m}^3$), 10m Wind (kt)

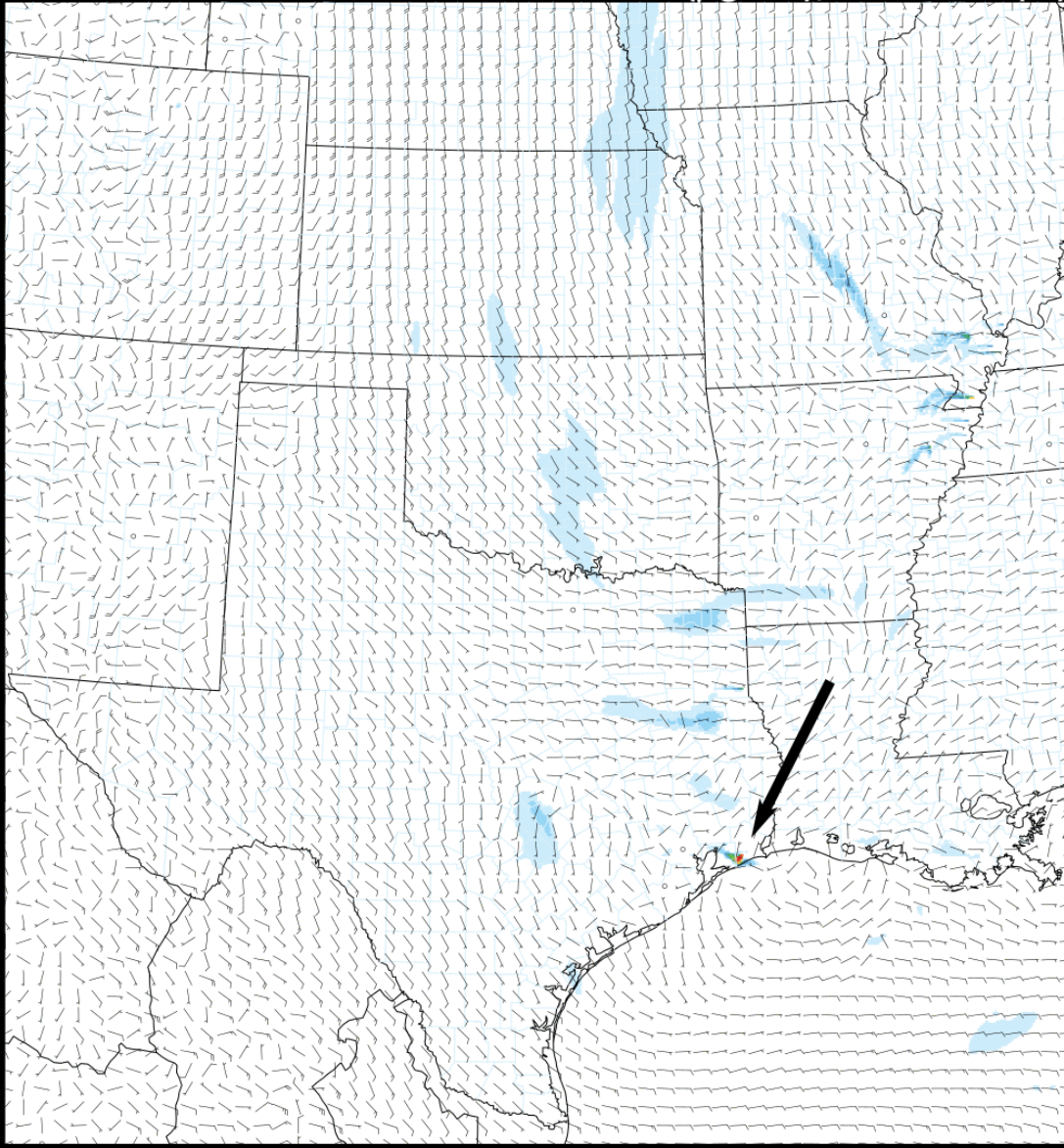


Figure 1-7: HRRR Near-Surface Smoke Modeling on June 20, 2022, 06:00 UTC

HRRR-NCEP 06/20/2022 (12:00) 4h fcst Valid 06/20/2022 16:00 UTC
Near-Surface Smoke ($\mu\text{g}/\text{m}^3$), 10m Wind (kt)

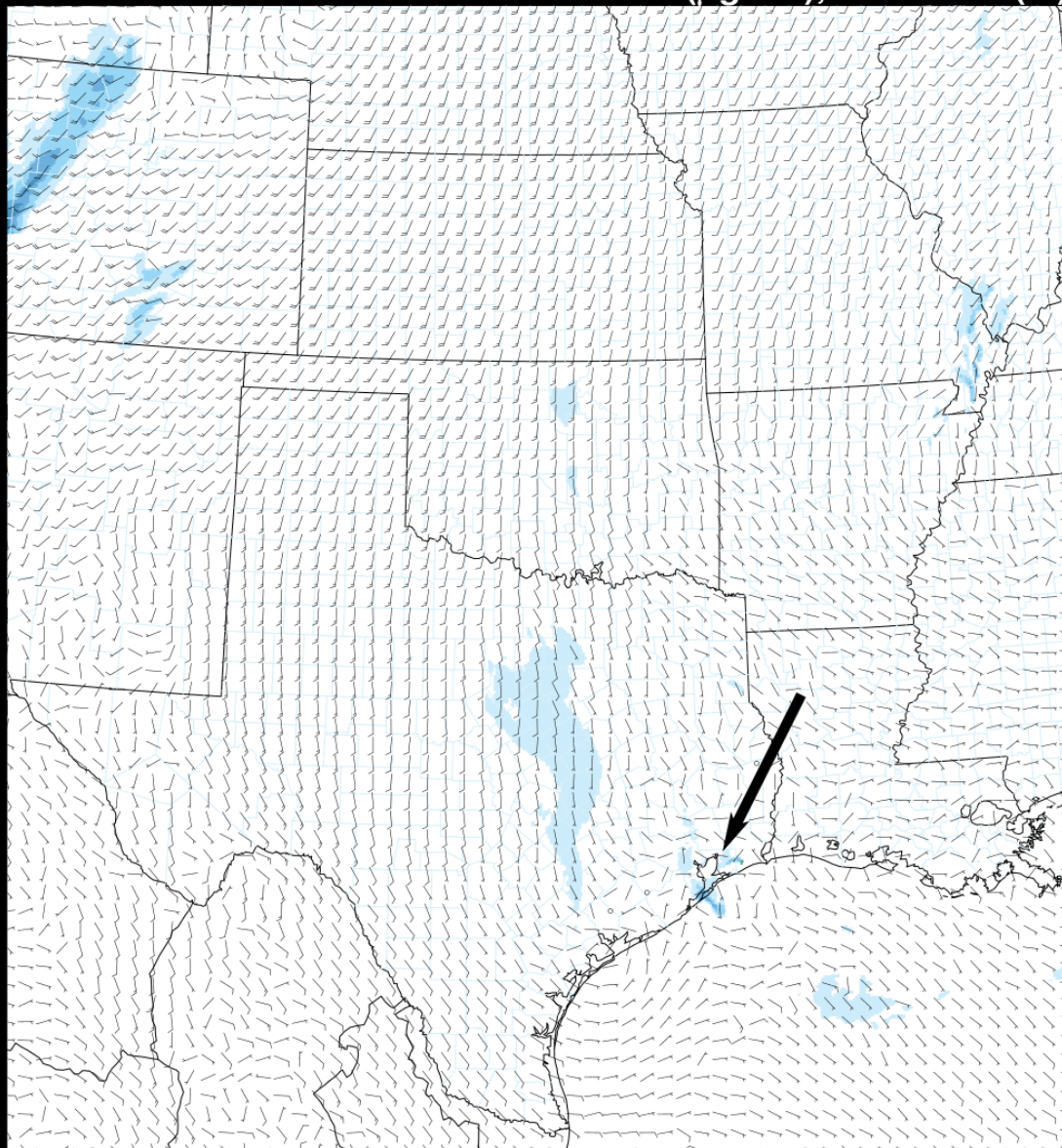


Figure 1-8: HRRR Near-Surface Smoke Modeling on June 20, 2022, 16:00 UTC

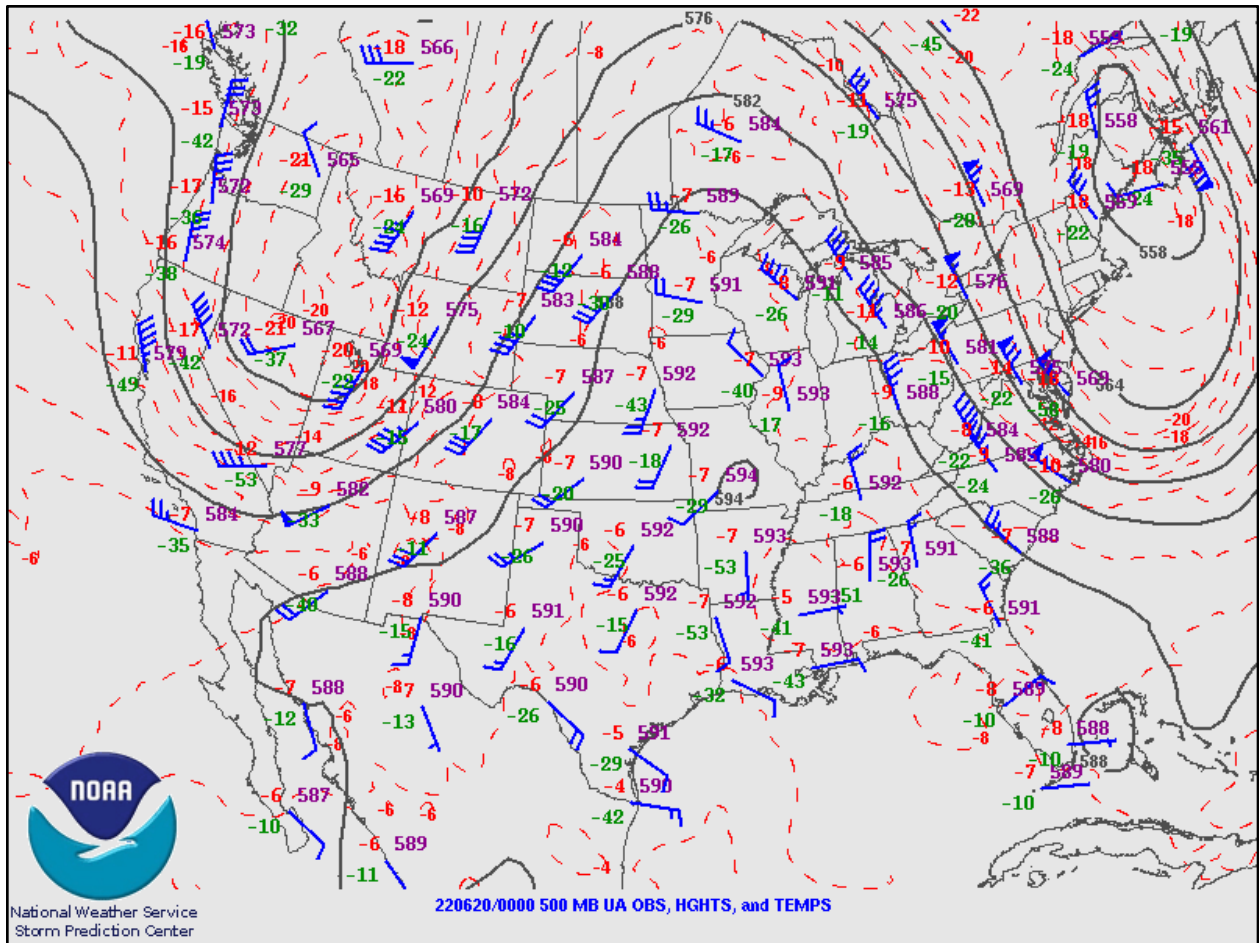


Figure 1-9: NOAA 500 mb Height and Wind Analysis at 7:00 PM CDT June 20, 2022

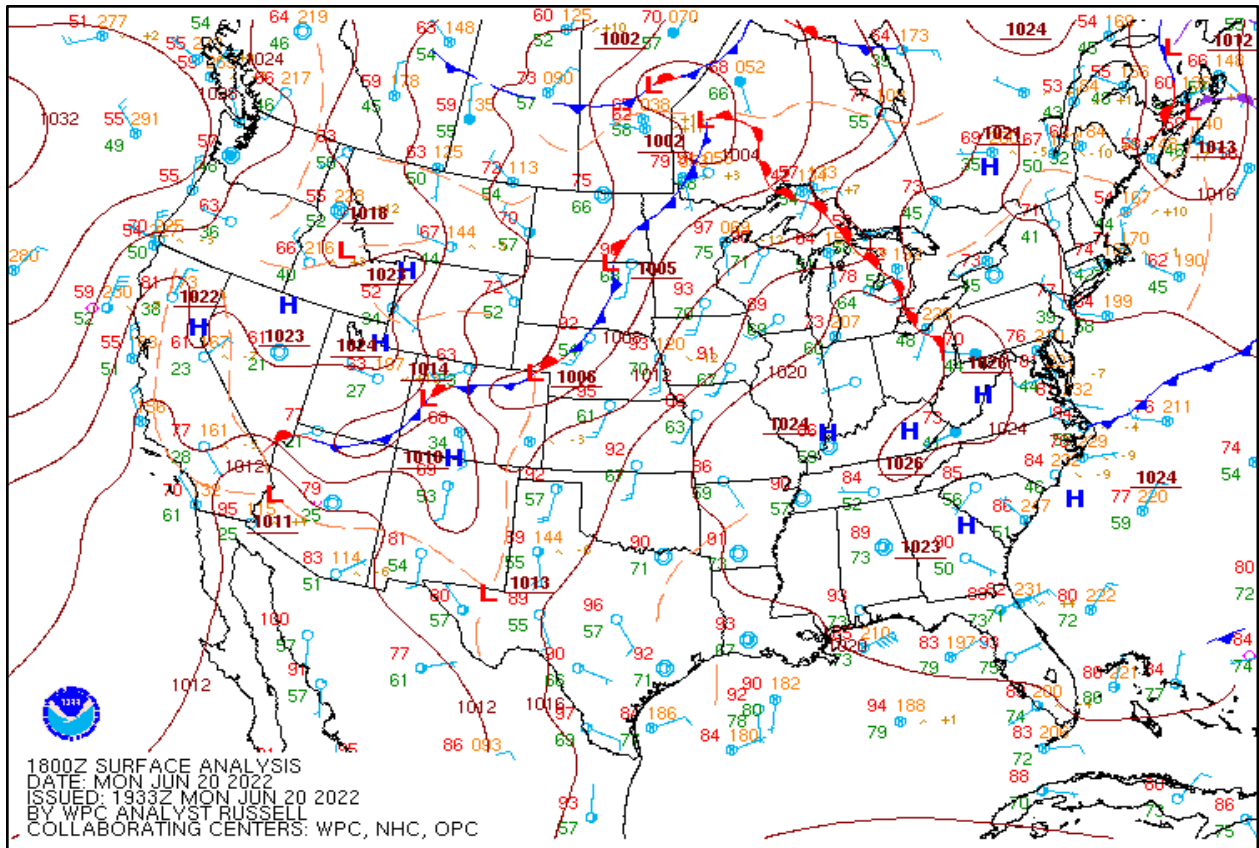


Figure 1-10: NOAA Surface Analysis at 7:00 PM CDT June 20, 2022

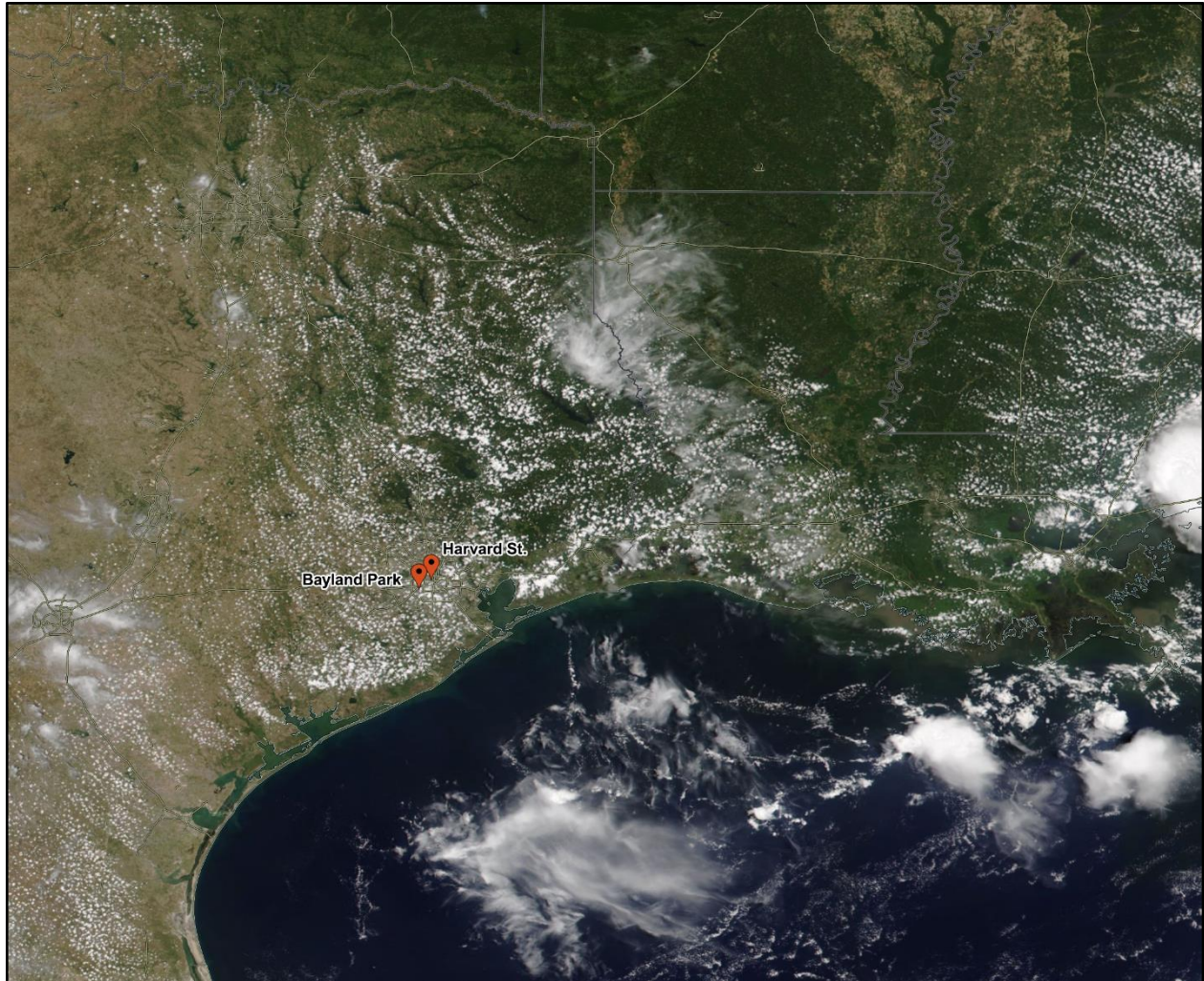


Figure 1-11: NOAA-20 VIIRS True Color Satellite Imagery on June 20, 2022

1.3.3 Characteristics of the September 13, 2022 High Ozone Event

High temperatures and drought conditions (see Figure 1-12: *Drought Conditions on September 13, 2022*) were present before and during the event. These conditions are conducive to wildfire development which created smoke plumes that later influenced the HGB area (see Figure 1-13: *NOAA HMS Fire and Smoke Product on September 13, 2022*). On the night of September 12, 2022, multiple fires in northeast Louisiana and north of Houston began (see Figure 1-14: *HRRR Near-Surface Smoke Modeling on September 13, 2022, 01:00 UTC*). Smoke from these fires then lofted into the HGB area in the morning as conditions in the area typically become highly conducive to ozone formation (see Figure 1-15: *HRRR Near-Surface Smoke Modeling on September 13, 2022, 13:00 UTC*), and continued to cover the area into the following day. This movement is consistent with the flow seen in the 500 mb weather charts (see Figure 1-16: *NOAA 500 mb Height and Wind Analysis at 7:00 PM CDT September 13, 2022*).

Figure 1-17: *NOAA Surface Analysis at 7:00 PM CDT September 13, 2022* shows evidence of a surface high pressure system centered over southern Arkansas and northern Louisiana. The wind barbs on the surface analysis show clockwise flow, bringing air to Southeast Texas from central Arkansas and eastern Oklahoma. The

NOAA-20 VIIRS satellite (see Figure 1-18: *NOAA-20 VIIRS True Color Satellite Imagery on September 13, 2022*) shows smoke over this area of the country. The lack of cloud cover on satellite imagery also indicates there was wide scale subsidence just north of the HGB area which may have brought air from aloft to ground level.

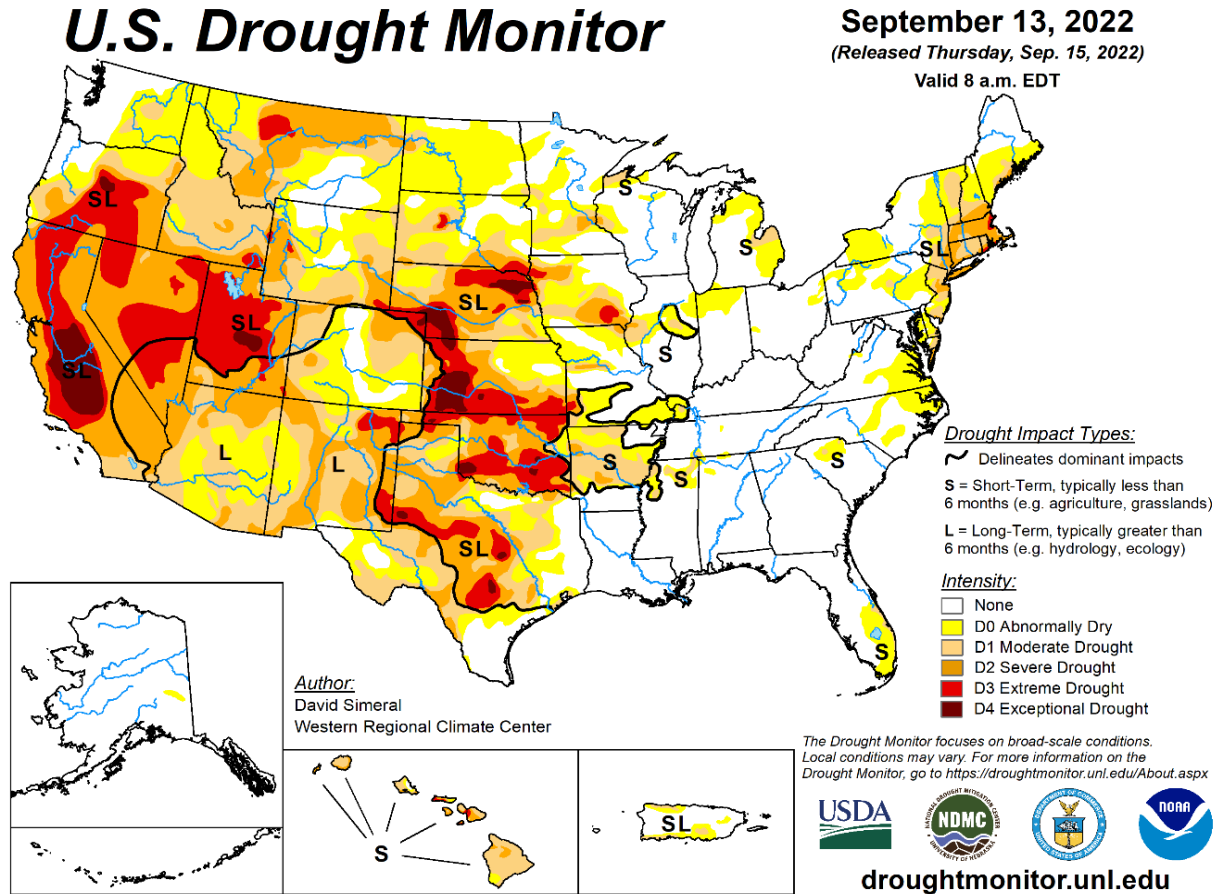


Figure 1-12: Drought Conditions on September 13, 2022

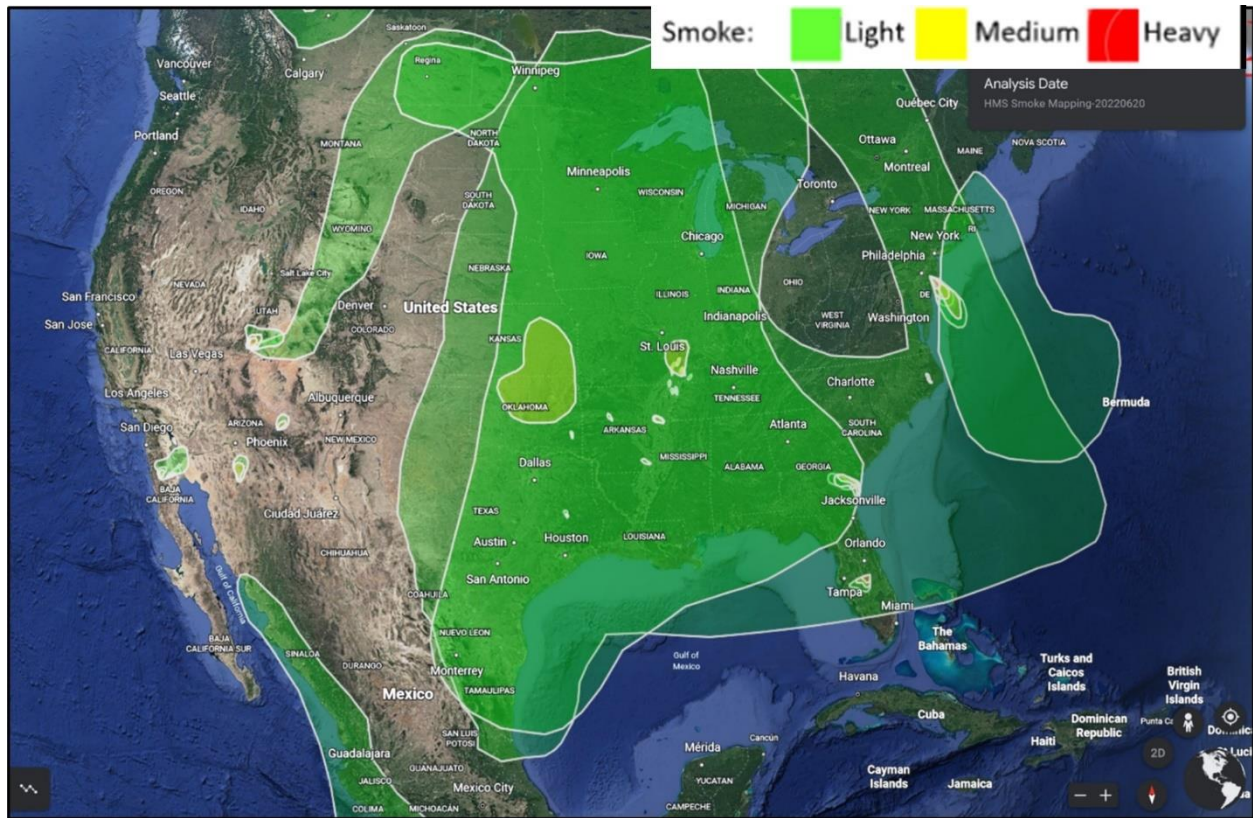


Figure 1-13: NOAA HMS Fire and Smoke Product on September 13, 2022

HRRR-NCEP 09/13/2022 (00:00) 1h fcst Valid 09/13/2022 01:00 UTC
Near-Surface Smoke ($\mu\text{g}/\text{m}^3$), 10m Wind (kt)

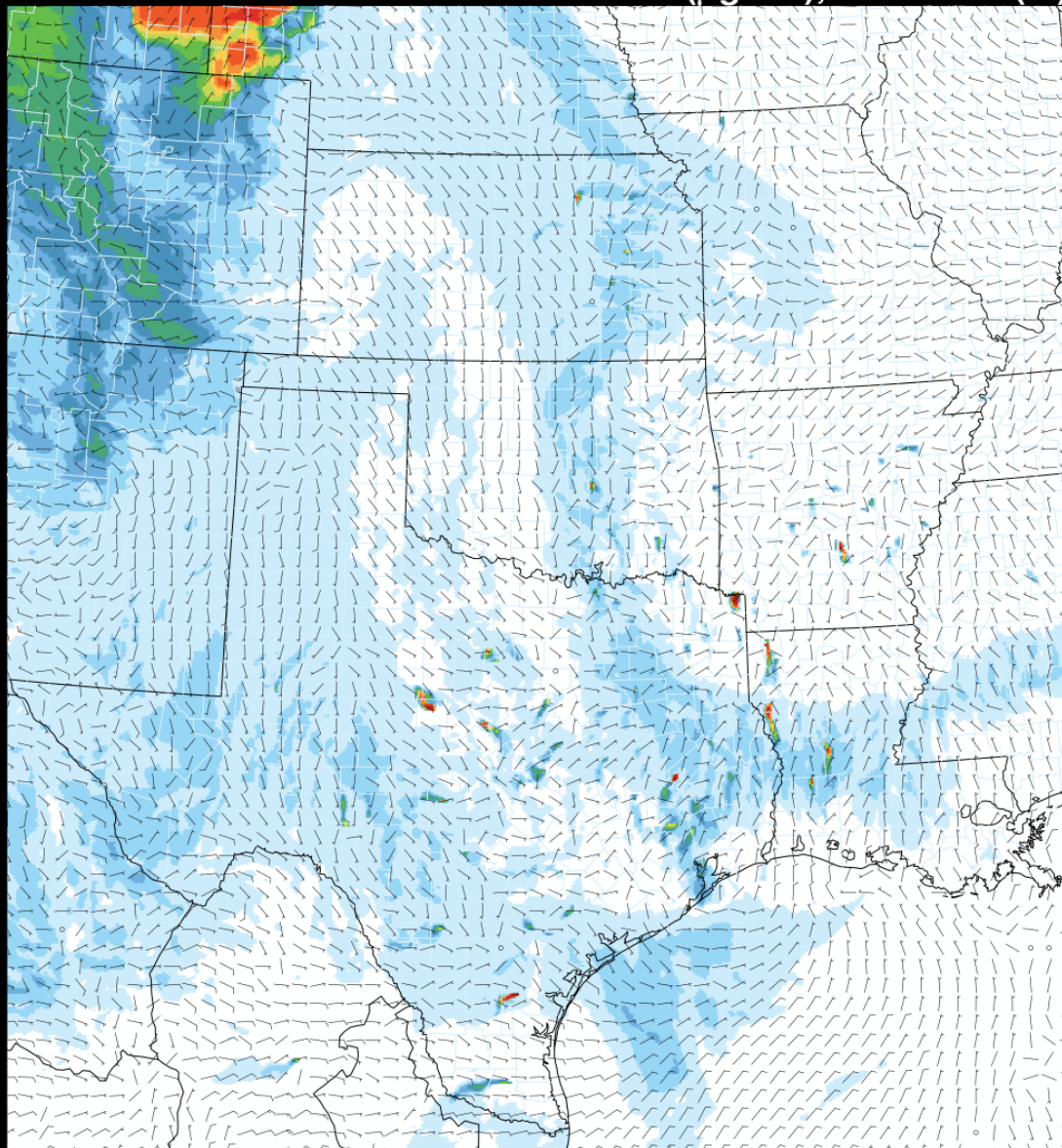


Figure 1-14: HRRR Near-Surface Smoke Modeling on September 13, 2022, 01:00 UTC

HRRR-NCEP 09/13/2022 (06:00) 7h fcst Valid 09/13/2022 13:00 UTC
Near-Surface Smoke ($\mu\text{g}/\text{m}^3$), 10m Wind (kt)

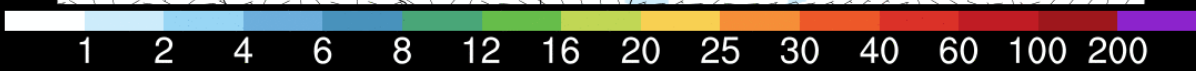
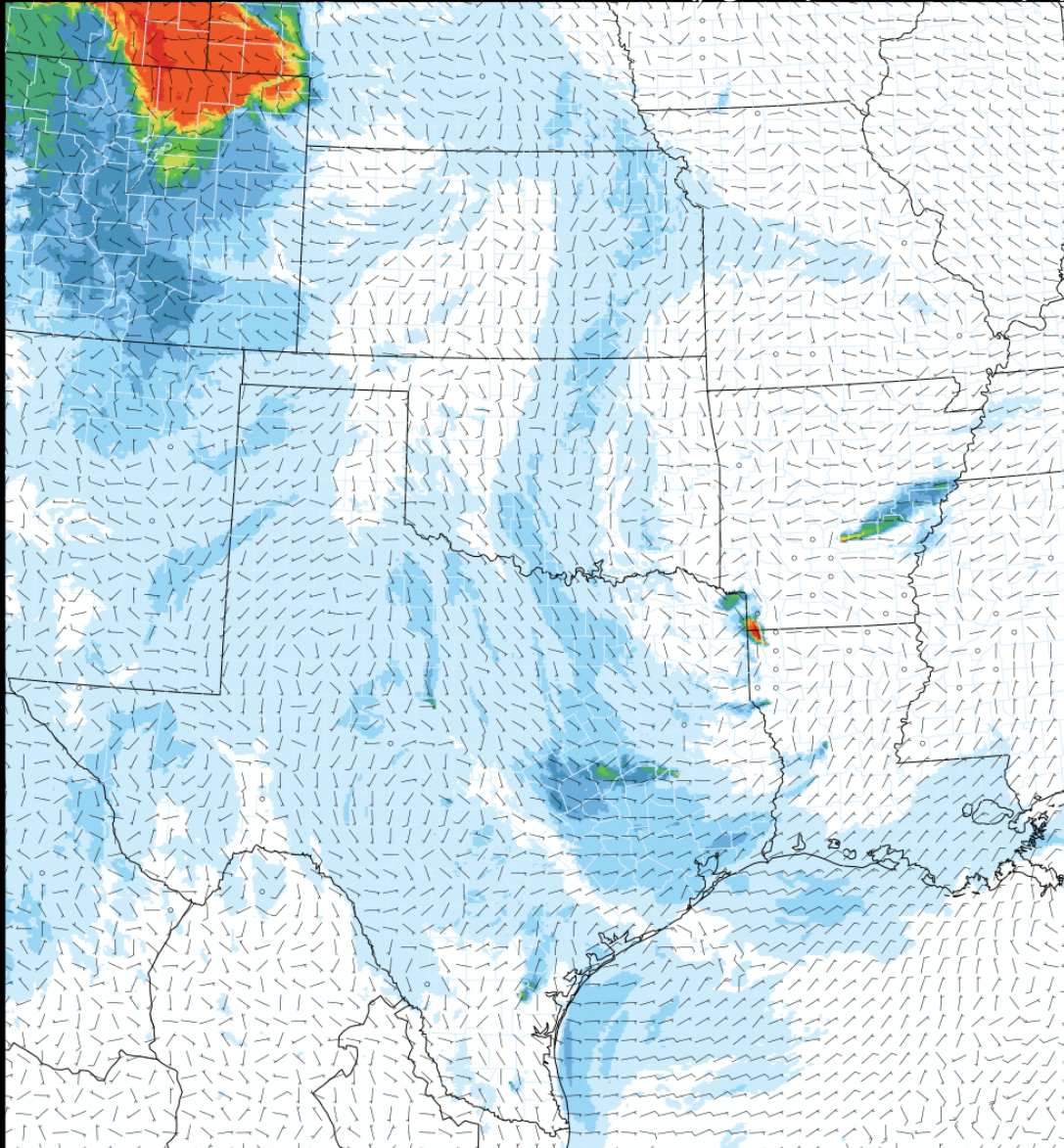


Figure 1-15: HRRR Near-Surface Smoke Modeling on September 13, 2022, 13:00 UTC

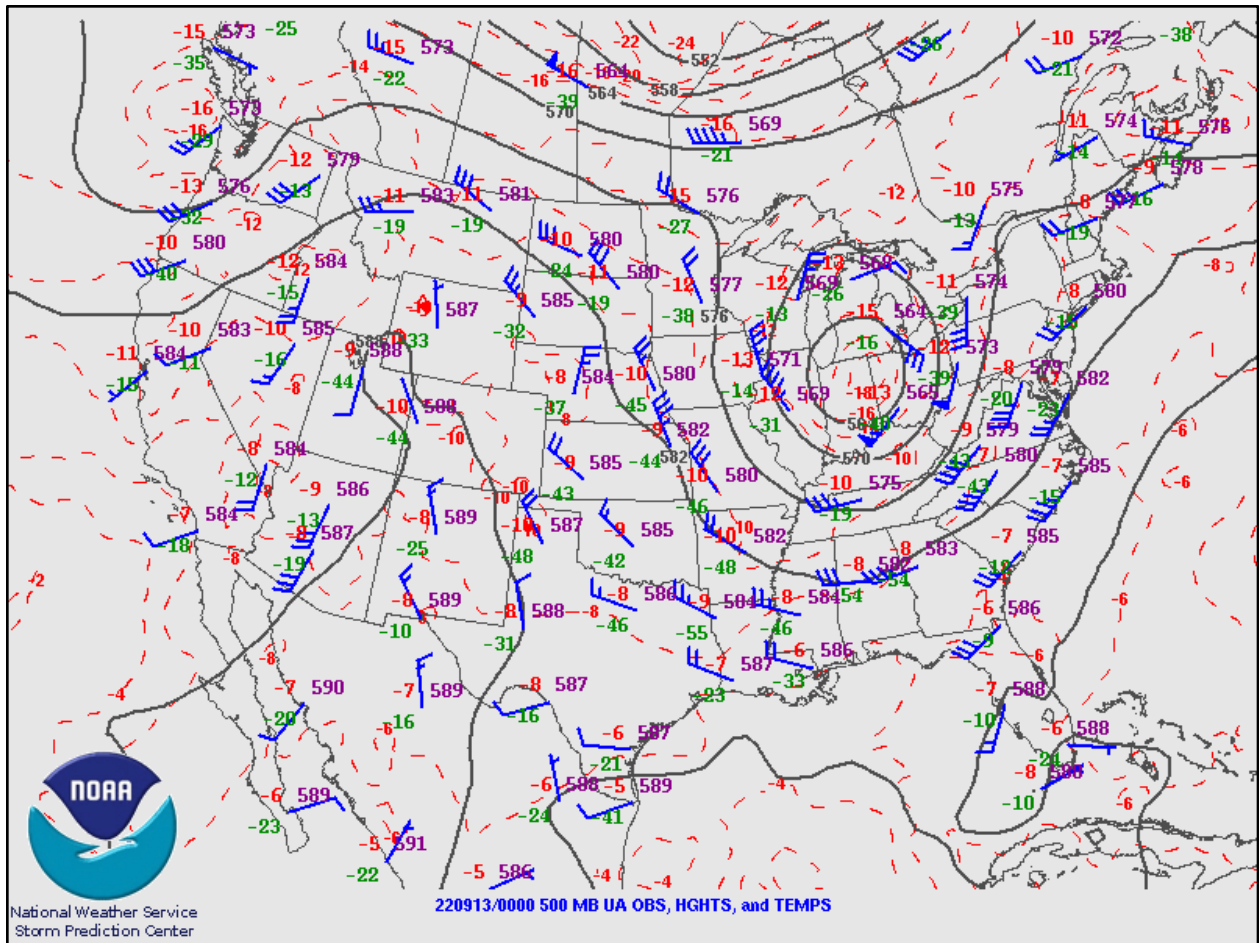


Figure 1-16: NOAA 500 mb Height and Wind Analysis at 7:00 PM CDT September 13, 2022

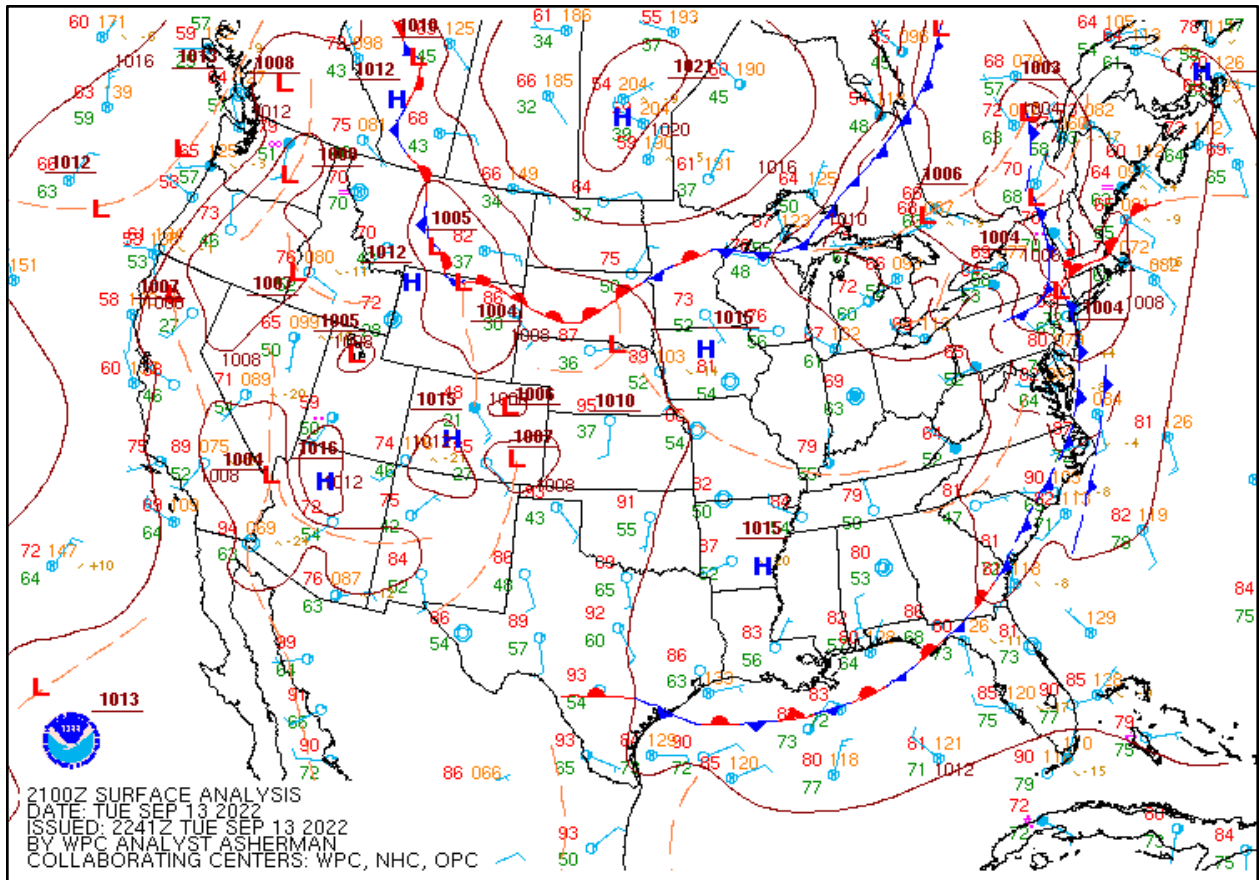


Figure 1-17: NOAA Surface Analysis at 7:00 PM CDT September 13, 2022

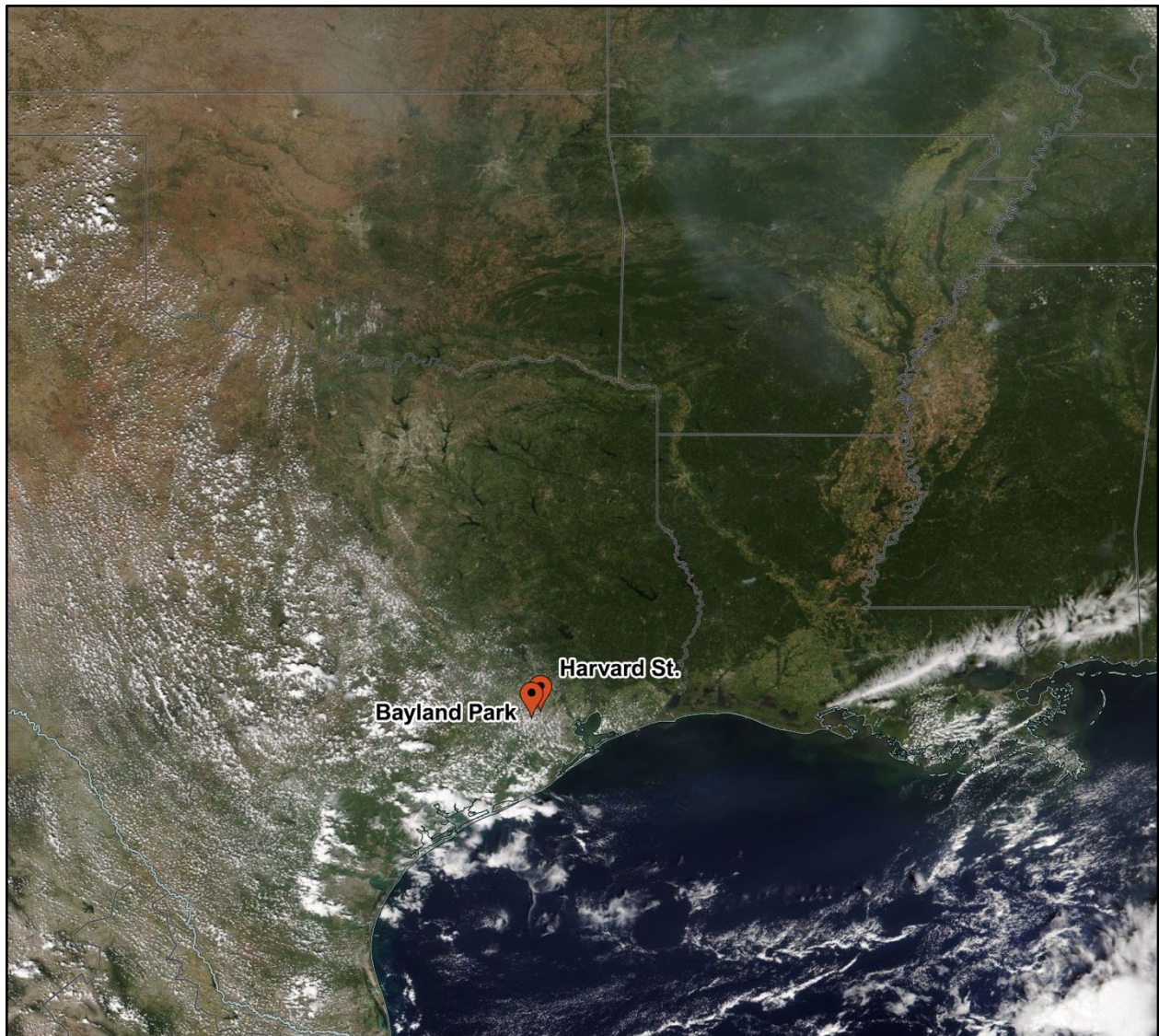


Figure 1-18: NOAA-20 VIIRS True Color Satellite Imagery on September 13, 2022

1.3.4 Characteristics of the September 21, 2022 High Ozone Event

Above average heat and mild drought conditions in parts of Texas and Alabama (see Figure 1-19: *Drought Conditions on September 21, 2022*) were present before and during the event. These conditions are conducive to wildfire development which created smoke plumes that later influenced the HGB area (see Figure 1-20: *NOAA HMS Fire and Smoke Product on September 21, 2022*).

The morning of September 20, 2022, multiple fires across Alabama began (see Figure 1-21: *HRRR Near-Surface Smoke Modeling on September 20, 2022, 11:00 UTC*). Smoke from these fires was carried across the Gulf of Mexico (see Figure 1-22: *HRRR Near-Surface Smoke Modeling on September 21, 2022, 00:00 UTC*) then lofted into the HGB area as conditions in the area typically become highly conducive to ozone formation (see Figure 1-23: *HRRR Near-Surface Smoke Modeling on September 21, 2022, 19:00 UTC*) and continued to cover the area into the following day.

This movement is consistent with the flow seen in the 500 mb weather charts (see Figure 1-24: *NOAA 500 mb Height and Wind Analysis at 7:00 PM CDT September 21, 2022*). Figure 1-25: *NOAA Surface Analysis at 7:00 PM CDT September 21, 2022* shows evidence of a strong surface high pressure system over the Ark-La-Tex region. The surface winds barbs indicate clockwise flow around the center of this high-pressure system. As shown on the surface analysis, the surface winds were bringing air from Coastal Louisiana into the HGB area. The NOAA-20 VIIRS satellite shows smoke plumes in this area. On September 21, 2022, smoke that lofted from Alabama to the HGB area from the Gulf of Mexico can be seen by the NOAA-20 VIIRS satellite (see Figure 1-26: *NOAA-20 VIIRS True Color Satellite Imagery on September 21, 2022*). The lack of cloud cover on satellite imagery also indicates there was wide scale subsidence just north of the HGB area which may have brought air from aloft to ground level.

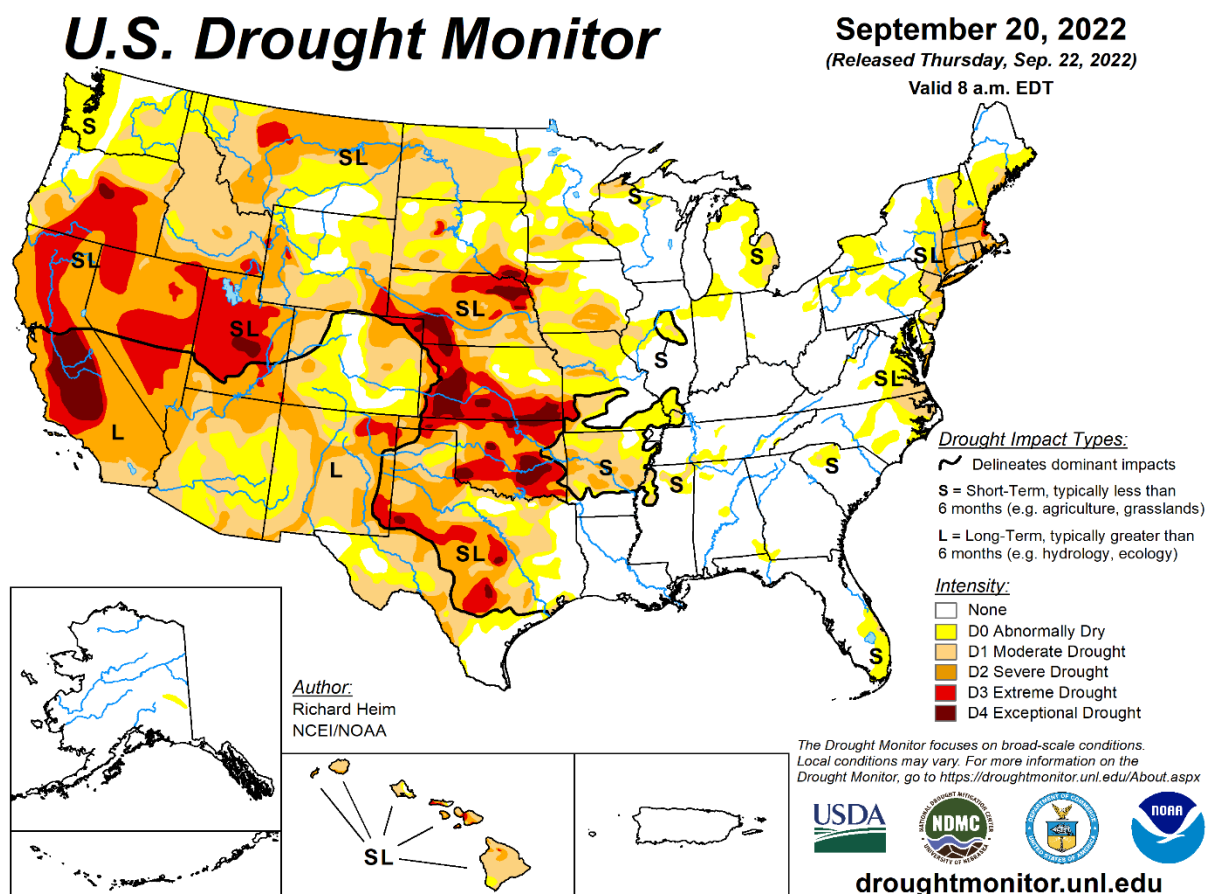


Figure 1-19: Drought Conditions on September 21, 2022

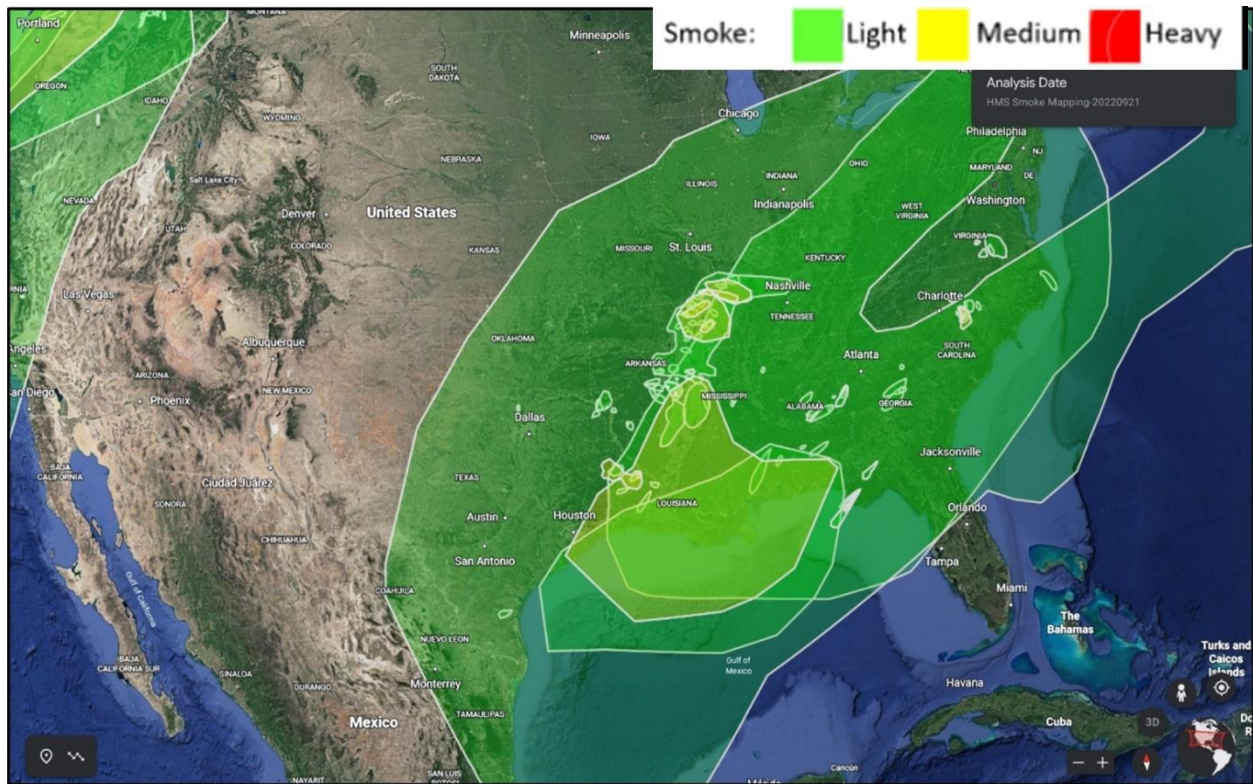
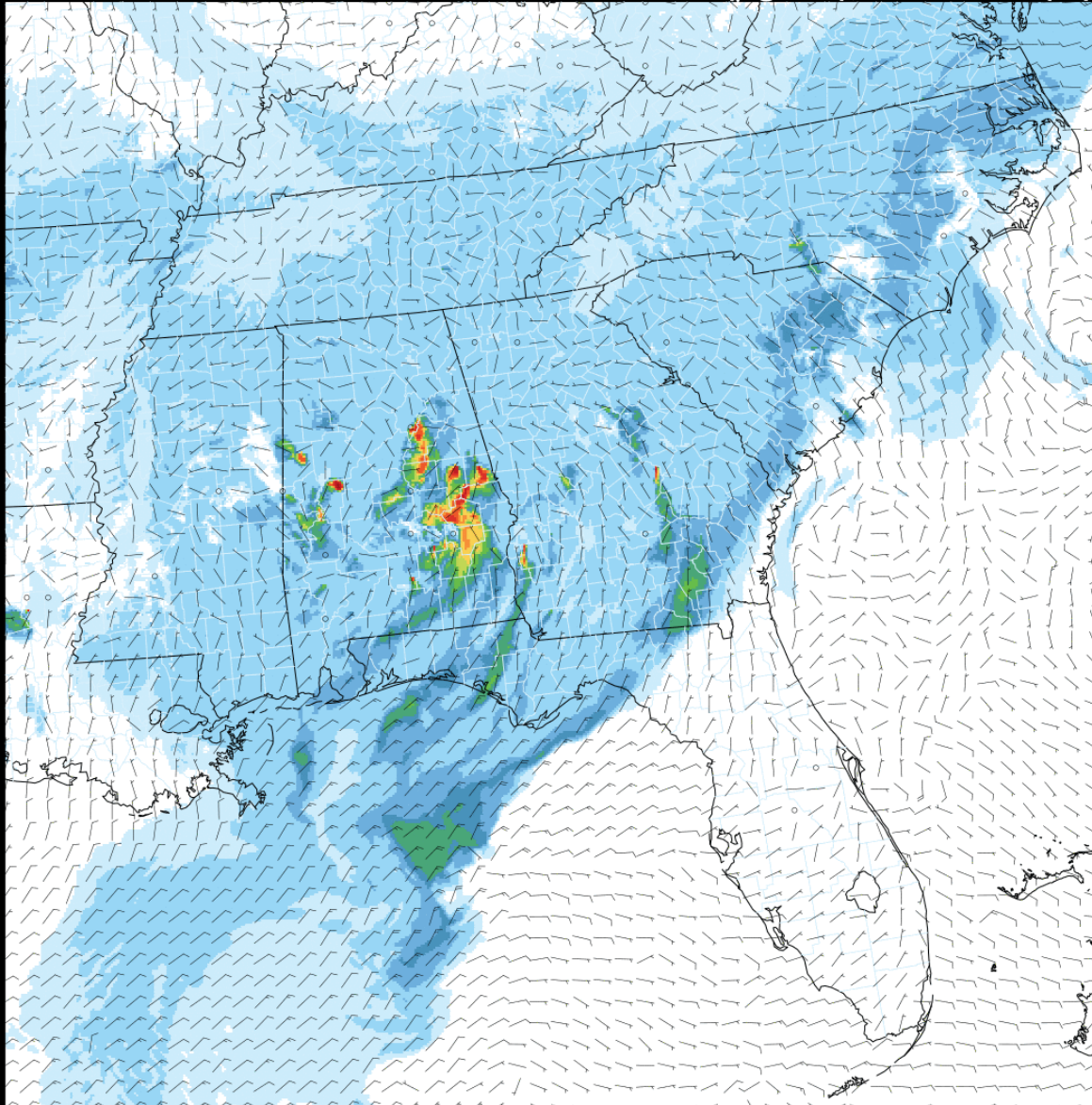


Figure 1-20: NOAA HMS Fire and Smoke Product on September 21, 2022

HRRR-NCEP 09/20/2022 (06:00) 5h fcst

Valid 09/20/2022 11:00 UTC

Near-Surface Smoke ($\mu\text{g}/\text{m}^3$), 10m Wind (kt)



1 2 4 6 8 12 16 20 25 30 40 60 100 200

Figure 1-21: HRRR Near-Surface Smoke Modeling on September 20, 2022, 11:00 UTC

HRRR-NCEP 09/21/2022 (00:00) 0h fcst Valid 09/21/2022 00:00 UTC
Near-Surface Smoke ($\mu\text{g}/\text{m}^3$), 10m Wind (kt)

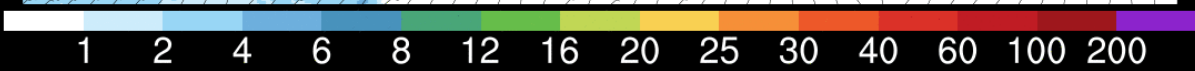
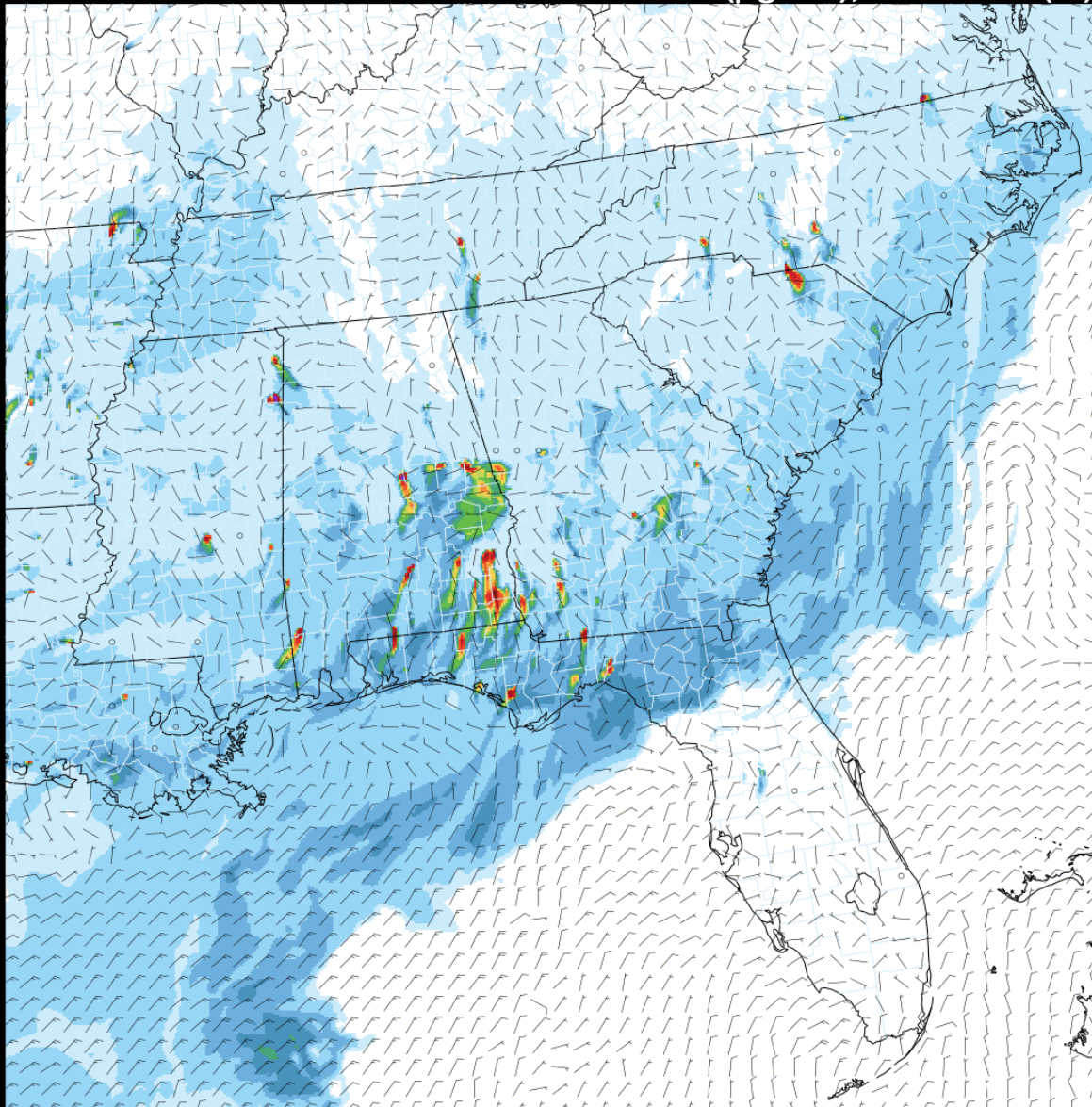


Figure 1-22: HRRR Near-Surface Smoke Modeling on September 21, 2022, 00:00 UTC

HRRR-NCEP 09/21/2022 (18:00) 1h fcst Valid 09/21/2022 19:00 UTC
Near-Surface Smoke ($\mu\text{g}/\text{m}^3$), 10m Wind (kt)

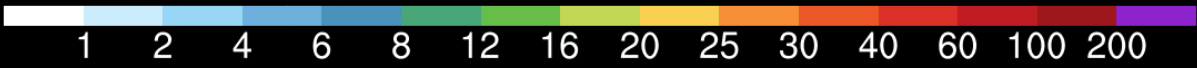
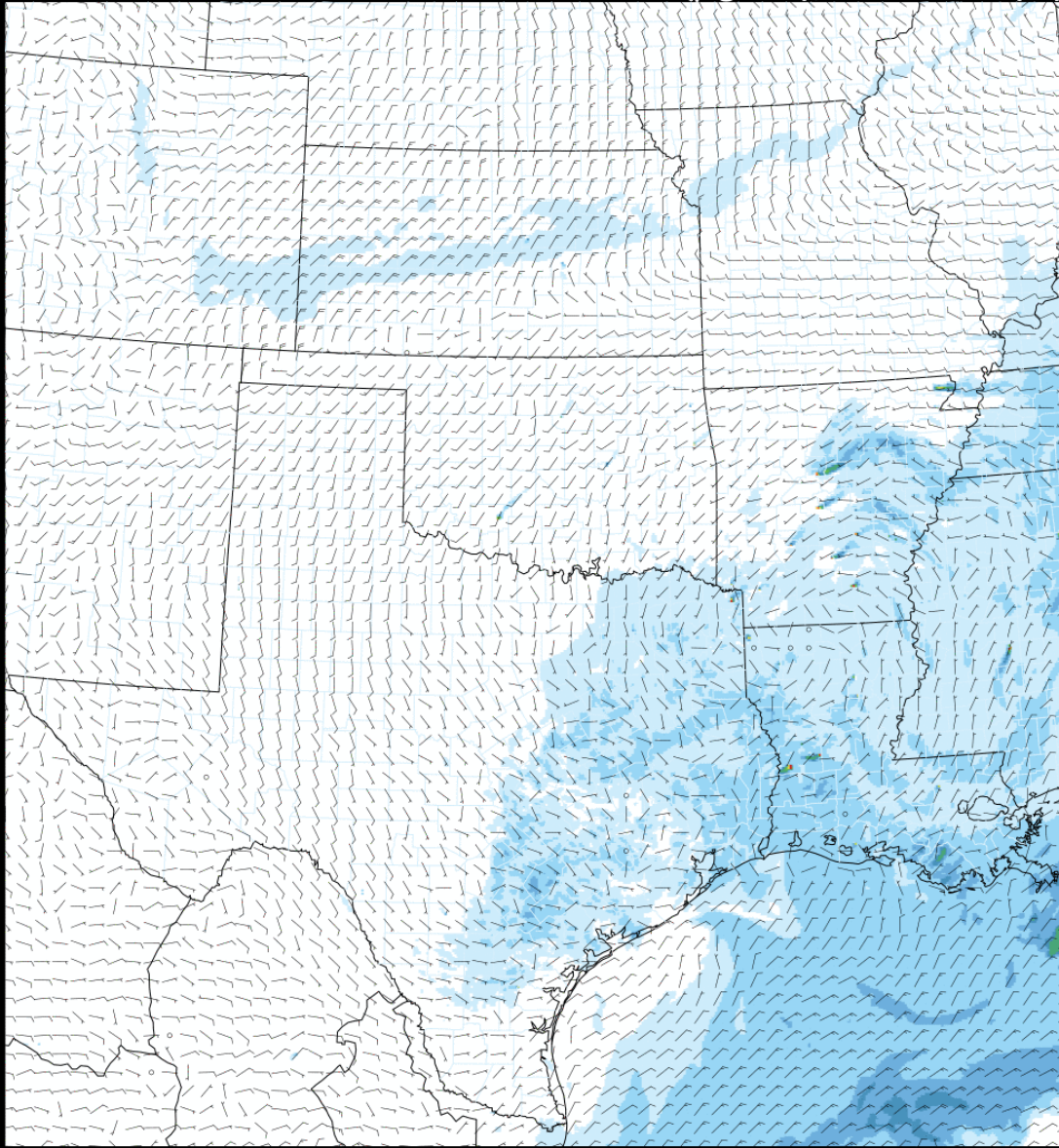


Figure 1-23: HRRR Near-Surface Smoke Modeling on September 21, 2022, 19:00 UTC

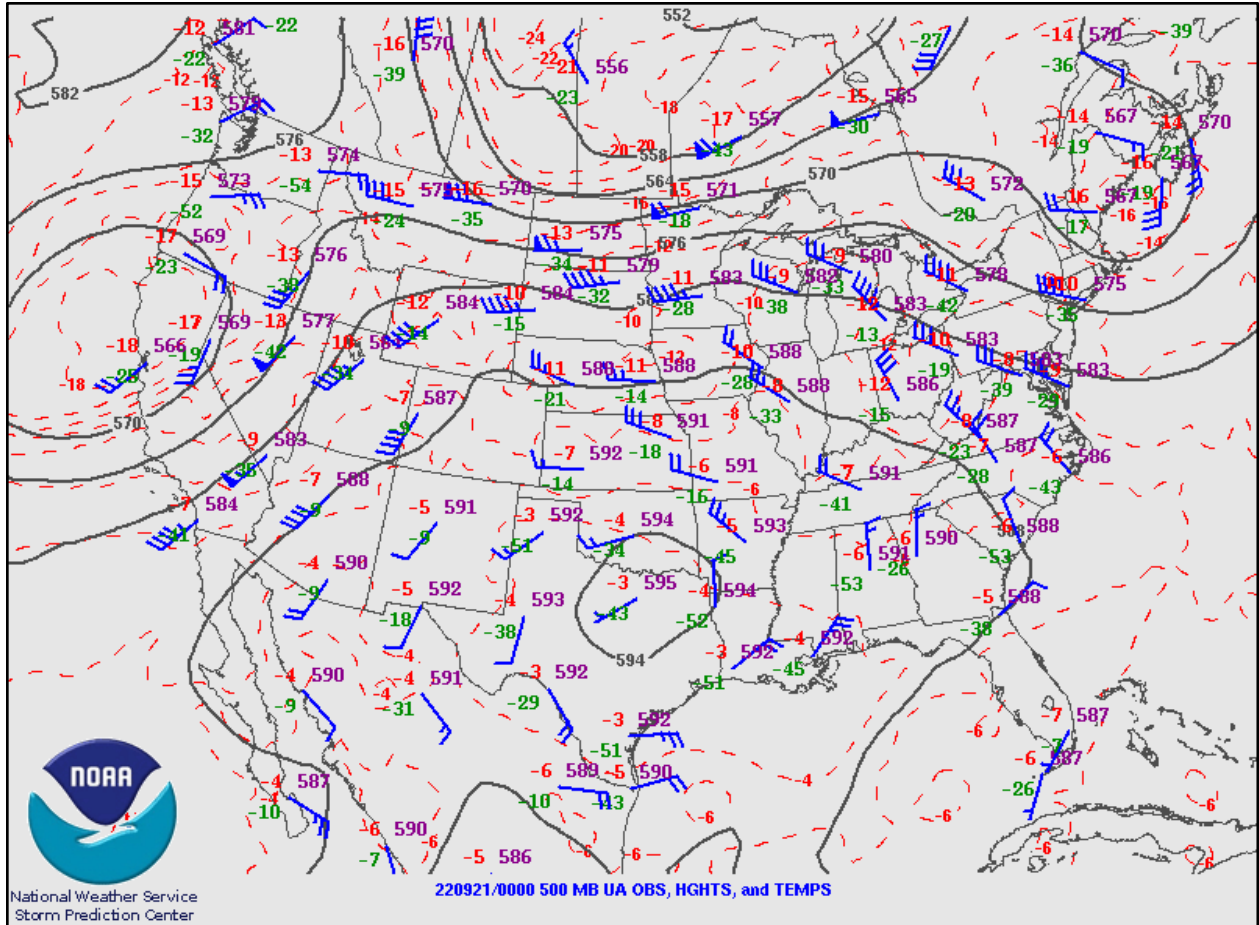


Figure 1-24: NOAA 500 mb Height and Wind Analysis at 7:00 PM CDT September 21, 2022

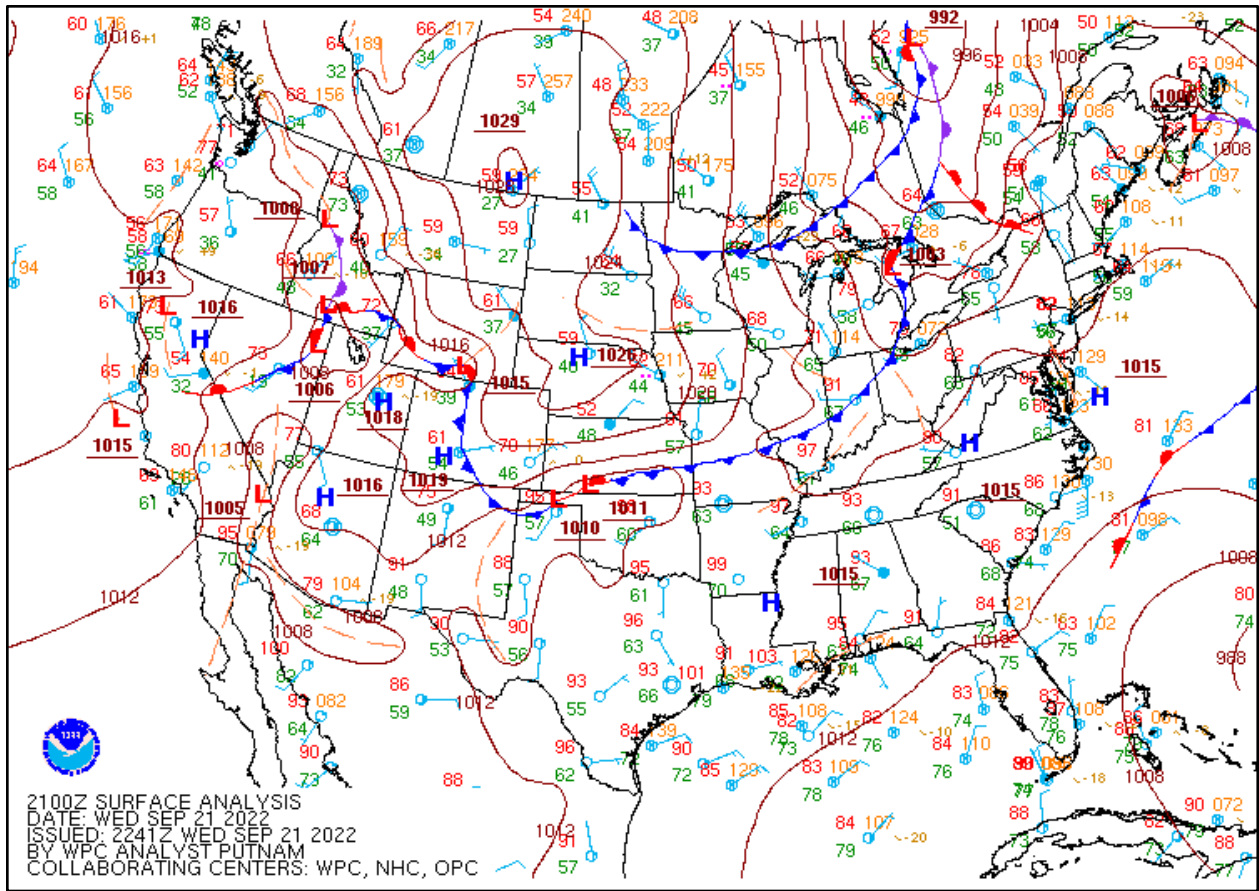


Figure 1-25: NOAA Surface Analysis at 7:00 PM CDT September 21, 2022

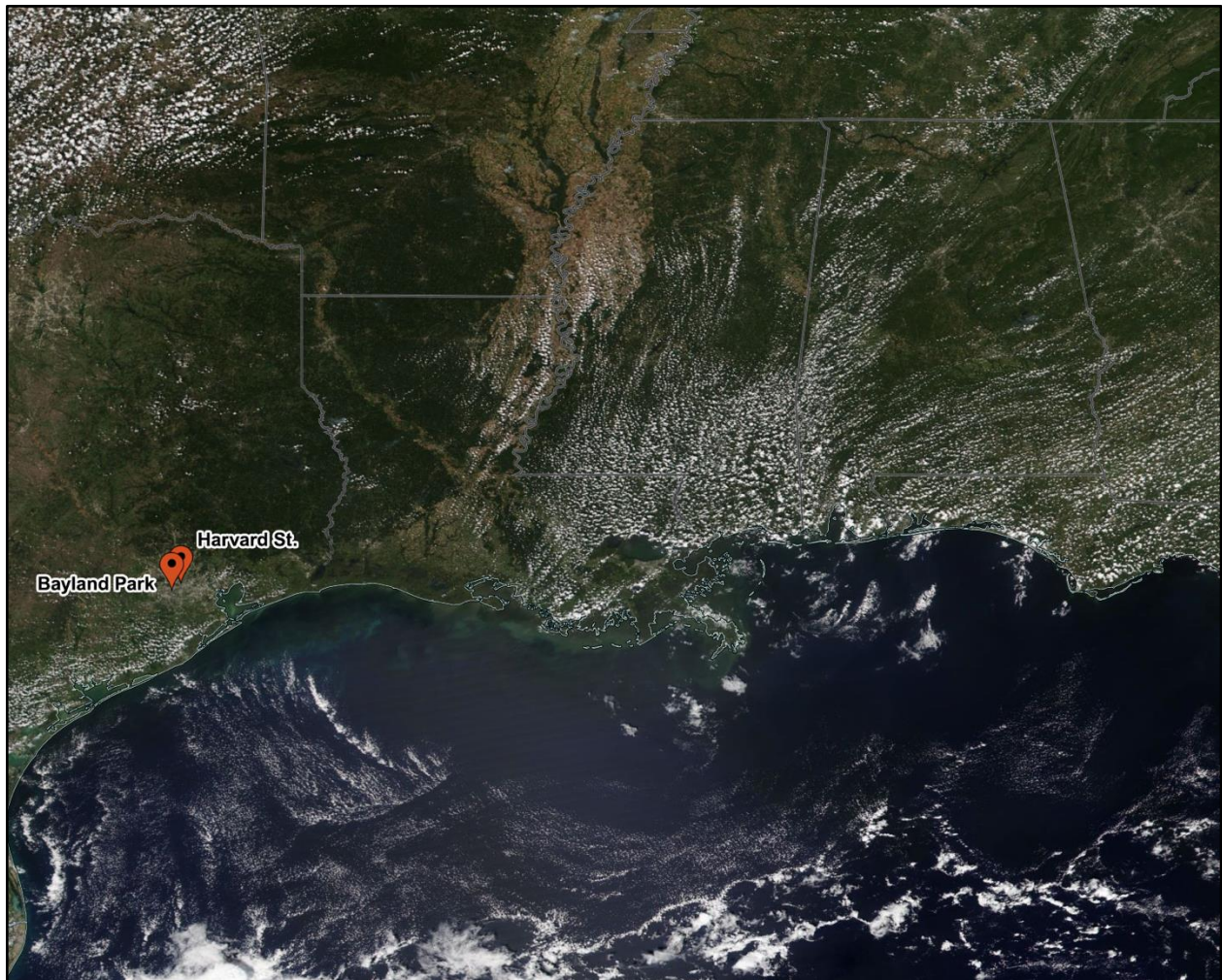


Figure 1-26: NOAA-20 VIIRS True Color Satellite Imagery on September 21, 2022

1.3.5 Characteristics of the October 8, 2022 High Ozone Event

Extremely warm and dry conditions in the south-central United States (see Figure 1-27: *Drought Conditions on October 11, 2022*) were present before and during the event. These conditions were conducive to wildfire development, which created smoke plumes that later influenced the HGB area.

From October 5 through October 7, 2022, multiple fires persisted across northern Louisiana and central Mississippi (see Figure 1-28: *NOAA HMS Fire and Smoke Product on October 8, 2022*). Smoke from these fires was carried overnight across east Texas towards the HGB area (see Figure 1-29: *HRRR Near-Surface Smoke Modeling on October 7, 2022, 13:00 UTC*). This smoke lofted into the HGB area as conditions in the area typically became highly conducive to ozone formation (see Figure 1-30: *HRRR Near-Surface Smoke Modeling on October 7, 2022, 07:00 UTC* and Figure 1-31: *HRRR Near-Surface Smoke Modeling on October 8, 2022, 17:00 UTC*.) and continued to cover the area for most of the day.

This movement is consistent with the flow seen in the 500 mb weather charts (see Figure 1-32: *NOAA 500 mb Height and Wind Analysis at 7:00 PM CDT October 8, 2022*).

Figure 1-33: NOAA Surface Analysis at 7:00 PM CDT October 8, 2022 shows evidence of a trough moving eastward just north of the Great Lakes region dragging a cold front southward over the HGB area. The surface analysis shows, behind the front, winds flowing into the HGB area were from the northeast. Additionally, the post-frontal conditions on October 8, 2022, were favorable for ozone formation as local winds were light and relative humidity had dropped to 57% during the afternoon. On October 7, 2022, visible smoke from the aforementioned wildfires can be seen by the NOAA-20 VIIRS satellite (see Figure 1-34: NOAA-20 VIIRS True Color Satellite Imagery on October 8, 2022). This smoke then lofted into the HGB area on October 8, 2022.

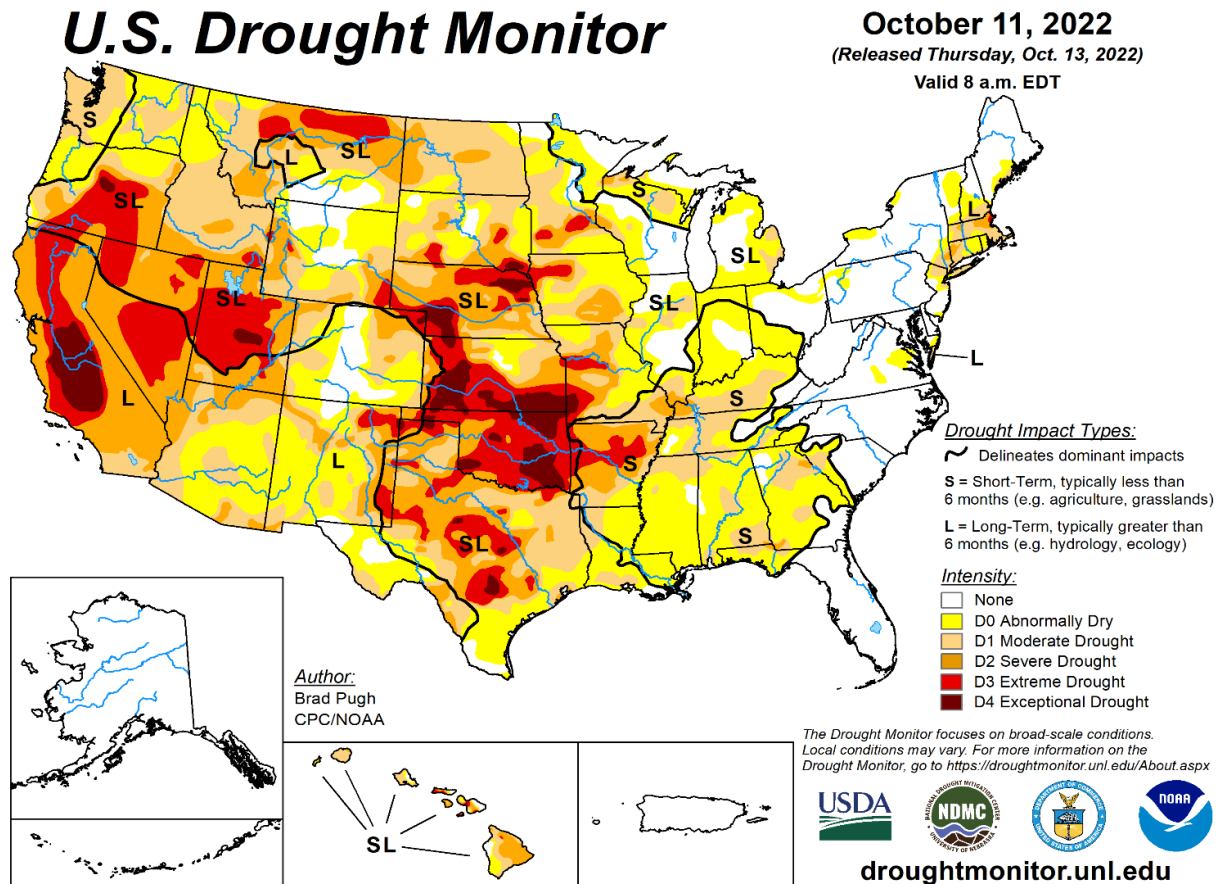


Figure 1-27: Drought Conditions on October 11, 2022

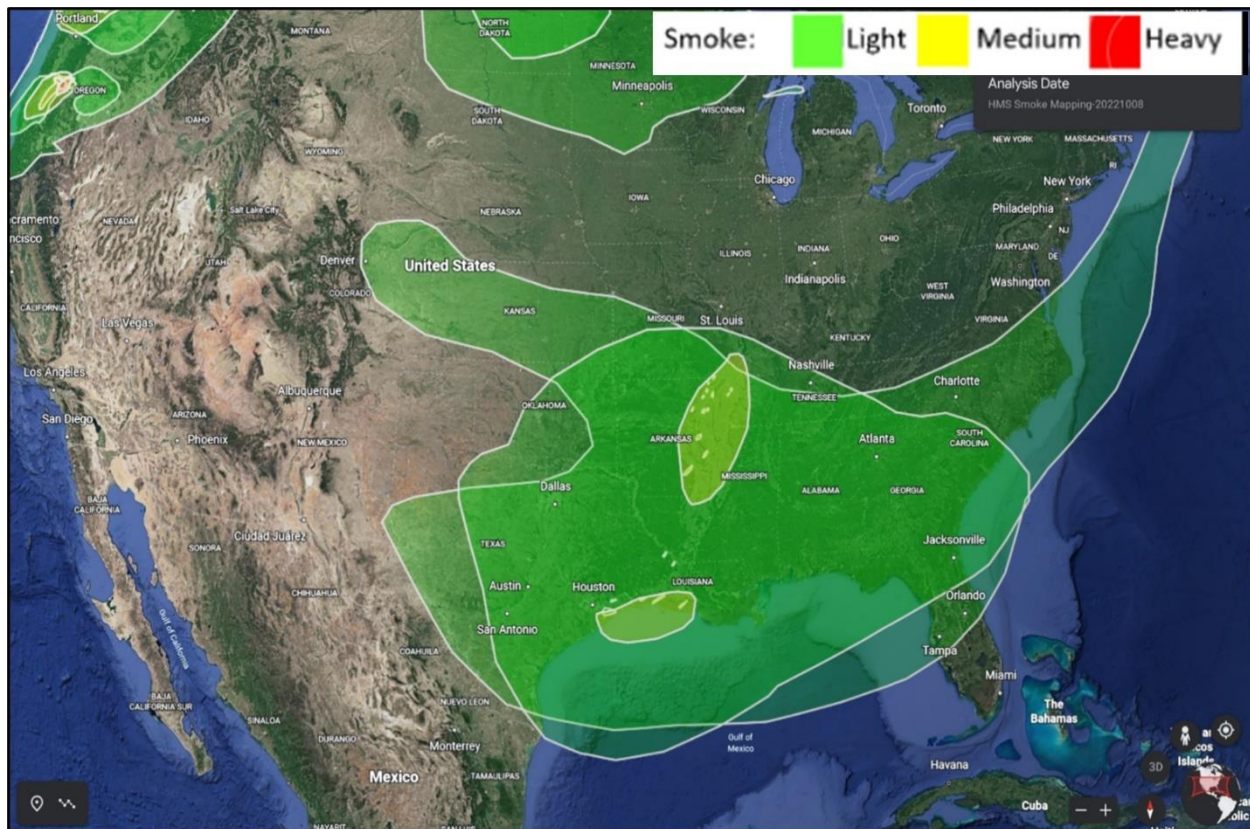


Figure 1-28: NOAA HMS Fire and Smoke Product on October 8, 2022

HRRR-NCEP 10/07/2022 (12:00) 1h fcst Valid 10/07/2022 13:00 UTC
Near-Surface Smoke ($\mu\text{g}/\text{m}^3$), 10m Wind (kt)

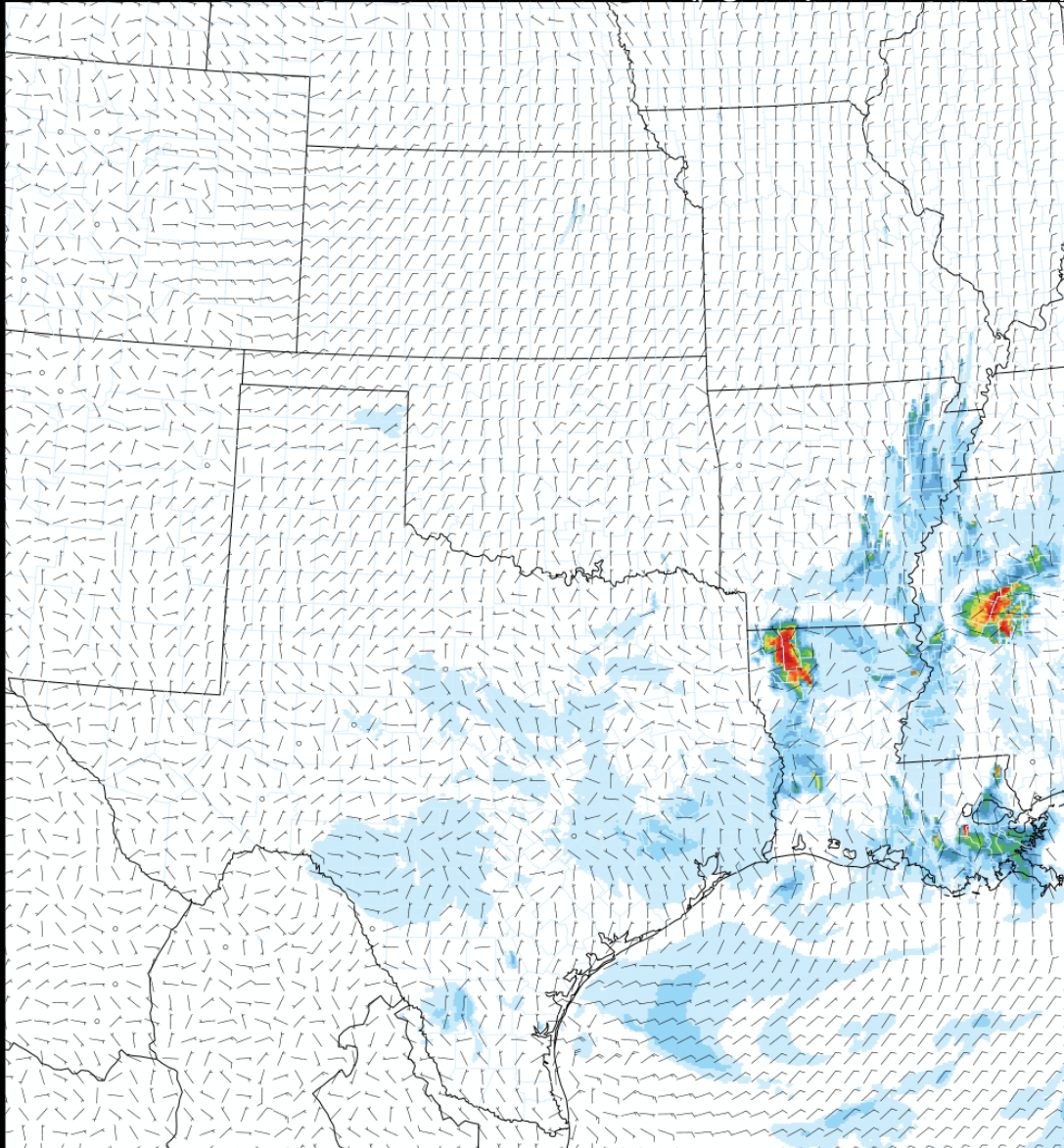


Figure 1-29: HRRR Near-Surface Smoke Modeling on October 7, 2022, 13:00 UTC

HRRR-NCEP 10/08/2022 (06:00) 1h fcst Valid 10/08/2022 07:00 UTC
Near-Surface Smoke ($\mu\text{g}/\text{m}^3$), 10m Wind (kt)

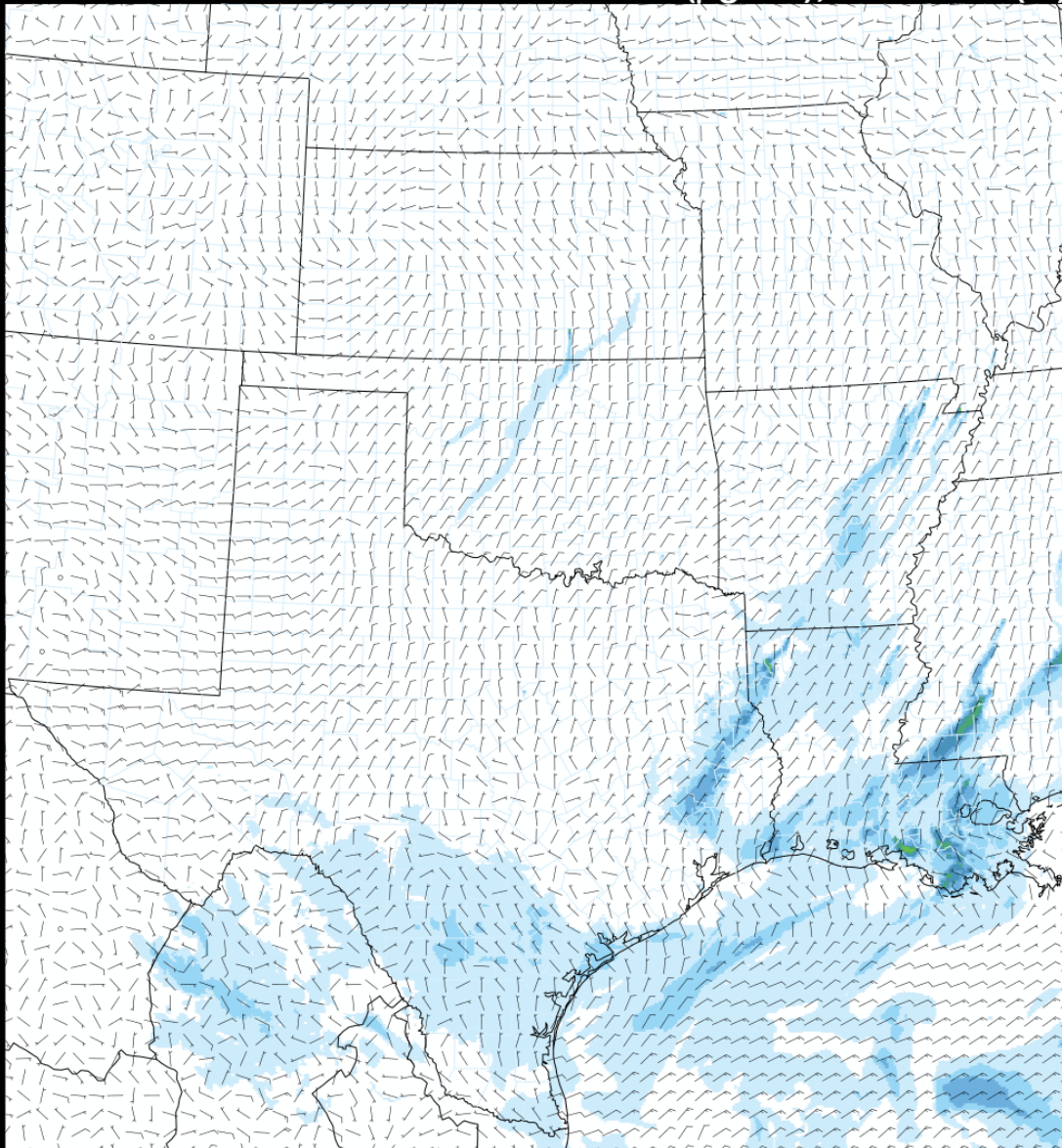


Figure 1-30: HRRR Near-Surface Smoke Modeling on October 7, 2022, 07:00 UTC

HRRR-NCEP 10/08/2022 (12:00) 5h fcst Valid 10/08/2022 17:00 UTC
Near-Surface Smoke ($\mu\text{g}/\text{m}^3$), 10m Wind (kt)

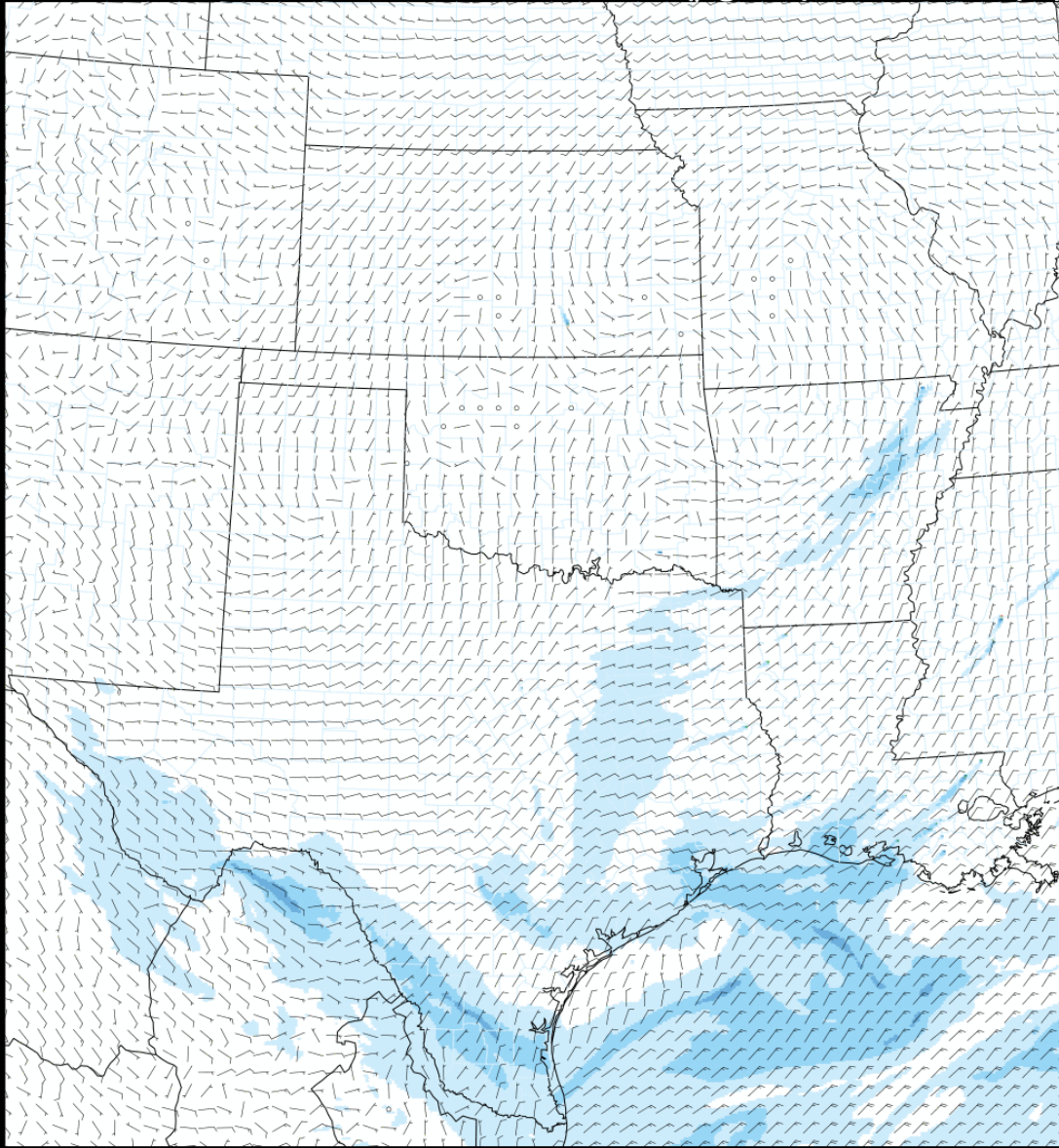


Figure 1-31: HRRR Near-Surface Smoke Modeling on October 8, 2022, 17:00 UTC

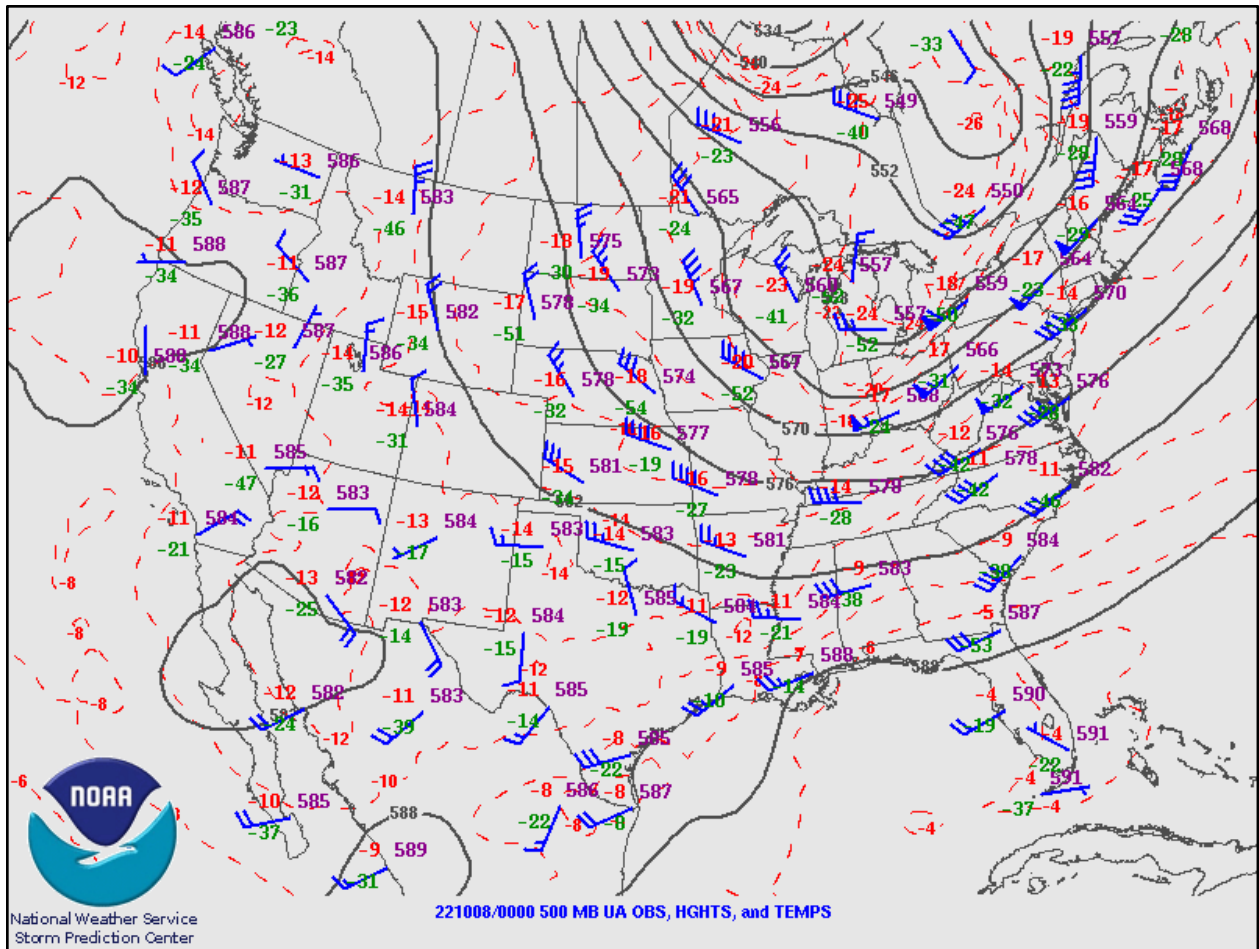


Figure 1-32: NOAA 500 mb Height and Wind Analysis at 7:00 PM CDT October 8, 2022

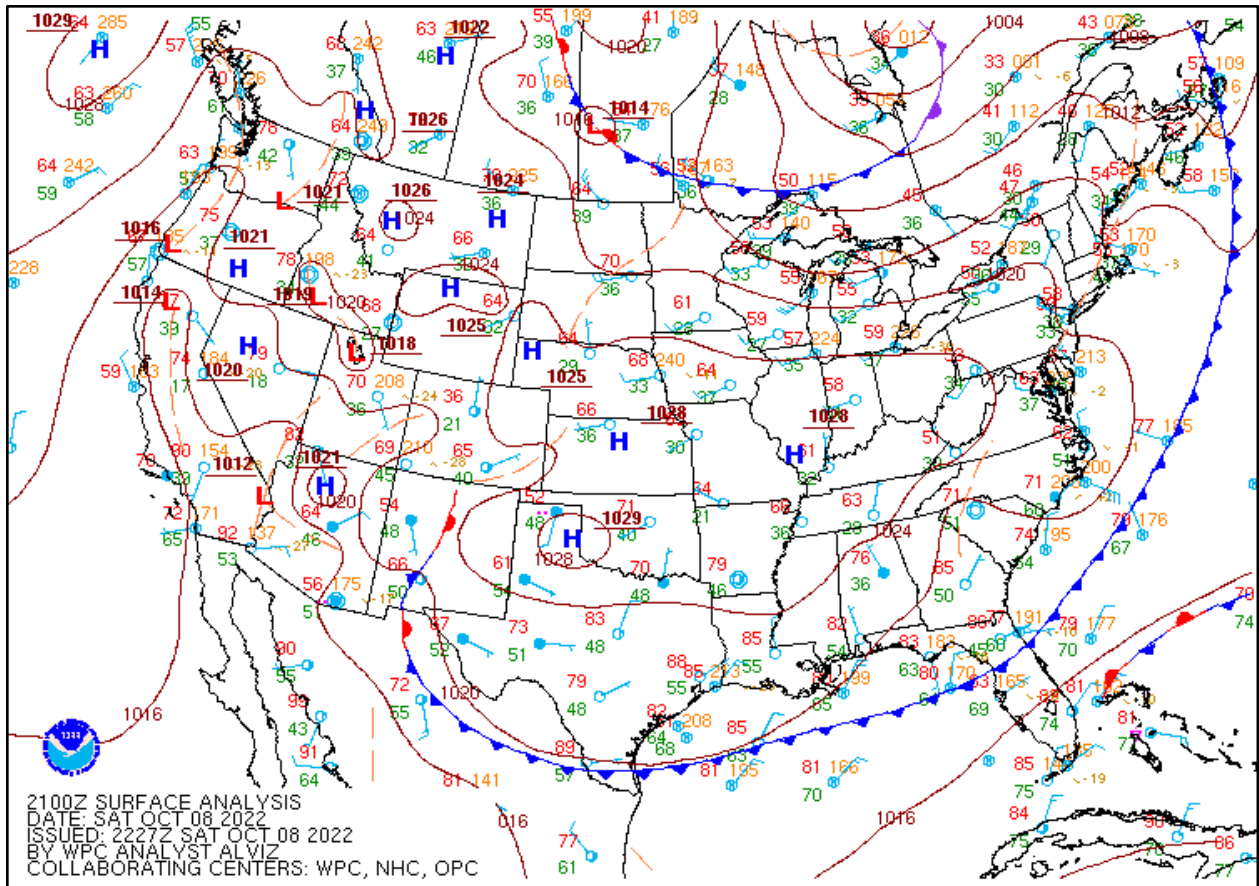


Figure 1-33: NOAA Surface Analysis at 7:00 PM CDT October 8, 2022

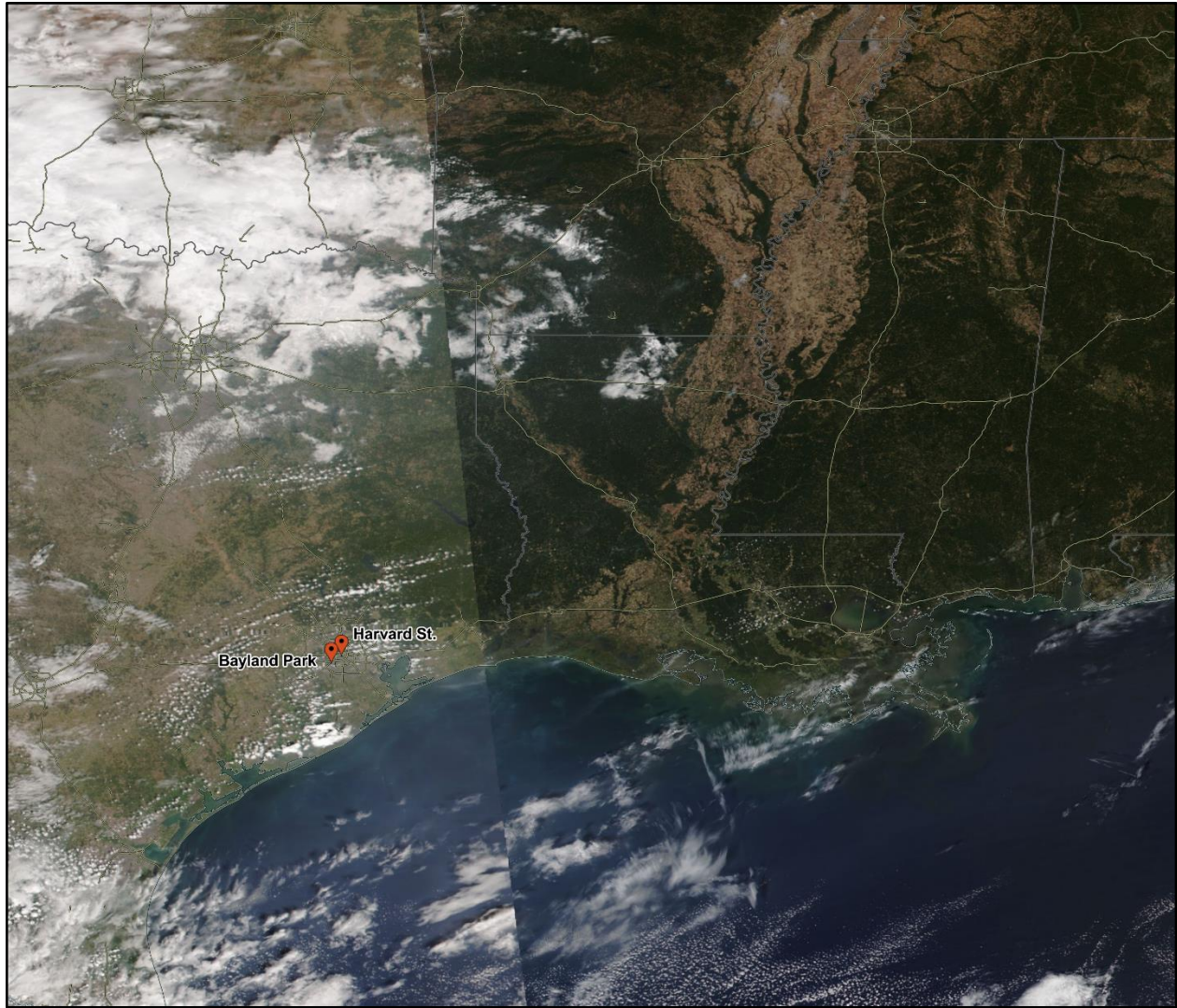


Figure 1-34: NOAA-20 VIIRS True Color Satellite Imagery on October 8, 2022

1.4 FIRES INFLUENCING EXCEEDANCES IN THE HGB AREA

During the June through October 2022 period, there were fire regions in Texas, Louisiana, Alabama, and Mississippi with wildfires that affected the HGB area. The wildfire locations and corresponding dates are: the area between Galveston Bay and Beaumont-Port Arthur on June 20 (see Figure 1-35: *Location of Fire That Impacted HGB on June 20, 2022*); East of Centerville, Texas and Northwest Louisiana on September 13 (see Figure 1-36: *Location of Fires That Impacted HGB on September 13, 2022*); Southeast and central east Alabama on September 21 (see Figure 1-37: *Location of Fires That Impacted HGB on September 21, 2022*); and northern Louisiana and western Mississippi on October 8, 2022 (see Figure 1-38: *Location of Fires That Impacted HGB on October 8, 2022*). Table 1-2: *Wildfires That Impacted HGB Area* contains additional information on these fires.

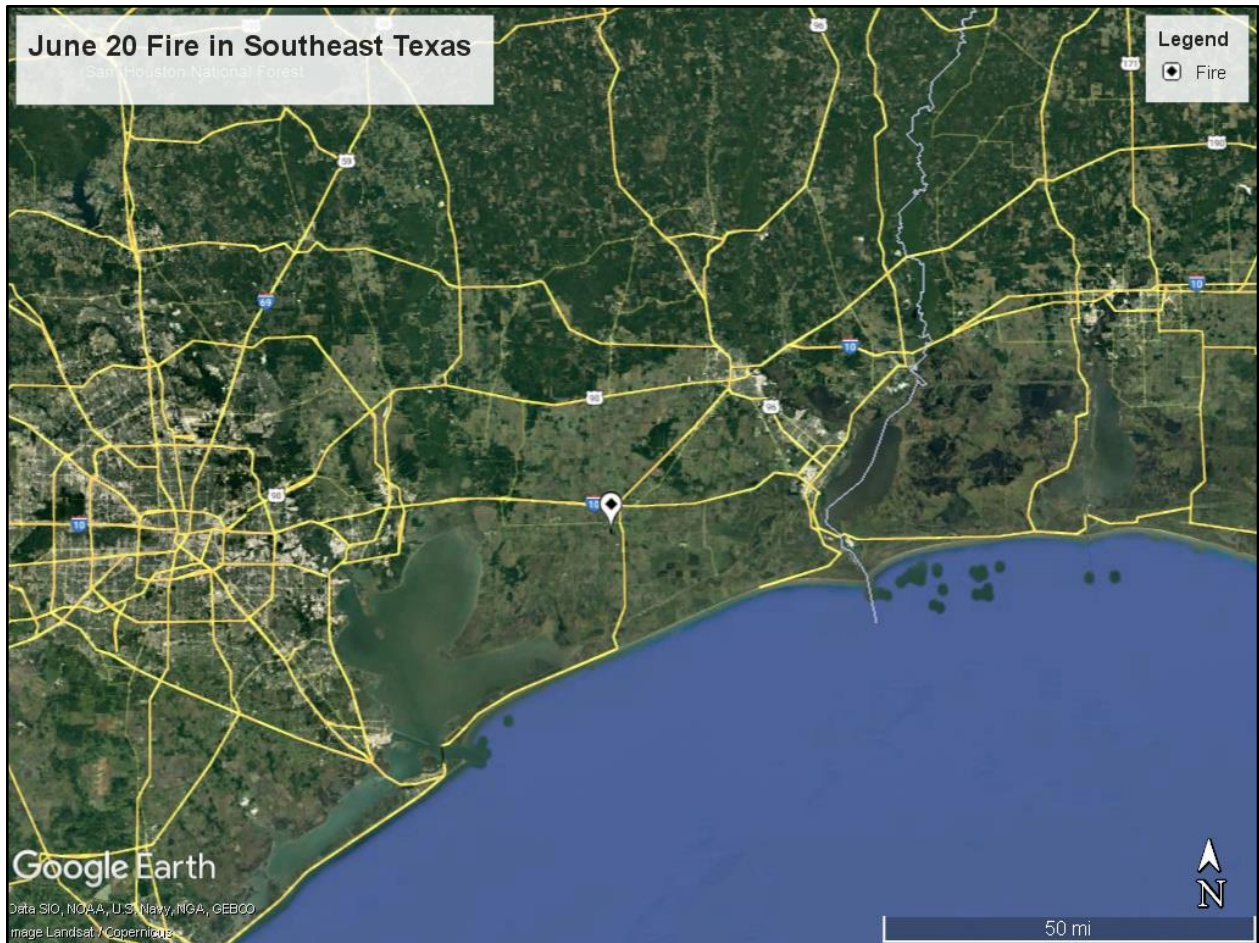


Figure 1-35: Location of Fire That Impacted HGB on June 20, 2022

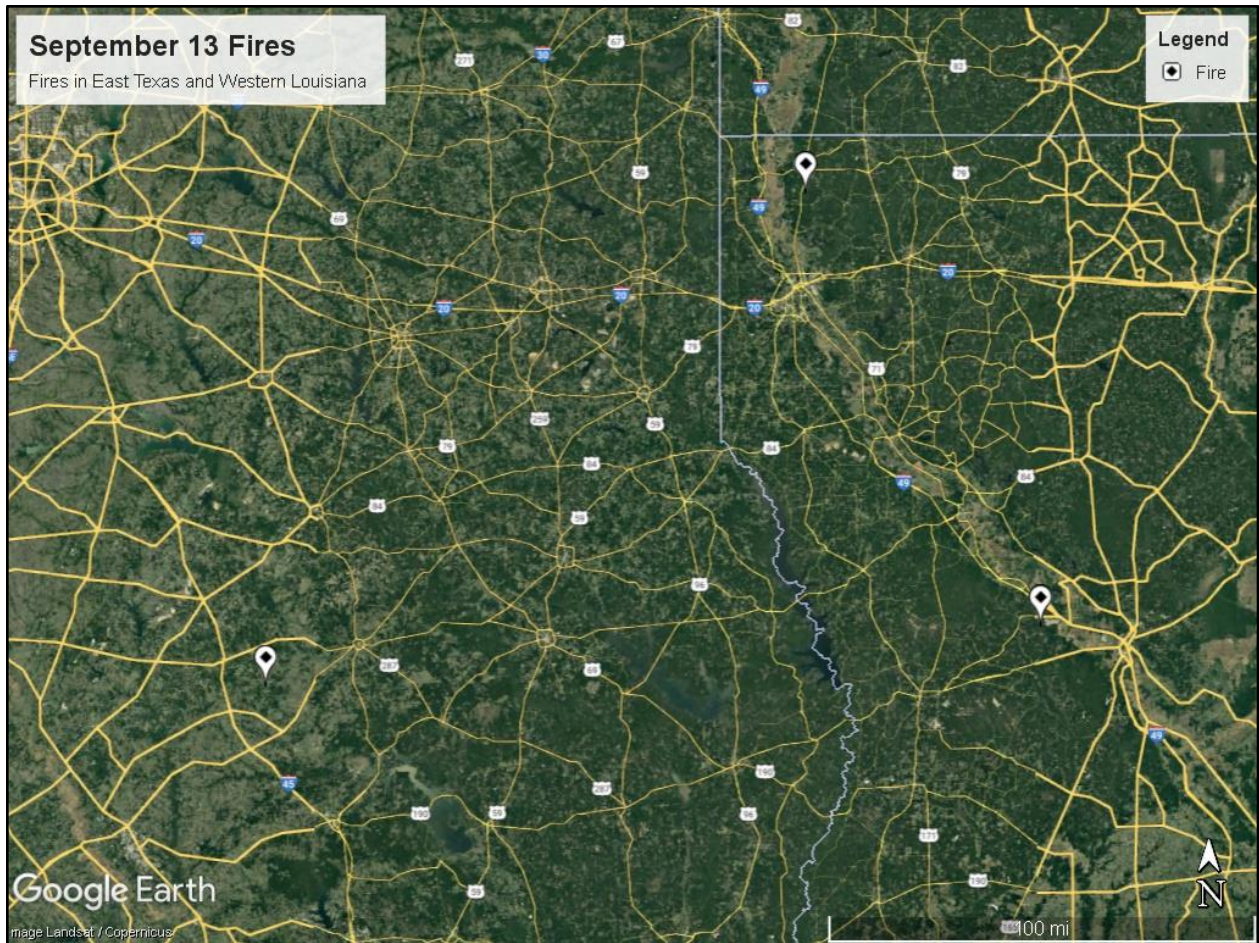


Figure 1-36: Location of Fires That Impacted HGB on September 13, 2022

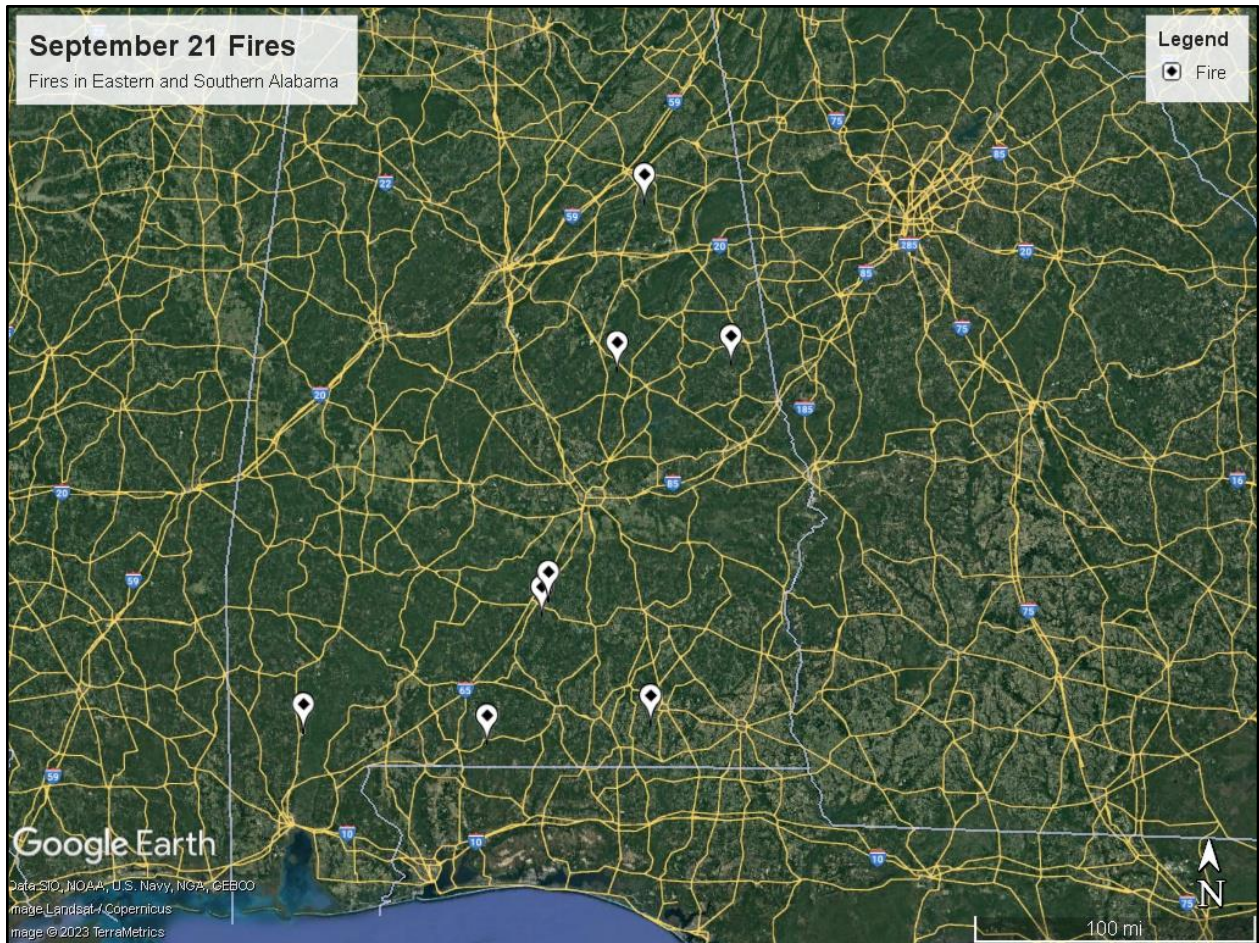


Figure 1-37: Location of Fires That Impacted HGB on September 21, 2022

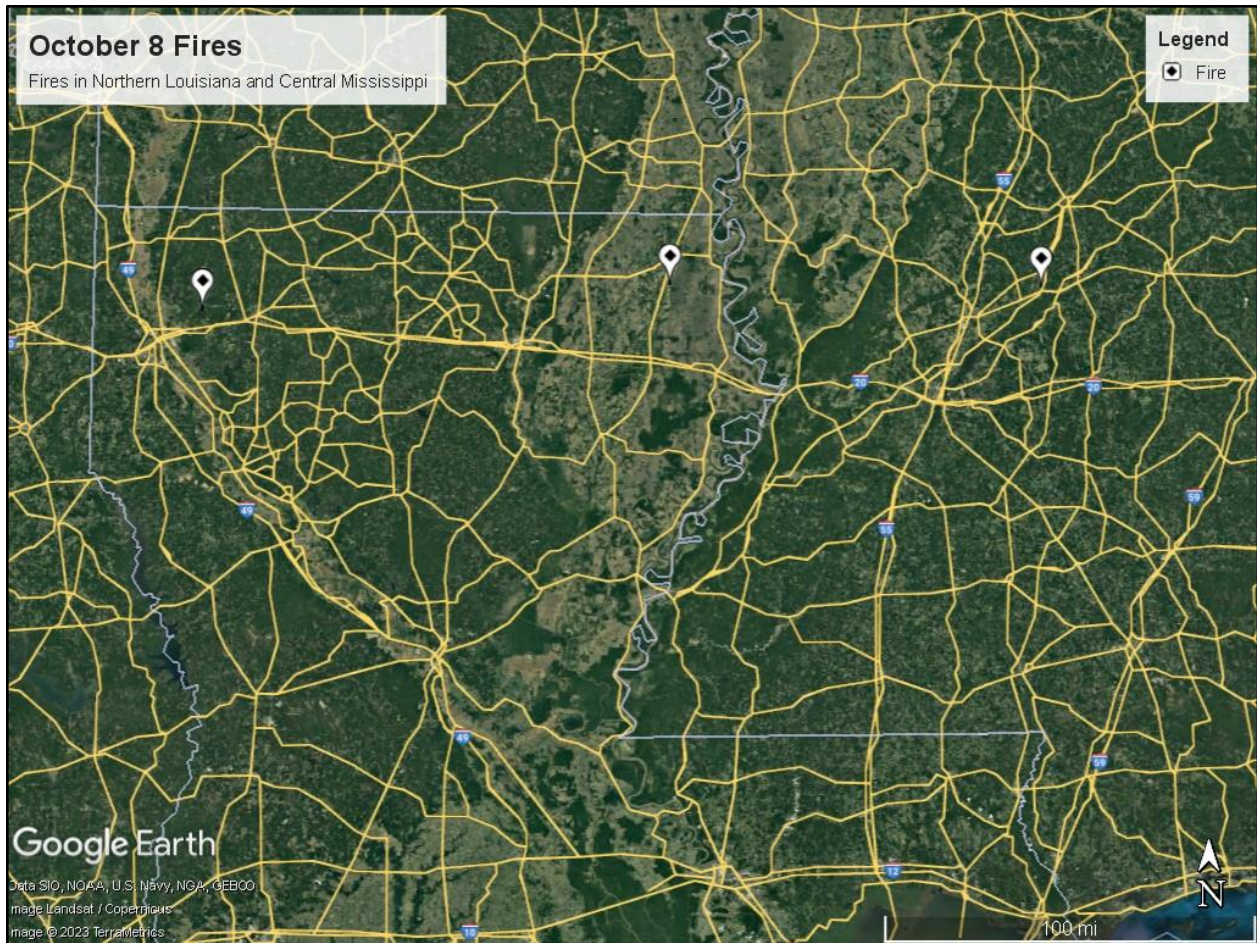


Figure 1-38: Location of Fires That Impacted HGB on October 8, 2022

Table 1-2: Wildfires That Impacted HGB Area

Wildfire	State	Date	Reference Latitude	Reference Longitude
June 20 Fire	Texas	6/20/2022	29.7715	-94.4041
September 13 Fire A	Louisiana	9/10/22 through 9/12/22	32.8268	-93.7022
September 13 Fire B	Louisiana	9/10/22 through 9/12/22	31.169	-95.8228
September 13 Fire C	Louisiana	9/10/22 through 9/12/22	31.3701	-92.7896
September 21 Fire A	Alabama	9/17/22 through 9/20/22	33.0321	-85.4627
September 21 Fire B	Alabama	9/17/22 through 9/20/22	31.113	-86.8972
September 21 Fire C	Alabama	9/17/22 through 9/20/22	31.7652	-86.5814
September 21 Fire D	Alabama	9/17/22 through 9/20/22	31.1497	-87.9844

Wildfire	State	Date	Reference Latitude	Reference Longitude
September 21 Fire E	Alabama	9/17/22 through 9/20/22	33.8452	-85.9866
September 21 Fire F	Alabama	9/17/22 through 9/20/22	32.9977	-86.1451
September 21 Fire G	Alabama	9/17/22 through 9/20/22	31.2215	-85.9347
September 21 Fire H	Alabama	9/17/22 through 9/20/22	31.841	-86.5433
October 8 Fire A	Louisiana	10/5/22 through 10/7/22	32.62738	-93.5393
October 8 Fire B	Louisiana	10/5/22 through 10/7/22	32.7138	-89.7085
October 8 Fire C	Mississippi	10/5/22 through 10/7/22	32.73425	-91.4053

CHAPTER 2: EXCEPTIONAL EVENT REQUIREMENTS FOR STATES

2.1 RELEVANT REGULATORY DOCUMENTS

The United States (U.S.) Environmental Protection Agency (EPA) has provided several documents that address exceptional event demonstration requirements, including:

- the 2016 revisions to the 2007 Exceptional Events Rule (EER) (U.S. EPA, 2016a);
- “Guidance on the Preparation of Exceptional Events Demonstrations for Wildfire Events that May Influence Ozone Concentrations” (U.S. EPA, 2016b); and
- “2016 Revisions to the Exceptional Events Rule: Update to Frequently Asked Questions” (U.S. EPA, 2020).

2.2 REQUIREMENTS FOR AN EXCEPTIONAL EVENT

On October 3, 2016, the EPA revised its EER (40 Code of Federal Regulations (CFR) §50.14(c)(3)), to specify six fundamental elements that a state’s demonstration must contain. Those elements and the parts of this demonstration that fulfill those requirements are shown in Table 2-1: *40 CFR §50.14(c)(3) Exceptional Event Demonstration Requirements*.

Table 2-1: 40 CFR §50.14(c)(3) Exceptional Event Demonstration Requirements

40 CFR §50.14(c)(3) Requirement	Demonstration Chapter
A narrative conceptual model that describes the event(s) causing the exceedance or violation and a discussion of how emissions from the event(s) led to the exceedance or violation at the affected monitor(s).	Chapter 1.3
A demonstration that the event affected air quality in such a way that there exists a clear causal relationship between the specific event and the monitored exceedance or violation.	Chapter 1.2, Chapter 1.3, Chapter 3
Analyses comparing the claimed event-influenced concentration(s) to concentrations at the same monitoring site at other times. The Administrator shall not require a State to prove a specific percentile point in the distribution of data.	Chapter 1.2
A demonstration that the event was both not reasonably controllable and not reasonably preventable.	Chapter 2.3
A demonstration that the event was caused by human activity that is unlikely to recur at a particular location or was a natural event.	Chapter 2.4
Documentation that the submitting air agency followed the public comment process.	Chapter 2.5, Appendix A

The Texas Commission on Environmental Quality (TCEQ) documents compliance with the EER mitigation requirements in 40 CFR §51.930 with respect public notification, public education, and implementation of appropriate measures to protect health in Table 2-2: *40 CFR §51.930 Exceptional Event Demonstration Requirements*.

Table 2-2: 40 CFR §51.930 Exceptional Event Demonstration Requirements

40 CFR §51.930 Requirement	Demonstration Chapter
Provide for prompt public notification whenever air quality concentrations exceed or are expected to exceed an applicable ambient air quality standard.	Chapter 2.6.1
Provide for public education concerning actions that individuals may take to reduce exposures to unhealthy levels of air quality during and following an exceptional event.	Chapter 2.6.2
Provide for public education concerning actions that individuals may take to reduce exposures to unhealthy levels of air quality during and following an exceptional event.	Chapter 2.6.3

2.3 THE EVENT IS NOT REASONABLY CONTROLLABLE OR PREVENTABLE

The June 20, 2022 fire occurred in the area between Galveston Bay and Beaumont-Port Arthur, Texas. The TCEQ is not aware of any evidence clearly demonstrating that prevention or control efforts beyond those made would have been reasonable. Therefore, emissions from these fires were not reasonably controllable or preventable. The fires occurring outside the State of Texas (Louisiana, Mississippi, and Alabama) were not reasonably controllable or preventable by the State of Texas and are essentially treated as wildfires in this demonstration. The states of Louisiana, Alabama and Mississippi maintain robust programs aimed at responding to wildfires and preventing future ones.

Information on the Louisiana Department of Agriculture and Forestry is available at <https://www.ldaf.state.la.us/forestry/>

Information on the Alabama Forestry Commission is available at <https://forestry.alabama.gov/>

Information on the Mississippi Forestry Commission is available at <https://www.mfc.ms.gov/wildfires/>

2.4 THE EVENT IS NOT LIKELY TO RECUR OR IS NATURAL

The wildfires determined to have caused the subject ozone exceedance were a result of both natural causes (lightning strikes) and human actions. Once an area has been burned out, the likelihood of that area burning again declines for an extended period (assuming that the fire was completely extinguished), and the biomass available to burn is significantly reduced such that a fire in the same area in the next several years would likely yield significantly fewer emissions. Any of the fires attributable to human causes that occur outside of Texas are not controllable or preventable by the State of Texas.

2.5 THE TCEQ FOLLOWED THE PUBLIC COMMENT PROCESS

The draft demonstration is being provided by the TCEQ for stakeholders and the public to comment for 30 days as required by federal rules. All comments received will be included in the final version of this demonstration.

2.6 MITIGATION REQUIREMENTS OF 40 CFR §51.930

The EER (40 CFR §51.930) requires that “a State requesting to exclude air quality data due to exceptional events must take appropriate and reasonable actions to protect public health from exceedances or violations of the national ambient air quality standards.” The TCEQ addresses each of the specific requirements individually below.

2.6.1 Prompt Public Notification

The first mitigation requirement is to “provide for prompt public notification whenever air quality concentrations exceed or are expected to exceed an applicable ambient air quality standard.” The TCEQ provided (and continues to provide) ozone, Fine Particulate Matter (PM_{2.5}), and Particulate Matter less than or equal to 10 microns in diameter (PM₁₀) Air Quality Index (AQI) forecasts for the current day and the next three days for 14 areas in Texas including the Houston-Galveston-Brazoria (HGB) area. These forecasts are available to the public on the [Today’s Texas Air Quality Forecast](#) webpage of the TCEQ website (http://www.tceq.texas.gov/airquality/monops/forecast_today.html), and on the EPA’s [AirNow](#) website (<http://airnow.gov/>).

The TCEQ provides near real-time hourly ozone measurements from monitors across the state, including the HGB area, which the public may access on the [Current Ozone Levels](#) page of the TCEQ website (http://www.tceq.texas.gov/cgi-bin/compliance/monops/select_curlev.pl). The TCEQ also publishes an AQI Report for many Texas metropolitan areas including the HGB area on the [AQI and Data Reports](#) page of the TCEQ website (<https://www.tceq.texas.gov/airquality/monops/data-reports>), which displays current and historical daily AQI measurements. Finally, the TCEQ publishes daily updates to its air quality forecast to interested parties through electronic mail and Twitter. Any person wishing to receive these updates may register on the [Air Quality Forecast and Ozone Action Day Alerts](#) page on the TCEQ website (http://www.tceq.texas.gov/airquality/monops/ozone_email.html). These measures provide daily and near real-time notification to the public, including the media, of current, expected, and changing air quality conditions.

2.6.2 Public Education

The second mitigation requirement is to “provide for public education concerning actions that individuals may take to reduce exposures to unhealthy levels of air quality during and following an exceptional event.” Through its website, the TCEQ provides the public with technical, health, personal activity, planning, and legal information and resources concerning ozone pollution. Besides its website, the TCEQ publishes daily updates to its air quality forecast to interested parties through electronic mail and Twitter to provide daily and near real-time notification to the public of current, expected, and changing air quality conditions.

The TCEQ maintains an ozone fact sheet (<http://www.tceq.texas.gov/airquality/monops/ozonefacts.html>), which provides important information regarding the health effects of ozone, steps that individuals can take to limit ozone formation, and actions they may wish to take to reduce their exposure to higher levels of ozone. A hyperlink to this fact sheet is located on the TCEQ daily air quality forecast page. The fact sheet points individuals towards

additional health-related information from the Centers for Disease Control, the Texas Department of State Health Services, and the EPA.

The TCEQ's main [Air](http://www.tceq.texas.gov/agency/air_main.html) webpage (http://www.tceq.texas.gov/agency/air_main.html) provides air quality information on topics such as advisory groups, emissions inventories, air quality modeling and data analysis, scientific field studies, state implementation plan (SIP) revisions, air permits, rules, air monitoring data, and how to file complaints.

The TCEQ provides a specific [Air Pollution from Ozone](http://www.tceq.texas.gov/airquality/sip/criteria-pollutants/sip-ozone) webpage (<http://www.tceq.texas.gov/airquality/sip/criteria-pollutants/sip-ozone>), which provides the latest information on air quality planning activities by both the TCEQ and the EPA.

The TCEQ's website provides a hyperlink to the Texas [AirNow](https://www.airnow.gov/) website operated by the EPA (<https://www.airnow.gov/>). This website links the public to additional information regarding health effects of ozone, strategies for reducing one's exposure to ozone, and actions that individuals can take to reduce pollution levels.

The Texas Department of Transportation sponsors the public education and awareness through the [Drive Clean Across Texas](http://www.drivecleanacrosstexas.org) campaign (<http://www.drivecleanacrosstexas.org>). The campaign raises awareness about the impact of vehicle emissions on air quality and motivates drivers to take steps to reduce air pollution. The campaign's activities are concentrated during the summer months when ozone levels rise.

The TCEQ sponsors the [Take Care of Texas](http://takecareoftexas.org/air-quality) program (<http://takecareoftexas.org/air-quality>), which addresses air quality and provides the public with proactive steps to reduce air pollution particularly on days when air quality forecasts are issued predicting greater potential for ozone formation.

2.6.3 Implementation of Measures to Protect Public Health

The HGB area is designated as moderate nonattainment for the 2015 eight-hour ozone NAAQS and the U.S. EPA reclassified the HGB area to severe nonattainment for the 2008 eight-hour ozone NAAQS, effective November 7, 2022. As a result of this, the TCEQ is required to submit severe attainment demonstration and reasonable further progress SIP revisions to the EPA by May 7, 2024. In 2020, the TCEQ adopted a revised attainment demonstration SIP revision for the HGB area for the 2008 eight-hour ozone NAAQS. The HGB SIP Section 4.2 contains information on existing control measures. The SIP revision can be accessed via the link ([HGB Serious Attainment Demonstration SIP Revision for 2008 Ozone NAAQS Adoption \(archive-it.org\) https://wayback.archive-it.org/https://www.tceq.texas.gov/assets/public/implementation/air/sip/hgb/hgb_serious_AD_SIP_19077SIP_adoption_web.pdf](https://wayback.archive-it.org/https://www.tceq.texas.gov/assets/public/implementation/air/sip/hgb/hgb_serious_AD_SIP_19077SIP_adoption_web.pdf)). More detailed information about the state's ozone reduction strategies can be found on the following webpages:

- [Control Ozone Pollution](http://www.tceq.texas.gov/airquality/stationary-rules/ozone), Strategies for Stationary Sources (<http://www.tceq.texas.gov/airquality/stationary-rules/ozone>);
- [Controlling On-Road Mobile Source Vehicle Emissions](http://www.tceq.texas.gov/airquality/mobilesource/mobile_source.html) (http://www.tceq.texas.gov/airquality/mobilesource/mobile_source.html)
- [Air Permitting](http://www.tceq.texas.gov/permitting/air) (<http://www.tceq.texas.gov/permitting/air>); and

- Texas Emissions Reduction Plan's [Emissions Reduction Incentive Grants](http://www.tceq.texas.gov/airquality/terp/erig.html) (<http://www.tceq.texas.gov/airquality/terp/erig.html>).

CHAPTER 3: CAUSAL RELATIONSHIP

The Texas Commission on Environmental Quality (TCEQ) completed analyses of meteorological, pollutant, and remote sensing data that support the conclusion that a clear causal relationship exists between surrounding wildfires and exceedances of the 2008 eight-hour ozone National Ambient Air Quality Standard (NAAQS) at the Houston Bayland Park and Houston Harvard Street monitoring sites in the Houston-Galveston-Brazoria (HGB) area on June 20, September 13, September 21, and October 8, 2022. The TCEQ's analysis of data at the Bayland Park and Harvard Street monitors indicates that wildfire emissions affected ground-level air quality in the HGB area.

3.1 PERIOD OF ANALYSIS

When considering the amount of data that states should use in an exceptional event demonstration, the United States (U.S.) Environmental Protection Agency (EPA) (2020, p. 14) notes that "For seasonal comparisons, an approvable demonstration will ideally include all available seasonal data from at least 5 years, if available." For this demonstration, the TCEQ used the data for 2017 through 2022, a five-year period. The TCEQ's monitoring from 2022 has not been certified and should be viewed as preliminary. Exceptions to this time-period will be noted on a case-by-case basis.

3.2 TIERED ANALYSIS

In its September 2016 guidance for exceptional event demonstrations related to wildfire events, the EPA introduced a tiered approach for addressing the causal relationship in a wildfire-caused ozone exceptional event demonstration.

"Tier 1 clear causal analyses should be used for wildfire events that cause clear ozone impacts in areas or during times of year that typically experience lower ozone concentrations and are thus simpler and less resource intensive than analyses for other events. Tier 2 clear causal analyses are appropriate when the impacts of the wildfire on ozone levels are less clear and require more supportive documentation than Tier 1 analyses. Tier 3 clear causal analyses should be used for events in which the relationship between the wildfire and the ozone exceedance or violation is more complicated than the relationship in a Tier 2 analysis, and thus would require more supportive documentation than Tier 2 analyses." (U.S. EPA, 2016a, p. 4).

As a result of discussions between the TCEQ and the EPA, this demonstration provides a Tier 3 analysis.

3.3 HAZARD MAPPING SYSTEM PLUME

As part of its Hazard Mapping System (HMS), the National Oceanic and Atmospheric Administration (NOAA) produces daily fire and smoke plume maps depicting the location of fires and smoke plumes detected by satellites (NOAA, 2003). The maps for June 20, September 13, September 21, and October 8 are shown below in Figure 3-1: *NOAA HMS Plume Map for June 20, 2022*, Figure 3-2: *NOAA HMS Plume Map for September 13, 2022*, Figure 3-3: *NOAA HMS Plume Map for September 21, 2022*, and Figure 3-4: *NOAA HMS Plume Map for October 8, 2022*. All four figures clearly show the presence of smoke plumes over the HGB area.

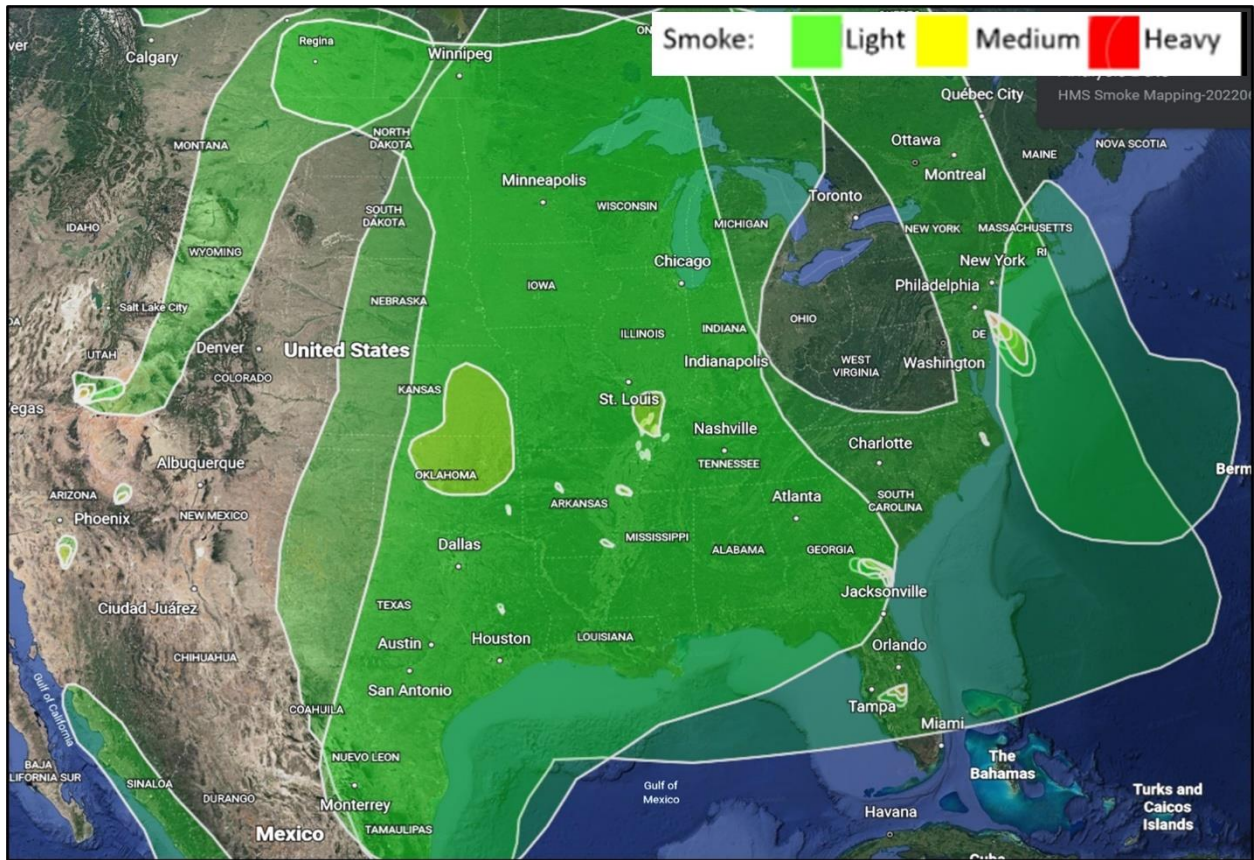


Figure 3-1: NOAA HMS Plume Map for June 20, 2022

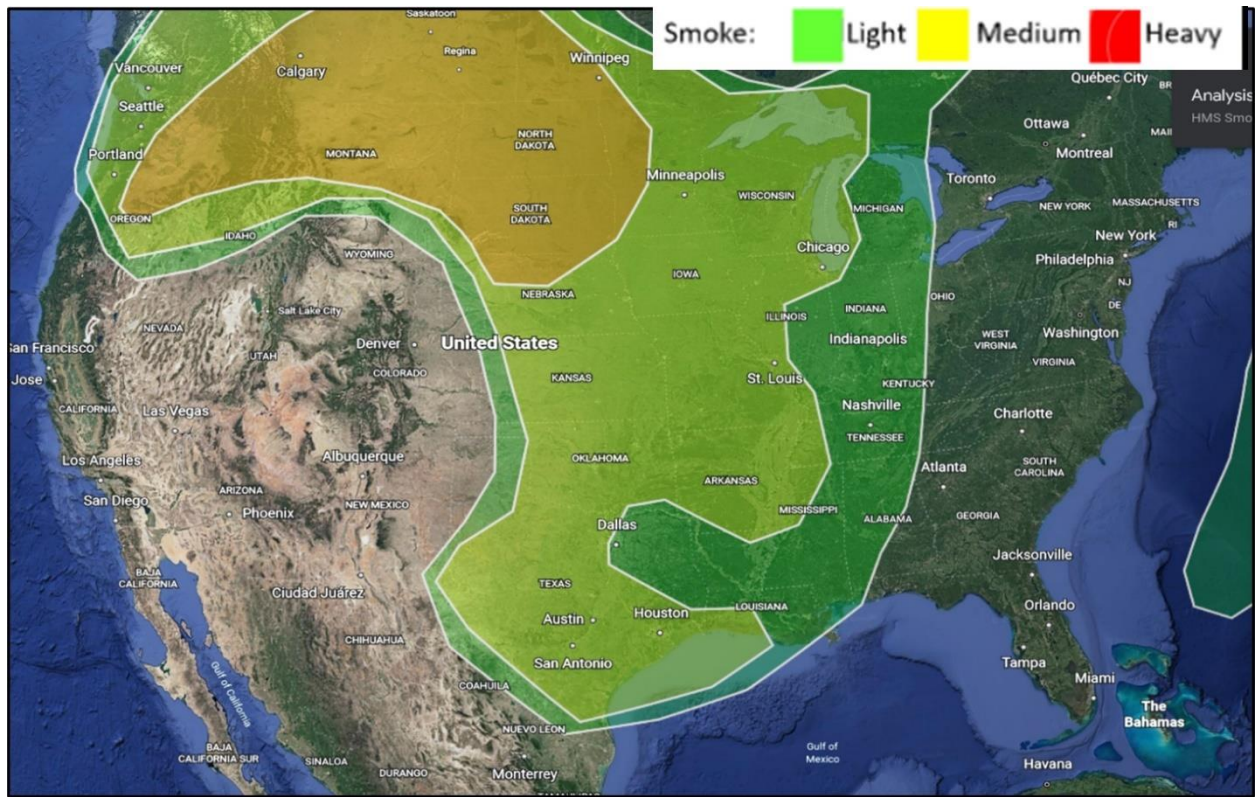


Figure 3-2: NOAA HMS Plume Map for September 13, 2022

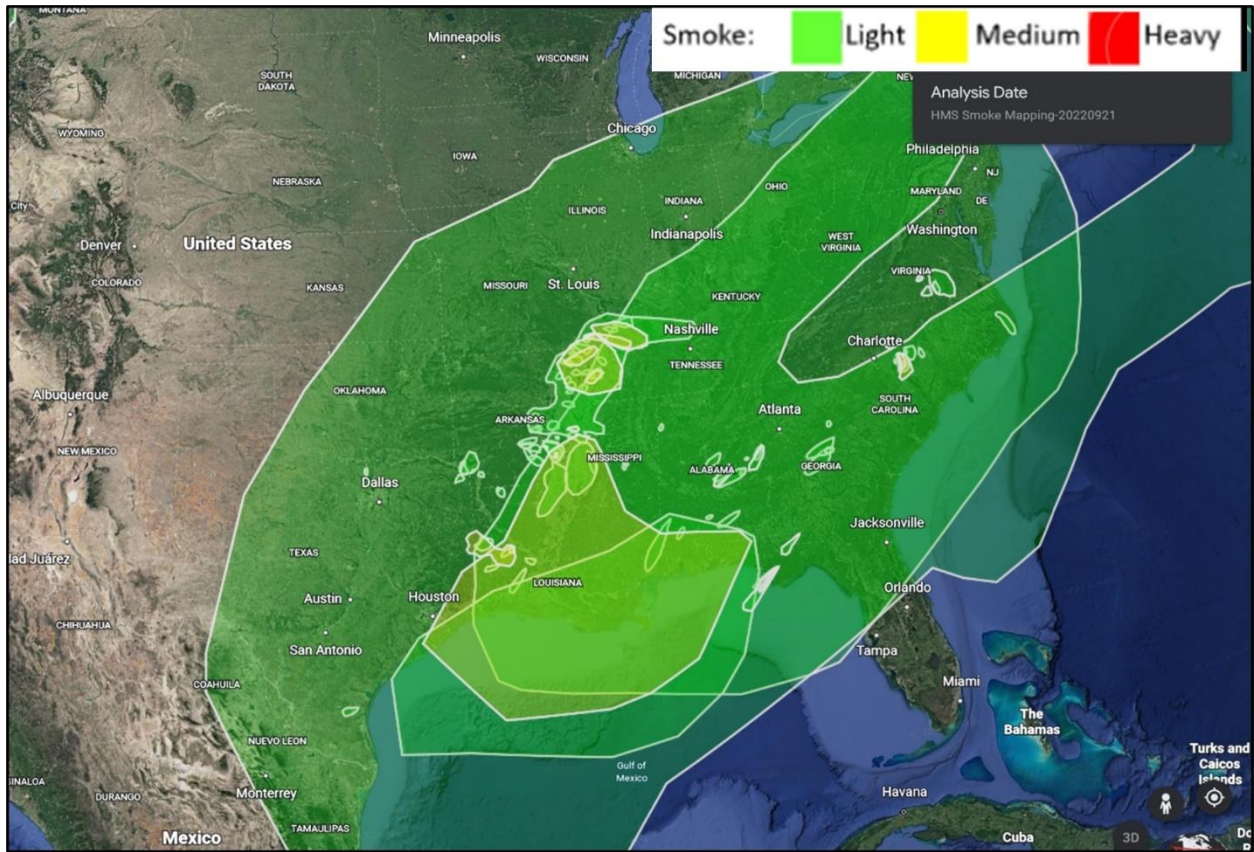


Figure 3-3: NOAA HMS Plume Map for September 21, 2022

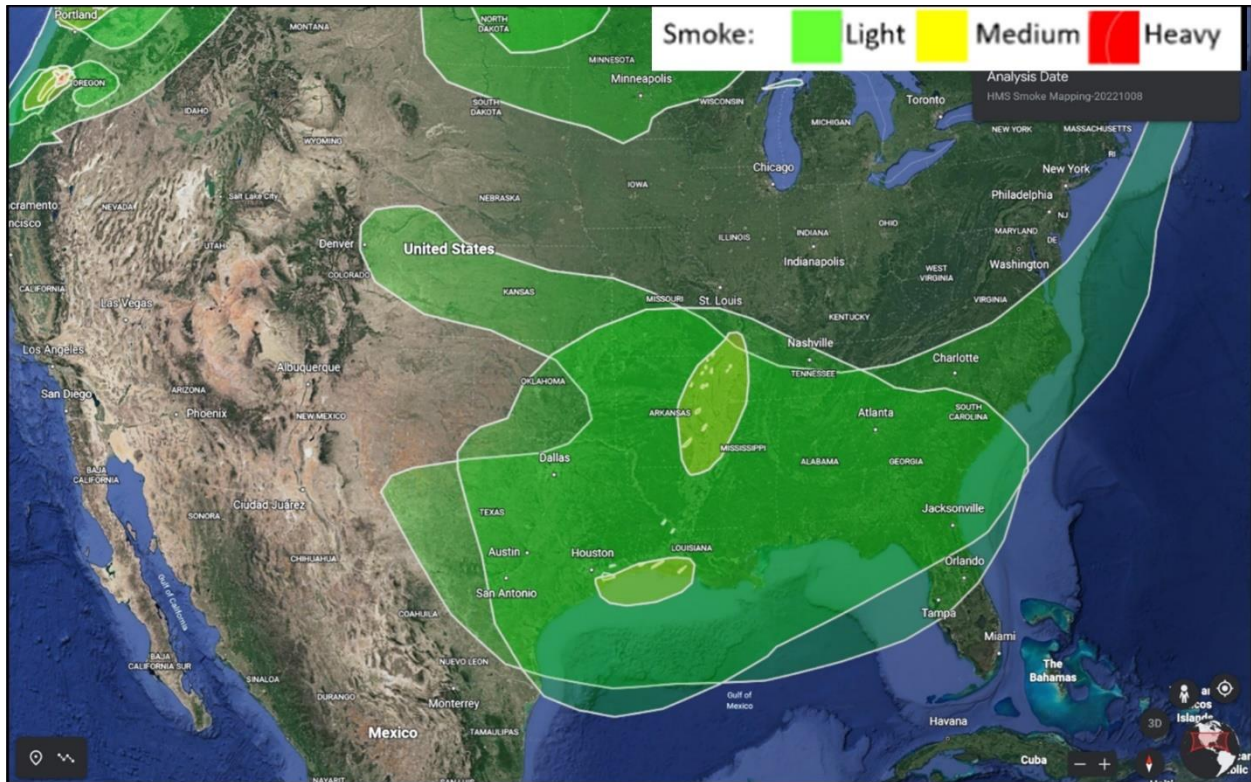


Figure 3-4: NOAA HMS Plume Map for October 8, 2022

3.4 TRUE COLOR SATELLITE IMAGERY SHOWS TRANSPORT TO HGB MONITORS

The TCEQ used satellite imagery available through the National Aeronautics and Space Administration’s (NASA) Worldview website (NASA, 2023) to analyze the transport of wildfire emissions from surrounding areas to the Harvard Street and Bayland Park monitors.

The Terra satellite uses five instruments to observe Earth’s atmosphere, ocean, land, snow and ice, and energy budget. Like Suomi-NPP, Terra follows a circular sun-synchronous polar orbit that takes it from north to south (on the daylight side of the Earth) every 99 minutes. One of Terra’s instruments, the Moderate Resolution Imaging Spectroradiometer (MODIS) has imaging bands very sensitive to fires. The bands can distinguish flaming from smoldering burns and provide more accurate estimates of the amounts of aerosols and gases that fires release into the atmosphere. With its 2,330-kilometer-wide imaging swath, MODIS captures every point on the earth’s surface every one or two days.

The smoke and emissions transported from the Texas Gulf Coast to the Harvard Street and Bayland Park monitors on June 20, 2022 are shown in Figure 3-5: *Terra Modis True Color Imagery on June 20, 2022.*

The smoke and emissions transported from northwest Louisiana to the Harvard Street and Bayland Park monitors are shown in Figure 3-6: *Terra Modis True Color Imagery on September 13, 2022.*

The smoke and emissions transported from southeast and central-east Alabama to the Harvard Street and Bayland Park monitors are shown in Figure 3-7: *Terra Modis True Color Imagery on September 21, 2022.*

The smoke and emissions transported from Louisiana and western Mississippi wildfire smoke to the Harvard Street and Bayland Park monitor in Figure 3-8: *Terra Modis True Color Imagery on October 8, 2022.*

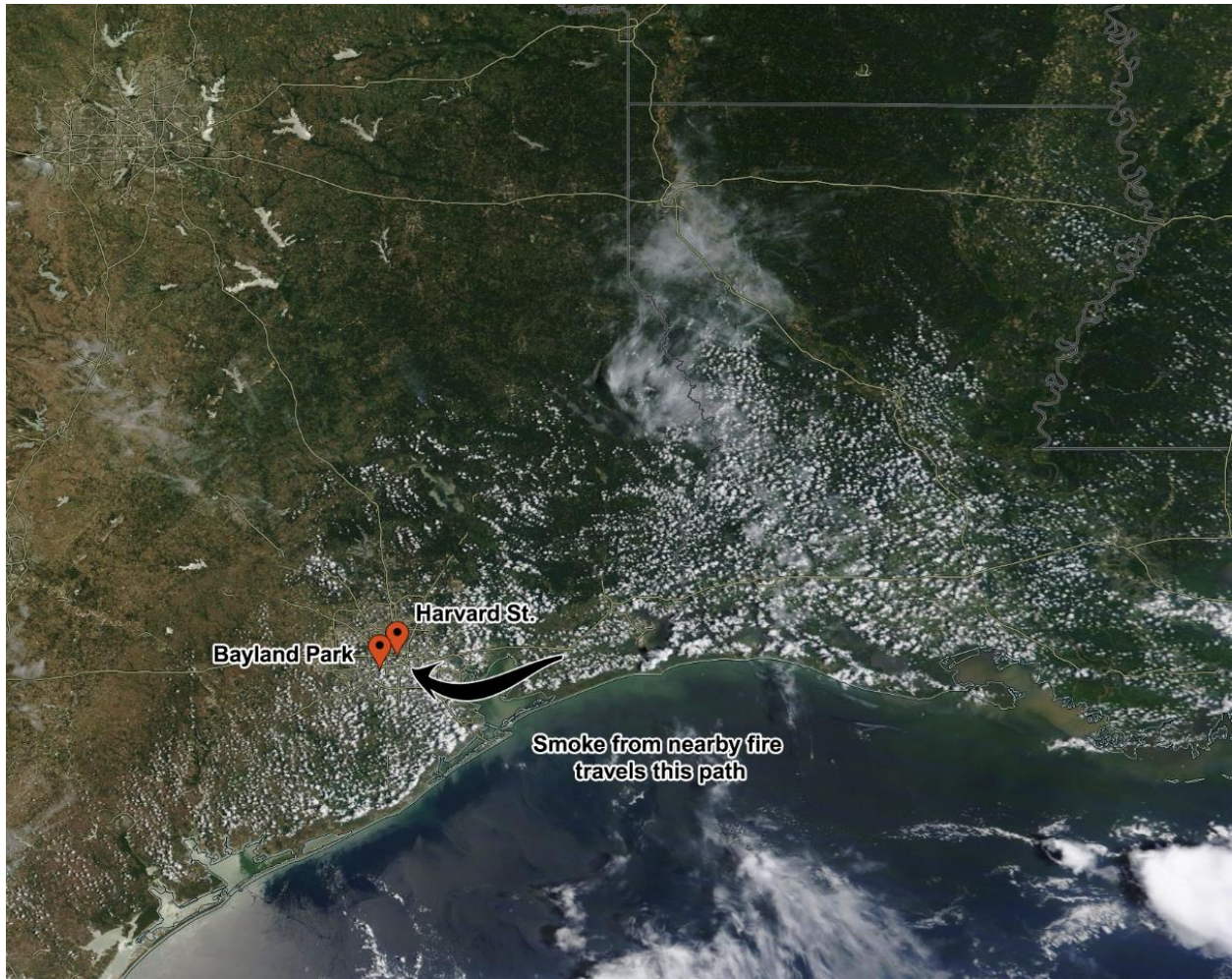


Figure 3-5: Terra Modis True Color Imagery on June 20, 2022

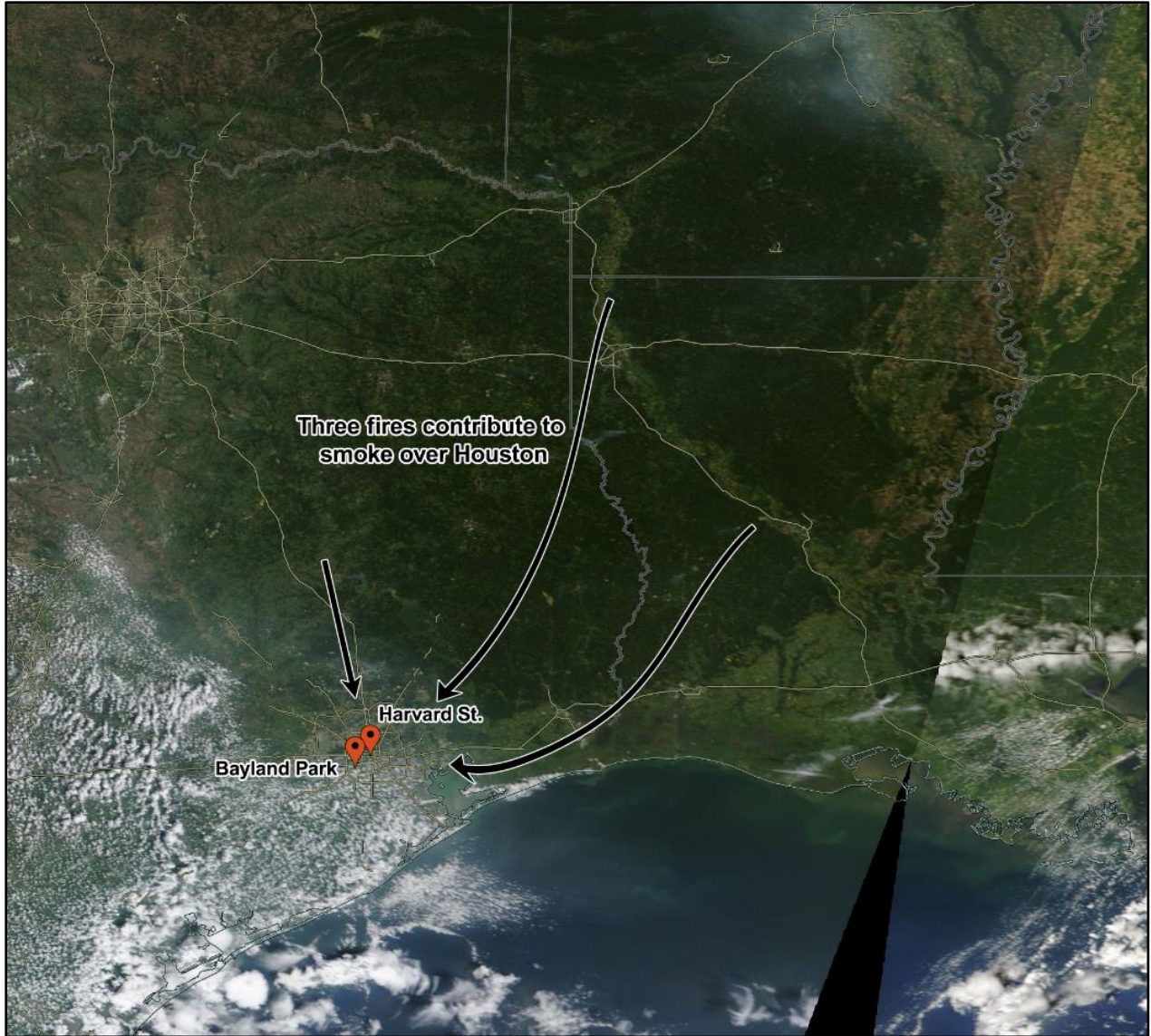


Figure 3-6: Terra Modis True Color Imagery on September 13, 2022

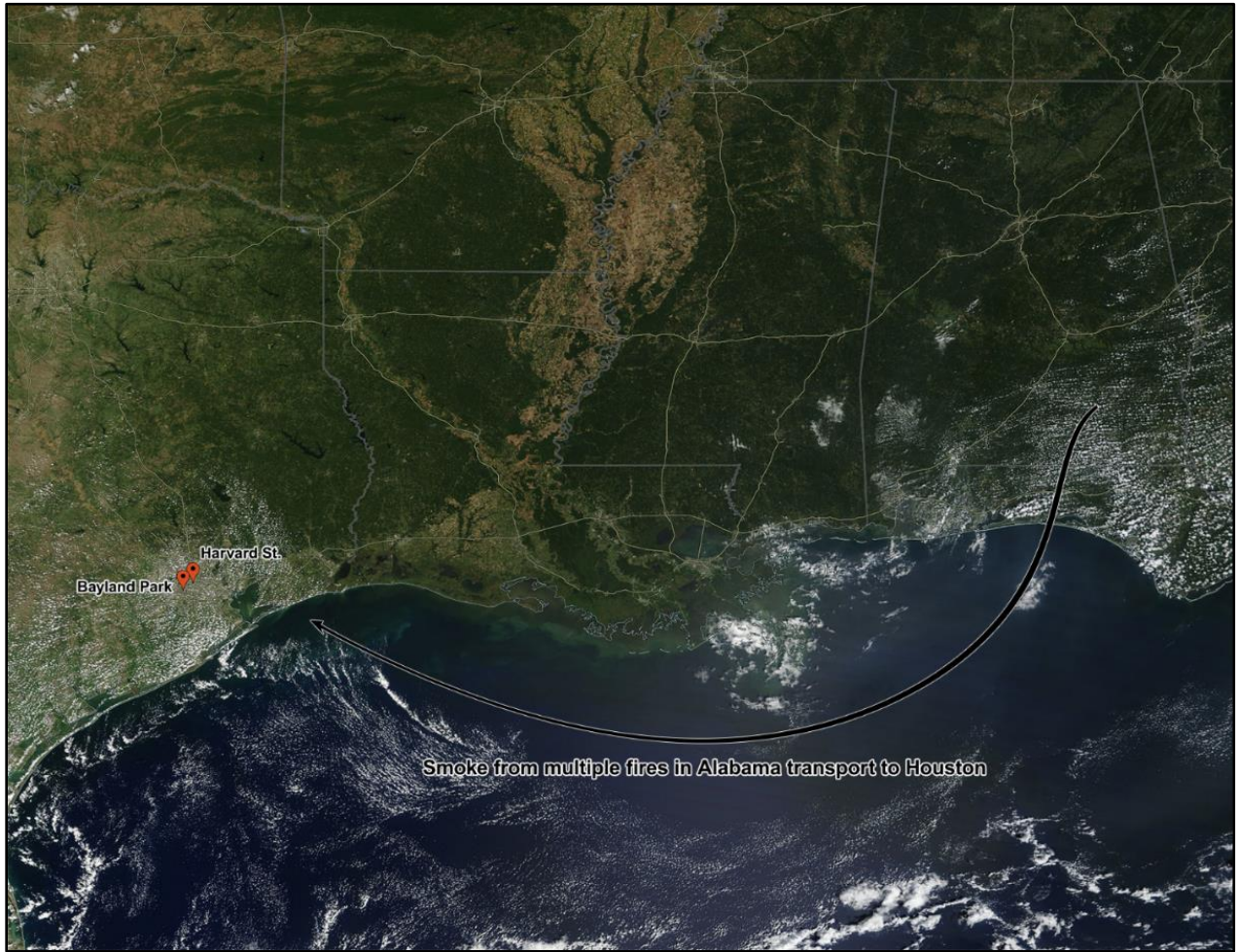


Figure 3-7: Terra Modis True Color Imagery on September 21, 2022

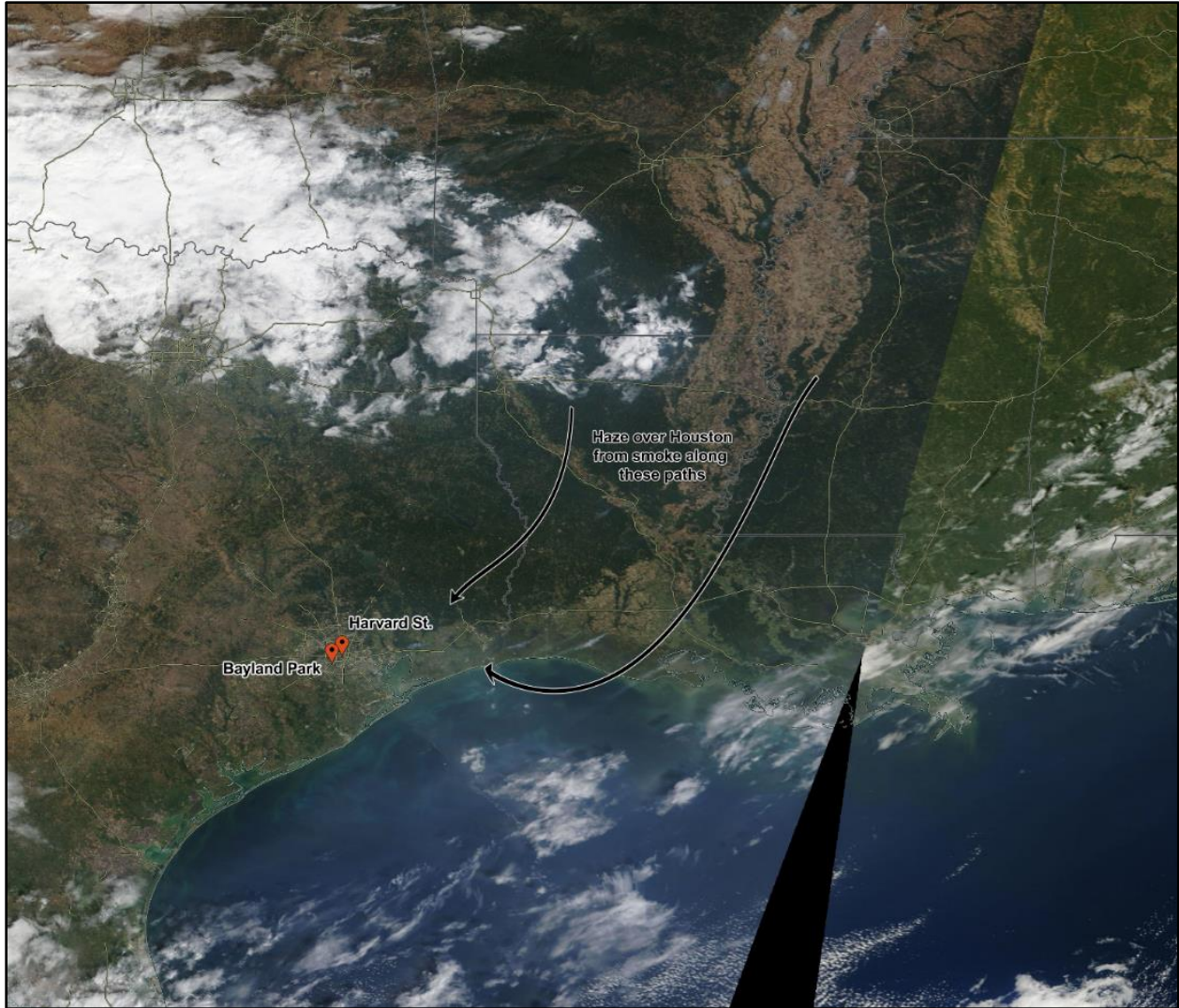


Figure 3-8: Terra Modis True Color Imagery on October 8, 2022

3.5 AEROSOL OPTICAL DEPTH MEASUREMENTS

Aerosol optical depth (AOD) is a unitless measure of extinction of radiation by particles in the atmosphere, such as dust, smoke, and other constituents of air pollution, known as aerosols. Aerosols are a complex mixture of many atmospheric compounds, which can have adverse human health effects when breathed. In addition, constituents in aerosols, such as nitrogen compounds and volatile organic compounds (VOC) can contribute to ozone formation, especially downwind of fires.

Aerosol particles block radiation by absorbing or scattering specific wavelengths. AOD can be determined remotely using instruments on the ground, by observing incoming solar radiation, or satellites, by observing radiation emitted or reflected from the Earth's surface. Use of instruments to detect aerosols from a distance is referred to as "remote sensing," in contrast to methods that directly sample discrete parcels of air to determine their constituents.

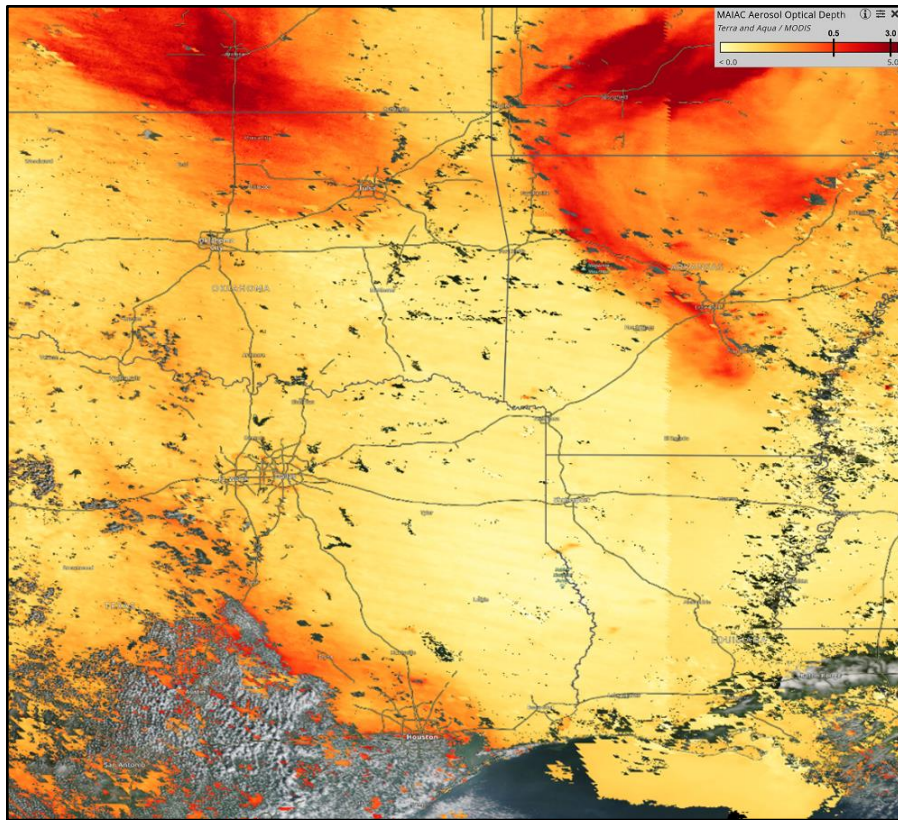


Figure 3-10: MAIAC Combined AOD on September 13, 2022

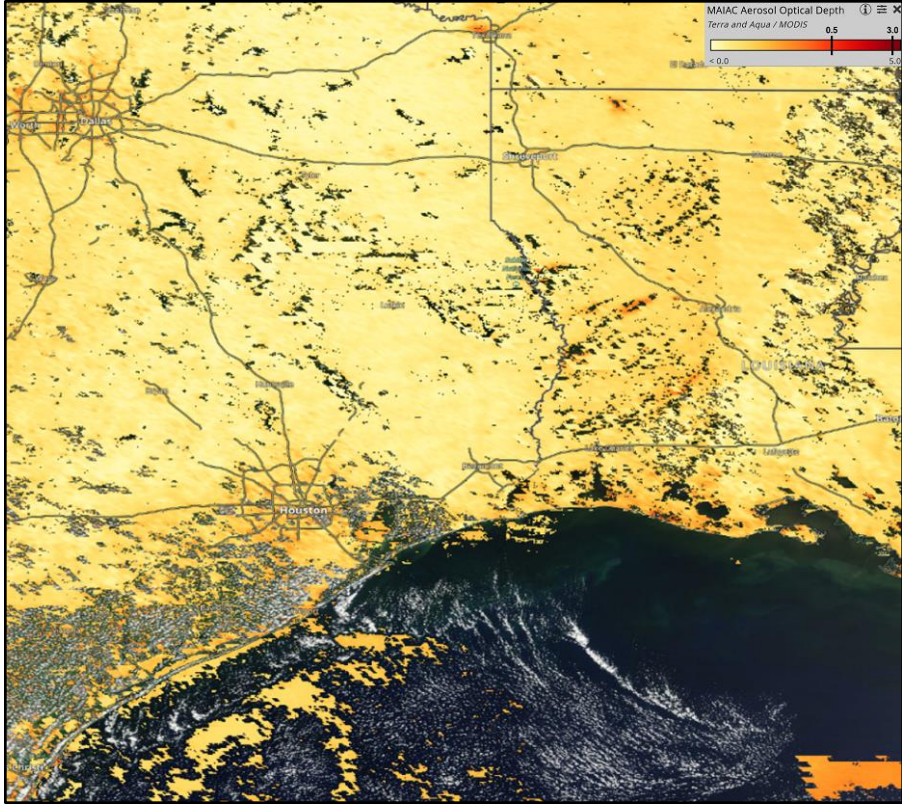


Figure 3-11: MAIAC Combined AOD on September 21, 2022

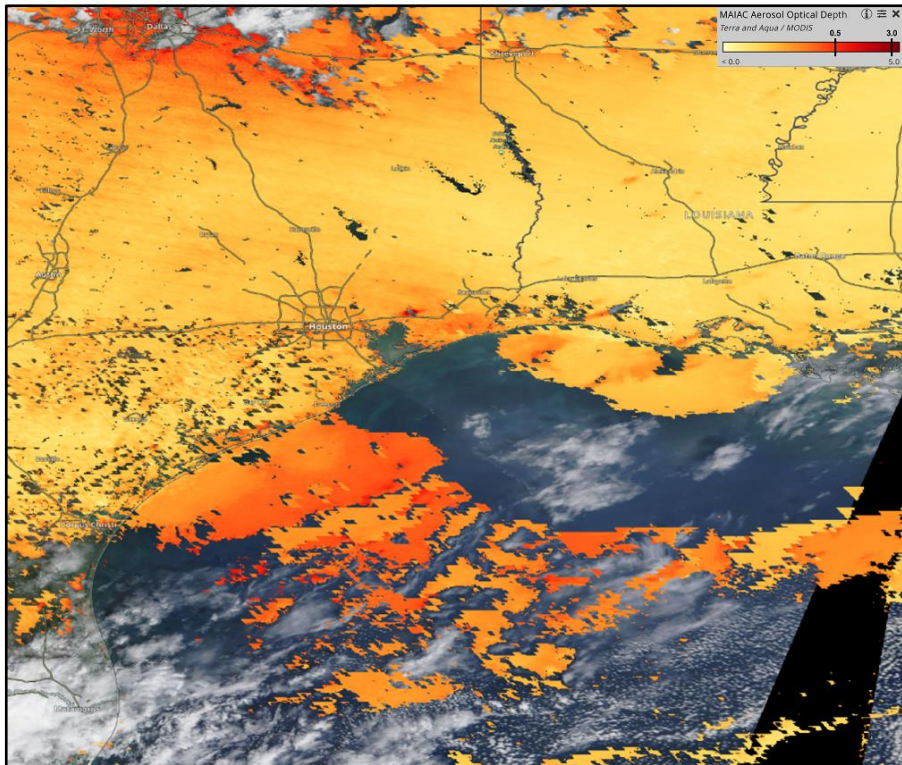


Figure 3-12: MAIAC Combined AOD on October 8, 2022

3.6 WILDFIRE EMISSIONS TRANSPORTED TO BAYLAND PARK AND HARVARD STREET MONITORS

As shown by remote-sensing data presented above and trajectory analysis presented below, wildfire emissions from surrounding areas were transported to the Bayland Park and Harvard Street monitors and caused exceedances on June 20, September 13, September 21, and October 8, 2022.

The TCEQ generated a series of backward (in time) air parcel trajectories that show how wildfire emissions were transported to the monitors. The NOAA HYSPLIT software (NOAA, 2023) (Stein, et al., 2015) was used to compute the trajectories from the Bayland Park and Harvard Street monitors. If the trajectory shows air moved from the wildfire locations toward the vicinity of a monitor, it is valuable evidence that the air quality around the monitor was likely affected by the fire.

The meteorological input to HYSPLIT was a subset of model output from NOAA's North American Mesoscale Forecast System (NAM). The NAM system is a major forecast model run by NOAA's National Center for Environmental Prediction for the North American continent at several different resolutions. The subset used has a horizontal resolution of 12 km and comprises 26 vertical layers ranging from the surface to 50 hectopascals (hPa).

Backward trajectories of 96-hours length from the Bayland Park and Harvard Street monitors were calculated using termination/starting heights of 100, 500, and 1000 meters. Other information about the HYSPLIT configuration used is presented in Table 3-1: *HYSPLIT Model Information*.

Table 3-1: HYSPLIT Model Information

Model Parameter	Configuration
HYSPLIT Version	5.2.1 (May 2022)
Model Top	10,000 meters
Vertical Motion Method	Input model data
Input Meteorology	NAM 12 km

Figure 3-13: *Backward HYSPLIT Trajectories on June 20, 2022* shows 96-hour back trajectories initiated from the Bayland Park monitor at 18:00 local time on June 20, 2022. Trajectories indicate winds coming from the area of the fire and off the Texas and Gulf coasts, and then recirculating over HGB.

Figure 3-14: *Backward HYSPLIT Trajectories on September 13, 2022* shows 96-hour back trajectories initiated from the Bayland Park monitor at 18:00 local time on September 13, 2022. Trajectories indicate winds coming from the areas of the Louisiana and Alabama wildfires, with smoke and emissions arriving within the mixing layer above the Bayland Park monitor.

Figure 3-15: *Backward HYSPLIT Trajectories on September 21, 2022* shows similar evidence that wildfire smoke and emissions were transported to the Bayland Park monitor from Louisiana and Mississippi on September 21, 2022.

Figure 3-16: *Backward HYSPLIT Trajectories on October 8, 2022* shows similar evidence that wildfire smoke and emissions were transported to the Bayland Park monitor from Louisiana, Alabama, and Mississippi on October 8, 2022.

Figure 3-17: *Backward HYSPLIT Trajectories on June 20, 2022* shows 96-hour back trajectories initiated from the Harvard Street monitor at 18:00 local time, with winds coming from the area of the fire and off the Texas and Gulf coasts, and then recirculating over HGB.

Figure 3-18: *Backward HYSPLIT Trajectories on September 21, 2022* shows similar evidence that wildfire smoke and emissions were transported to the Harvard Street monitor from Louisiana and Mississippi on September 21, 2022.

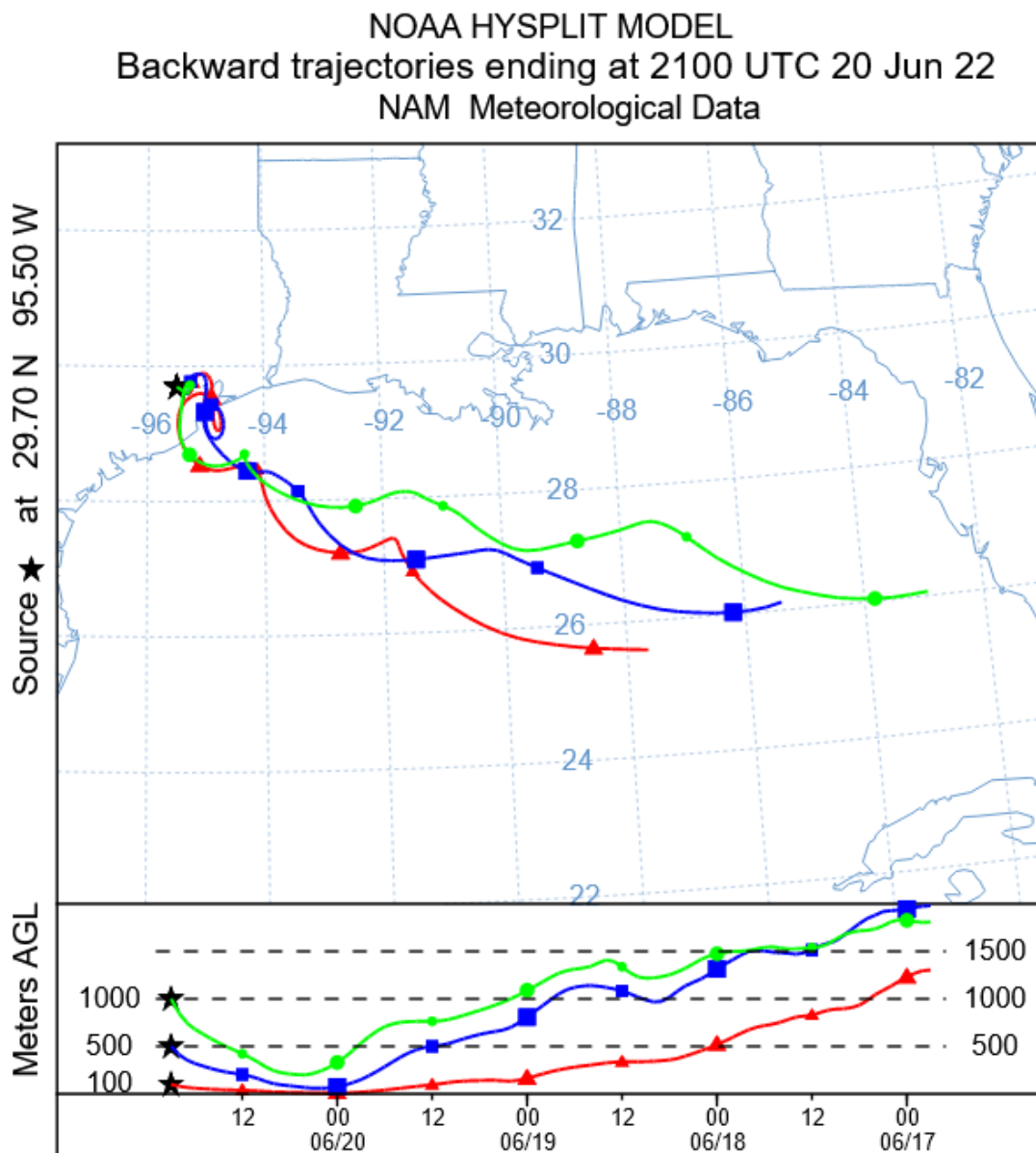


Figure 3-13: *Backward HYSPLIT Trajectories on June 20, 2022*

NOAA HYSPLIT MODEL
 Backward trajectories ending at 2000 UTC 13 Sep 22
 NAM Meteorological Data

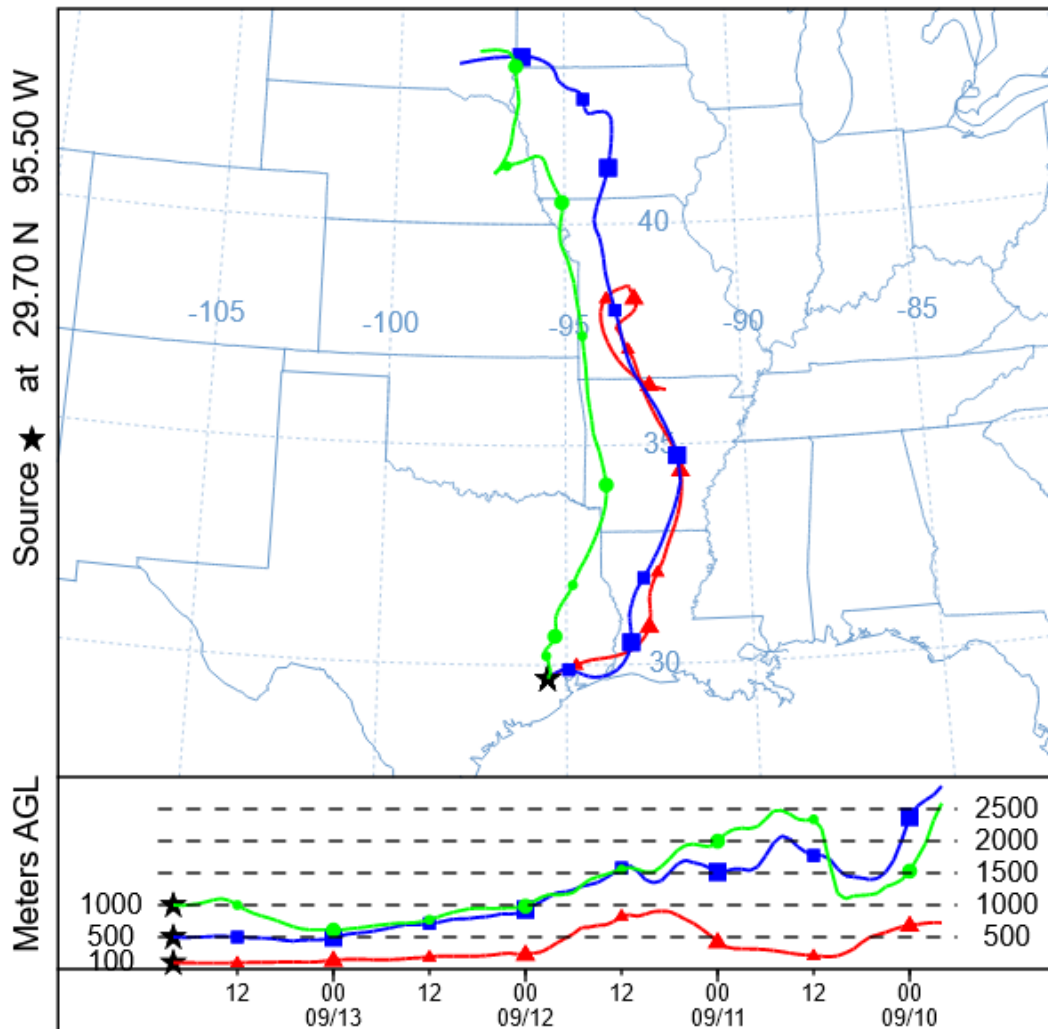


Figure 3-14: Backward HYSPLIT Trajectories on September 13, 2022

NOAA HYSPLIT MODEL
 Backward trajectories ending at 2100 UTC 21 Sep 22
 NAM Meteorological Data

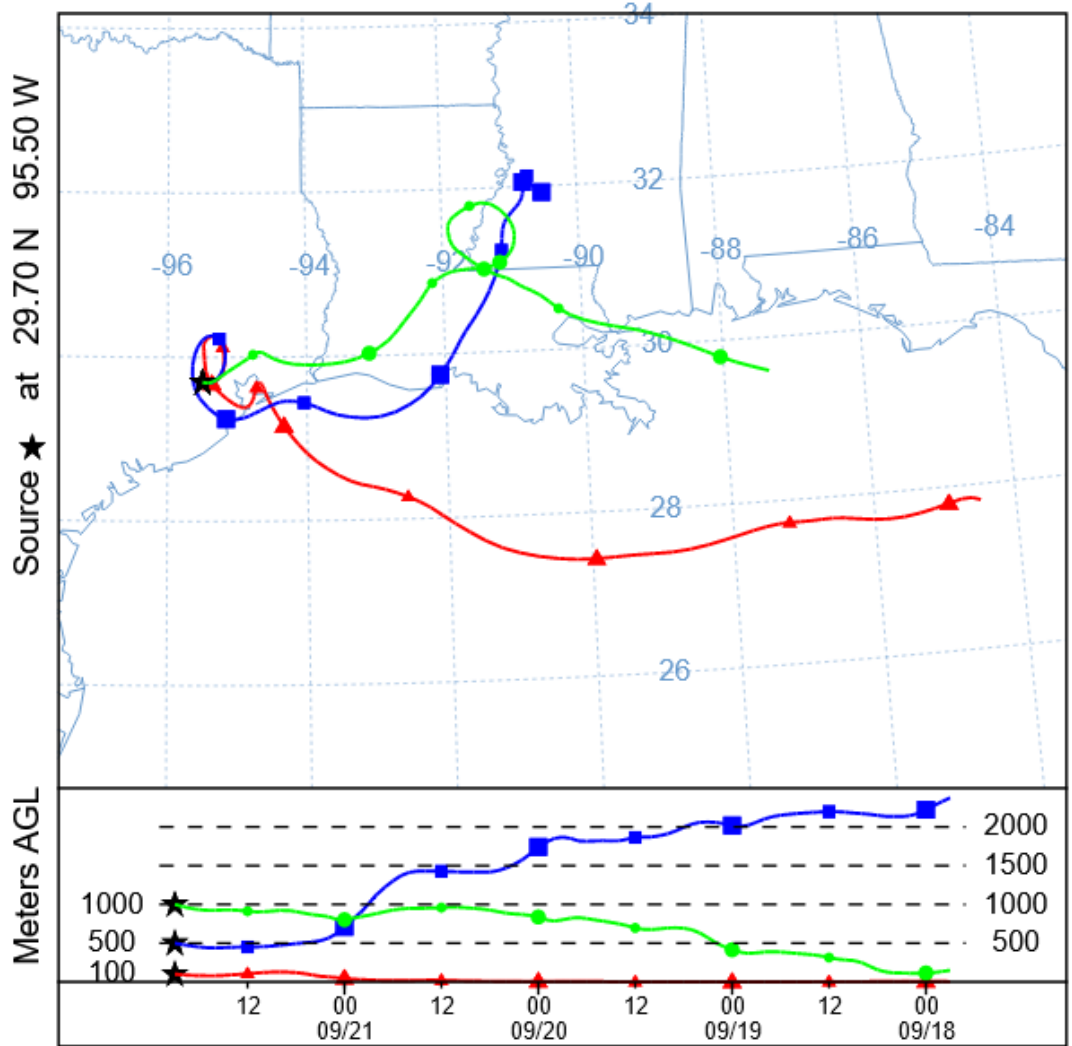


Figure 3-15: Backward HYSPLIT Trajectories on September 21, 2022

NOAA HYSPLIT MODEL
 Backward trajectories ending at 1900 UTC 08 Oct 22
 NAM Meteorological Data

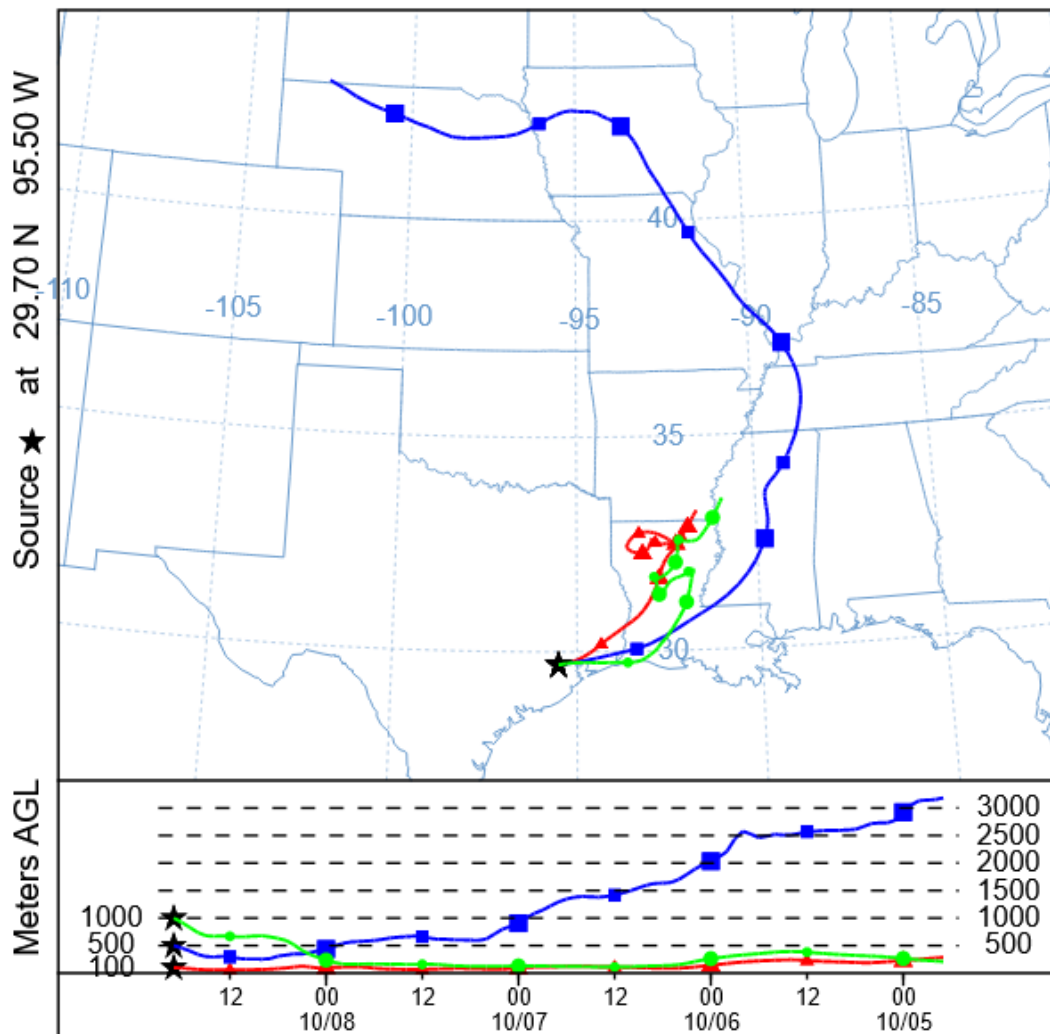


Figure 3-16: Backward HYSPLIT Trajectories on October 8, 2022

NOAA HYSPLIT MODEL
 Backward trajectories ending at 2000 UTC 20 Jun 22
 NAM Meteorological Data

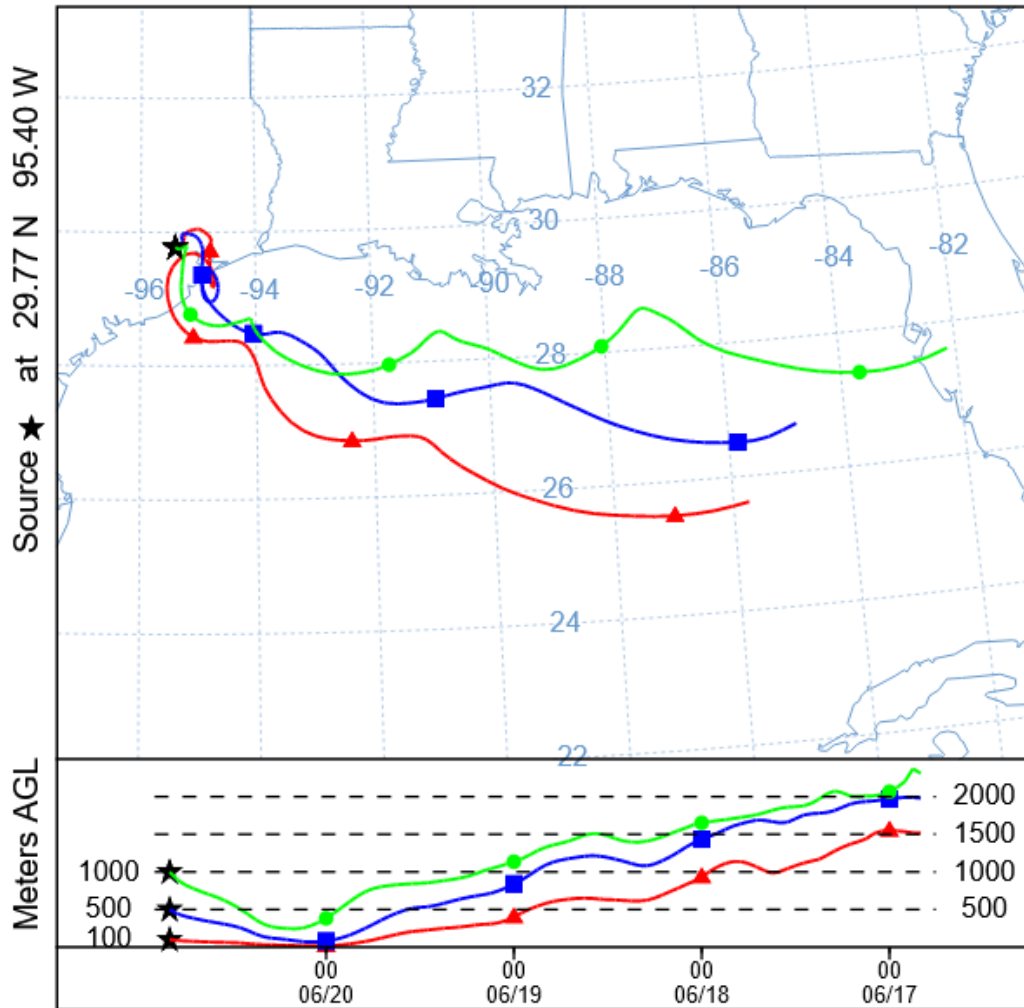


Figure 3-17: Backward HYSPLIT Trajectories on June 20, 2022

NOAA HYSPLIT MODEL
 Backward trajectories ending at 2100 UTC 21 Sep 22
 NAM Meteorological Data

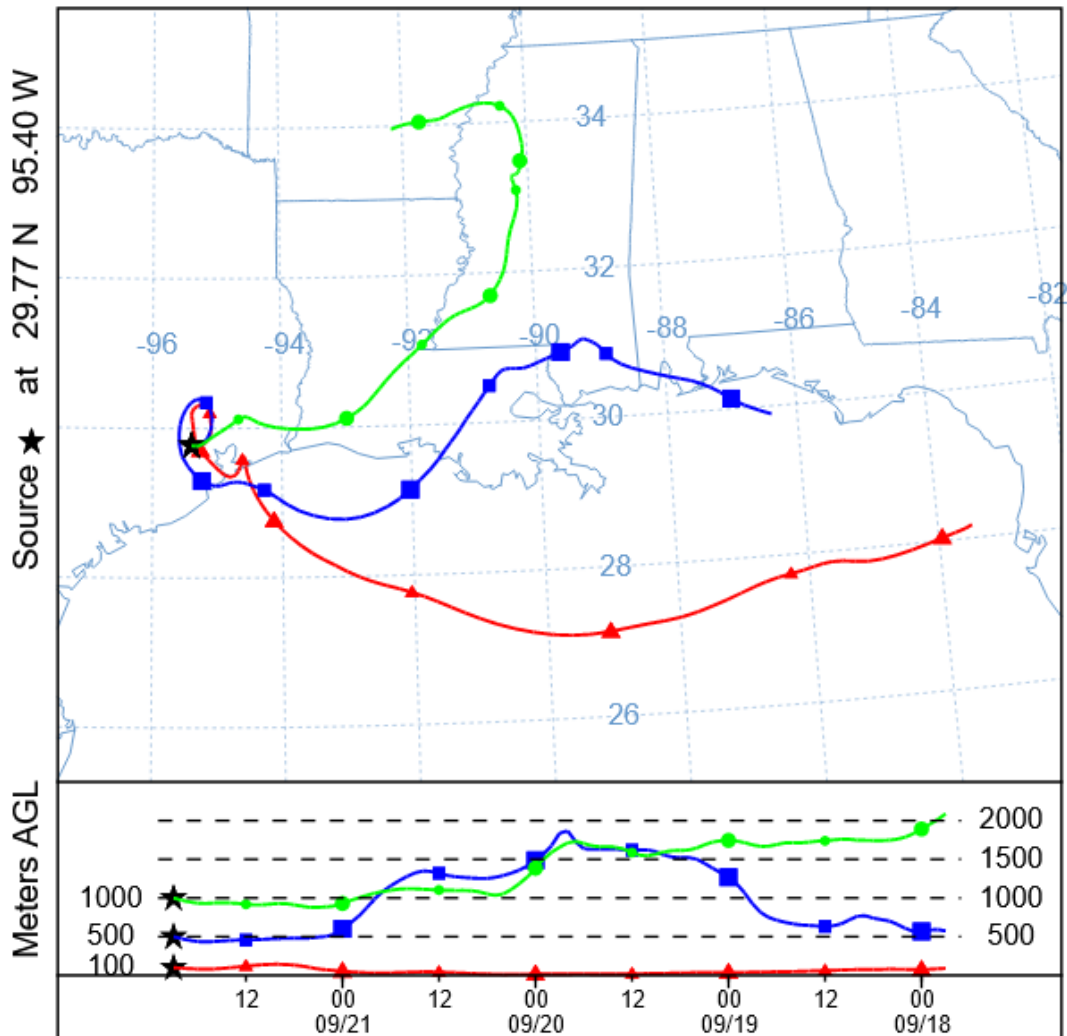


Figure 3-18: Backward HYSPLIT Trajectories on September 21, 2022

3.7 ANALYSIS OF MEASURED POLLUTANTS

In Section 1.2 *Comparison of Historical Ozone Data*, the maximum daily average eight-hour (MDA8) ozone concentrations on June 20, September 13, September 21, and October 8, 2022 were demonstrated to be above the Bayland Park and Harvard Street monitors' historical 99th percentile. This section presents additional supporting evidence for ozone and other pollutants.

3.7.1 The Regional Effect of Wildfire Emissions

The EPA EER requires states that submit demonstrations to compare ozone measurements on candidate exceptional event days to historical measurements to obtain the percentile of the candidate measurements over the historical period. To assess how widely wildfire emissions affected the HGB area, the TCEQ expanded this historical comparison to include all 21 regulatory ozone monitors across the region.

For each day from January 1, 2018, through December 31, 2022, the TCEQ evaluated how many sites reported a MDA8 ozone at or above the 95th percentile for that site. It is uncommon for large numbers of monitoring sites across an area to measure ozone values above their respective 95th percentile. This metric provides an indicator of how widespread the impact of wildfire emissions was because exceedances of the 95th percentile across multiple monitors are rare.

Table 3-2: *Monitoring Sites Above the 95th Percentile* shows that 19 monitoring sites measured ozone concentrations above their 95th percentile on June 20, 2022. This places June 20, 2022 in the 99th percentile for this period. On September 13, 2022, 13 monitoring sites measured ozone concentrations above the 95th percentile, placing September 13, 2022 in the 97th percentile for this period. On September 21, 2022, 16 monitoring sites measured ozone concentrations above their 95th percentile, placing September 21, 2022 in the 98th percentile for this period. On October 8, 2022, 17 monitoring sites measured ozone concentrations above their 95th percentile, placing October 8, 2022 in the 99th percentile for this period. These findings are consistent with NOAA HMS maps showing widespread plumes over the HGB area.

Table 3-2: Monitoring Sites Above the 95th Percentile

Number of Monitors	Days Above 95th Percentile	Percentage	Cumulative Percentage
0	1500	82.19%	82.19%
1	90	4.93%	87.12%
2	41	2.25%	89.37%
3	32	1.75%	91.12%
4	19	1.04%	92.16%
5	20	1.10%	93.26%
6	17	0.93%	94.19%
7	11	0.60%	94.79%
8	11	0.60%	95.40%
9	14	0.77%	96.16%
10	8	0.44%	96.60%
11	10	0.55%	97.15%
12	6	0.33%	97.48%
13	7	0.38%	97.86%
14	6	0.33%	98.19%
15	2	0.11%	98.30%
16	6	0.33%	98.63%

Number of Monitors	Days Above 95th Percentile	Percentage	Cumulative Percentage
17	9	0.49%	99.12%
18	5	0.27%	99.40%
19	5	0.27%	99.67%
20	6	0.33%	100.00%
21	0	0.00%	100.00%
Total Days	1825		

As plumes travel, they tend to disperse, so the fact that many air quality monitors are influenced in the HGB area is consistent with what would be expected when wildfire emissions have transported over a long distance (Jaffe et al., 2020). Figure 3-19: *Monitoring Sites Above Their 95th Percentile on June 20, 2022* shows nineteen monitoring sites on June 20, 2022 with measurements above their 95th percentile. These nineteen monitoring sites are widely distributed in the HGB area. Figure 3-20: *Monitoring Sites Above Their 95th Percentile on September 13, 2022* shows how widespread the effects of wildfire emissions are on September 13, 2022. Figure 3-21: *Monitoring Sites Above Their 95th Percentile on September 21, 2022* and Figure 3-22: *Monitoring Sites Above Their 95th Percentile on October 8, 2022* show the widespread nature of the historically high ozone values measured on September 21 and October 8, 2022.

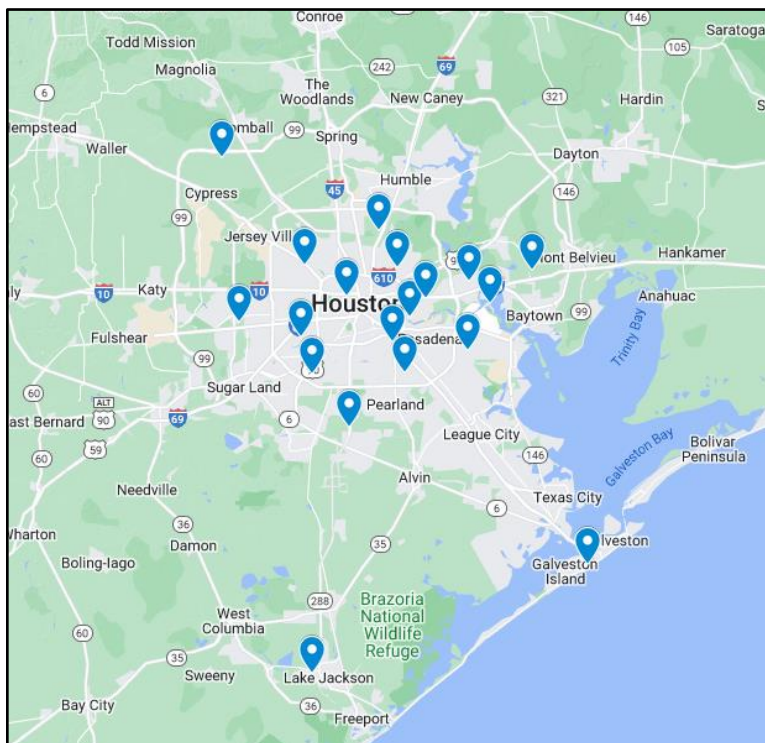


Figure 3-19: Monitoring Sites Above Their 95th Percentile on June 20, 2022

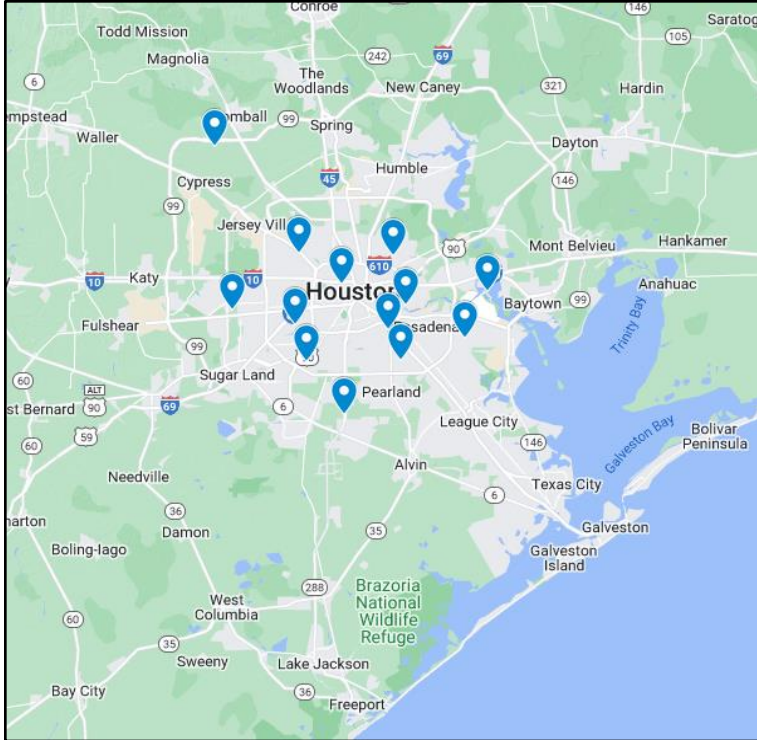


Figure 3-20: Monitoring Sites Above Their 95th Percentile on September 13, 2022

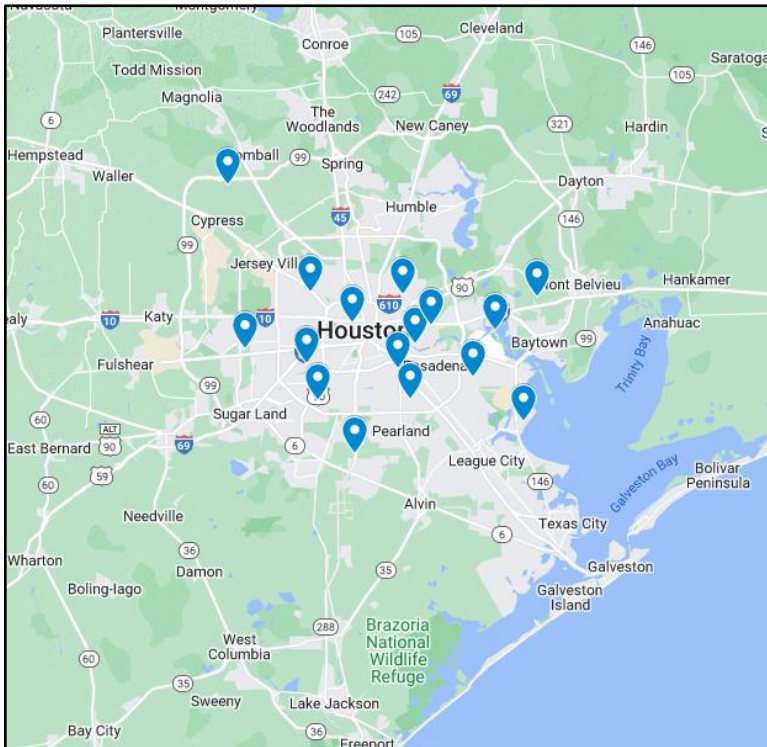


Figure 3-21: Monitoring Sites Above Their 95th Percentile on September 21, 2022

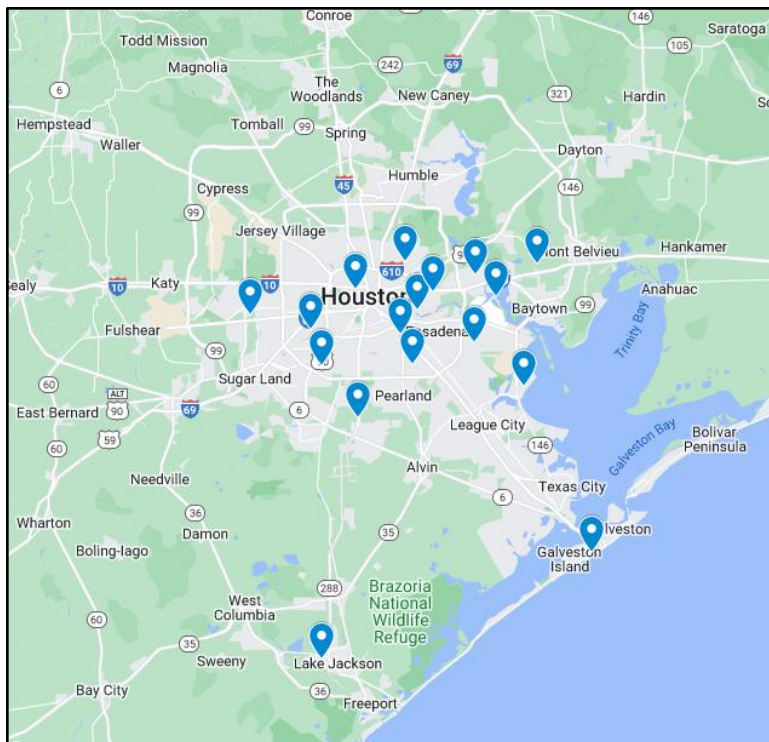


Figure 3-22: Monitoring Sites Above Their 95th Percentile on October 8, 2022

3.7.2 Analysis of Ground Based Monitoring Data

3.7.2.1 VOC to NO_x Ratios

Given the large number of VOC species that can be present in a wildfire plume, it is not surprising that monitors would see an enhancement of VOC on days influenced by wildfires. In a 2021 presentation, Dr. Dan Jaffe (Jaffe, 2021) noted that high VOC to nitrogen oxides (NO_x) ratios (i.e., 25-75) may indicate a biomass burning event. In preparing this demonstration, the TCEQ analyzed VOC/NO_x ratios from five monitoring sites with co-located automated gas chromatographs (auto-GCs) and NO_x monitors: Channelview, Clinton, Oyster Creek, Wallisville Road, and Texas City 34th Street. Diurnal VOC/NO_x ratios from the four event days were compared to hourly diurnal distributions of ozone season VOC/NO_x ratios from 2018-2022 (April through October). In the figures below, the box and whisker plots depict the historical distribution of VOC/NO_x ratios for each hour of the day. The red line depicts the diurnal pattern of VOC/NO_x ratio of that event day.

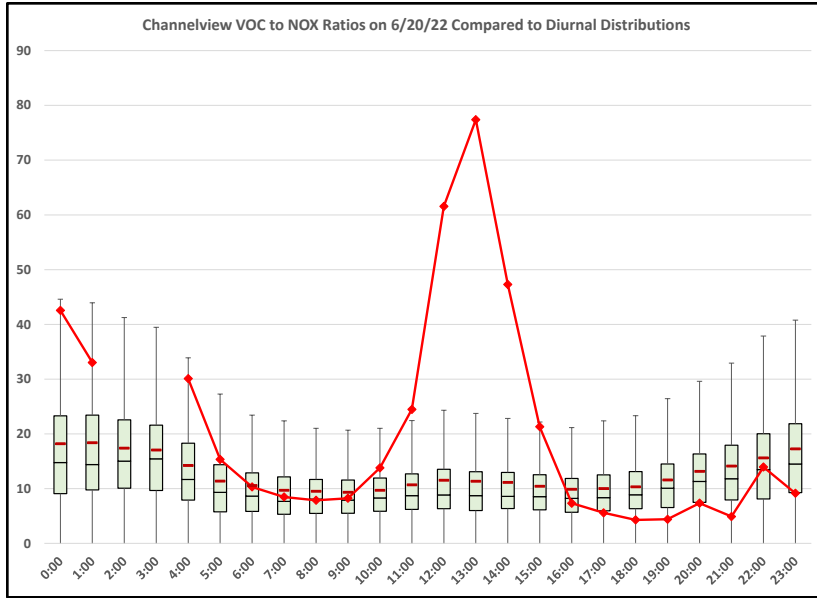


Figure 3-23: VOC/NO_x Ratios at Channelview Monitoring Site on June 20, 2022

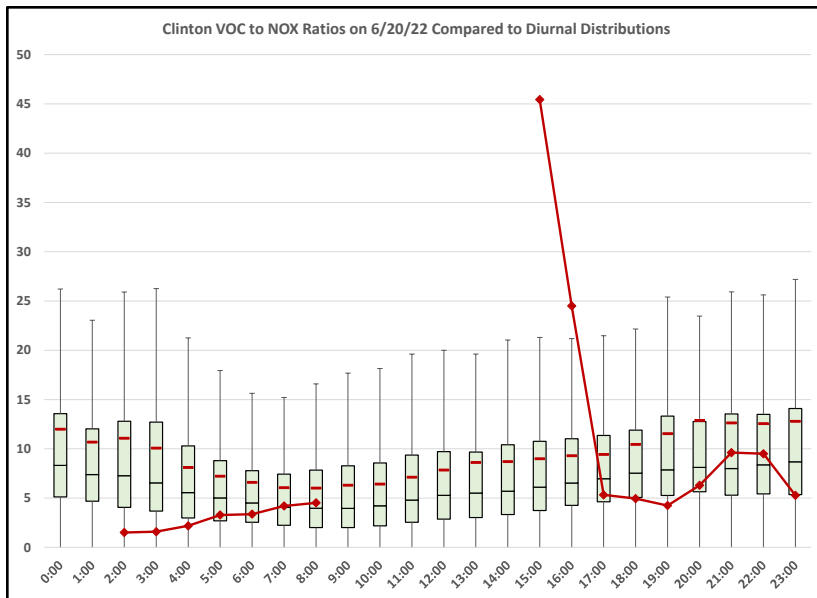


Figure 3-24: VOC/NO_x Ratios at Clinton Monitoring Site on June 20, 2022

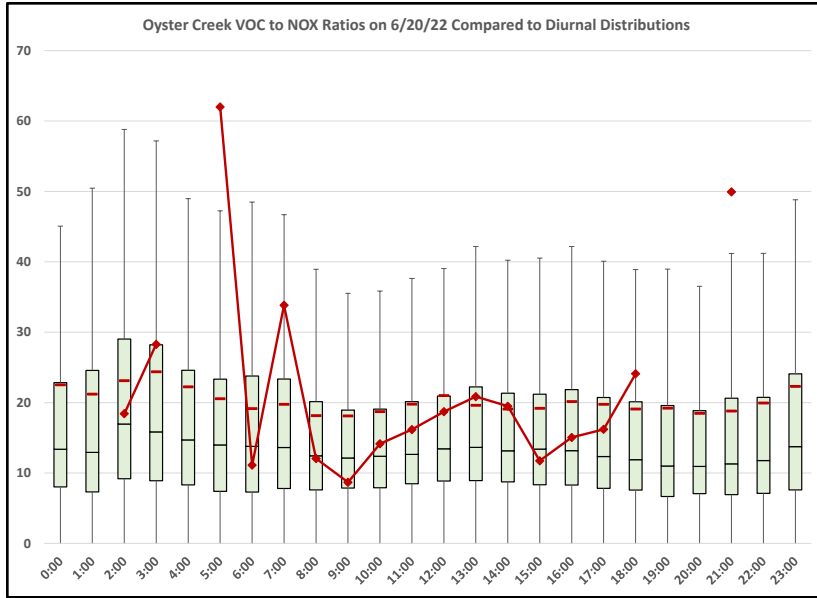


Figure 3-25: VOC/NO_x Ratios at Oyster Creek Monitoring Site on June 20, 2022

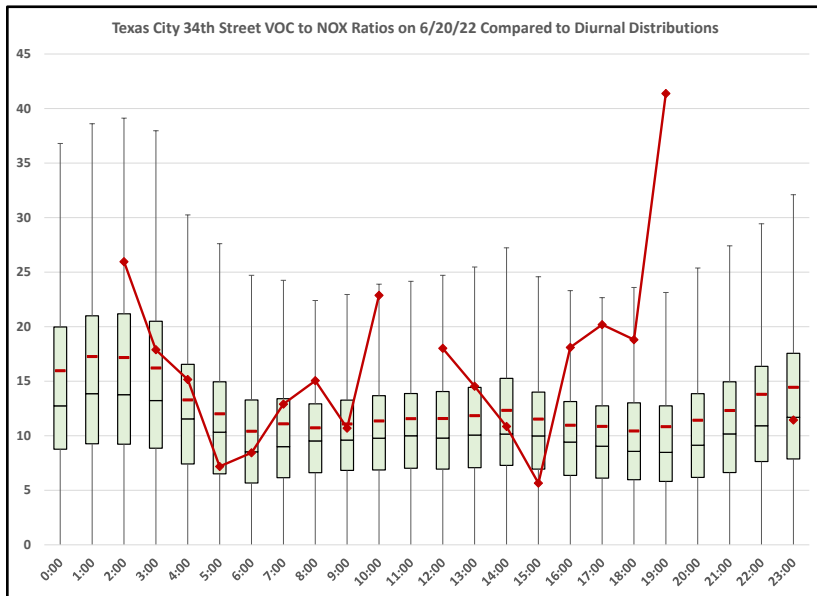


Figure 3-26: VOC/NO_x Ratios at Texas City 34th Street Monitoring Site on June 20, 2022

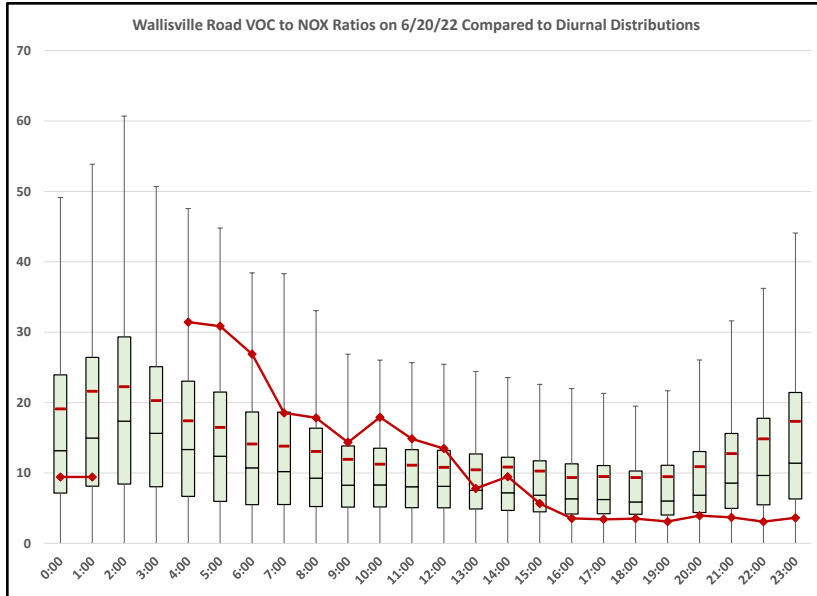


Figure 3-27: VOC/NO_x Ratios at Wallisville Monitoring Site on June 20, 2022

Figure 3-23: VOC/NO_x Ratios at Channelview Monitoring Site on June 20, 2022, Figure 3-24: VOC/NO_x Ratios at Clinton Monitoring Site on June 20, 2022, Figure 3-25: VOC/NO_x Ratios at Oyster Creek Monitoring Site on June 20, 2022, Figure 3-26: VOC/NO_x Ratios at Texas City 34th Street Monitoring Site on June 20, 2022, and Figure 3-27: VOC/NO_x Ratios at Wallisville Monitoring Site on June 20, 2022 all show VOC/NO_x ratios greater than 25, which offers support to the hypothesis of wildfire emissions influencing air quality in the HGB area.

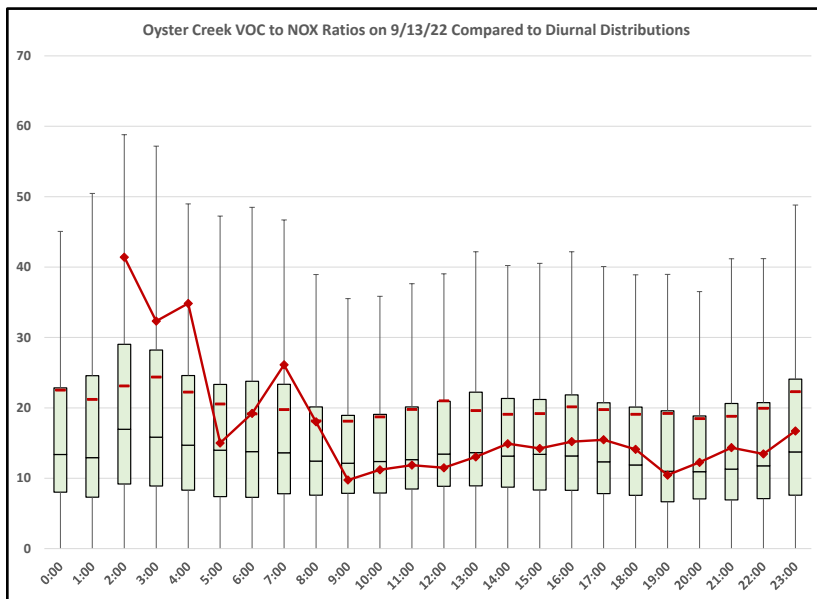


Figure 3-28: VOC/NO_x Ratios at Oyster Creek Monitoring Site on September 13, 2022

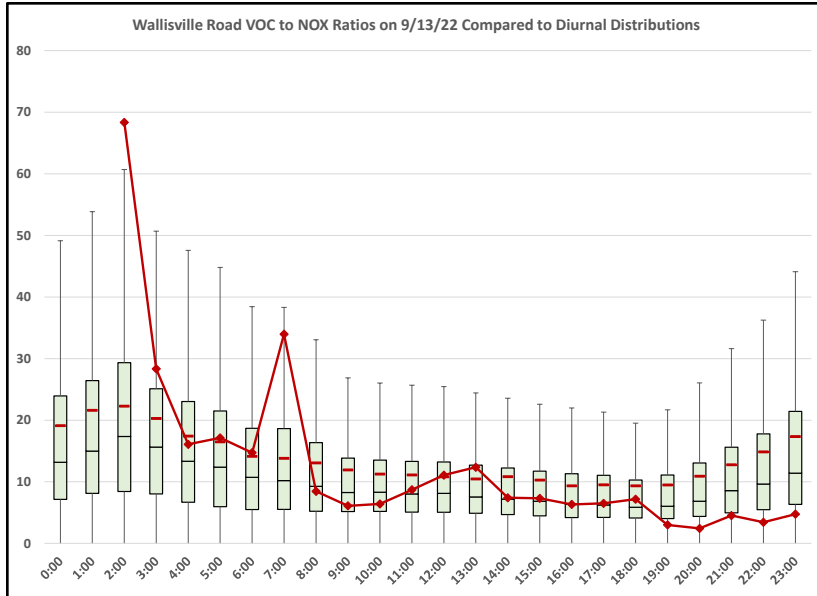


Figure 3-29: VOC/NO_x Ratios at Wallisville Road Monitoring Site on September 13, 2022

Figure 3-28: VOC/NO_x Ratios at Oyster Creek Monitoring Site on September 13, 2022 and Figure 3-29: VOC/NO_x Ratios at Wallisville Road Monitoring Site on September 13, 2022 show high VOC/NO_x ratios, and suggest wildfire emissions influenced ground-level air quality on this day as well.

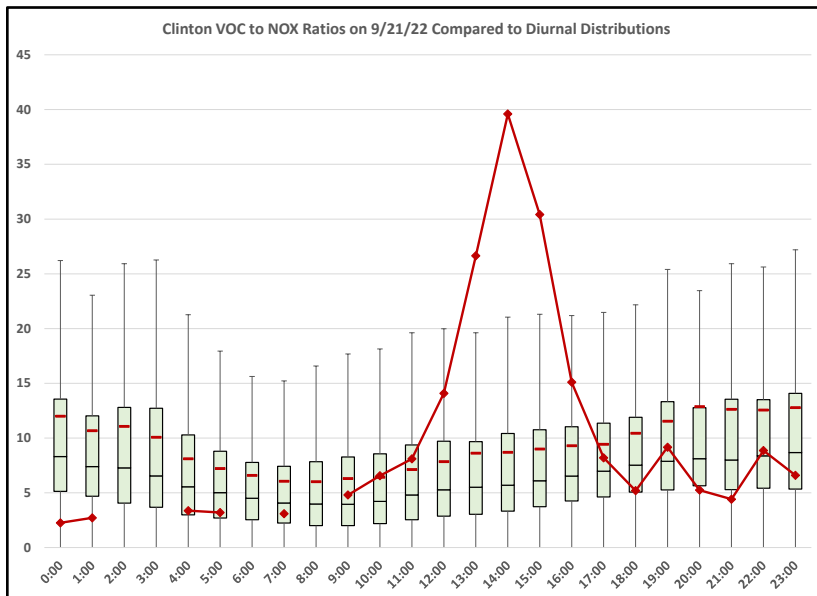


Figure 3-30: VOC/NO_x Ratios at Clinton Monitoring Site on September 21, 2022

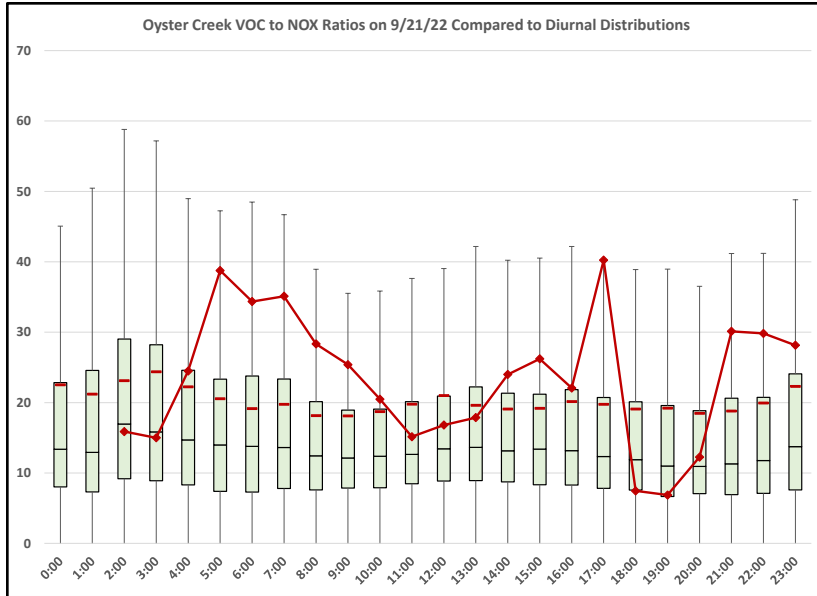


Figure 3-31: VOC/NO_x Ratios at Oyster Creek Monitoring Site on September 21, 2022

Figure 3-30: VOC/NO_x Ratios at Clinton Monitoring Site on September 21, 2022 and Figure 3-31: VOC/NO_x Ratios at Oyster Creek Monitoring Site on September 21, 2022 show that VOC/NO_x ratios reached levels supportive of the conclusion that wildfire emissions influenced air quality in the HGB area on September 21, 2022.

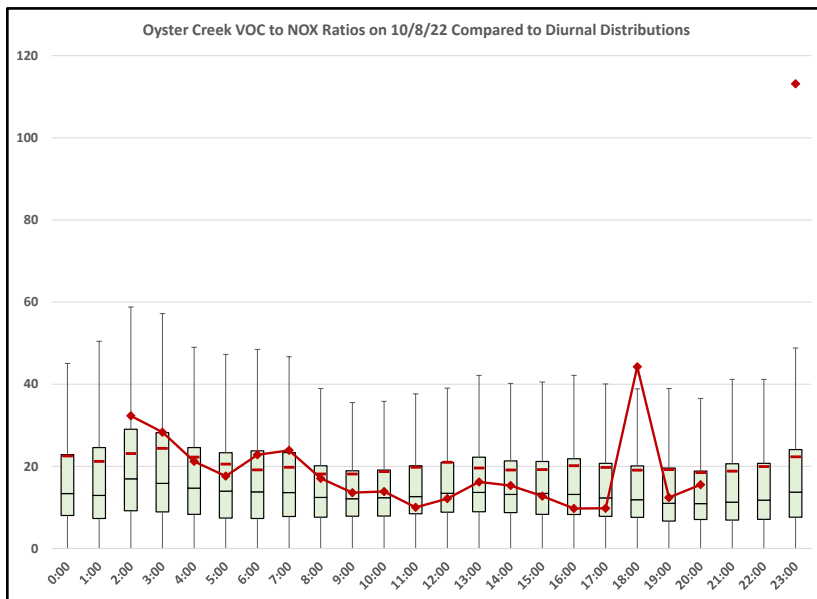


Figure 3-32: VOC/NO_x Ratios at Oyster Creek Monitoring Site on October 8, 2022

Figure 3-32: VOC/NO_x Ratios at Oyster Creek Monitoring Site on October 8, 2022 shows that VOC/NO_x ratios at Oyster Creek reached above 25 at 6:00 CST on October 8, 2022.

3.7.2.2 High Sensitivity CO Measurements

High CO levels are another indicator of wildfire emissions. For this demonstration, the TCEQ analyzed five years of historical CO data from the Clinton monitoring site.

Hourly CO measurements for exceptional event days were compared to hourly distributions of CO data for the years 2018-2022 (April through October). High sensitivity CO data was not available for June 20, 2022. In the figures below, the box and whisker plots depict the historical distribution of CO measurements for each hour of the day. The red line depicts the diurnal pattern of CO measurements of that event day.

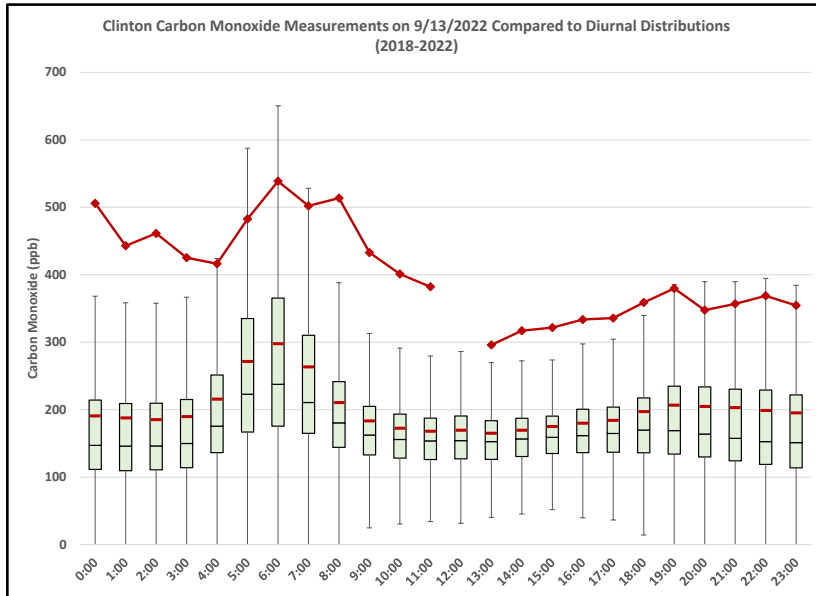


Figure 3-33: CO Measurements at Clinton Monitoring Site on September 13, 2022

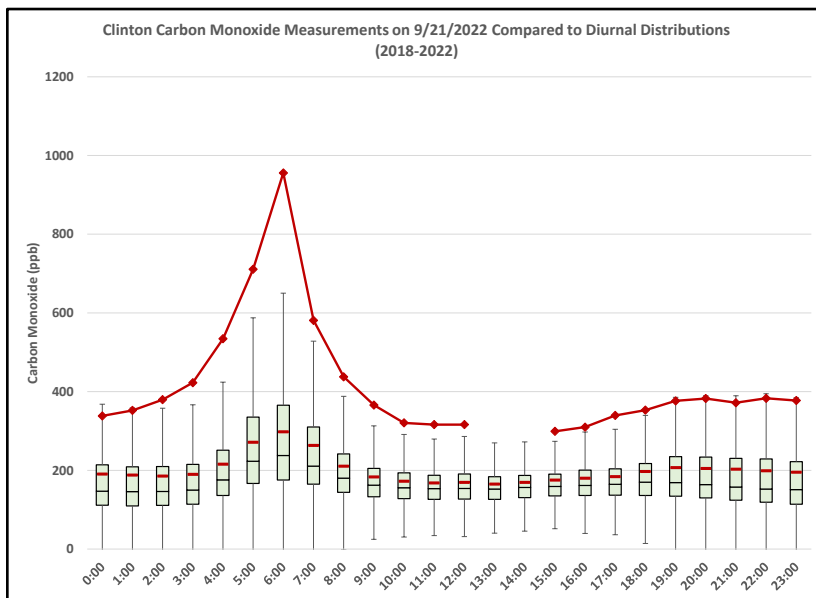


Figure 3-34: CO Measurements at Clinton Monitoring Site on September 21, 2022

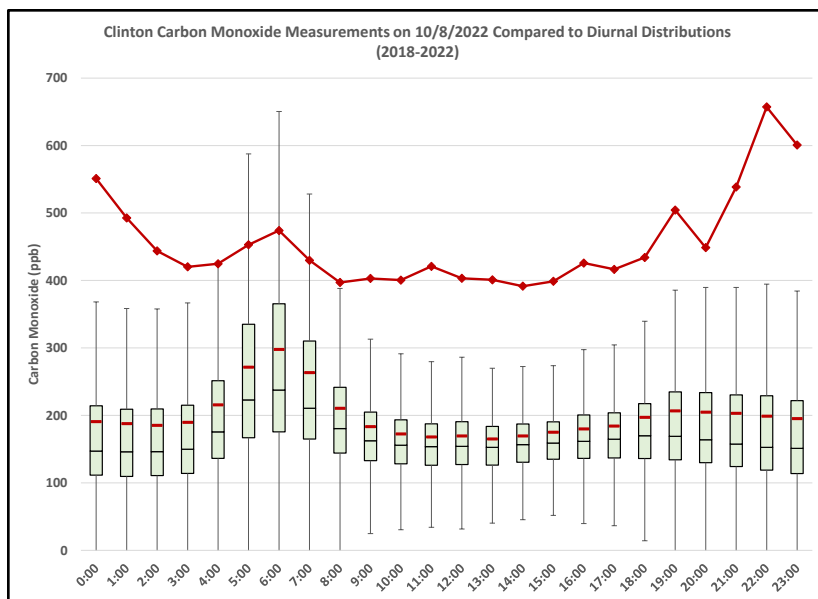


Figure 3-35: CO Measurements at Clinton Monitoring Site on October 8, 2022

Figure 3-33: *CO Measurements at Clinton Monitoring Site on September 13, 2022*, Figure 3-34: *CO Measurements at Clinton Monitoring Site on September 21, 2022*, and Figure 3-35: *CO Measurements at Clinton Monitoring Site on October 8, 2022* each show unusually high levels of CO. This supports the contention that air quality in the HGB area was influenced by wildfire emissions on these days.

3.7.2.3 Benzene to Toluene Ratios

The TCEQ also looked at benzene to toluene ratios observed at auto-GCs selected to achieve a geographic diversity in the HGB area. Research by Permar (Permar et al. 2021, 14-15) and Sullivan and Jaffe (2022) indicate that benzene and toluene occur at a ratio of 3 to 2 downwind of wildfires studied in the Western Wildfire Experiment for Cloud Chemistry, Aerosol Absorption, and Nitrogen field campaign in summer 2018. The ratio of benzene and toluene makes a good indicator because it tends to be fairly steady and does not have a strong diurnal cycle over the course of a day.

The TCEQ examined benzene to toluene ratios at the Texas City 34th Street, Wallisville Road, Houston Clinton, Channelview, Oyster Creek, and Cesar Chavez monitoring sites on the event days and compared them to hourly distributions at these monitoring sites observed over the 2018-2022 ozone seasons (April through October). In the figures below, the box and whisker plots depict the historical distribution of benzene to toluene ratios for each hour of the day. The red line depicts the diurnal pattern of benzene to toluene ratio of that event day.

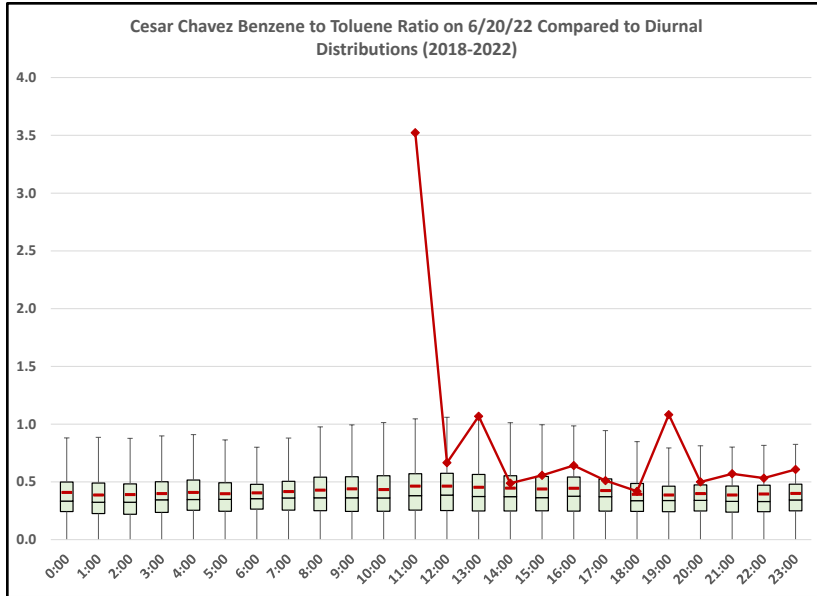


Figure 3-36: Benzene to Toluene Ratios at the Cesar Chavez Monitoring Site on June 20, 2022

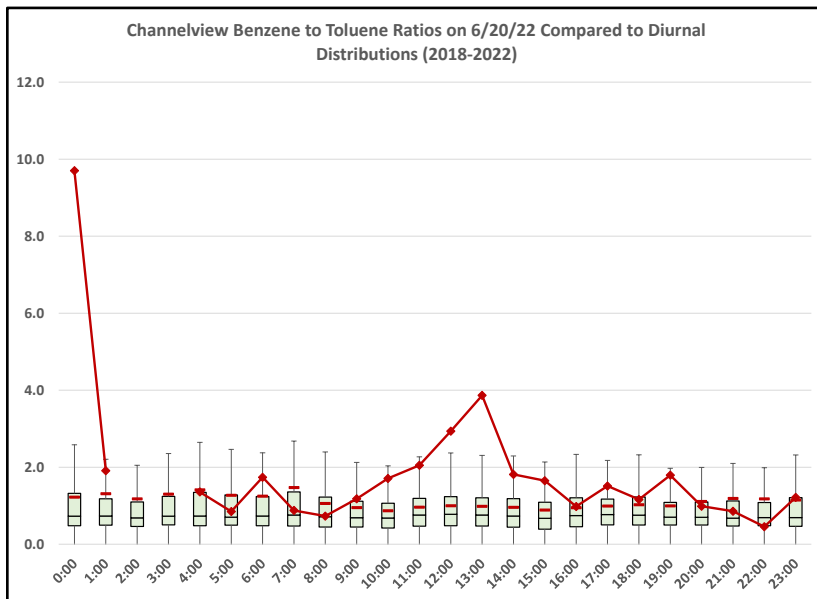


Figure 3-37: Benzene to Toluene Ratios at the Channelview Monitoring Site on June 20, 2022

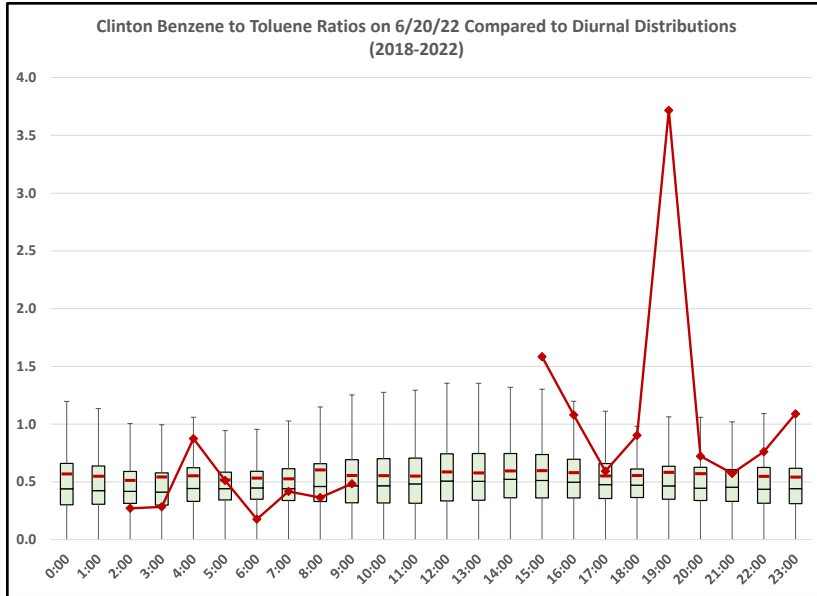


Figure 3-38: Benzene to Toluene Ratios at the Clinton Monitoring Site on June 20, 2022

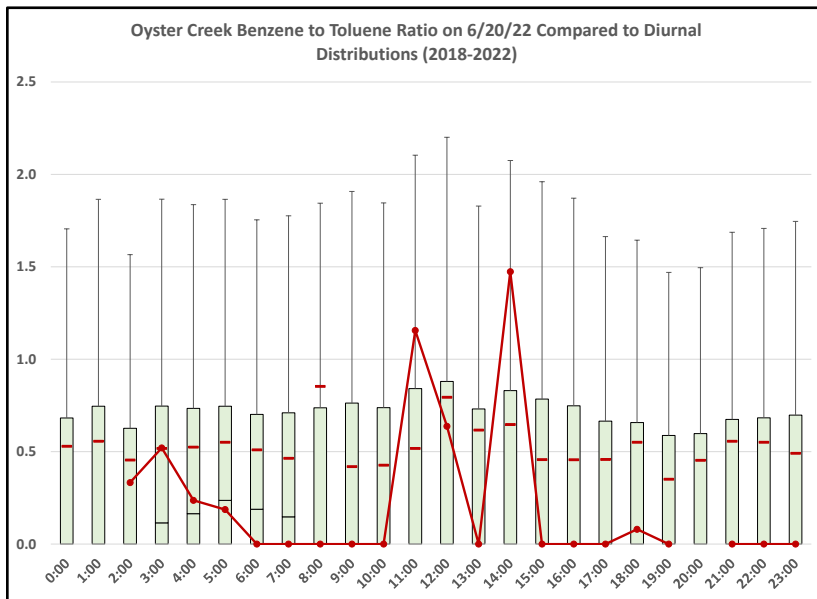


Figure 3-39: Benzene to Toluene Ratios at the Oyster Creek Monitoring Site on June 20, 2022

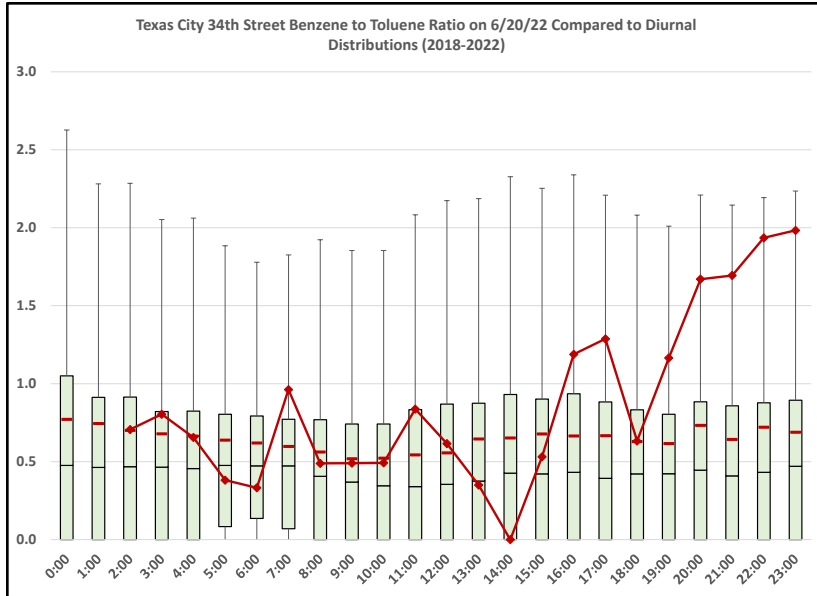


Figure 3-40: Benzene to Toluene Ratios at the Texas City 34th Street Monitoring Site on June 20, 2022

Figure 3-36: Benzene to Toluene Ratios at the Cesar Chavez Monitoring Site on June 20, 2022, Figure 3-37: Benzene to Toluene Ratios at the Channelview Monitoring Site on June 20, 2022, Figure 3-38: Benzene to Toluene Ratios at the Clinton Monitoring Site on June 20, 2022, Figure 3-39: Benzene to Toluene Ratios at the Oyster Creek Monitoring Site on June 20, 2022, and Figure 3-40: Benzene to Toluene Ratios at the Texas City 34th Street Monitoring Site on June 20, 2022 each show elevated benzene to toluene ratios, near 1.5, consistent with ratios found in wildfire plumes.

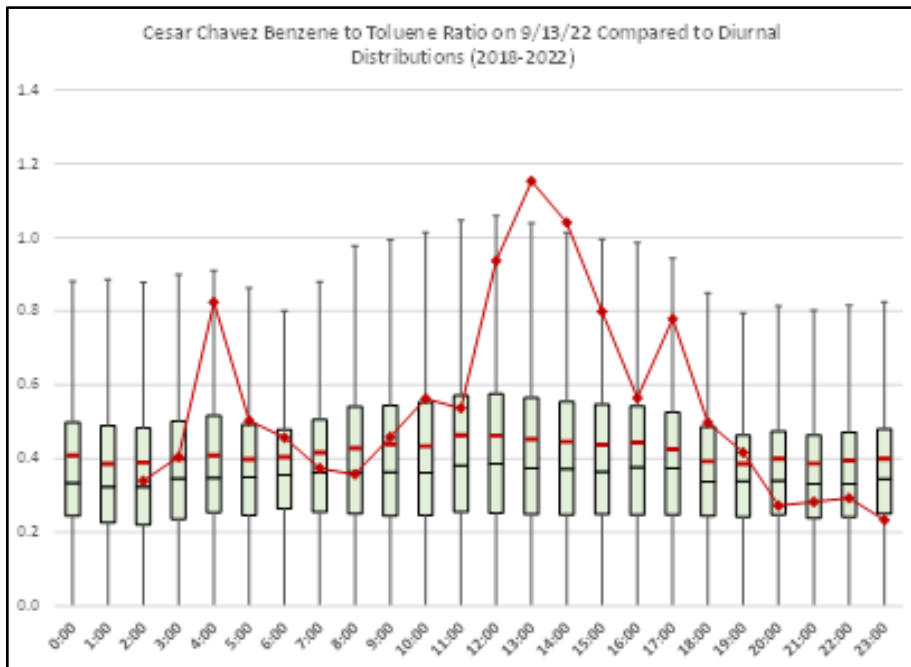


Figure 3-41: Benzene to Toluene Ratios at the Cesar Chavez Monitoring Site on September 13, 2022

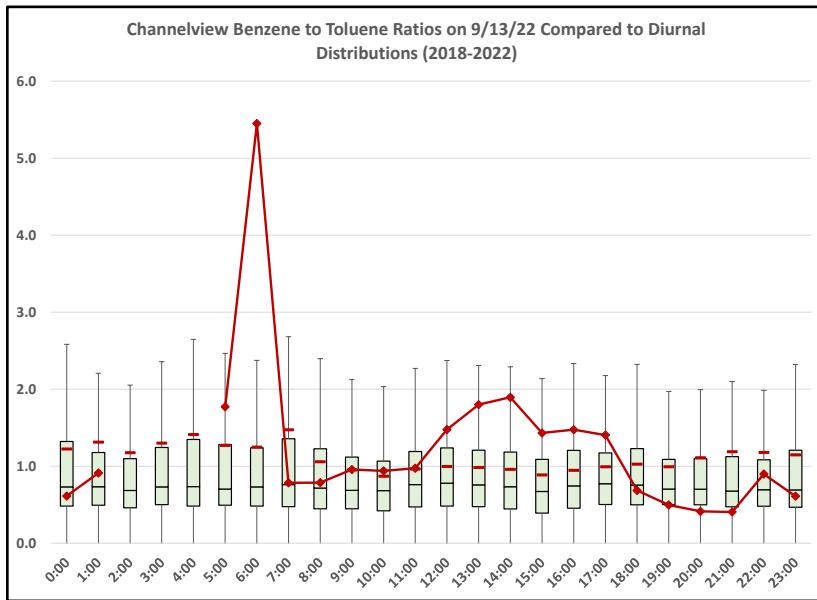


Figure 3-42: Benzene to Toluene Ratios at the Channelview Monitoring Site on September 13, 2022

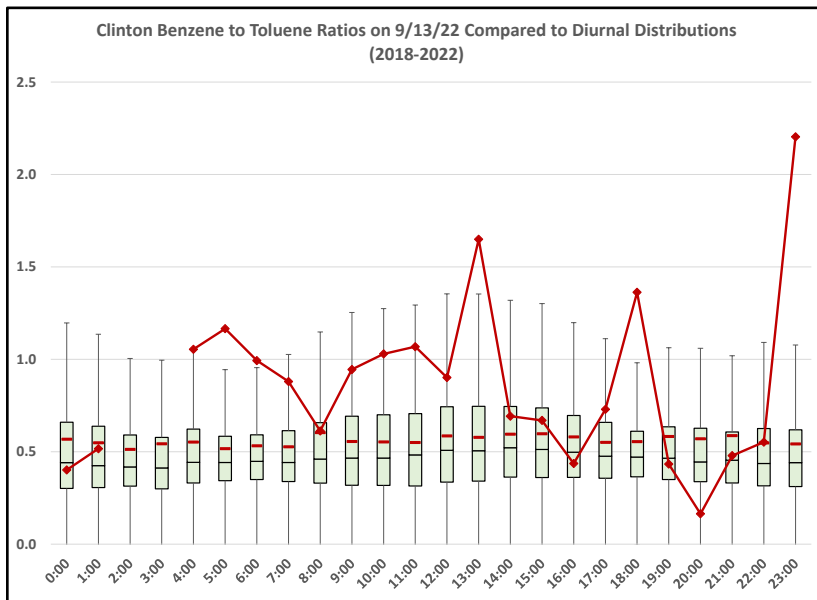


Figure 3-43: Benzene to Toluene Ratios at the Clinton Monitoring Site on September 13, 2022

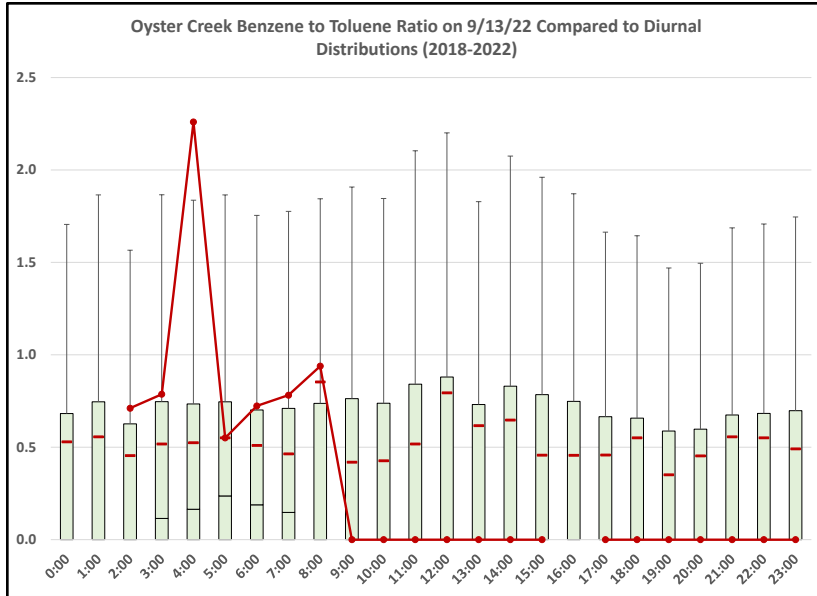


Figure 3-44: Benzene to Toluene Ratios at the Oyster Creek Monitoring Site on September 13, 2022

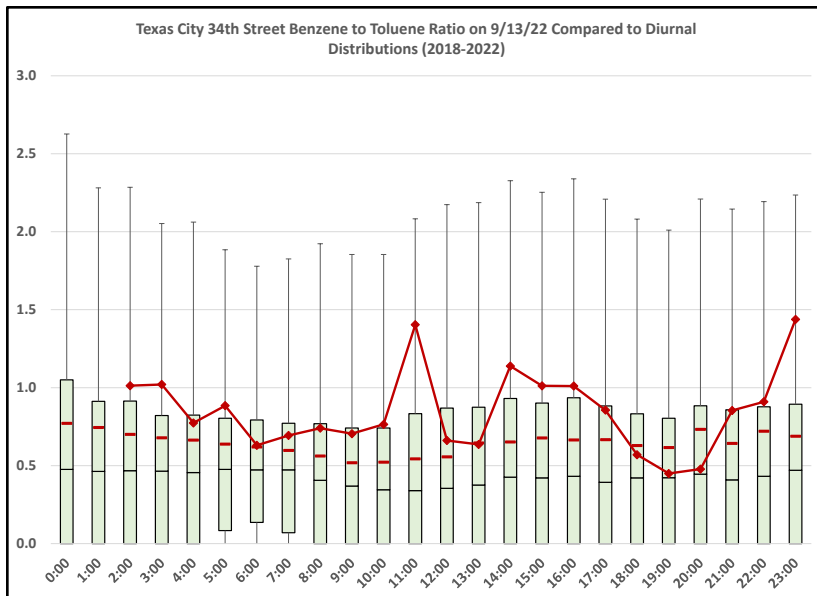


Figure 3-45: Benzene to Toluene Ratios at the Texas City 34th Street Monitoring Site on September 13, 2022

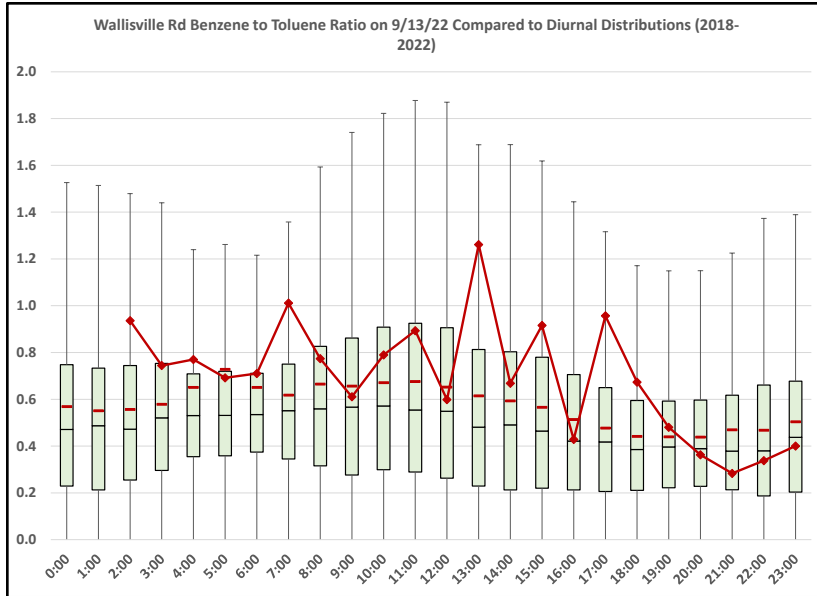


Figure 3-46: Benzene to Toluene Ratios at the Wallisville Road Monitoring Site on September 13, 2022

Figure 3-41: Benzene to Toluene Ratios at the Cesar Chavez Monitoring Site on September 13, 2022, Figure 3-42: Benzene to Toluene Ratios at the Channelview Monitoring Site on September 13, 2022, Figure 3-43: Benzene to Toluene Ratios at the Clinton Monitoring Site on September 13, 2022, Figure 3-44: Benzene to Toluene Ratios at the Oyster Creek Monitoring Site on September 13, 2022, Figure 3-45: Benzene to Toluene Ratios at the Texas City 34th Street Monitoring Site on September 13, 2022, and Figure 3-46: Benzene to Toluene Ratios at the Wallisville Road Monitoring Site on September 13, 2022 each show elevated benzene to toluene ratios, near 1.5, consistent with ratios found in wildfire plumes.

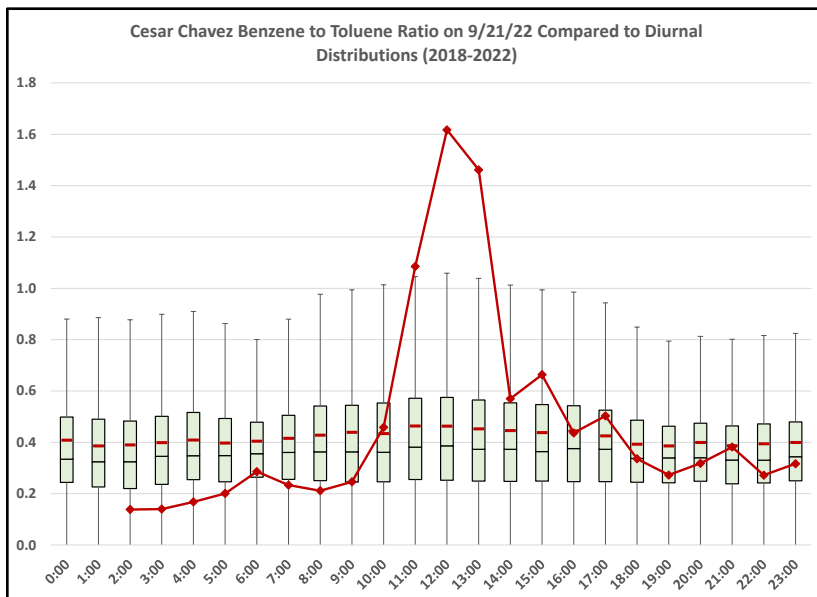


Figure 3-47: Benzene to Toluene Ratios at the Cesar Chavez Monitoring Site on September 21, 2022

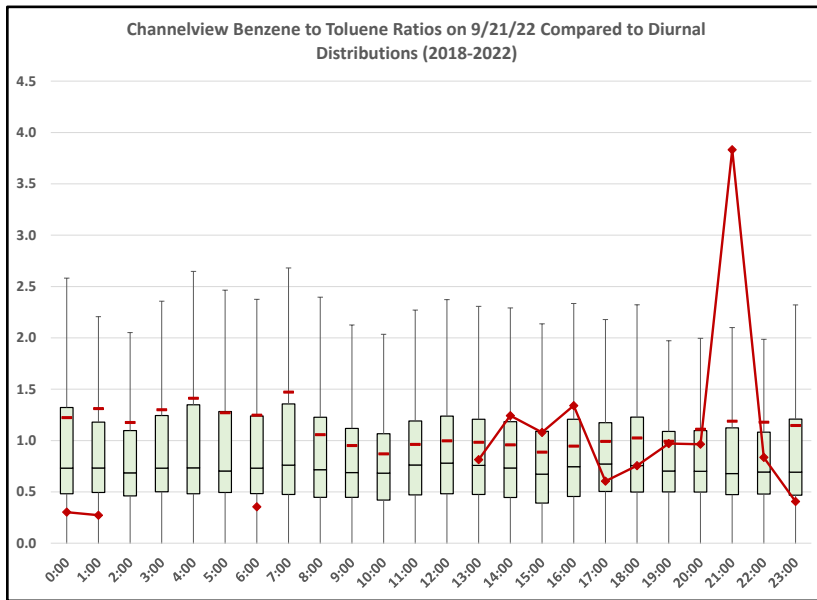


Figure 3-48: Benzene to Toluene Ratios at the Channelview Monitoring Site on September 21, 2022

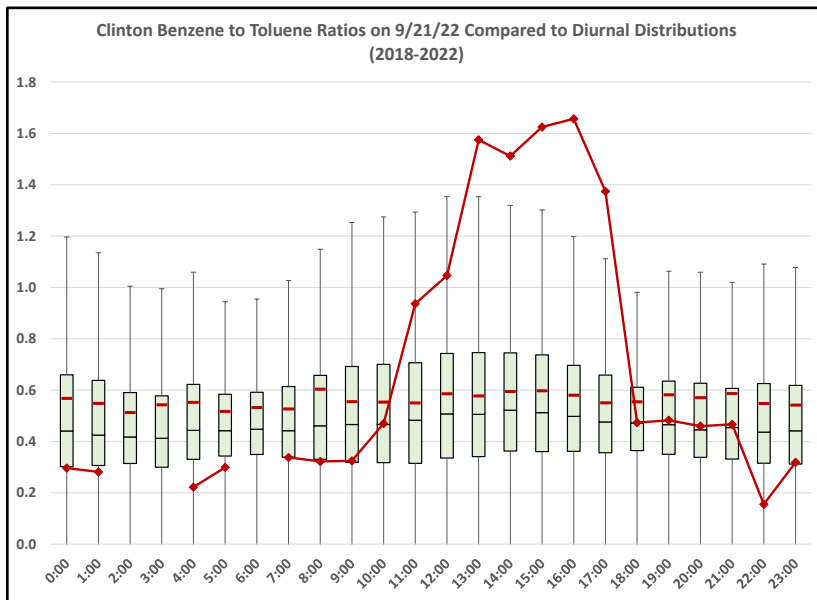


Figure 3-49: Benzene to Toluene Ratios at the Clinton Monitoring Site on September 21, 2022

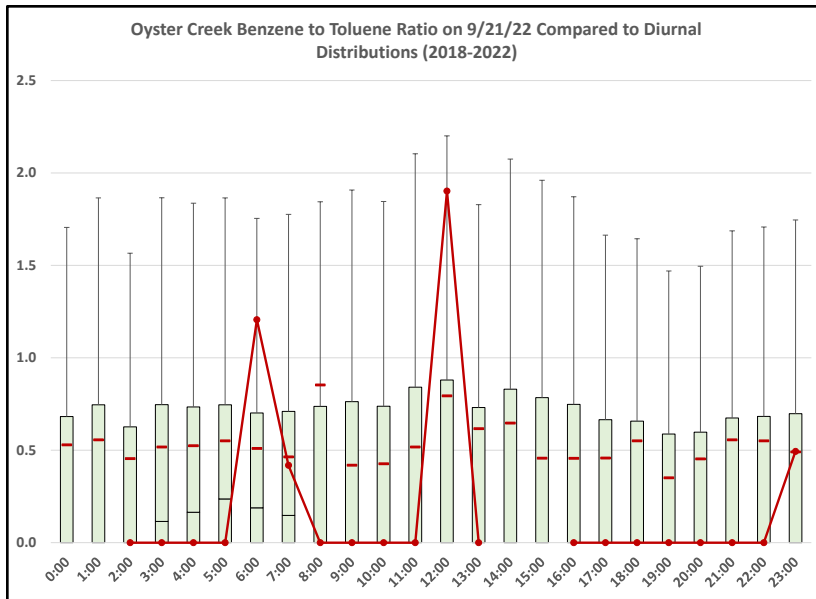


Figure 3-50: Benzene to Toluene Ratios at the Oyster Creek Monitoring Site on September 21, 2022

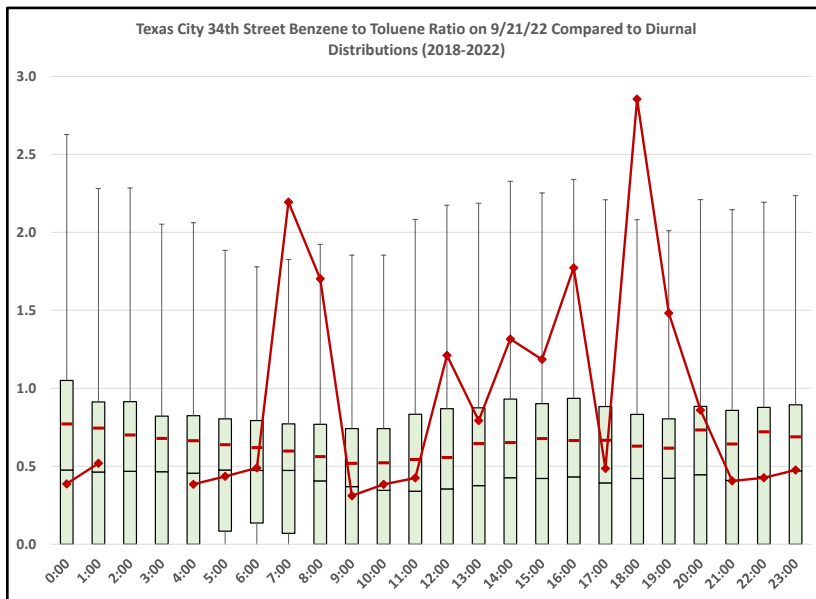


Figure 3-51: Benzene to Toluene Ratios at the Texas City 34th Street Monitoring Site on September 21, 2022

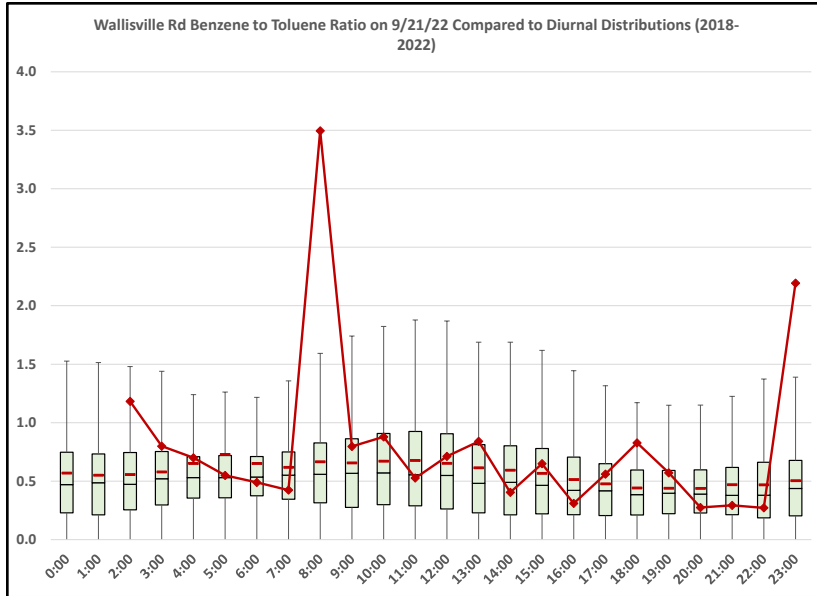


Figure 3-52: Benzene to Toluene Ratios at the Wallisville Road Monitoring Site on September 21, 2022

Figure 3-47: Benzene to Toluene Ratios at the Cesar Chavez Monitoring Site on September 21, 2022, Figure 3-48: Benzene to Toluene Ratios at the Channelview Monitoring Site on September 21, 2022, Figure 3-49: Benzene to Toluene Ratios at the Clinton Monitoring Site on September 21, 2022, Figure 3-50: Benzene to Toluene Ratios at the Oyster Creek Monitoring Site on September 21, 2022, Figure 3-51: Benzene to Toluene Ratios at the Texas City 34th Street Monitoring Site on September 21, 2022, and Figure 3-52: Benzene to Toluene Ratios at the Wallisville Road Monitoring Site on September 21, 2022 each show elevated benzene to toluene ratios consistent with ratios found in wildfire plumes.

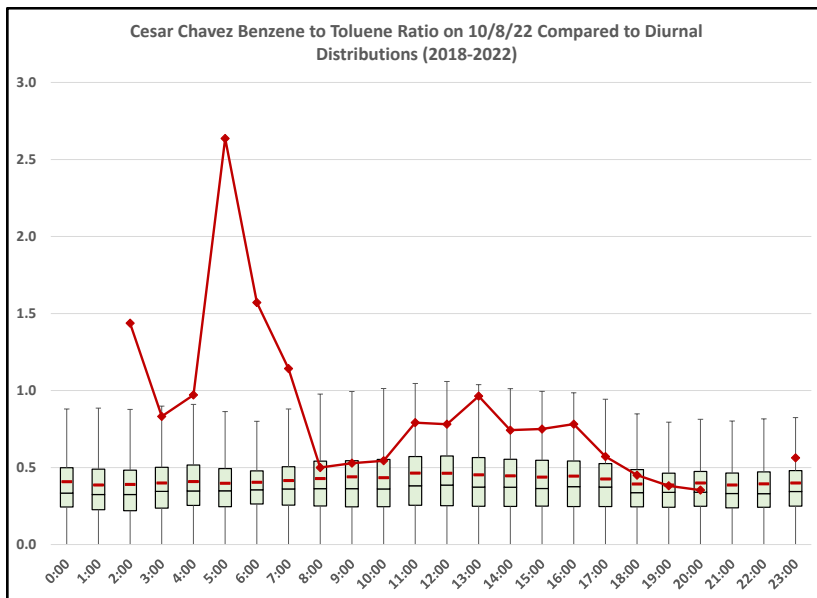


Figure 3-53: Benzene to Toluene Ratios at the Cesar Chavez Monitoring Site on October 8, 2022

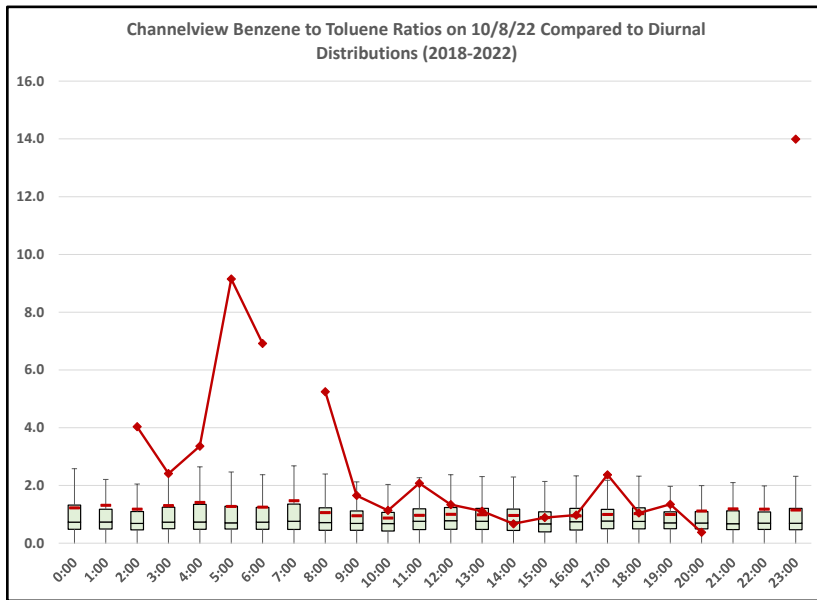


Figure 3-54: Benzene to Toluene Ratios at the Channelview Monitoring Site on October 8, 2022

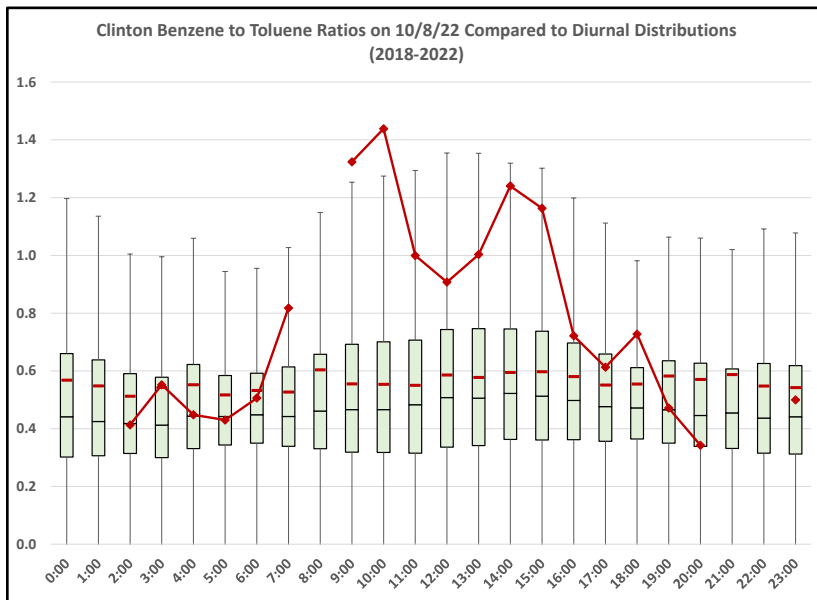


Figure 3-55: Benzene to Toluene Ratios at the Clinton Monitoring Site on October 8, 2022

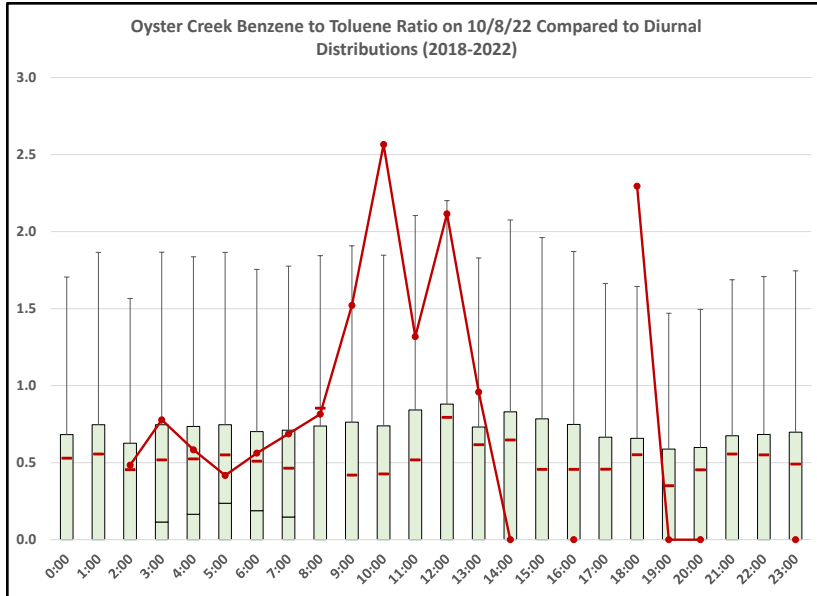


Figure 3-56: Benzene to Toluene Ratios at the Oyster Creek Monitoring Site on October 8, 2022

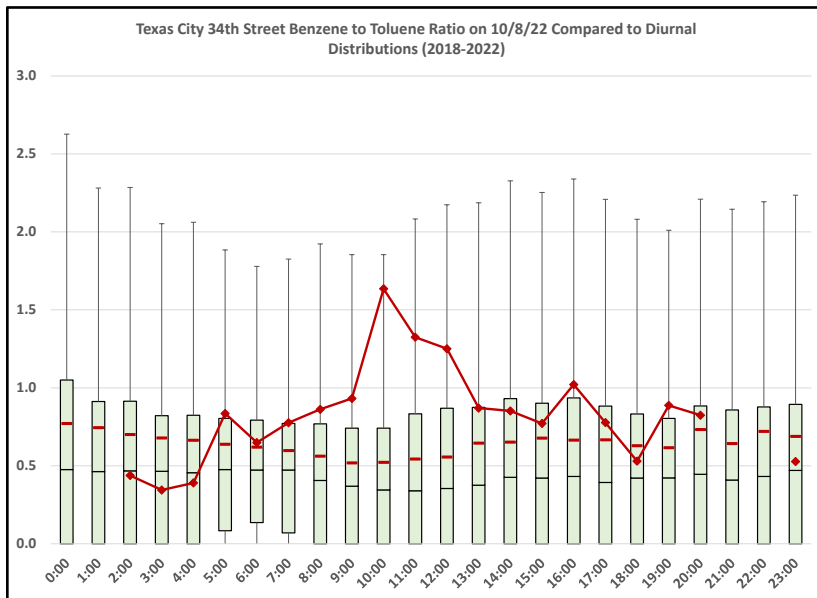


Figure 3-57: Benzene to Toluene Ratios at the Texas City 34th Street Monitoring Site on October 8, 2022

Figure 3-53: Benzene to Toluene Ratios at the Cesar Chavez Monitoring Site on October 8, 2022, Figure 3-54: Benzene to Toluene Ratios at the Channelview Monitoring Site on October 8, 2022, Figure 3-55: Benzene to Toluene Ratios at the Clinton Monitoring Site on October 8, 2022, Figure 3-56: Benzene to Toluene Ratios at the Oyster Creek Monitoring Site on October 8, 2022, Figure 3-57: Benzene to Toluene Ratios at the Texas City 34th Street Monitoring Site on October 8, 2022 each show elevated benzene to toluene ratios, near 1.5, consistent with ratios found in wildfire plumes.

3.7.2.4 Hourly Particulate Matter (PM) Measurements

Hourly measurements of fine particulate matter (PM_{2.5}) are often another important indicator that wildfire plumes have influenced air quality. While PM_{2.5} levels will vary from monitoring site to monitoring site, the existence of high levels of PM_{2.5} across a wide regional area on days with recognizable smoke plumes tends to support the hypothesis that wildfire emissions have influenced air quality. In this demonstration, the TCEQ has compared hourly PM_{2.5} measurements on the exceptional event days with historical hourly distributions (from the 2018-2022 ozone seasons) at various monitors across the HGB area. PM_{2.5} data only began to be collected in 2021 for the Westhollow monitoring site and in 2022 for the Bayland Park monitoring site. In the figures below, the box and whisker plots depict the historical distribution of hourly PM_{2.5} measurements for each hour of the day. The red line depicts the diurnal pattern of hourly PM_{2.5} measurements of that event day.

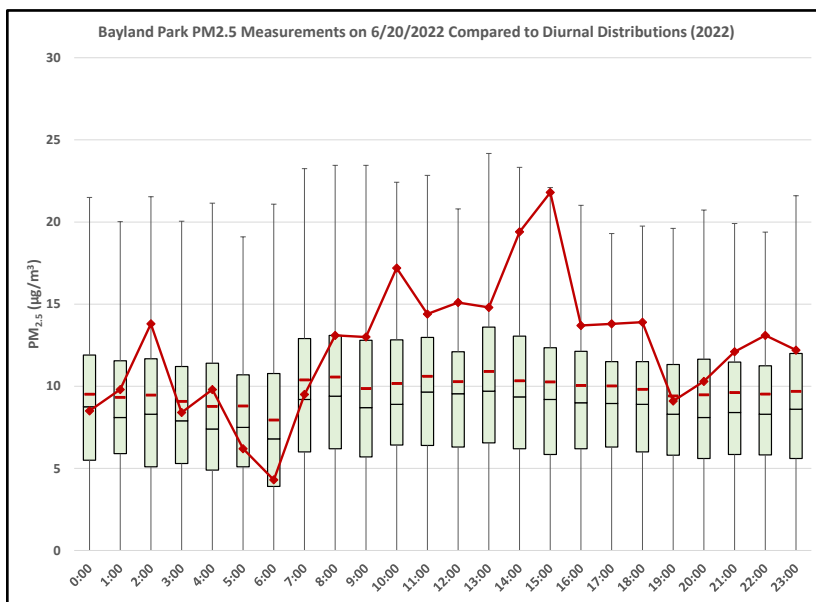


Figure 3-58: PM_{2.5} Levels at the Bayland Park Monitoring Site on June 20, 2022

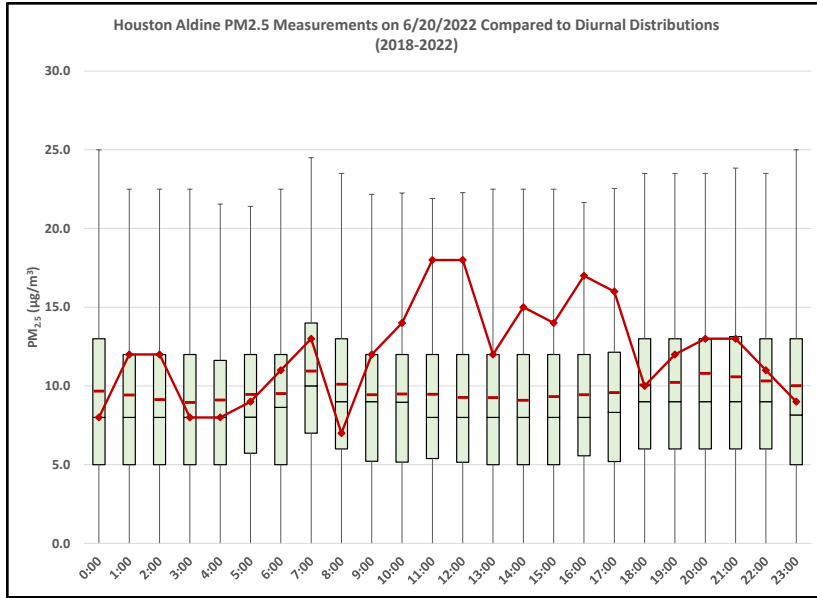


Figure 3-59: PM_{2.5} Levels at the Aldine Monitoring Site on June 20, 2022

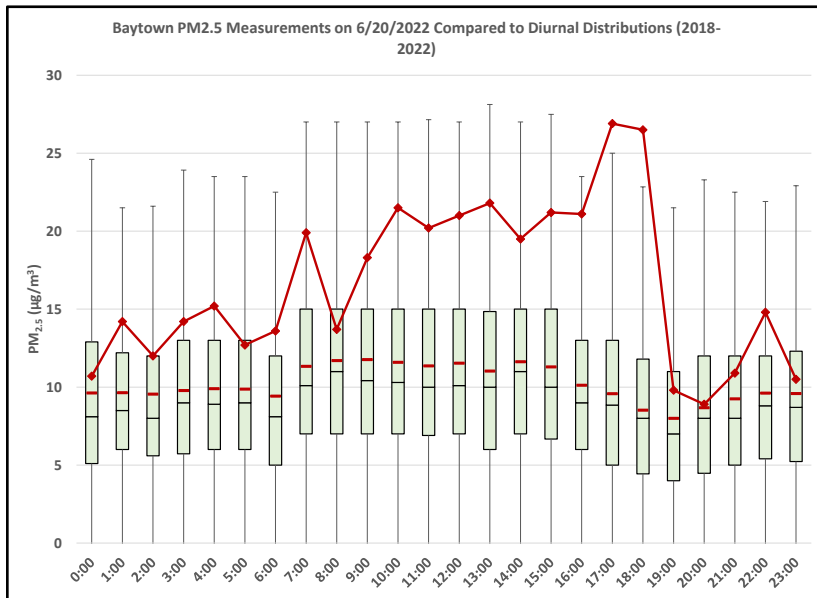


Figure 3-60: PM_{2.5} Levels at the Baytown Monitoring Site on June 20, 2022

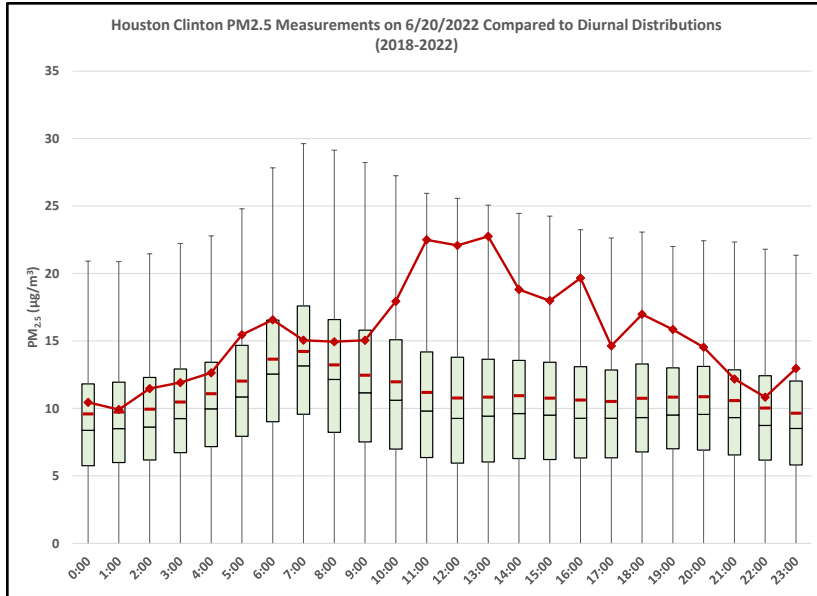


Figure 3-61: PM_{2.5} Levels at the Clinton Monitoring Site on June 20, 2022

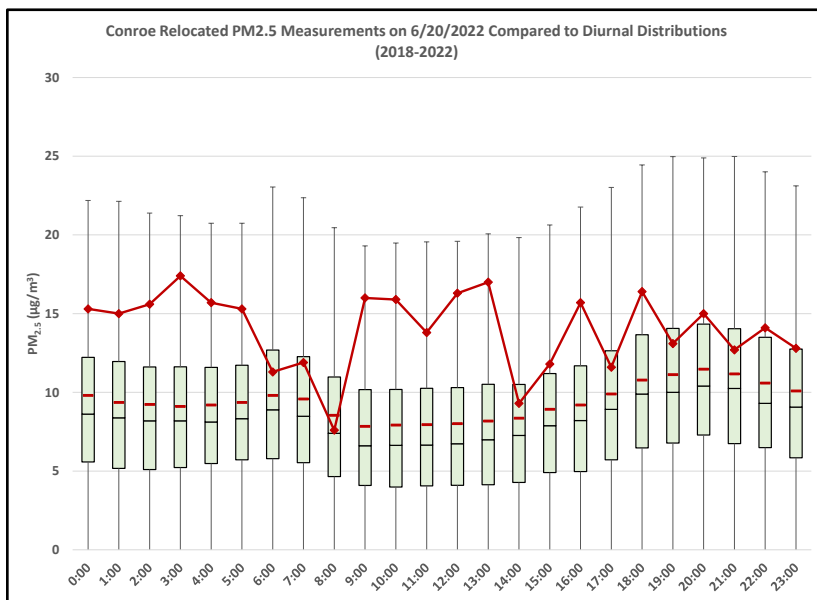


Figure 3-62: PM_{2.5} Levels at the Conroe-Relocated Monitoring Site on June 20, 2022

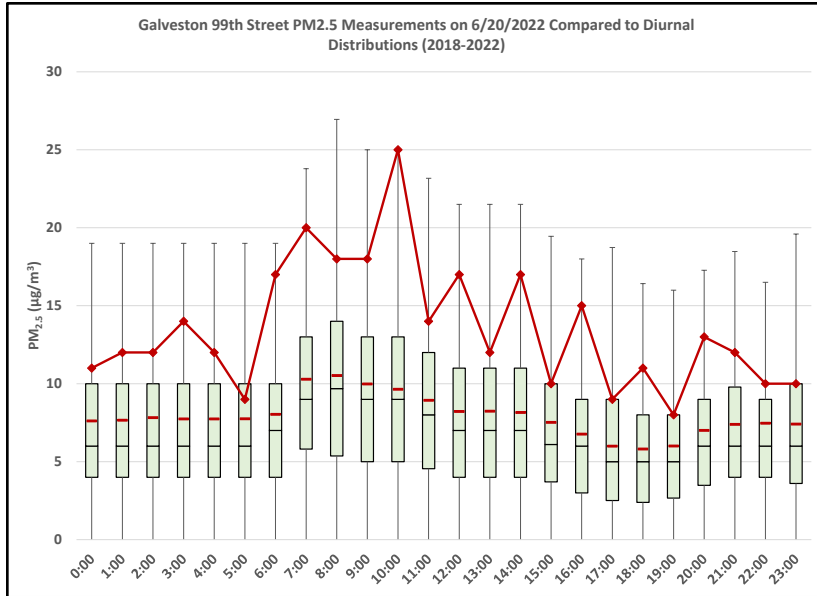


Figure 3-63: PM_{2.5} Levels at the Galveston 99th Street Monitoring Site on June 20, 2022

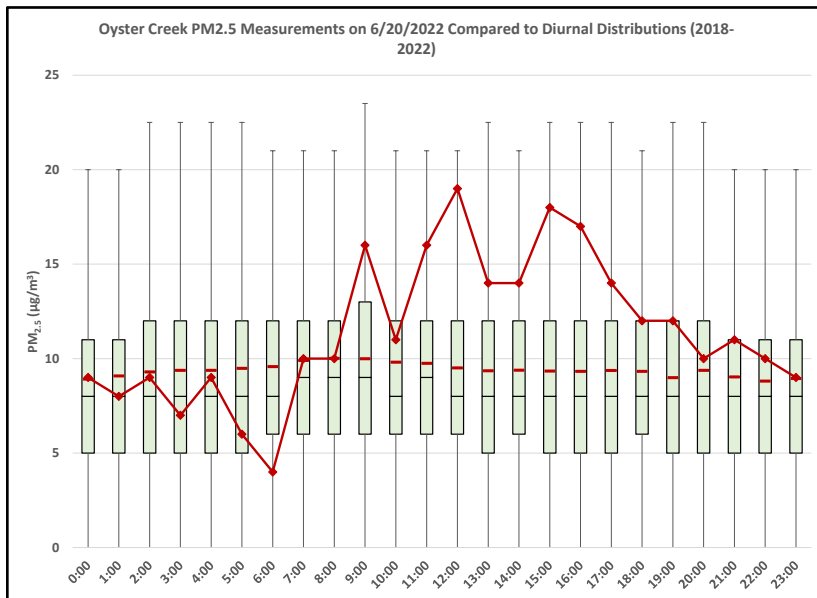


Figure 3-64: PM_{2.5} Levels at the Oyster Creek Monitoring Site on June 20, 2022

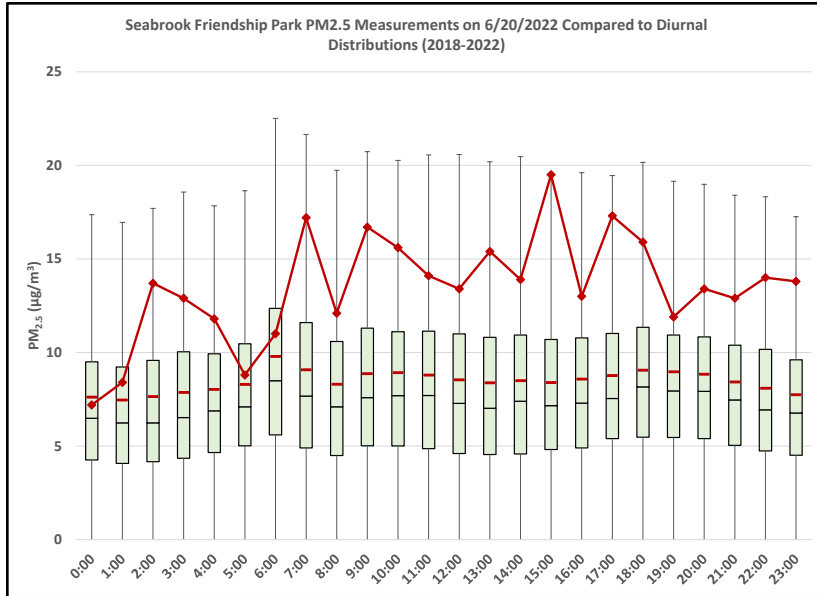


Figure 3-65: PM_{2.5} Levels at the Seabrook Friendship Park Monitoring Site on June 20, 2022

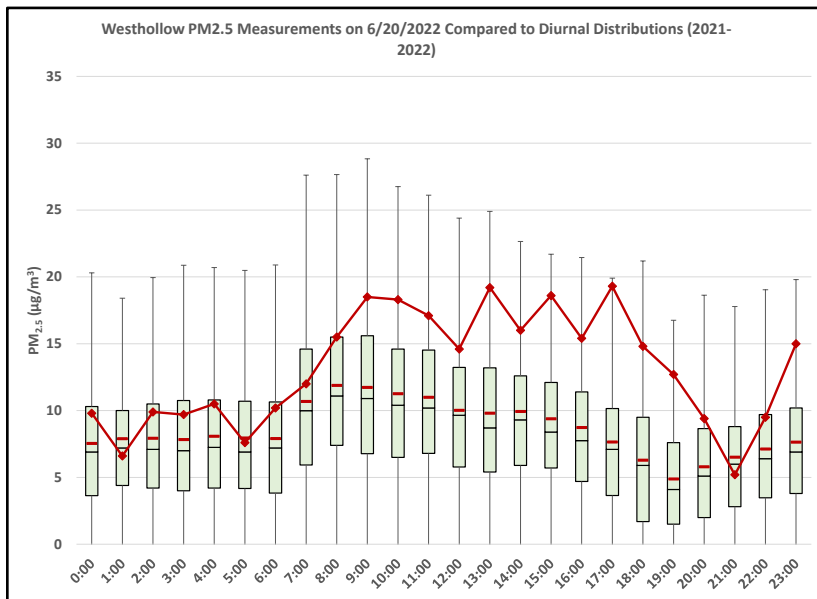


Figure 3-66: PM_{2.5} Levels at the Westhollow Monitoring Site on June 20, 2022

Figure 3-58: PM_{2.5} Levels at the Bayland Park Monitoring Site on June 20, 2022, Figure 3-59: PM_{2.5} Levels at the Aldine Monitoring Site on June 20, 2022, Figure 3-60: PM_{2.5} Levels at the Baytown Monitoring Site on June 20, 2022, Figure 3-61: PM_{2.5} Levels at the Clinton Monitoring Site on June 20, 2022, Figure 3-62: PM_{2.5} Levels at the Conroe-Relocated Monitoring Site on June 20, 2022, Figure 3-63: PM_{2.5} Levels at the Galveston 99th Street Monitoring Site on June 20, 2022, Figure 3-64: PM_{2.5} Levels at the Oyster Creek Monitoring Site on June 20, 2022, Figure 3-65: PM_{2.5} Levels at the Seabrook Friendship Park Monitoring Site on June 20, 2022, and Figure 3-66: PM_{2.5} Levels at the Westhollow Monitoring Site on June 20, 2022 all show comparatively high PM_{2.5}

measurements across the HGB area, and support the demonstration of an exceptional event.

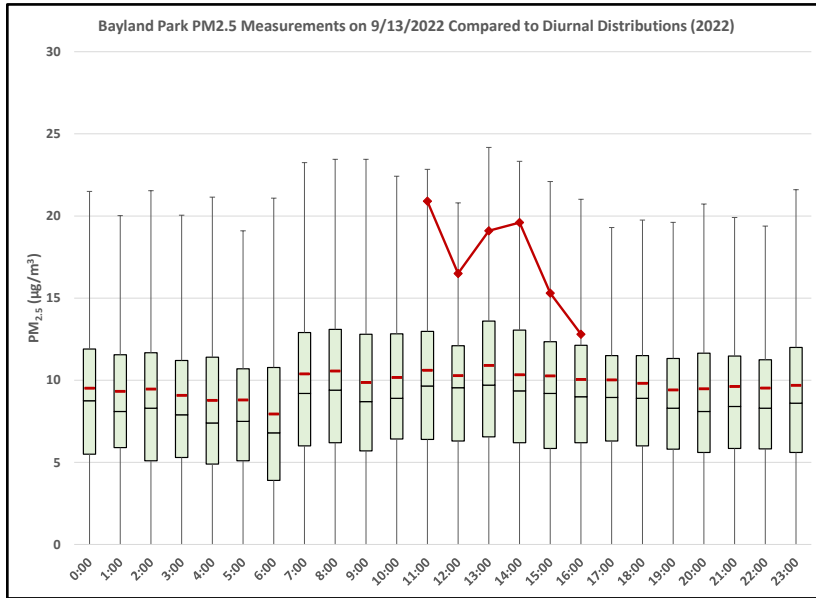


Figure 3-67: PM_{2.5} Levels at the Bayland Park Monitoring Site on September 13, 2022

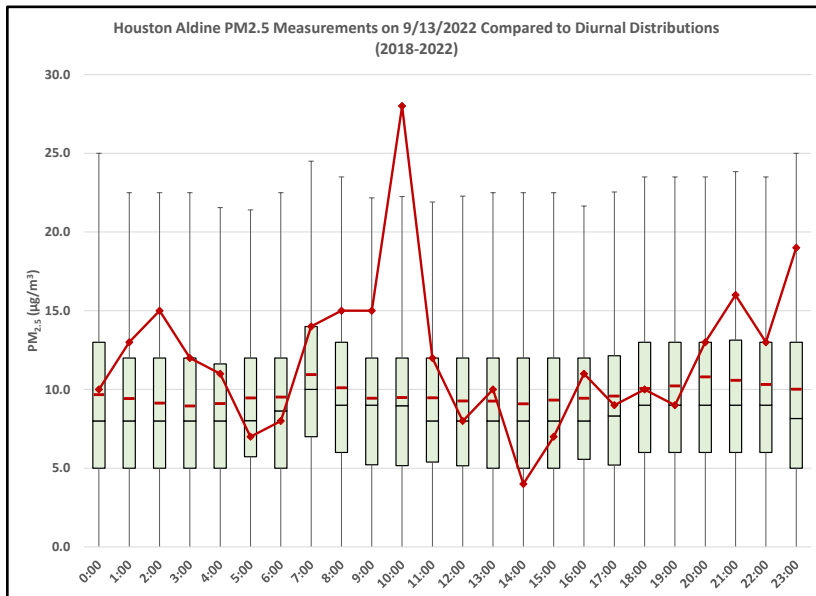


Figure 3-68: PM_{2.5} Levels at the Aldine Monitoring Site on September 13, 2022

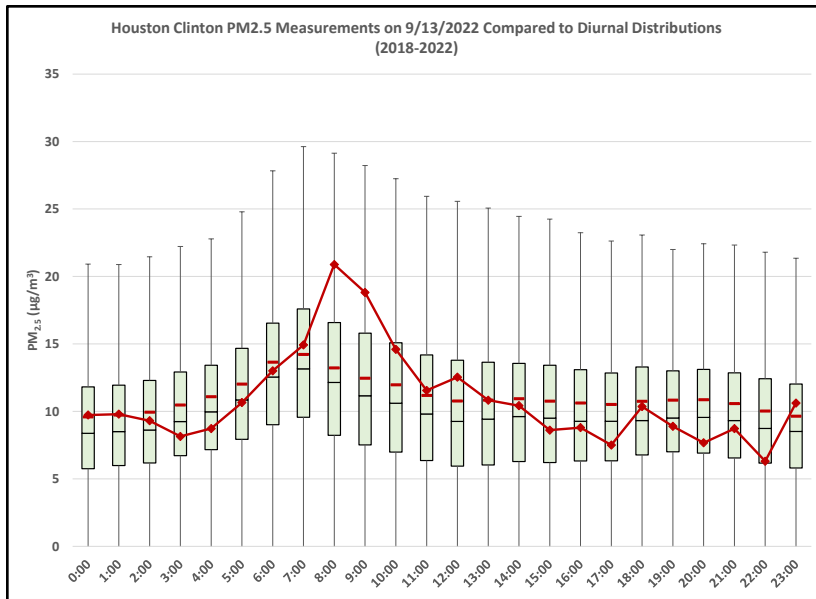


Figure 3-69: PM_{2.5} Levels at the Clinton Monitoring Site on September 13, 2022

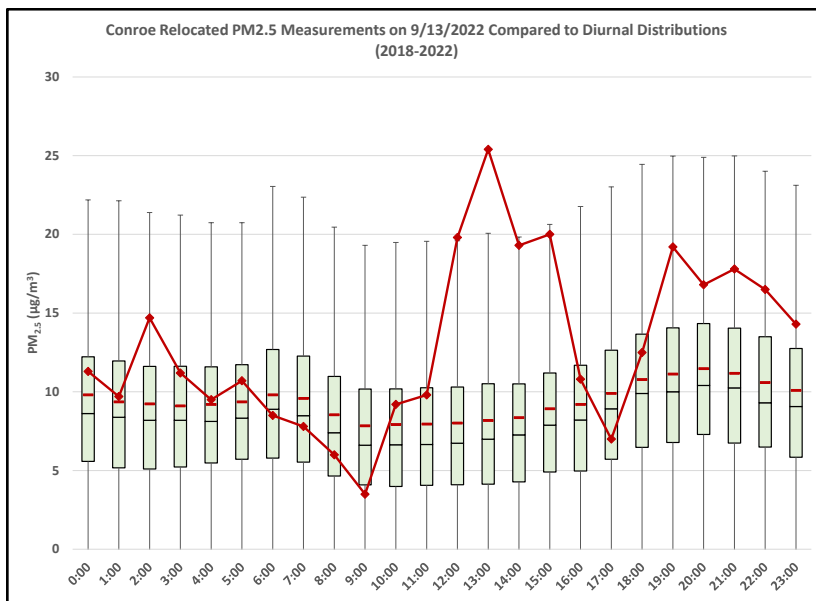


Figure 3-70: PM_{2.5} Levels at the Conroe-Relocated Monitoring Site on September 13, 2022

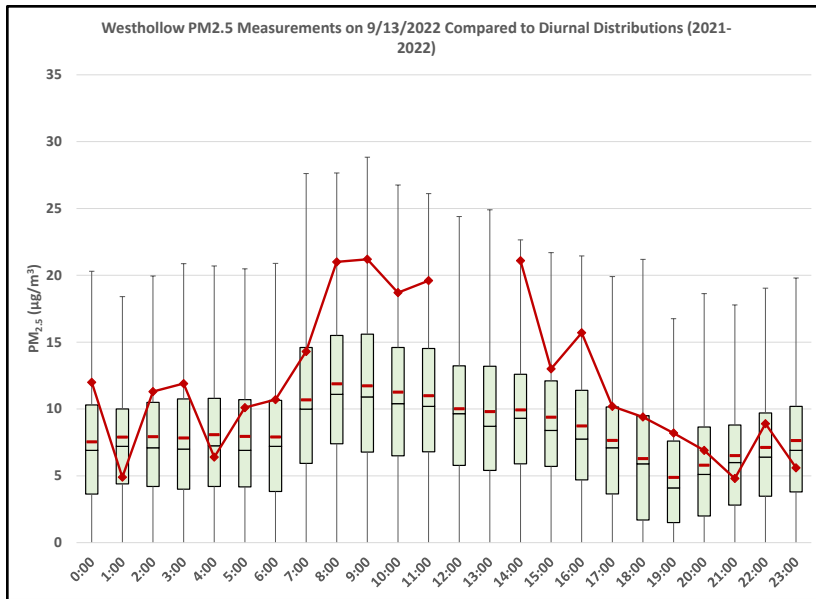


Figure 3-71: PM_{2.5} Levels at the Westhollow Monitoring Site on September 13, 2022

Figure 3-67: PM_{2.5} Levels at the Bayland Park Monitoring Site on September 13, 2022, Figure 3-68: PM_{2.5} Levels at the Aldine Monitoring Site on September 13, 2022, Figure 3-69: PM_{2.5} Levels at the Clinton Monitoring Site on September 13, 2022, Figure 3-70: PM_{2.5} Levels at the Conroe-Relocated Monitoring Site on September 13, 2022, and Figure 3-71: PM_{2.5} Levels at the Westhollow Monitoring Site on September 13, 2022 all show comparatively high PM_{2.5} measurements across the HGB area, and support the demonstration of an exceptional event.

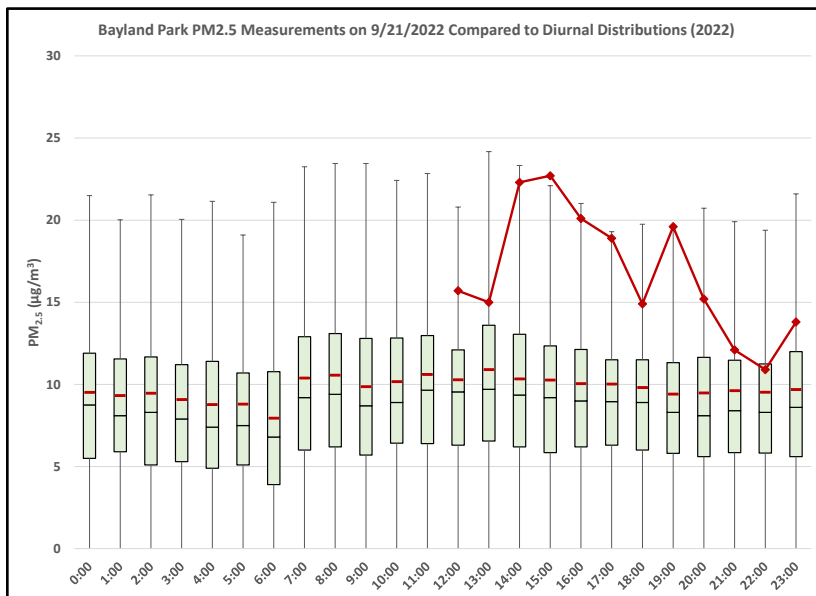


Figure 3-72: PM_{2.5} Levels at the Bayland Park Monitoring Site on September 21, 2022

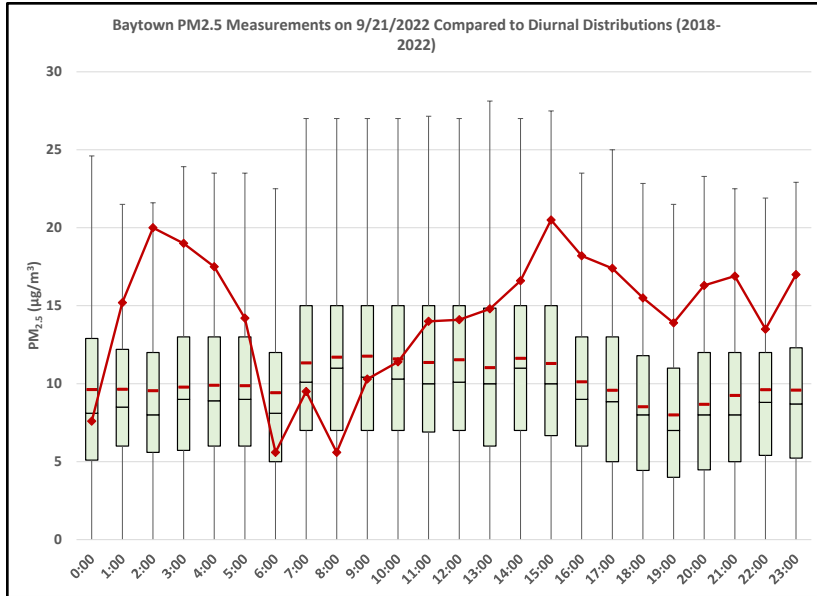


Figure 3-73: PM_{2.5} Levels at the Baytown Monitoring Site on September 21, 2022

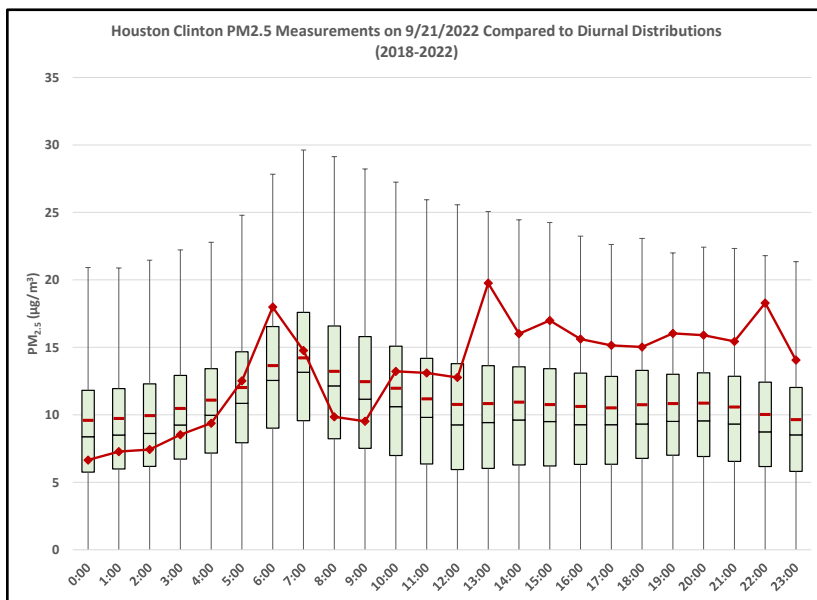


Figure 3-74: PM_{2.5} Levels at the Clinton Monitoring Site on September 21, 2022

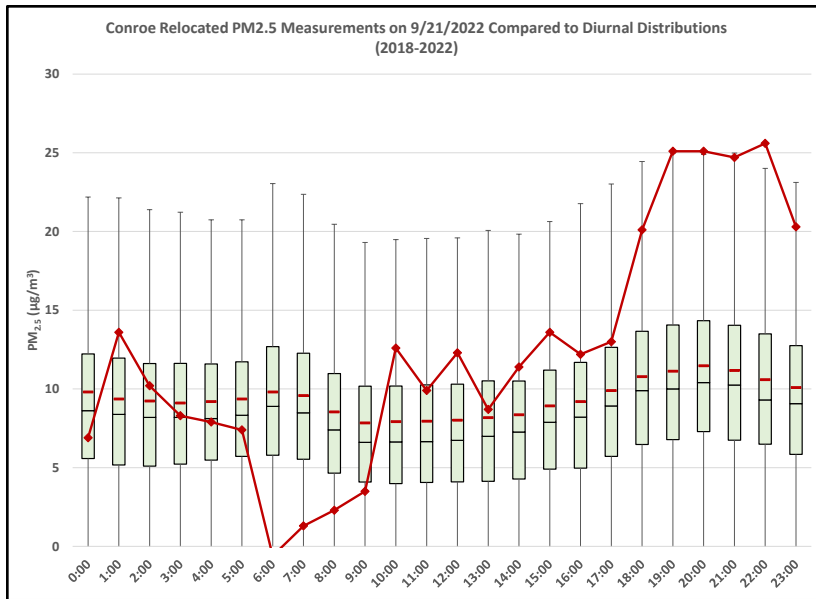


Figure 3-75: PM_{2.5} Levels at the Conroe-Relocated Monitoring Site on September 21, 2022

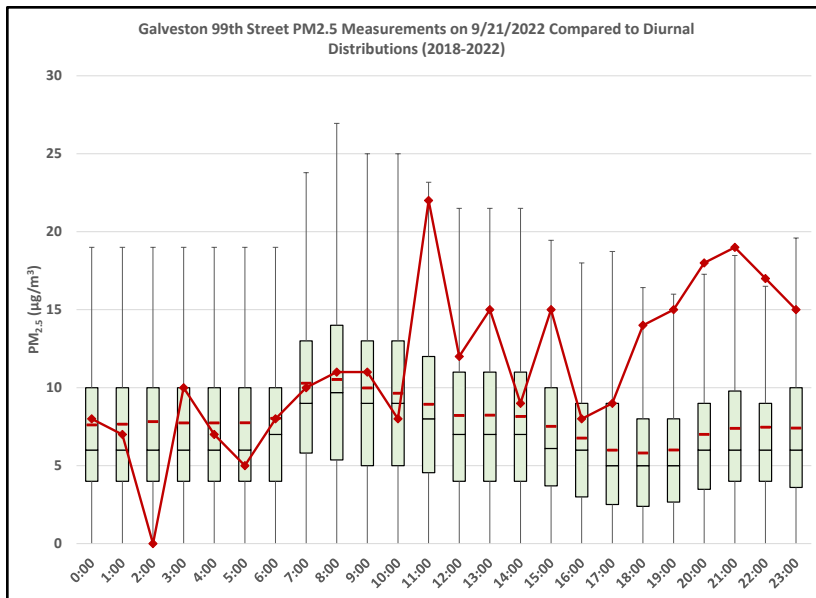


Figure 3-76: PM_{2.5} Levels at the Galveston 99th Street Monitoring Site on September 21, 2022

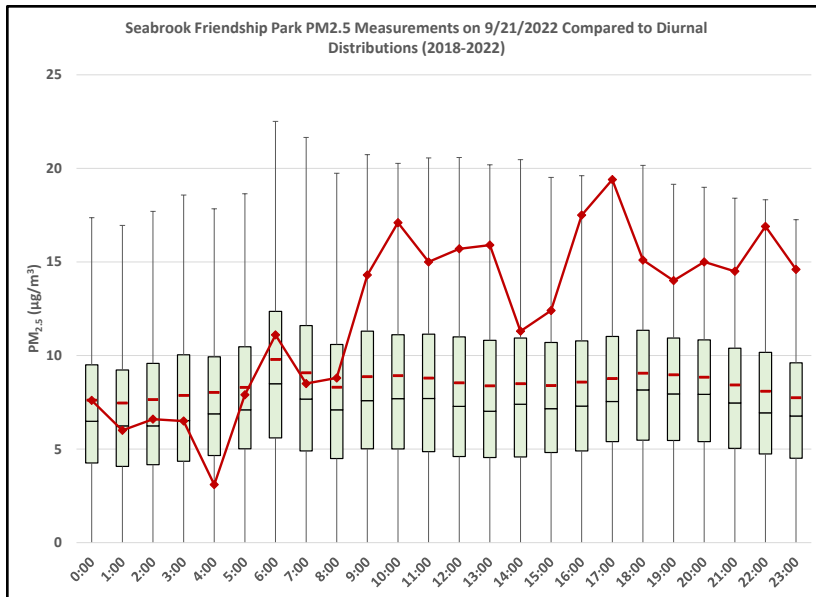


Figure 3-77: PM_{2.5} Levels at the Seabrook Friendship Park Monitoring Site on September 21, 2022

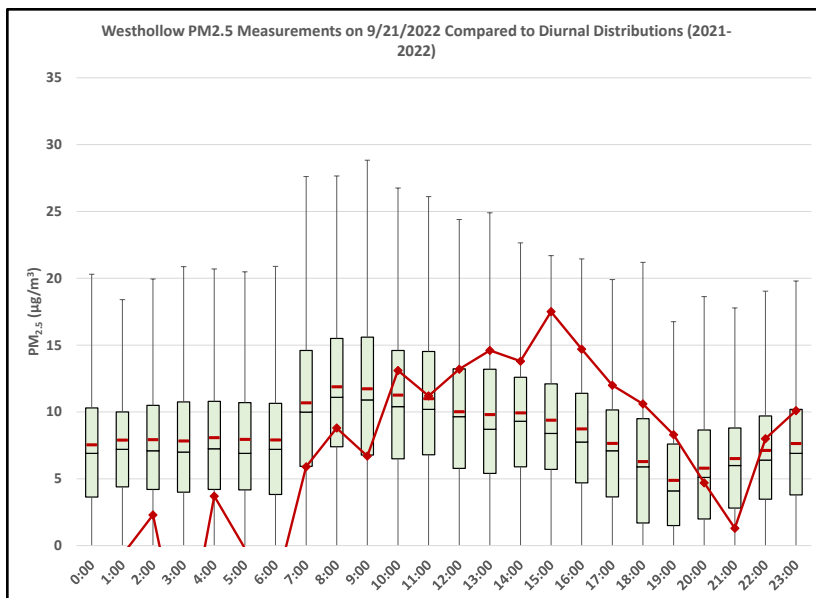


Figure 3-78: PM_{2.5} Levels at the Westhollow Monitoring Site on September 21, 2022

Figure 3-72: PM_{2.5} Levels at the Bayland Park Monitoring Site on September 21, 2022, Figure 3-73: PM_{2.5} Levels at the Baytown Monitoring Site on September 21, 2022, Figure 3-74: PM_{2.5} Levels at the Clinton Monitoring Site on September 21, 2022, Figure 3-75: PM_{2.5} Levels at the Conroe-Relocated Monitoring Site on September 21, 2022, Figure 3-76: PM_{2.5} Levels at the Galveston 99th Street Monitoring Site on September 21, 2022, Figure 3-77: PM_{2.5} Levels at the Seabrook Friendship Park Monitoring Site on September 21, 2022, and Figure 3-78: PM_{2.5} Levels at the Westhollow Monitoring Site on September 21, 2022 all show comparatively high PM_{2.5} measurements across the HGB area, and support the demonstration of an exceptional event.

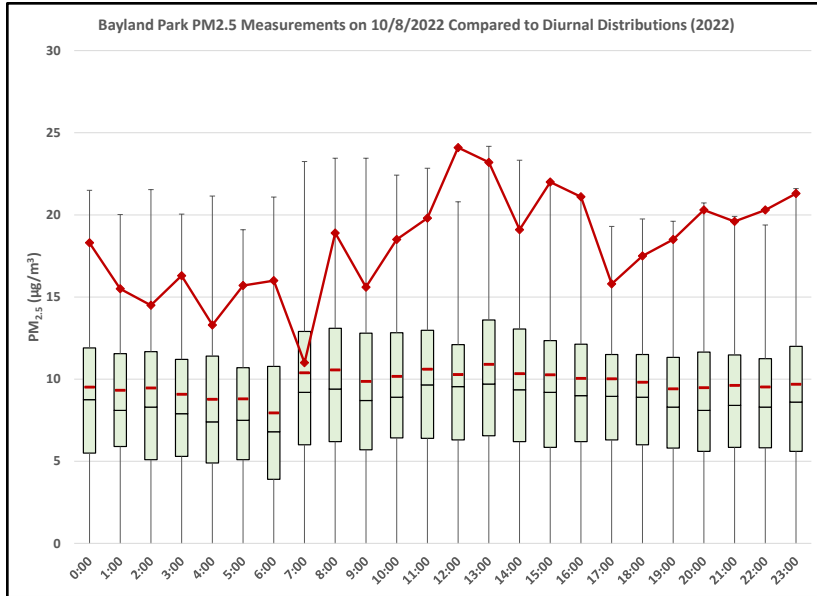


Figure 3-79: PM_{2.5} Levels at the Bayland Park Monitoring Site on October 8, 2022

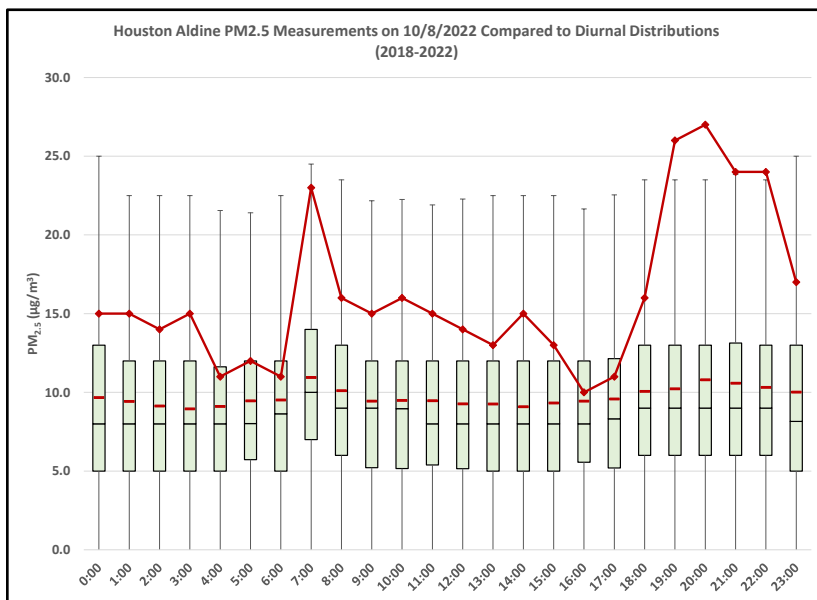


Figure 3-80: PM_{2.5} Levels at the Aldine Monitoring Site on October 8, 2022

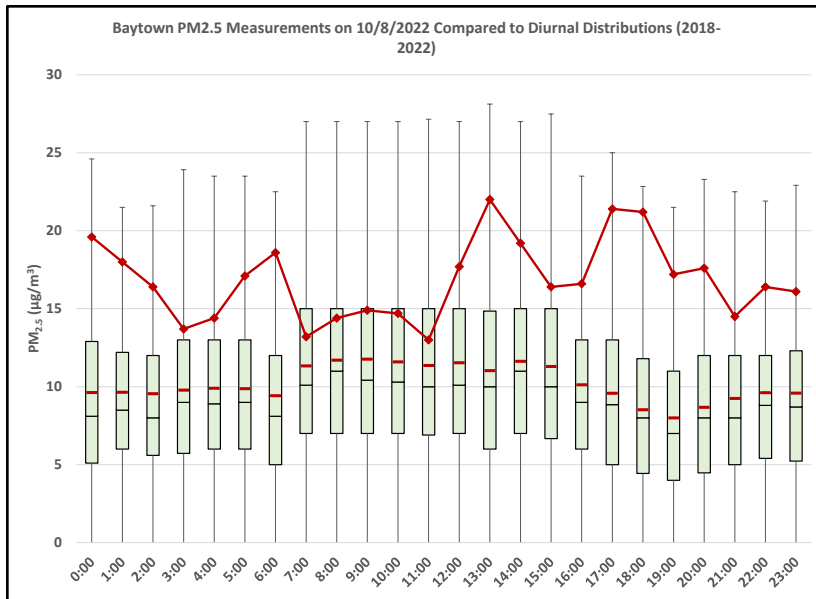


Figure 3-81: PM_{2.5} Levels at the Baytown Monitoring Site on October 8, 2022

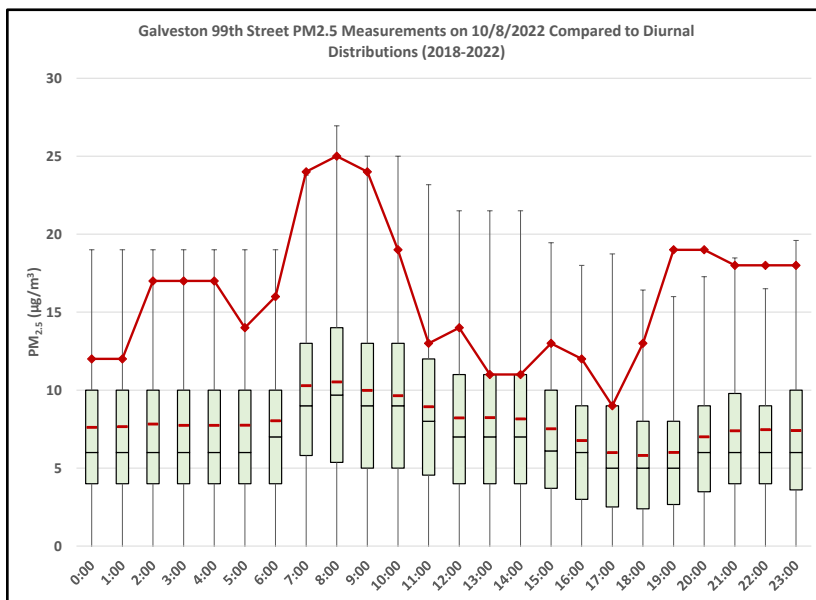


Figure 3-82: PM_{2.5} Levels at the Galveston 99th Street Monitoring Site on October 8, 2022

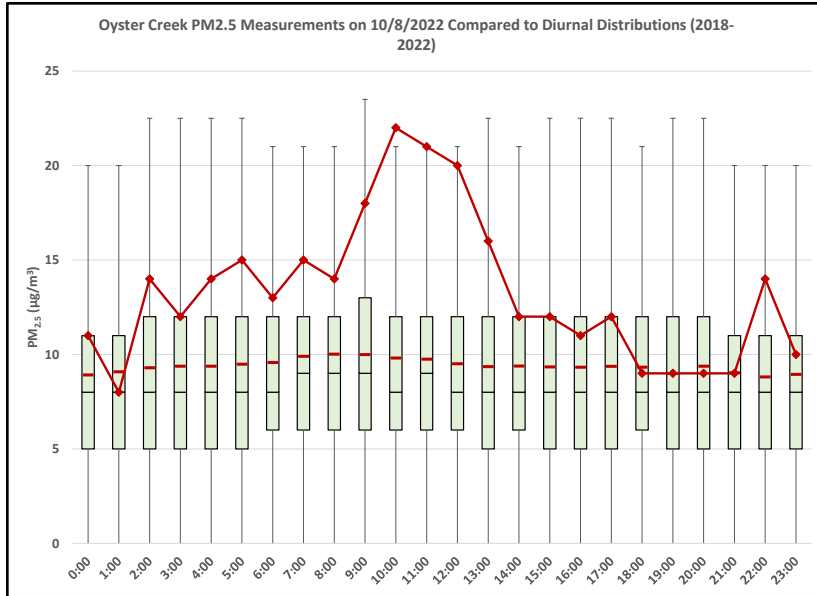


Figure 3-83: PM_{2.5} Levels at the Oyster Creek Monitoring Site on October 8, 2022

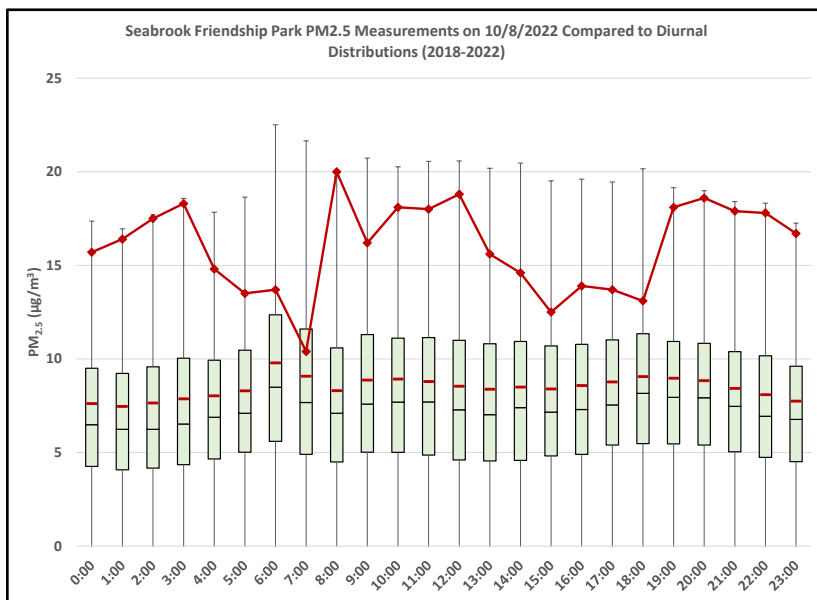


Figure 3-84: PM_{2.5} Levels at the Seabrook Friendship Park Monitoring Site on October 8, 2022

Figure 3-79: PM_{2.5} Levels at the Bayland Park Monitoring Site on October 8, 2022, Figure 3-80: PM_{2.5} Levels at the Aldine Monitoring Site on October 8, 2022, Figure 3-81: PM_{2.5} Levels at the Baytown Monitoring Site on October 8, 2022, Figure 3-82: PM_{2.5} Levels at the Galveston 99th Street Monitoring Site on October 8, 2022, Figure 3-83: PM_{2.5} Levels at the Oyster Creek Monitoring Site on October 8, 2022, and Figure 3-84: PM_{2.5} Levels at the Seabrook Friendship Park Monitoring Site on October 8, 2022 all show comparatively high PM_{2.5} measurements across the HGB area, and support the demonstration of an exceptional event.

3.7.2.5 Speciated PM_{2.5} Measurements

In support of this demonstration, the TCEQ analyzed speciated PM_{2.5} data from the North Wayside (northeast Houston) and Clinton (west end of Houston Ship Channel) monitoring sites. The analysis looked at organic carbon, potassium ion, and potassium data for September and October 2022. Data was not available for the June 20, 2022 exceptional event because it was not a scheduled sampling date. Validated data from the Clinton monitoring site was only available for one exceptional event day - October 8, 2022. Speciated monitoring only began at the North Wayside monitoring in July 2022 so no speciated data was available for the June 20, 2022, exceptional event. Organic carbon and potassium are known as possible markers for biomass burning. Data from the North Wayside monitoring site includes speciated data specifically for September 13, September 21, and October 8, 2022. Data from the Clinton monitoring site includes speciated data specifically for October 8, 2022.

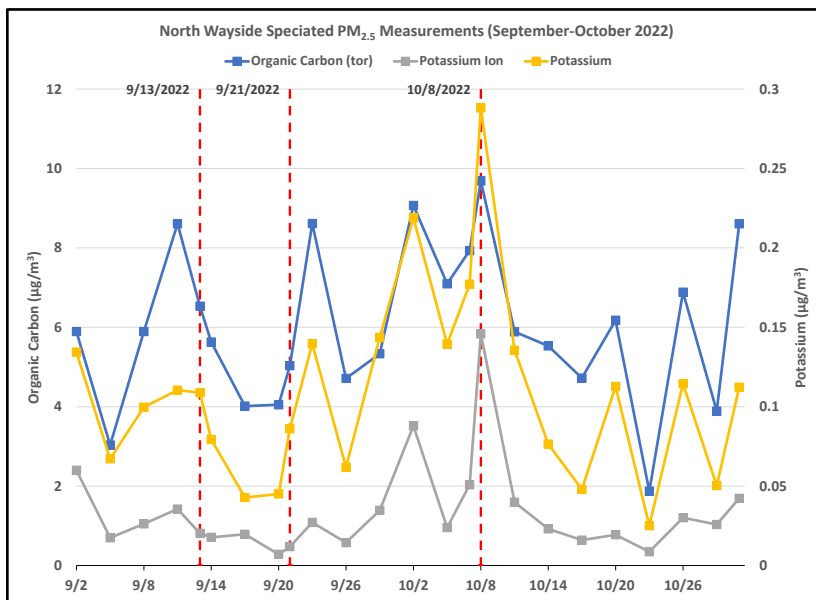


Figure 3-85: Speciated PM_{2.5} Data at the North Wayside Monitoring Site

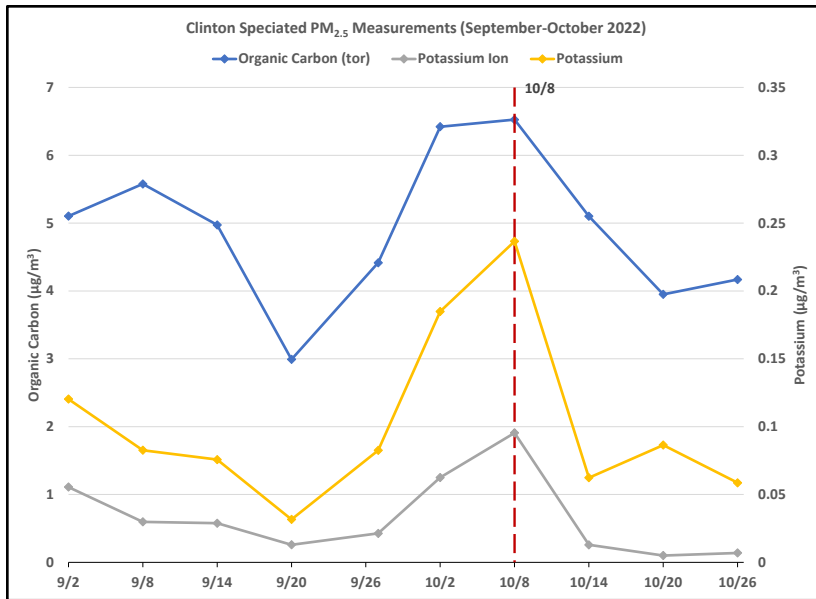


Figure 3-86: Speciated PM_{2.5} Measurements at the Clinton Monitoring Site

Figure 3-85: *Speciated PM_{2.5} Data at the North Wayside Monitoring Site* shows moderate to high levels of potassium and organic carbon on all exceptional event days in September and October 2022 and the jump in potassium and organic carbon measurements on October 8, 2022, shows that air quality on that day was influenced by biomass burning. Likewise, Figure 3-86: *Speciated PM_{2.5} Measurements at the Clinton Monitoring Site* shows excellent support for an exceptional event on October 8, 2022.

3.7.2.6 Ozone and PM_{2.5} Time Series

The TCEQ also analyzed time series of hourly ozone and PM_{2.5} for the week before and after each exceptional event day at the Bayland Park monitoring site and hourly ozone for the Harvard Street monitoring site.

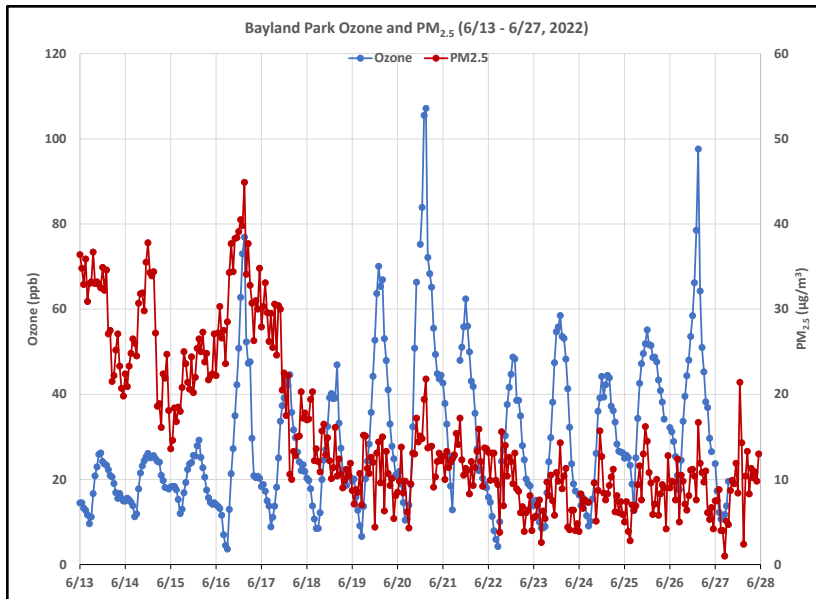


Figure 3-87: Bayland Park Ozone and PM_{2.5} Time Series for June 20, 2022

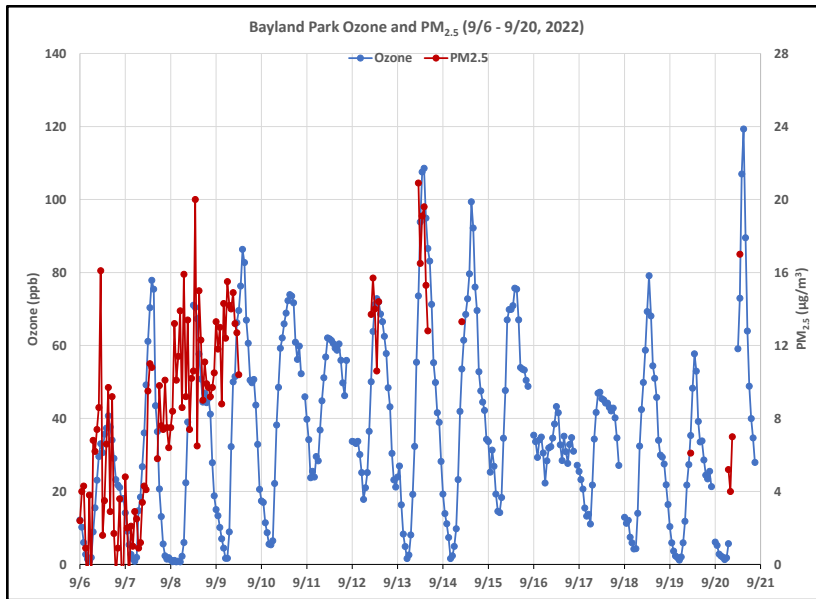


Figure 3-88: Bayland Park Ozone and PM_{2.5} Time Series for September 13, 2022

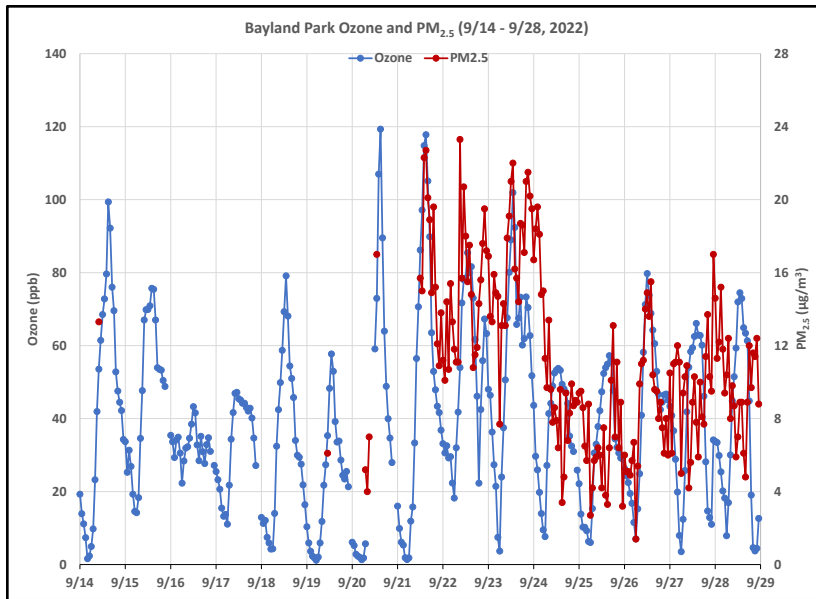


Figure 3-89: Bayland Park Ozone and PM_{2.5} Time Series for September 21, 2022

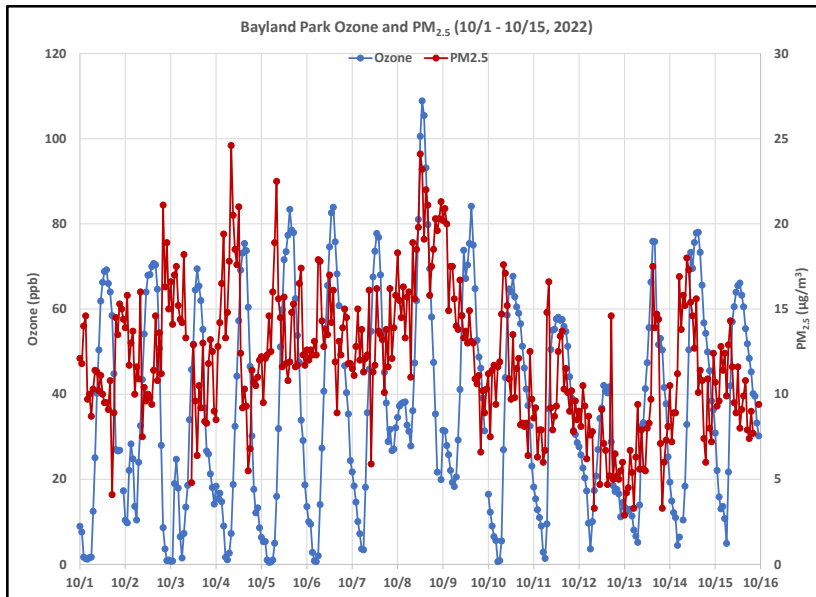


Figure 3-90: Bayland Park Ozone and PM_{2.5} Time Series for October 8, 2022

Figure 3-87: Bayland Park Ozone and PM_{2.5} Time Series for June 20, 2022, Figure 3-88: Bayland Park Ozone and PM_{2.5} Time Series for September 13, 2022, Figure 3-89: Bayland Park Ozone and PM_{2.5} Time Series for September 21, 2022, and Figure 3-90: Bayland Park Ozone and PM_{2.5} Time Series for October 8, 2022 show that maximum hourly ozone values stand out from most days before and after each exceptional event day. These figures also show that maximum daily PM_{2.5} values coincide with maximum daily ozone values. This suggests that the maximum daily ozone and PM_{2.5} values are related and caused by wildfires.

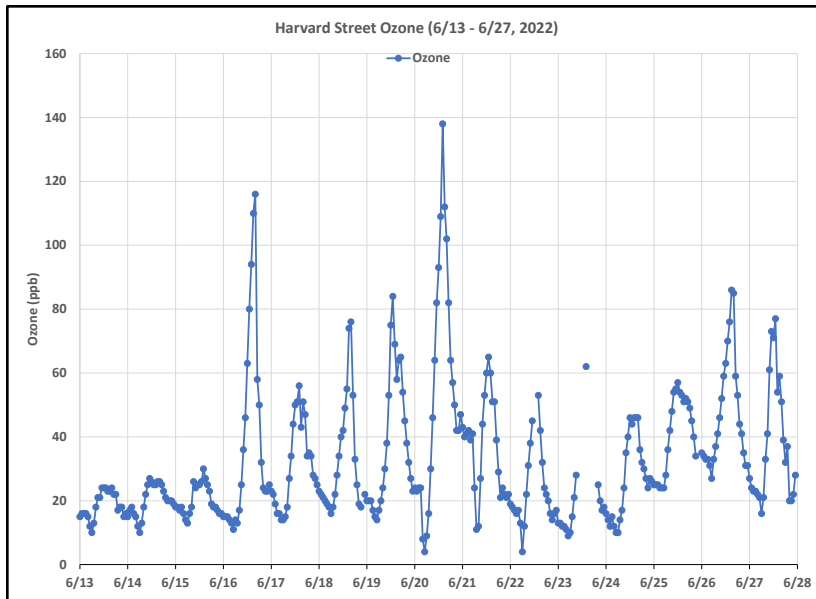


Figure 3-91: Harvard Street Ozone Time Series for June 20, 2022

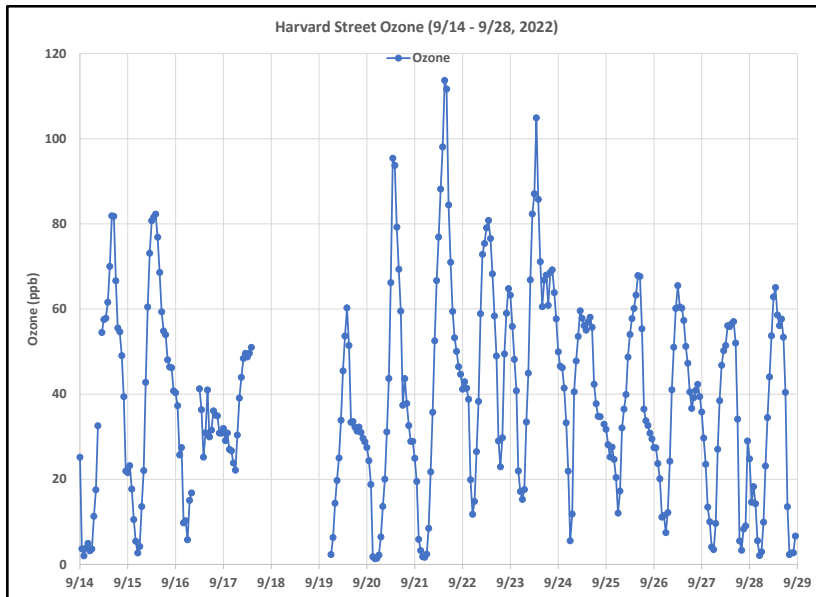


Figure 3-92: Harvard Street Ozone Time Series for September 21, 2022

Figure 3-91: *Harvard Street Ozone Time Series for June 20, 2022* and Figure 3-92: *Harvard Street Ozone Time Series for September 21, 2022* show time series for the June 20, 2022, and September 21, 2022 events at the Harvard Street monitor. The maximum hourly ozone value stands out on both exceptional event days.

3.7.2.7 Biomass Burning Indicator

The TCEQ also looked at data from the Black and Brown Carbon (BC2) project for the days of interest. The BC2 project assesses the impacts of biomass burning (BB) observed at select monitoring sites in Texas including HGB. BB, which can include wildfires, agricultural burning, and residential wood smoke, emits PM and a wide range of gas-phase pollutants. PM emissions from BB are predominantly carbonaceous, with aerosol absorbance from both black carbon (elemental carbon) and brown carbon

(light-absorbing organic carbon). This project is managed collaboratively through the University of Houston and Baylor University (Flynn, et.al., 2021). It uses Tricolor Absorption Photometer and nephelometer instruments to identify signals of BB events. The project identified BB events for the ozone season of 2022 to determine whether BB events coincided with the days of interest (June 20, September 13, September 21, and October 8, 2022). The project did not identify BB events on or ± 1 day of June 20, 2022. For September 13, September 21, and October 8, 2022, events were identified across the Houston network either on or within or ± 1 day of interest; so, according to this method of sampling, three of the four days of interest had BB influence within a day. The reason for doing ± 1 day is to allow for time difference in ozone chemistry in Houston versus plume transport.

The table below illustrates that BB influence was identified at all three Houston BC2 sites (Aldine, Galveston, and Liberty) on and around the September 13, 2022. For the September 21, 2022, BB influence was identified immediately following on September 22, 2022, at Aldine and Liberty. For October 8, 2022, BB influence was identified at all three Houston BC2 sites (Aldine, Galveston, and Liberty). Identification of BB influence at multiple sites gives a high degree of confidence that the BB plume had widespread influence. This is confirmed by the smoke products and back trajectories which are summarized in Table 3-3: *Biomass Burning Events at Each BC2 Site in Houston ± 1 Day of Event Days*. BB events identified at each BC2 site on the days of interest are marked in bold.

The Absorption Angström Exponent (AAE) is used to track the influence of BB through the quantification of the wavelength dependence which results in $AAE > 1$, while fossil combustion from motor vehicles has little wavelength dependence and an $AAE \sim 1$. The Scattering Angström Exponent (SAE) is used to track the influence of dust through the quantification of the wavelength dependence of aerosol scattering. Larger particles have an SAE approaching zero while smaller particles have an enhanced SAE. The AAE and SAE are monitored in real time to characterize the influence of wildfires and dust on urban air quality in Texas. The AAE threshold for each site is listed on the left column with site name. An $SAE > 1.0$ indicates limited influence from dust. HMS is the NOAA Hazard Mapping System; the Yes or No indicates whether there was smoke aloft. The back trajectory through smoke indicates whether the back trajectory from the site at that time traveled through an HMS smoke plume.

Table 3-3: Biomass Burning Events at Each BC2 Site in Houston ± 1 Day of Event Days

Site	Start	Stop	Average AAE	Average SAE	HMS Over head	Back Trajectory through Smoke
Aldine (AAE>1.32)	9/12/2022 22:20	9/13/2022 3:30	1.45	1.86	Yes	Yes
Aldine (AAE>1.32)	9/13/2022 20:35	9/14/2022 0:20	1.35	1.83	Yes	Yes
Aldine (AAE>1.32)	9/14/2022 22:25	9/15/2022 5:05	1.33	2.01	No	Yes
Aldine (AAE>1.32)	9/22/2022 18:35	9/23/2022 0:15	1.63	1.67	Yes	Yes

Site	Start	Stop	Average AAE	Average SAE	HMS Over head	Back Trajectory through Smoke
Aldine (AAE>1.32)	10/7/2022 15:50	10/7/2022 22:00	1.45	1.75	No	Yes
Aldine (AAE>1.32)	10/8/2022 19:35	10/8/2022 23:55	1.43	1.84	Yes	Yes
Galveston (AAE>1.14)	9/14/2022 0:25	9/14/2022 8:15	1.27	1.27	No	Yes
Galveston (AAE>1.14)	10/8/2022 16:05	10/9/2022 4:15	1.46	1.73	Yes	Yes
Galveston (AAE>1.14)	10/9/2022 21:00	10/10/2022 12:00	1.26	1.60	Yes	Yes
Liberty (AAE>1.18)	9/12/2022 14:10	9/12/2022 22:15	1.26	1.90	Yes	Yes
Liberty (AAE>1.18)	9/13/2022 20:05	9/14/2022 8:40	1.33	2.00	Yes	Yes
Liberty (AAE>1.18)	9/14/2022 20:30	9/15/2022 9:55	1.52	2.13	No	Yes
Liberty (AAE>1.18)	9/22/2022 18:25	9/23/2022 7:55	1.37	1.82	Yes	Yes
Liberty (AAE>1.18)	9/23/2022 18:00	9/24/2022 3:55	1.47	1.98	Yes	Yes
Liberty (AAE>1.18)	10/8/2022 0:05	10/8/2022 13:55	1.28	1.95	Yes	Yes

Figure 3-93: *Time Series of Aerosol Optical Properties at Aldine around September 13, 2022*, Figure 3-94: *Time Series of Aerosol Optical Properties at Liberty around September 13, 2022*, and Figure 3-95: *Time Series of Aerosol Optical Properties at Galveston around September 13, 2022* show gray shading for BB events. The graphs shows that the Aldine, Liberty, and Galveston sites had an influence of BB on or around September 13, 2022. Figure 3-96: *HMS and Back Trajectories on September 13, 2022* illustrates that the entire region had smoke aloft. The fire spots indicate potential influence of long-range transport from other states.

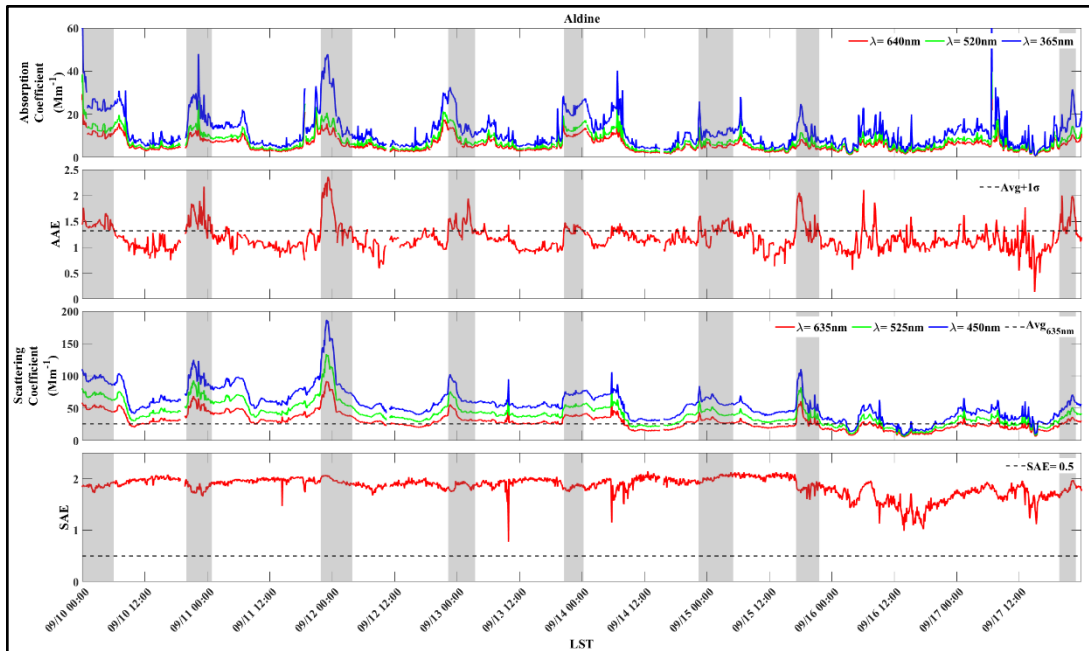


Figure 3-93: Time Series of Aerosol Optical Properties at Aldine around September 13, 2022

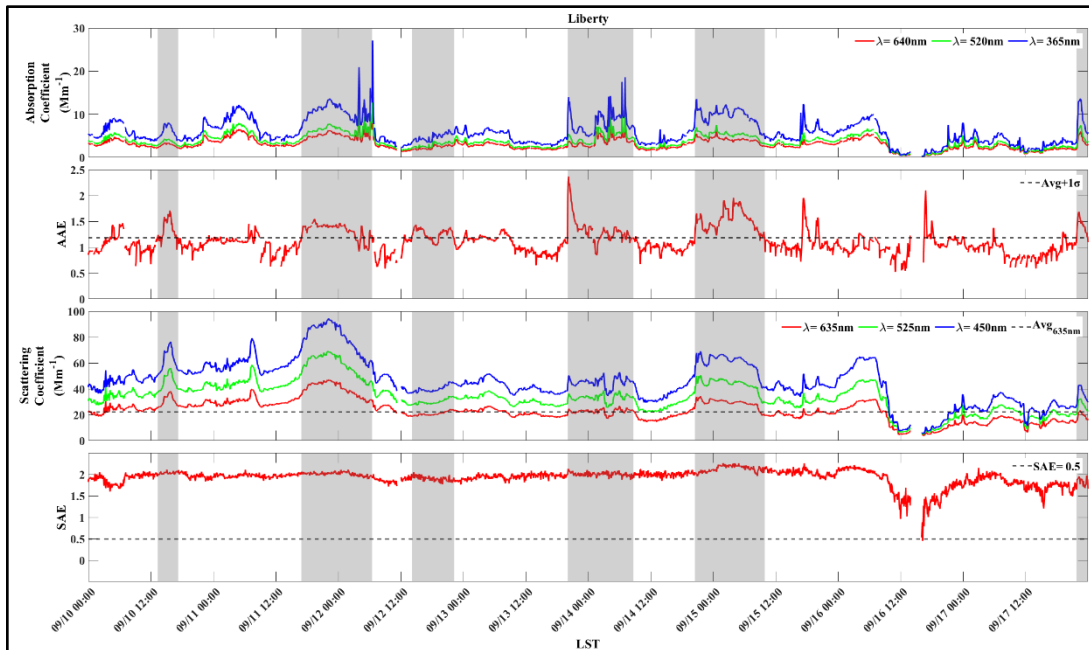


Figure 3-94: Time Series of Aerosol Optical Properties at Liberty around September 13, 2022

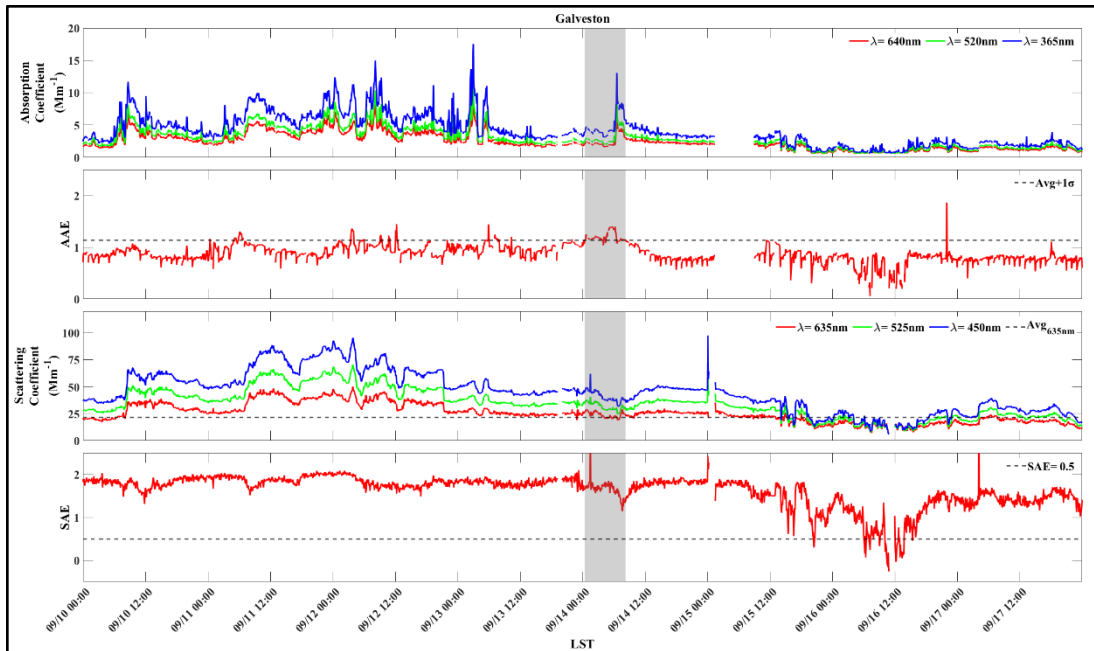


Figure 3-95: Time Series of Aerosol Optical Properties at Galveston around September 13, 2022

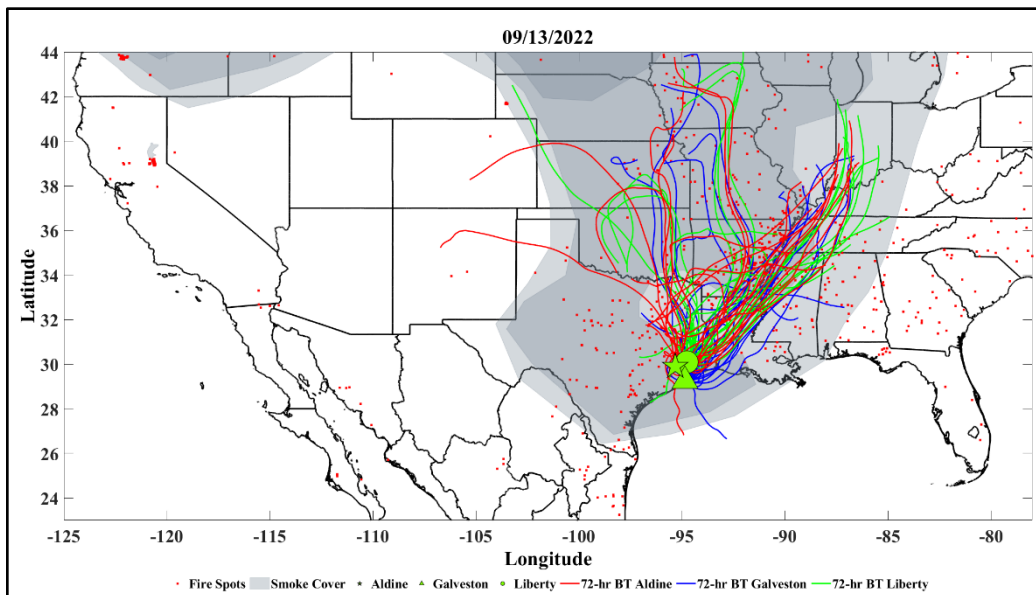


Figure 3-96: HMS and Back Trajectories on September 13, 2022

Figure 3-97: *Time Series of Aerosol Optical Properties at Aldine around September 21, 2022* and Figure 3-98: *Time Series of Aerosol Optical Properties at Liberty around September 21, 2022* show gray shading for BB events. The graphs show that Aldine and Liberty had an influence of BB on or around September 21, 2022. Figure 3-99: *Time series of Aerosol Optical Properties at Galveston around September 21, 2022* shows Galveston may not have had a BB signature on September 21, but there was a continental influence to the aerosol optical properties, which was most likely black carbon for absorbing aerosol as indicated by lower AAE value that remained around 1.

Figure 3-100: *HMS and Back Trajectories on September 21, 2022* illustrates that the entire region had smoke aloft. The fire spots indicate potential influence of long-range transport from other states, potentially Arkansas and the Southeast.

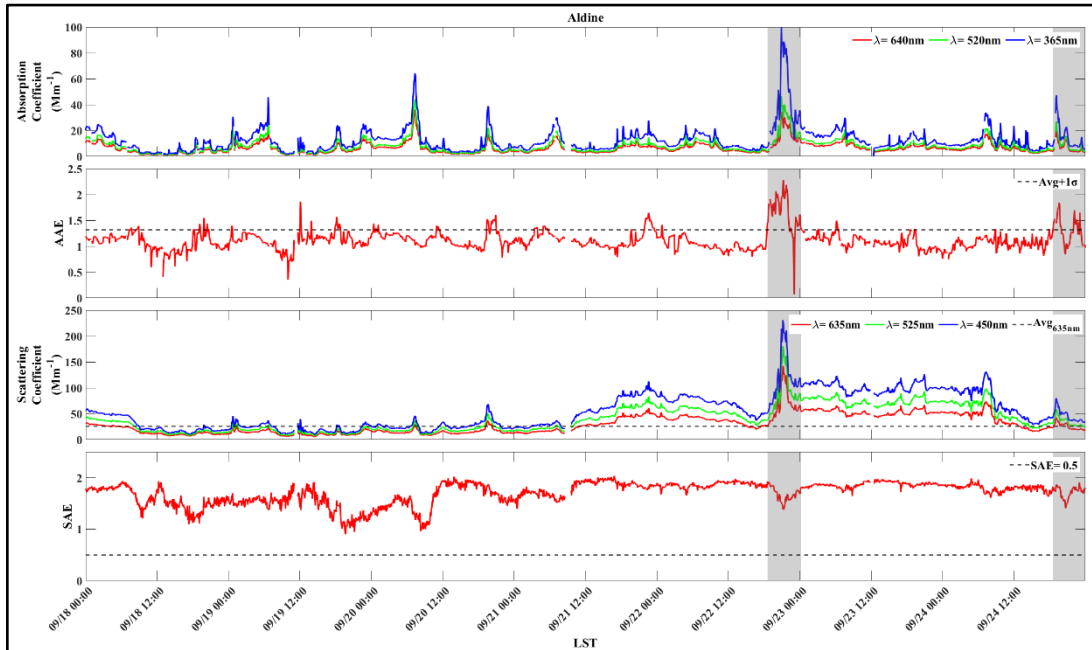


Figure 3-97: Time Series of Aerosol Optical Properties at Aldine around September 21, 2022

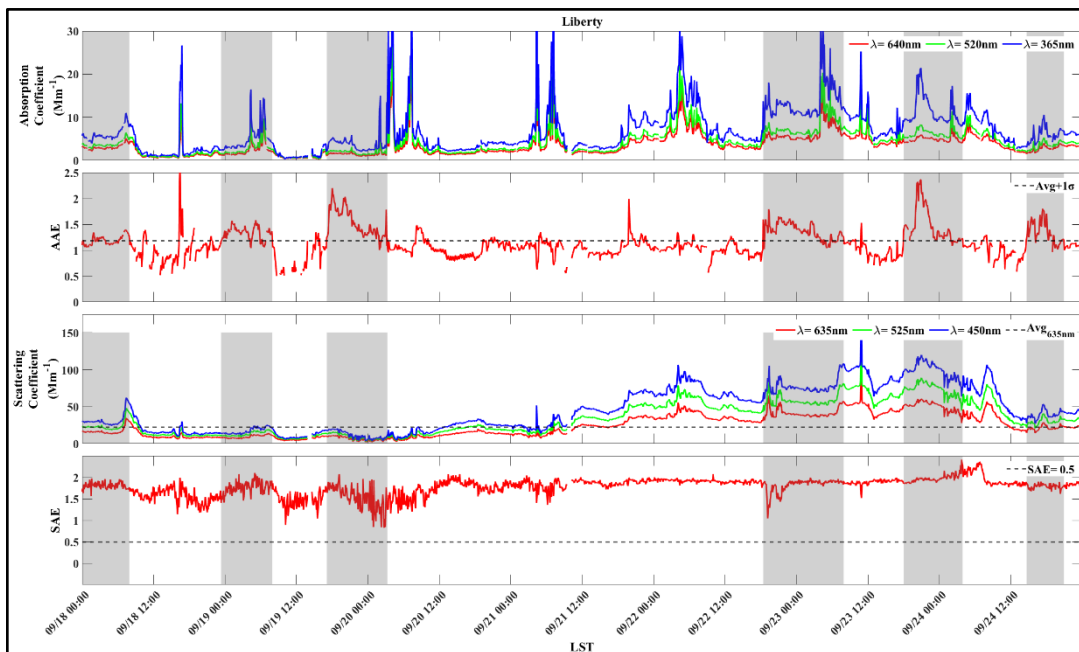


Figure 3-98: Time Series of Aerosol Optical Properties at Liberty around September 21, 2022

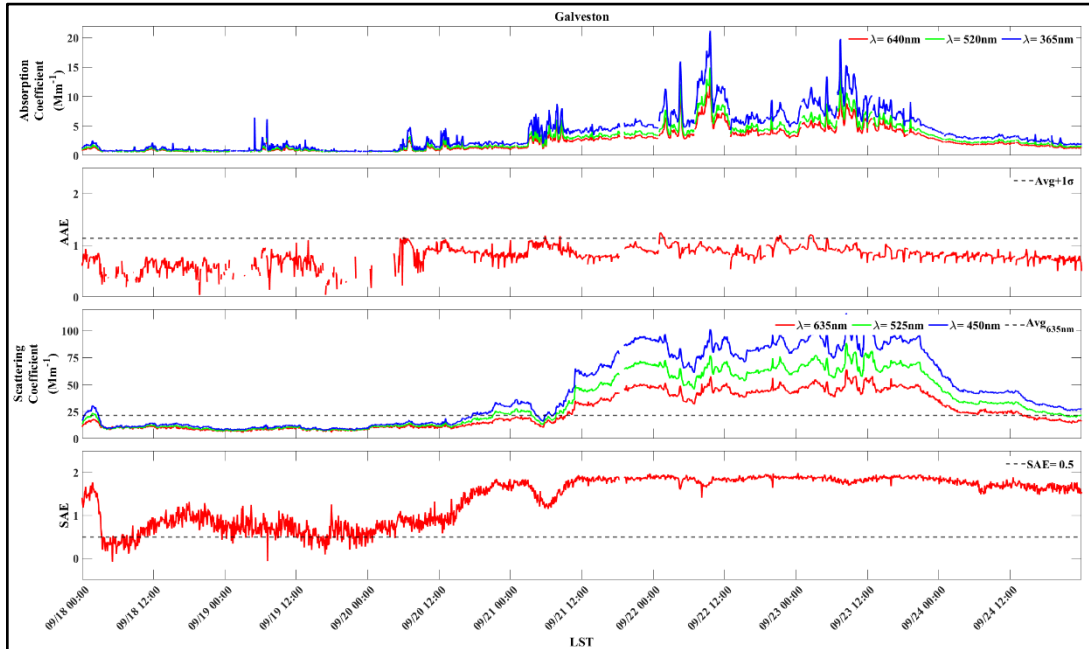


Figure 3-99: Time series of Aerosol Optical Properties at Galveston around September 21, 2022

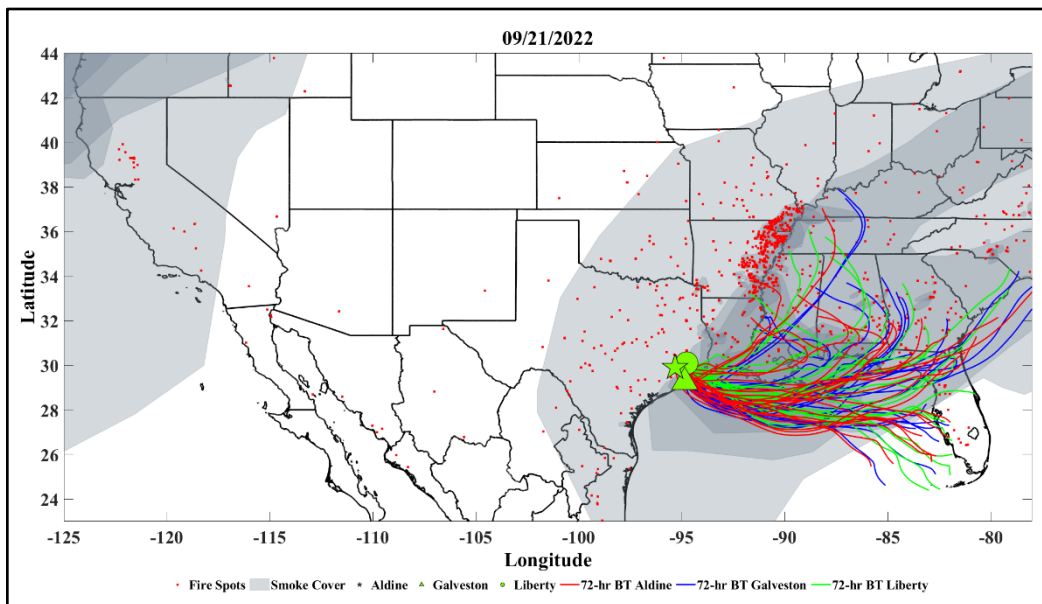


Figure 3-100: HMS and Back Trajectories on September 21, 2022

Figure 3-101: Time Series of Aerosol Optical Properties at Aldine around October 8, 2022, Figure 3-102: Time Series of Aerosol Optical Properties at Liberty around October 8, 2022, and Figure 3-103: Time Series of Aerosol Optical Properties at Galveston around October 8, 2022 show gray shading for BB events. The graphs shows that Aldine, Liberty, and Galveston had an influence of BB on or around October 8, 2022. Figure 3-104: HMS and Back Trajectories on October 8, 2022 illustrates that the entire region had smoke aloft. The fire spots indicate potential influence of long-range transport from other states.

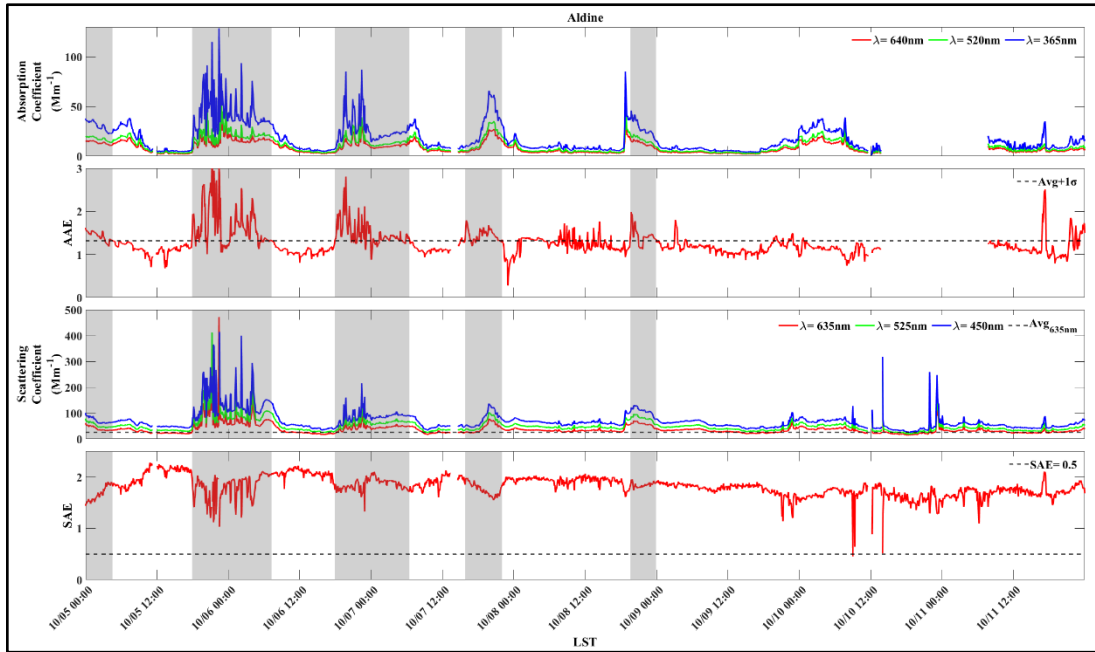


Figure 3-101: Time Series of Aerosol Optical Properties at Aldine around October 8, 2022



Figure 3-102: Time Series of Aerosol Optical Properties at Liberty around October 8, 2022

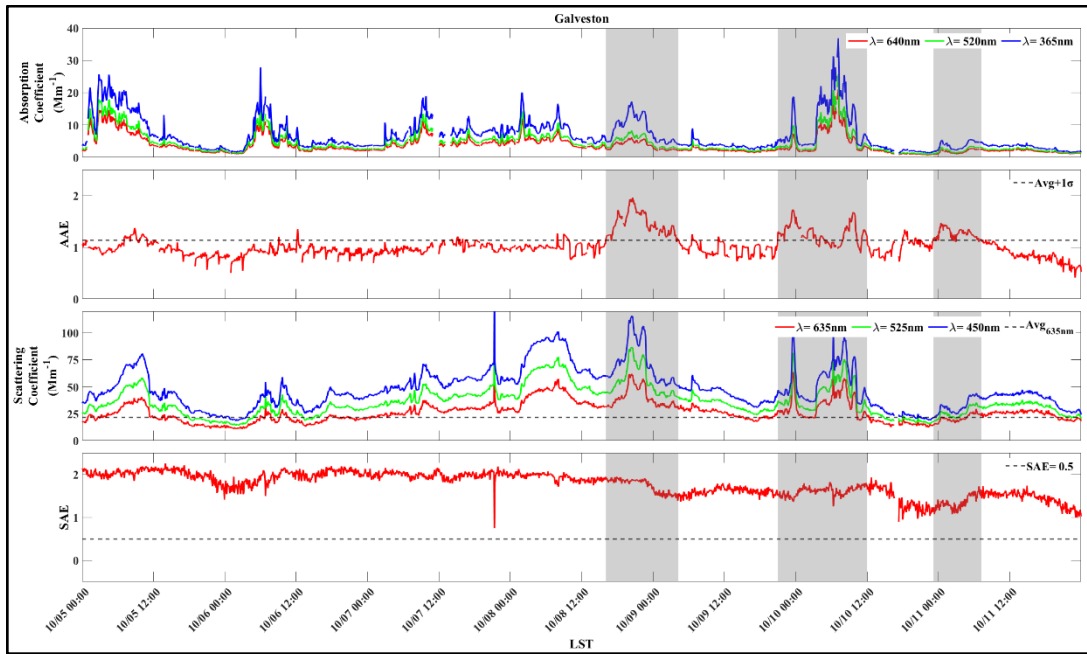


Figure 3-103: Time Series of Aerosol Optical Properties at Galveston around October 8, 2022

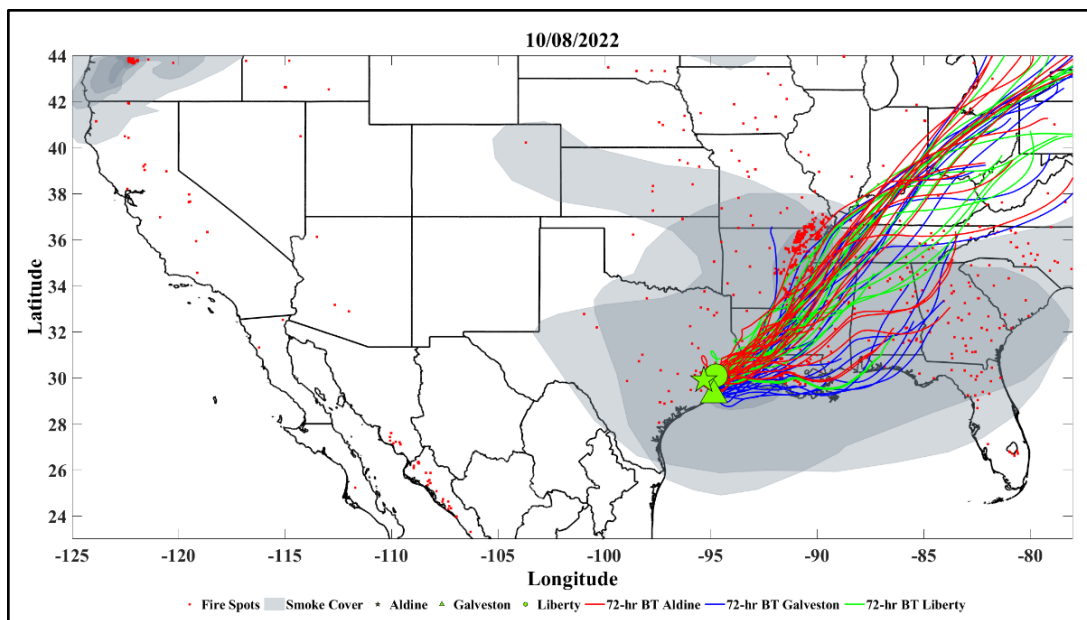


Figure 3-104: HMS and Back Trajectories on October 8, 2022

The BC2 network showed strong evidence of BB emissions mixing down to the surface on September 13, September 21, and October 8, 2022.

3.8 MATCHING DAY ANALYSIS

Ozone formation and transport depend greatly on meteorology. Consequently, a comparison of ozone meteorologically similar days with and without fire impacts can support a clear causal relationship between wildfires and monitored ozone concentrations. Because days with similar meteorology and seasonality usually have similar ozone concentrations, large differences in measured ozone concentrations with similar meteorology indicate influences from non-typical sources.

A typical approach to a "Matching Day" analysis involves meteorological parameters that strongly affect ozone concentrations near the monitor location. The parameters should be matched to the candidate day(s) within an appropriate tolerance. Matching days are usually chosen from a similar time of year as the candidate day(s). The EPA notes that "a similar day analysis of this type, when combined with a comparison of the qualitative description of the synoptic scale weather pattern (e.g., cold front location, high pressure system location), can show that the fire contributed to the elevated ozone concentrations" (U.S. EPA, 2016a, p. 27).

In undertaking its matching day analysis, the TCEQ chose to compare days according to synoptic conditions, backward trajectories, and the following parameters:

- average morning resultant wind speed (mph) and direction (°from North). Vector components of resultant wind speed and direction are averaged for the 7:00 AM through the 10:00 AM hours Central Standard Time (CST);
- average afternoon resultant wind speed (mph) and direction (°from North); Vector components of resultant wind speed and direction are averaged for the 1:00 PM through the 4:00 PM hours CST;

- daily Maximum Temperature (°F). The maximum hourly average temperature for each day; and
- daily Maximum Solar Radiation (Langley/minute). The maximum hourly solar radiation measurement for each day.

3.8.1 June 20, 2022

In reviewing information for June 20, 2022, the TCEQ identified a meteorologically similar day without smoke effects. On June 5, 2020, the Bayland Park monitor measured a maximum daily eight-hour ozone average of 44 parts per billion (ppb) and had no smoke plumes overhead. Table 3-4: *Meteorological Matching Parameters for June 20, 2022* shows the similarities of individual parameters. June 5, 2020, occurs at the same time of year as June 20 and shares many of the same general characteristics.

Table 3-4: Meteorological Matching Parameters for June 20, 2022

Meteorological Parameter	June 20, 2022	June 5, 2020
Maximum Eight-Hour Ozone Concentration (ppb)	82	44
0700-1000 CST Average Wind Direction	154.5	157.3
1300-600 CST Average Wind Direction	130.5	120.7
0700-1000 CST Average Wind Speed (mph)	2.9	4.0
1300-1600 CST Average Wind Speed (mph)	5.2	5.5
Maximum Daytime Temperature (°F)	98.2	94.0
Maximum Solar Radiation (Langley/minute)	1.34	1.30

Figure 3-105: *Backward Trajectories from the Bayland Park Monitor on June 20, 2022 and June 5, 2020* compares backward HYSPLIT trajectories initiated from the Bayland Park monitor at 15:00 local time on June 20, 2022 (left) to June 5, 2020 (right). The back trajectories are released at three heights, 100 meters, 300 meters, and 500 meters. Trajectories indicate winds coming out of the East-Southeast off the Texas and Louisiana coasts. This conclusion is confirmed by the NOAA (2003) Surface and 500-Millibar (mb) Weather Charts in Figure 3-106: *Weather Chart for June 20, 2022*, Figure 3-107: *Surface Weather Chart for June 5, 2020*, Figure 3-108: *500-mb Weather Chart for June 20, 2022*, and Figure 3-109: *500-mb Weather Chart for June 5, 2020*.

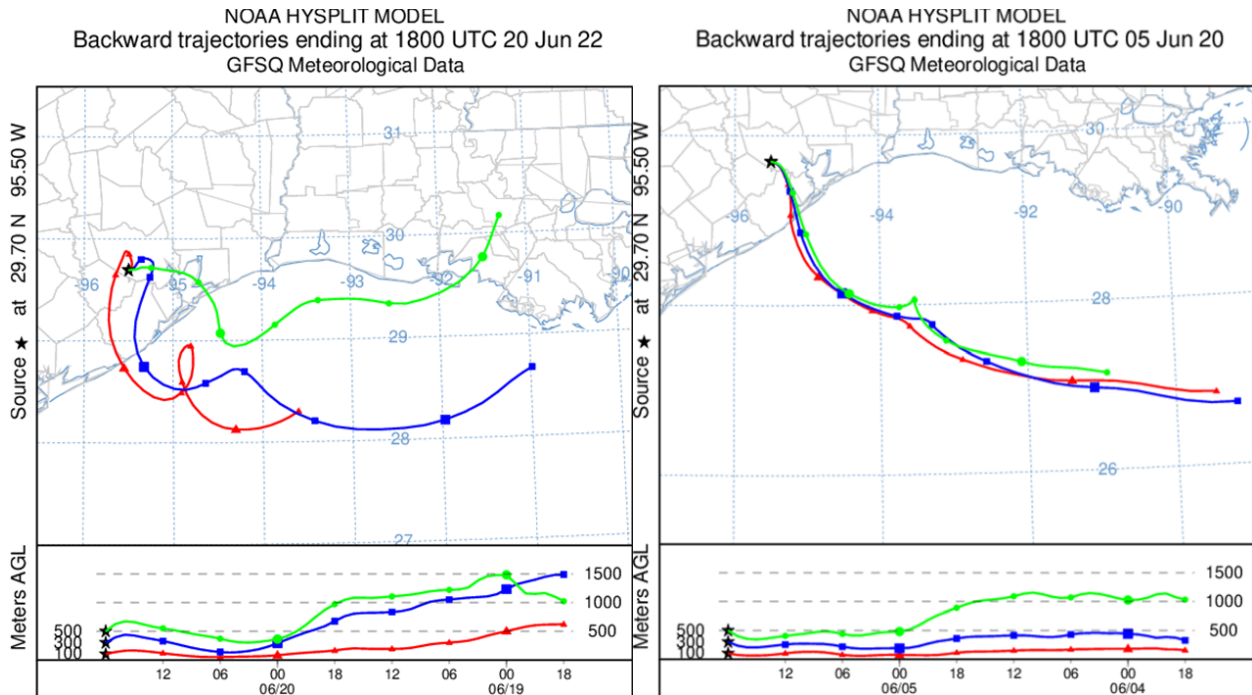


Figure 3-105: Backward Trajectories from the Bayland Park Monitor on June 20, 2022 and June 5, 2020

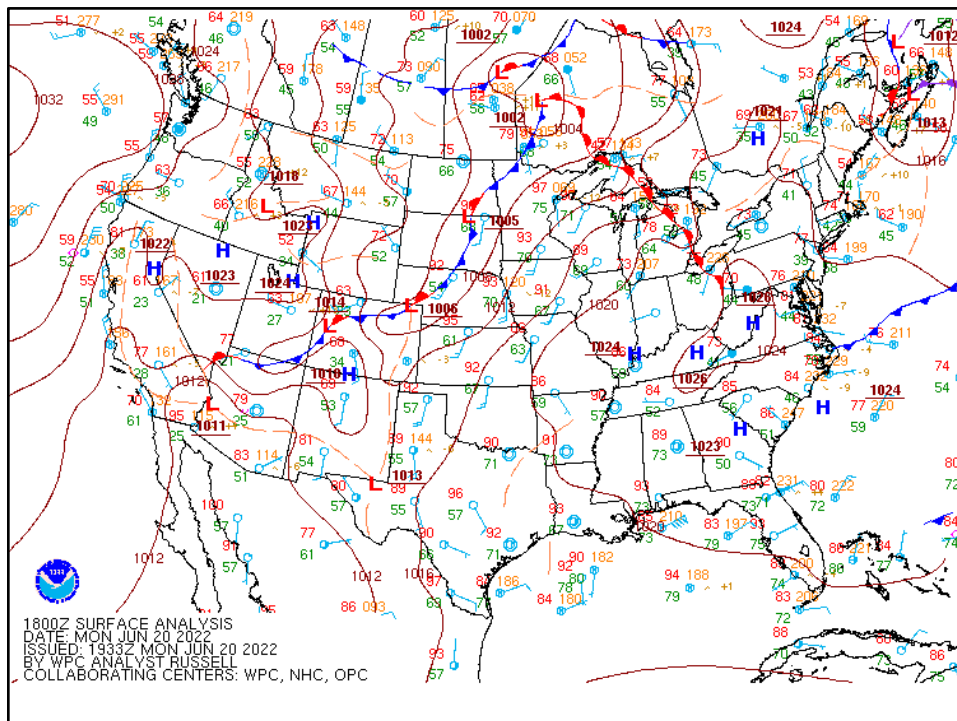


Figure 3-106: Weather Chart for June 20, 2022

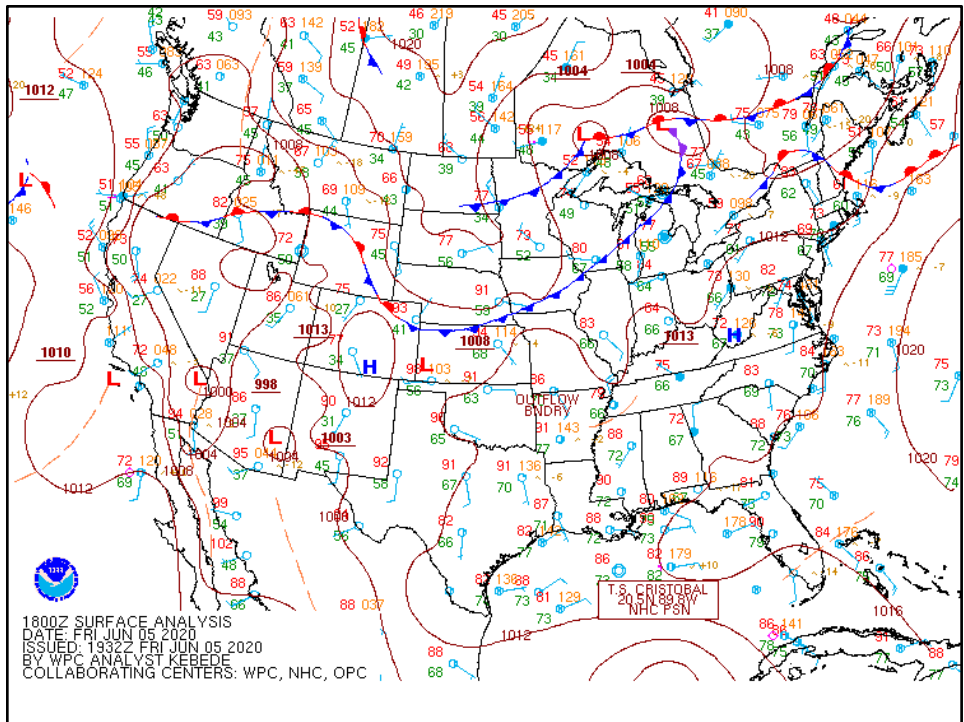


Figure 3-107: Surface Weather Chart for June 5, 2020

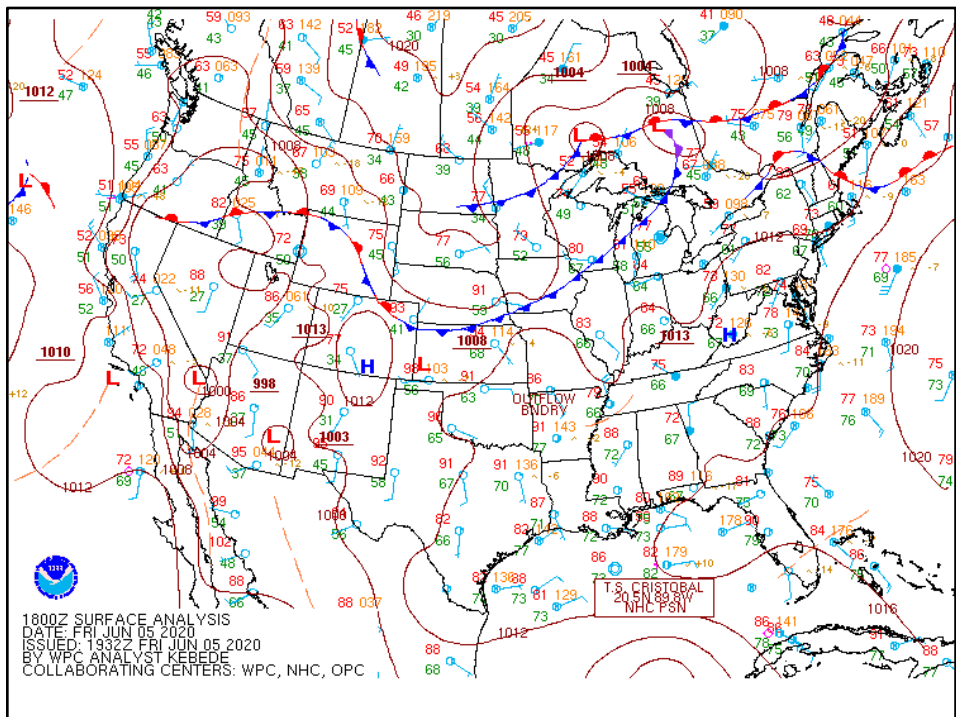


Figure 3-108: 500-mb Weather Chart for June 20, 2022

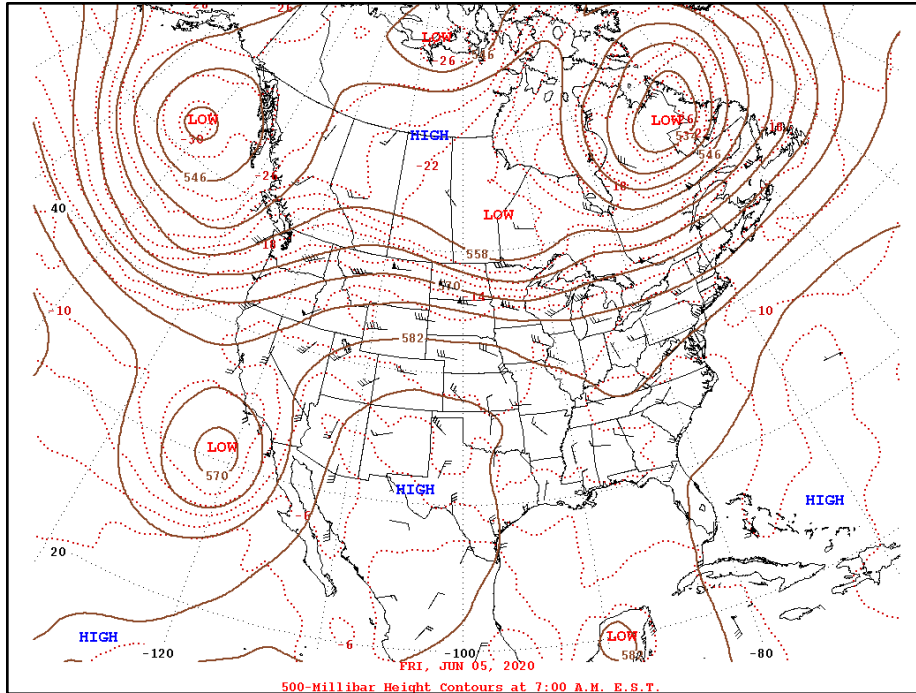


Figure 3-109: 500-mb Weather Chart for June 5, 2020

3.8.2 September 13, 2022

In reviewing information for September 13, 2022, the TCEQ identified a meteorologically similar day. On September 23, 2021, the Bayland Park monitor measured a maximum daily eight-hour ozone average of 73 ppb. Table 3-5: *Meteorological Matching Parameters for September 13, 2022* shows the similarities of individual parameters. September 23, 2021 occurs at the same time of year as September 13 and shares many of the same general characteristics.

Table 3-5: Meteorological Matching Parameters for September 13, 2022

Meteorological Parameter	September 13, 2022	September 23, 2021
Maximum Eight-Hour Ozone Concentration (ppb)	89	73
0700-1000 CST Average Wind Direction	74.3	80.8
1300-600 CST Average Wind Direction	102.8	117.0
0700-1000 CST Average Wind Speed (mph)	4.7	4.8
1300-1600 CST Average Wind Speed (mph)	3.2	4.7
Maximum Daytime Temperature (°F)	90	83
Maximum Solar Radiation (Langley/minute)	1.21	1.46

Figure 3-110: *Backward Trajectories from the Bayland Park Monitor on September 13, 2022, and September 23, 2021* compares backward HYSPLIT trajectories initiated from the Bayland Park monitor at 15:00 local time on September 13, 2022 (left) to September 23, 2021 (right). The back trajectories terminate at three heights, 100 meters, 300 meters, and 500 meters. Trajectories show continental flow into the HGB area in an anti-cyclonic manner. This is confirmed by the synoptic-scale flow shown in the surface and 500-millibar charts shown in Figure 3-111: *Surface Weather Chart for September 13, 2022*, Figure 3-112: *Surface Weather Chart for September 23, 2021*, Figure 3-113: *500-mb Weather Chart for September 13, 2022*, and Figure 3-114: *500-mb Weather Chart for September 23, 2021*.

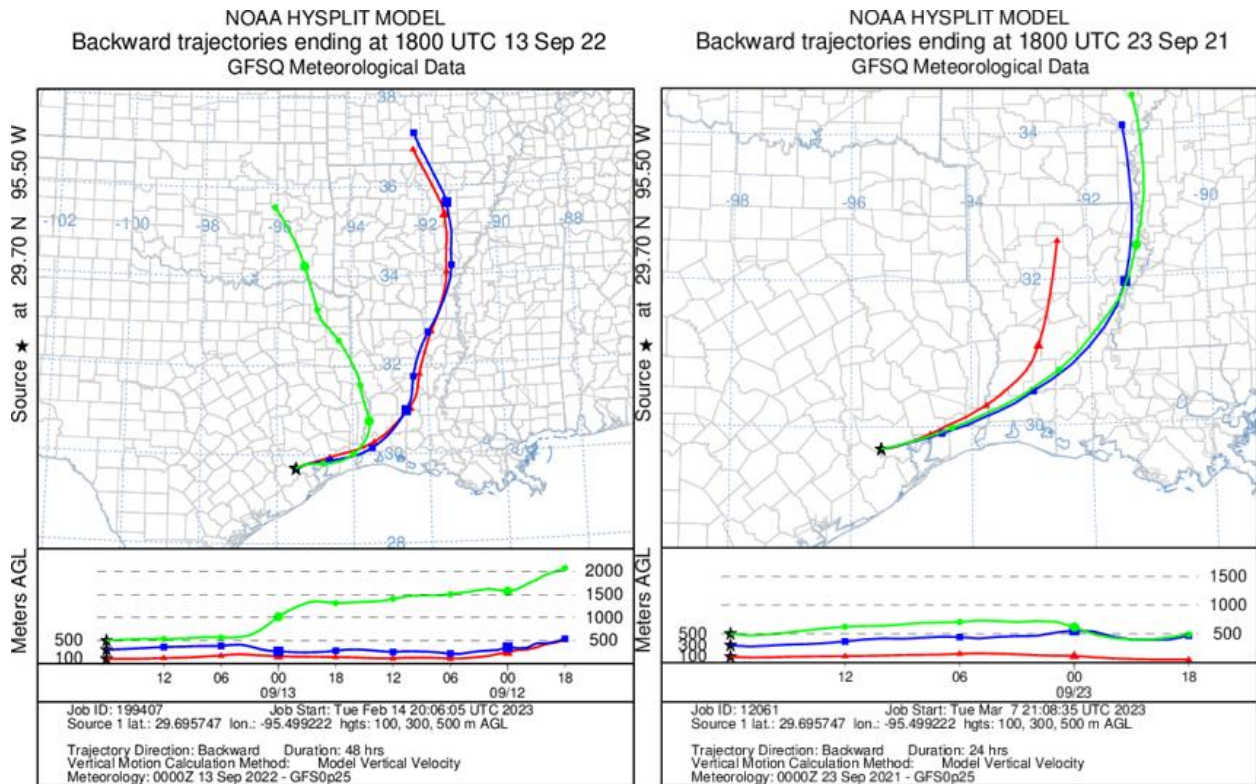


Figure 3-110: Backward Trajectories from the Bayland Park Monitor on September 13, 2022, and September 23, 2021

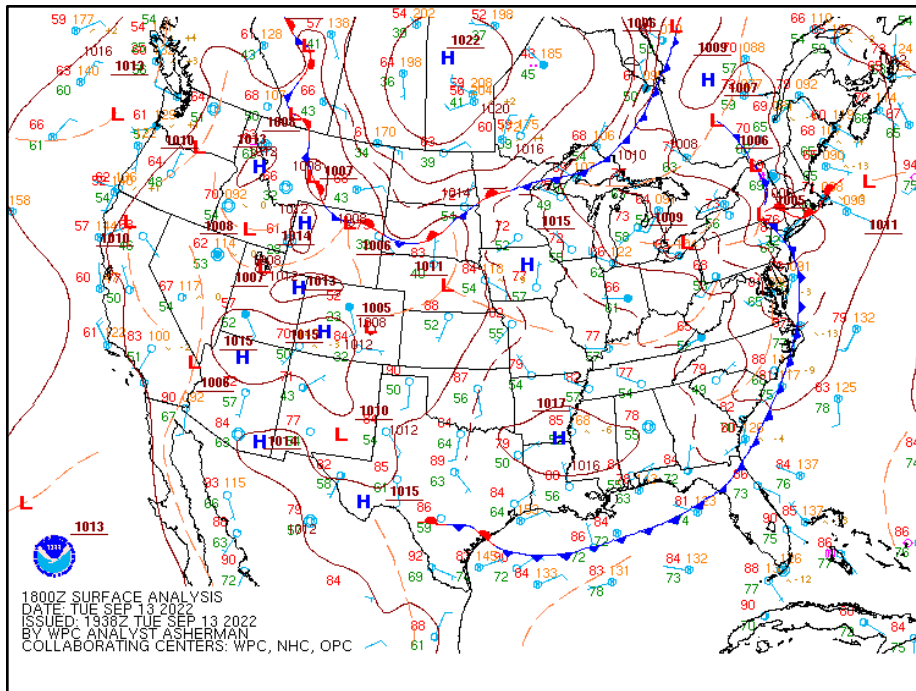


Figure 3-111: Surface Weather Chart for September 13, 2022

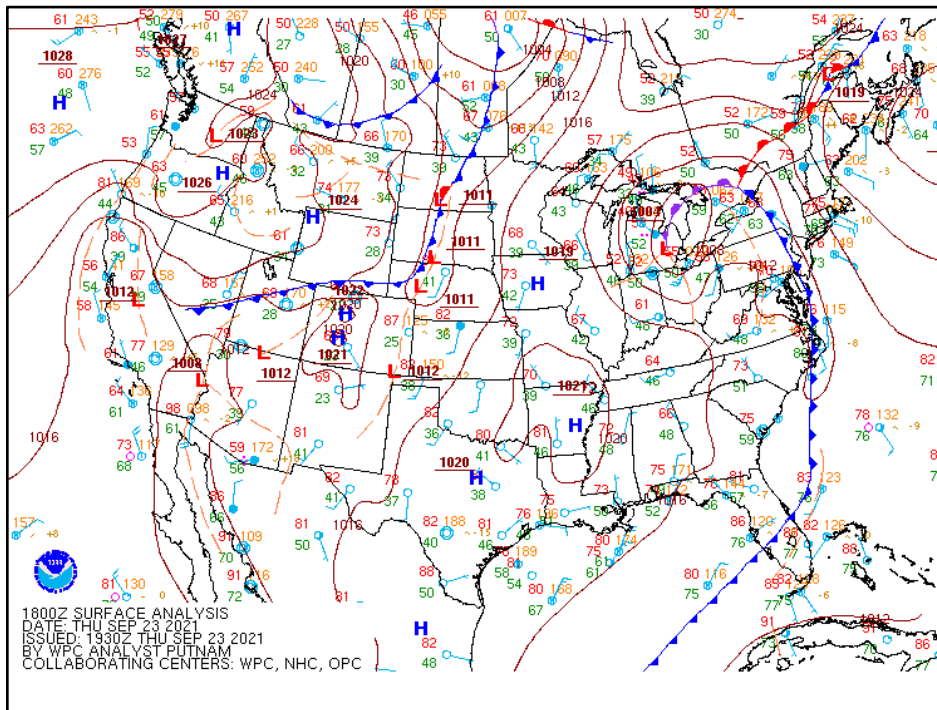


Figure 3-112: Surface Weather Chart for September 23, 2021

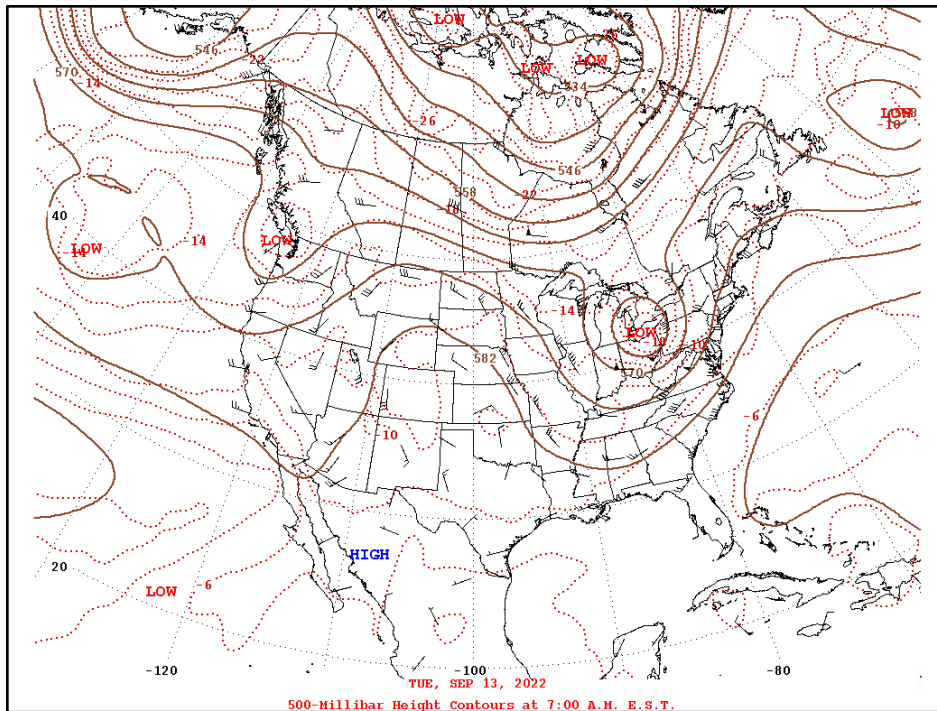


Figure 3-113: 500-mb Weather Chart for September 13, 2022

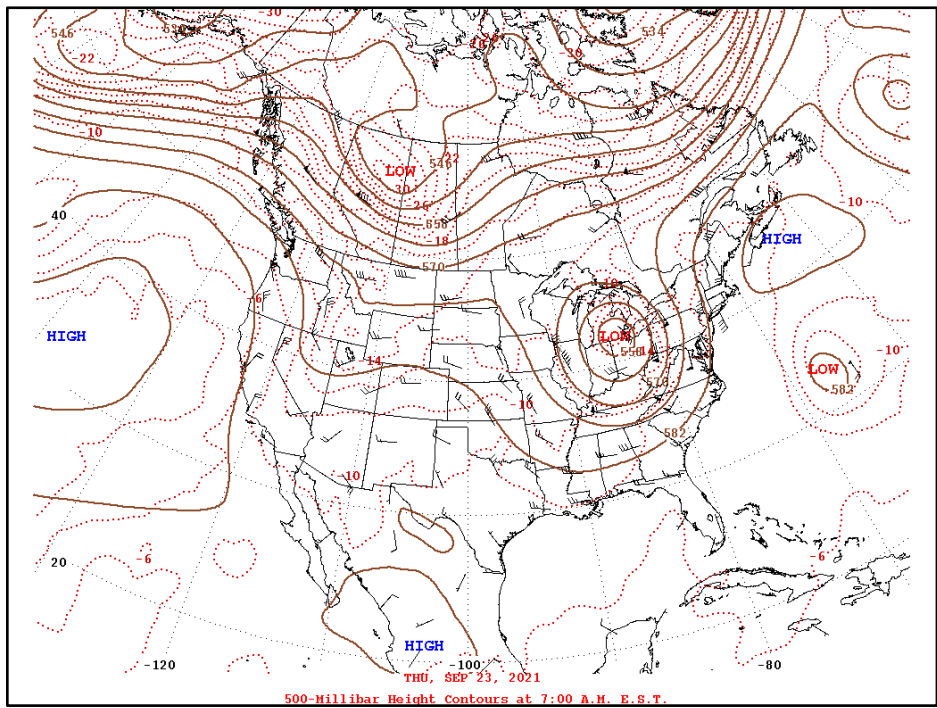


Figure 3-114: 500-mb Weather Chart for September 23, 2021

3.8.3 September 21, 2022

In reviewing information for September 21, 2022, the TCEQ identified a meteorologically similar day without smoke effects. On August 12, 2017, the Bayland Park monitor measured a maximum daily eight-hour ozone average of 28 ppb. Table

3-6: *Meteorological Matching Parameters for September 21, 2022* shows the similarities of individual parameters. August 12, 2017, occurs at the same time of year as September 21 and shares many of the same general characteristics.

Table 3-6: Meteorological Matching Parameters for September 21, 2022

Meteorological Parameter	September 21, 2022	August 12, 2017
Maximum Eight-Hour Ozone Concentration (ppb)	92	28
0700-1000 CST Average Wind Direction	187.8	216.6
1300-600 CST Average Wind Direction	131.0	182.4
0700-1000 CST Average Wind Speed (mph)	3.1	6.0
1300-1600 CST Average Wind Speed (mph)	5.0	5.3
Maximum Daytime Temperature (°F)	92.9	95.0
Maximum Solar Radiation (Langley/minute)	1.39	1.13

Figure 3-115: *Backward Trajectories from the Bayland Park Monitor on September 21, 2022 and August 12, 2017* compares backward HYSPLIT trajectories initiated from the Bayland Park monitor at 15:00 local time on September 21, 2022 (left) to August 12, 2017 (right). The back trajectories terminate at three heights, 100 meters, 300 meters, and 500 meters. Trajectories show a southerly flow bringing air in from the Gulf of Mexico. This is supported by the area of high pressure shown over the Texas and northern Gulf of Mexico areas in Figure 3-116: *Surface Weather Chart for September 21, 2022*, Figure 3-117: *Surface Weather Chart for August 12, 2017*, Figure 3-118: *500-mb Weather Chart for September 21, 2022*, and Figure 3-119: *500-mb Weather Chart for August 12, 2017*.

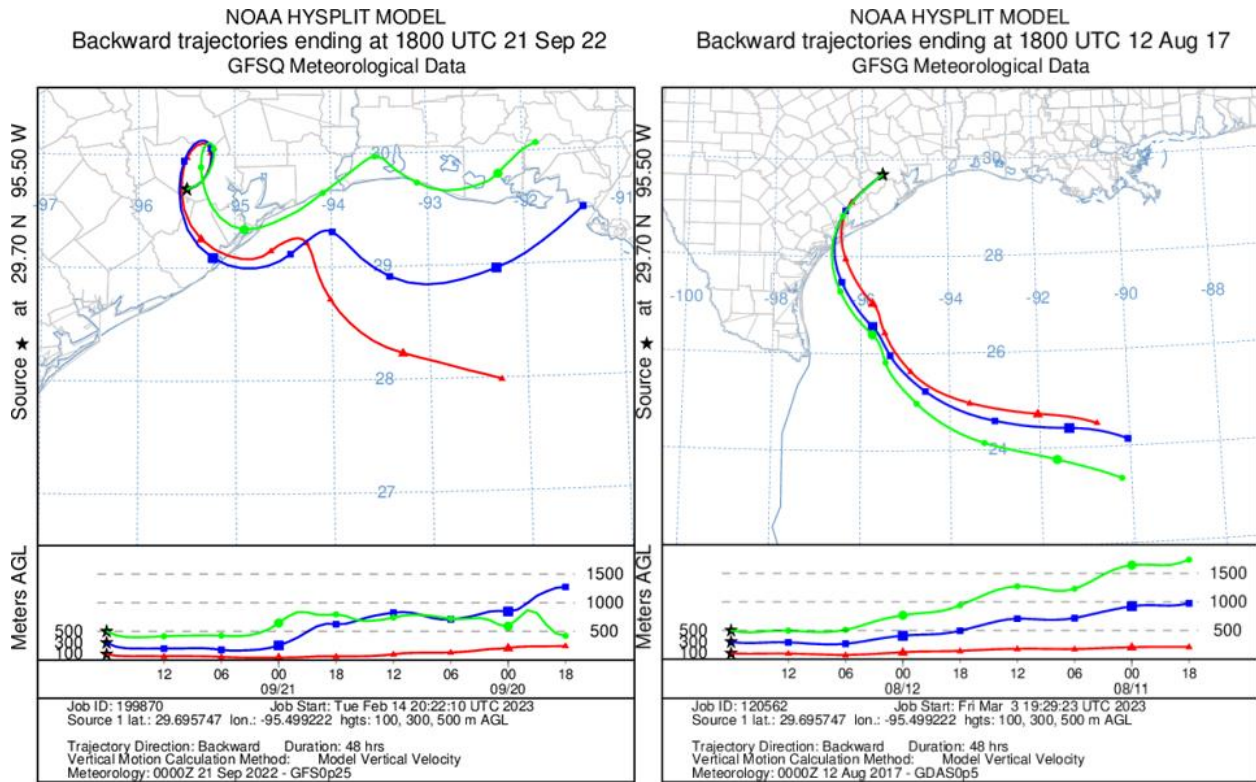


Figure 3-115: Backward Trajectories from the Bayland Park Monitor on September 21, 2022 and August 12, 2017

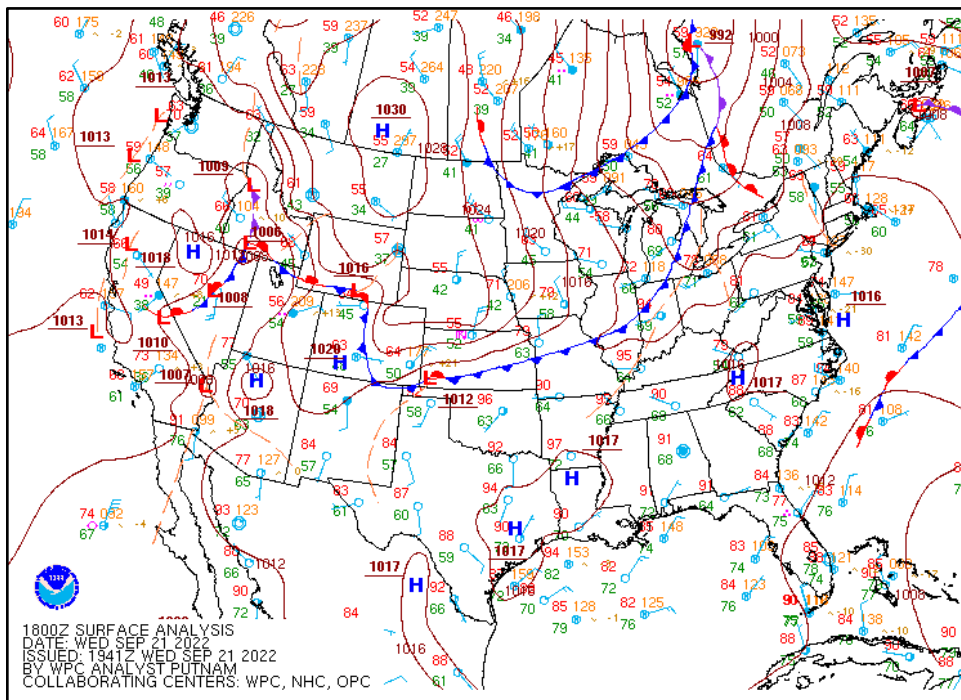


Figure 3-116: Surface Weather Chart for September 21, 2022

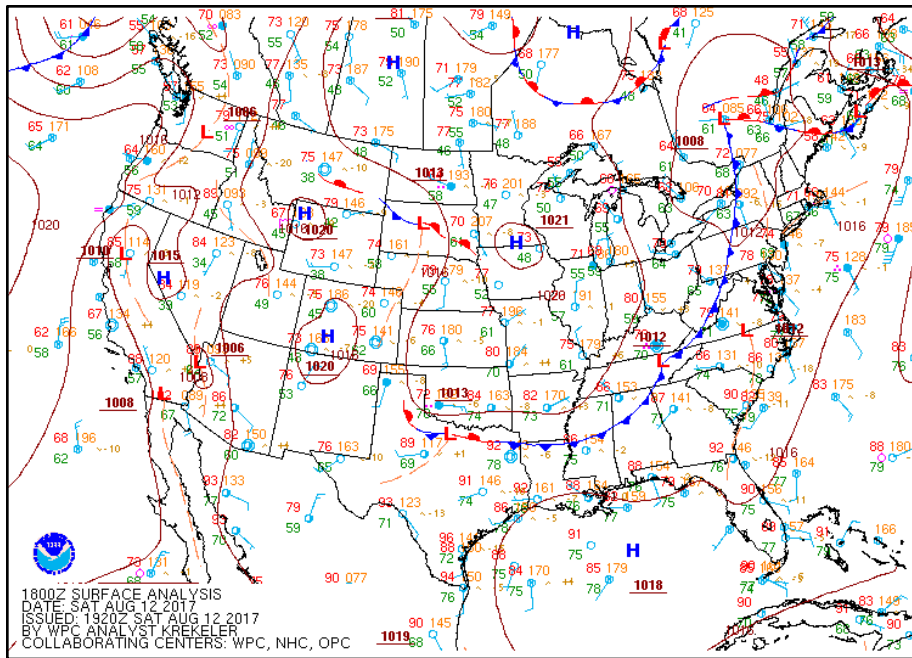


Figure 3-117: Surface Weather Chart for August 12, 2017

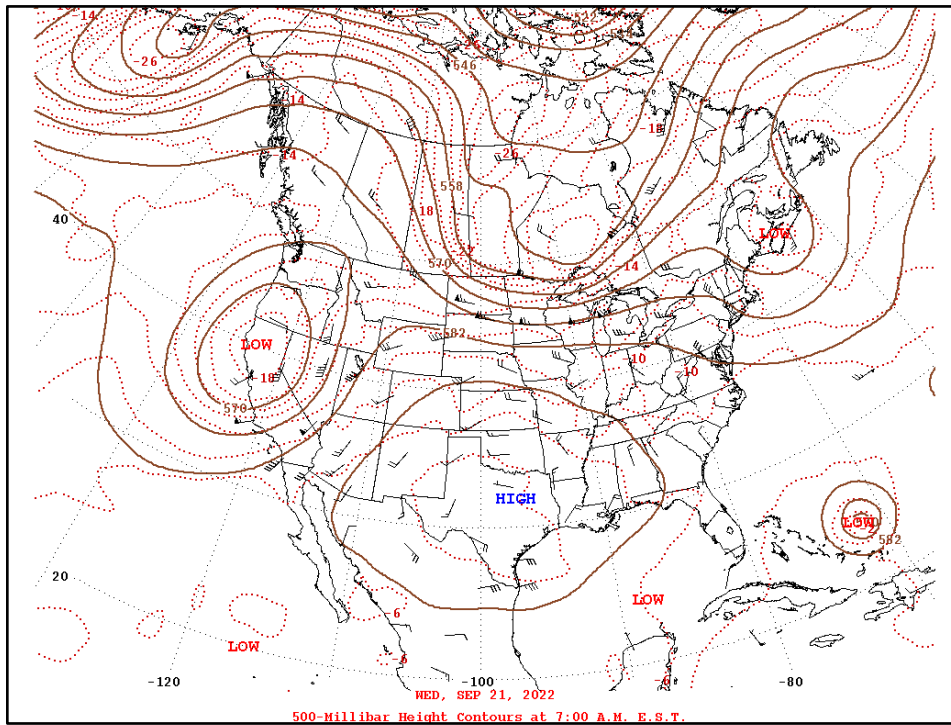


Figure 3-118: 500-mb Weather Chart for September 21, 2022

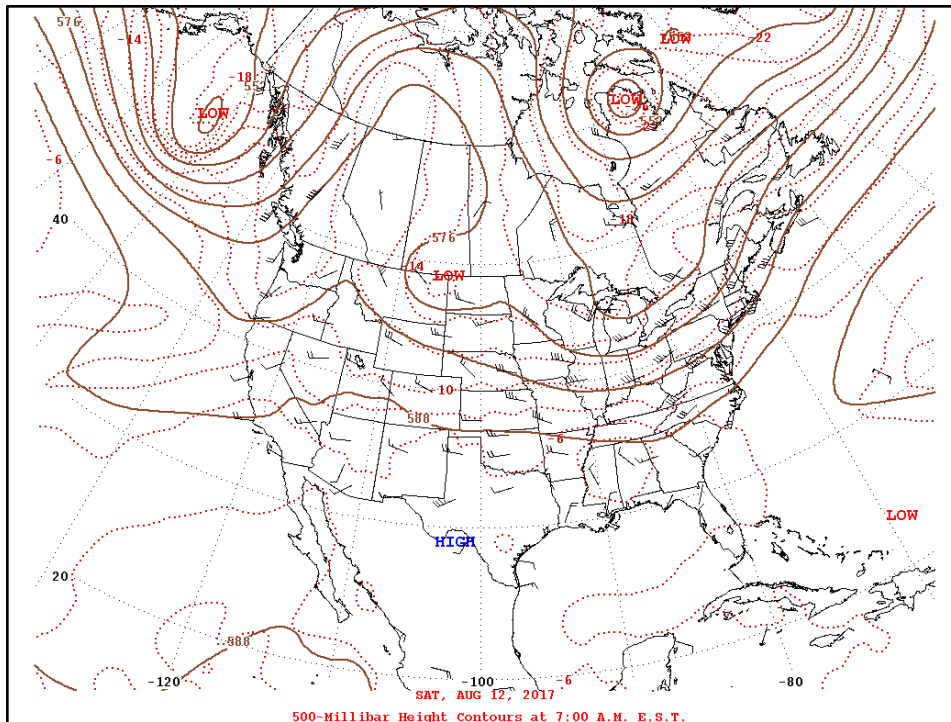


Figure 3-119: 500-mb Weather Chart for August 12, 2017

3.8.4 October 8, 2022

In reviewing information for October 8, 2022, the TCEQ identified a meteorologically similar day without smoke effects. On October 18, 2021, the Bayland Park monitor measured a maximum daily eight-hour ozone average of 58 ppb. Table 3-7: *Meteorological Matching Parameters for October 8, 2022* shows the similarities of individual parameters. October 18, 2021 occurs at the same time of year as October 8, 2022 and shares many of the same general characteristics.

Table 3-7: Meteorological Matching Parameters for October 8, 2022

Meteorological Parameter	October 8, 2022	October 18, 2021
Maximum Eight-Hour Ozone Concentration (ppb)	87	58
0700-1000 CST Average Wind Direction	55.8	61.8
1300-600 CST Average Wind Direction	86.3	115.2
0700-1000 CST Average Wind Speed (mph)	6.6	3.8
1300-1600 CST Average Wind Speed (mph)	7.5	5.1
Maximum Daytime Temperature (°F)	86.8	78.0
Maximum Solar Radiation (Langley/minute)	1.32	1.34

Figure 3-120: *Backward Trajectories from the Bayland Park Monitor on October 8, 2022 and October 18, 2021* compares backward HYSPLIT trajectories initiated from the Bayland Park monitor at the hour of maximum one-hour ozone on October 8, 2022 (left) to October 18, 2021 (right). The back trajectories terminate at three heights, 100 meters, 300 meters, and 500 meters. The trajectories show a similar synoptic pattern with an anticyclonic flow bringing continental air into the HGB area. This is supported by the surface and 500-millibar weather charts showing an area of high pressure over the central United States with a cold front pushing out through the east coast and the Gulf of Mexico in *Figure 3-121: Surface Weather Chart for October 8, 2022*, *Figure 3-122: Surface Weather Chart for October 18, 2021*, *Figure 3-123: 500-Millibar Weather Chart for October 8, 2022*, and *Figure 3-124: 500-Millibar Weather Chart for October 18, 2021*.

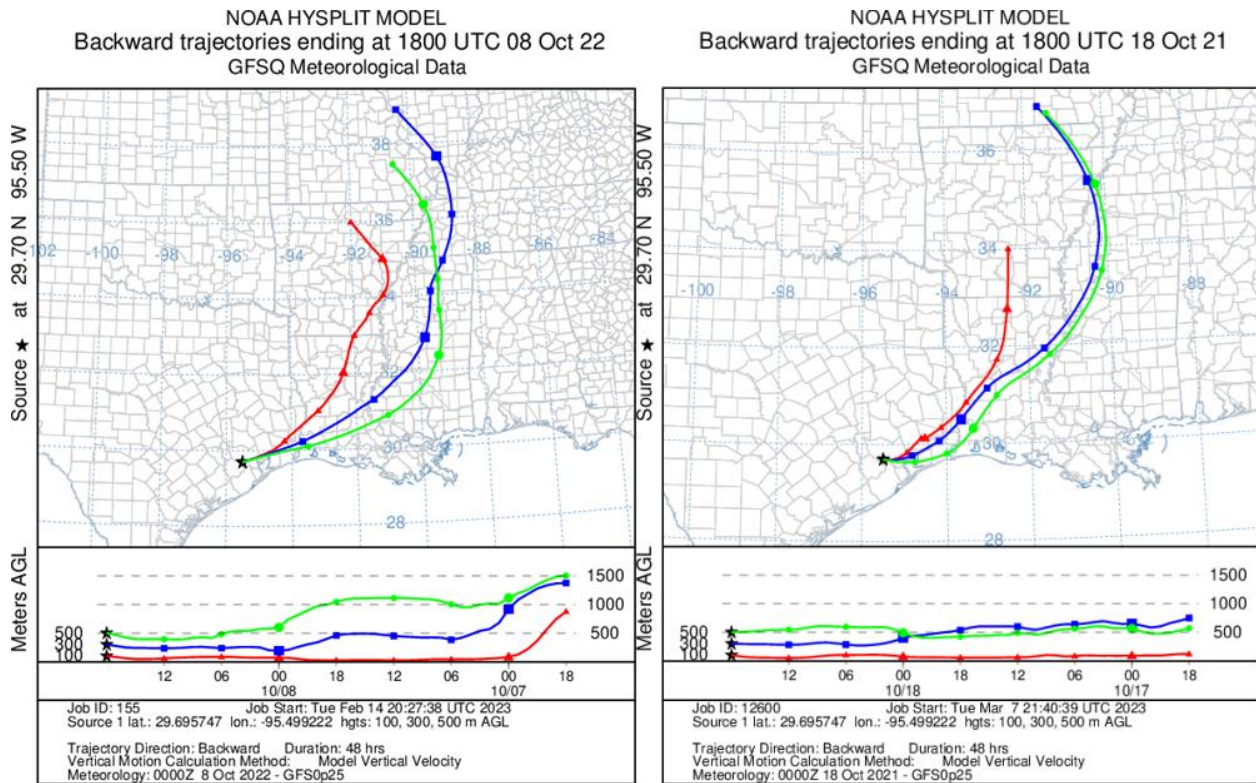


Figure 3-120: Backward Trajectories from the Bayland Park Monitor on October 8, 2022 and October 18, 2021

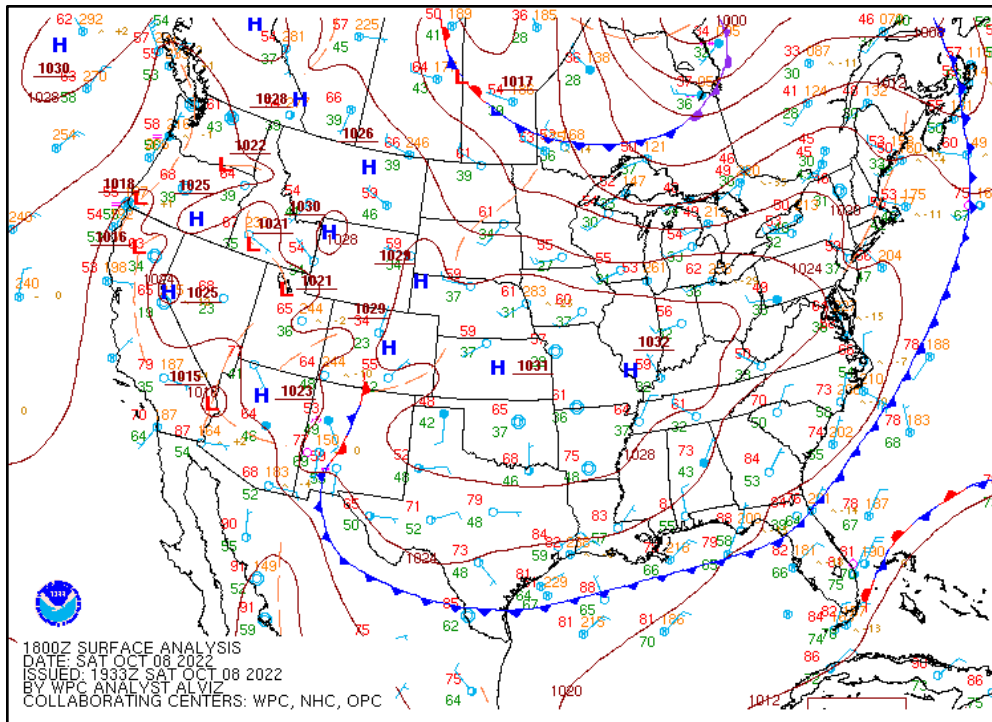


Figure 3-121: Surface Weather Chart for October 8, 2022

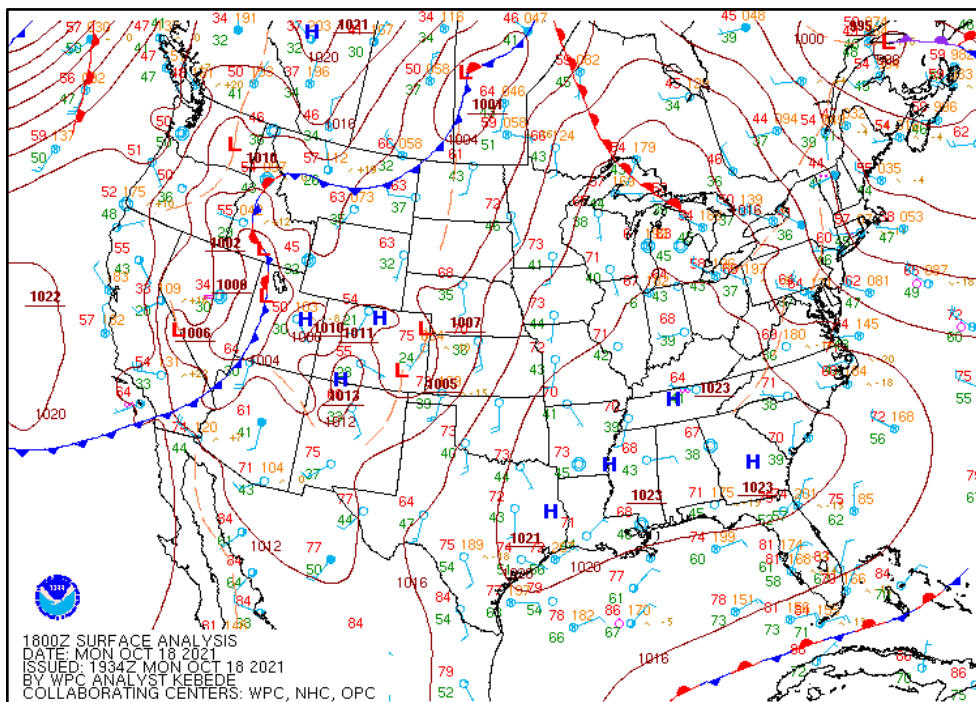


Figure 3-122: Surface Weather Chart for October 18, 2021

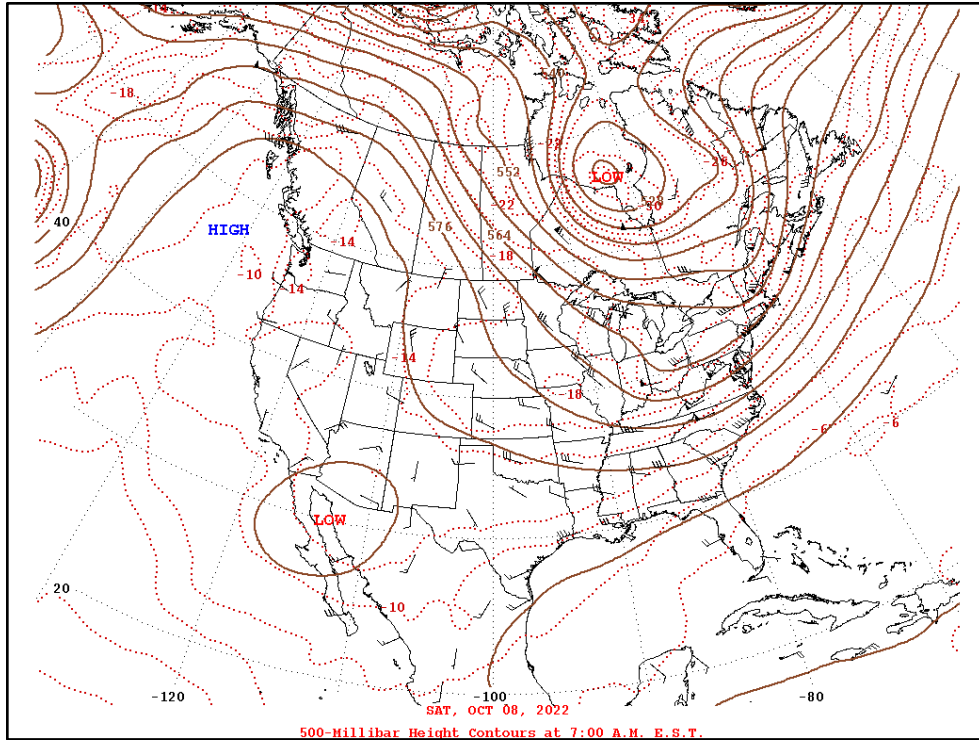


Figure 3-123: 500-Millibar Weather Chart for October 8, 2022

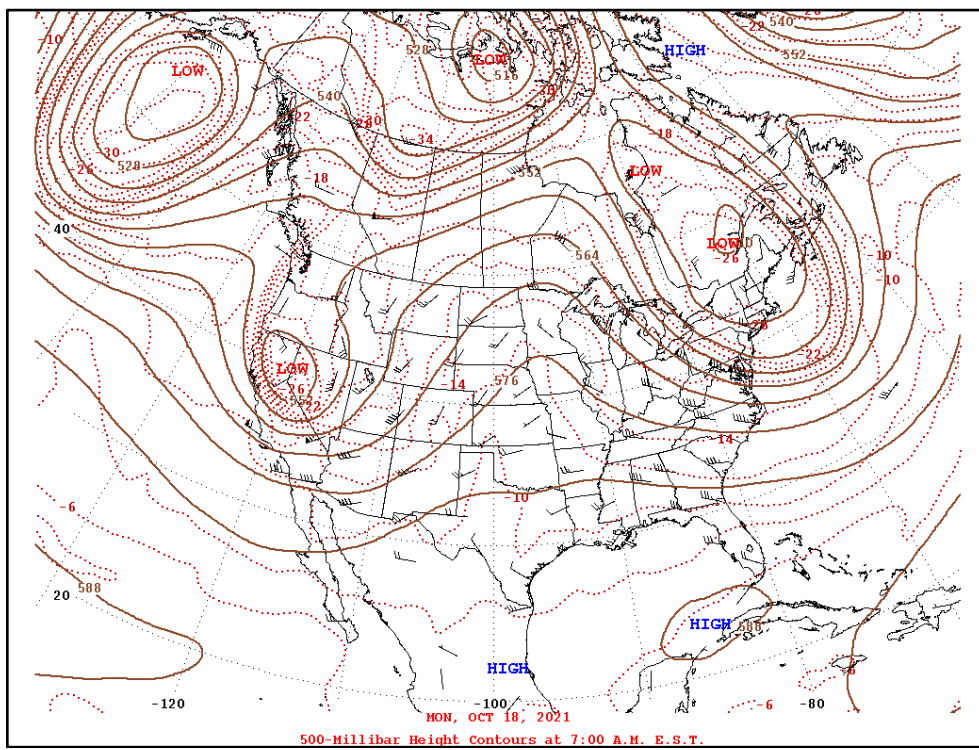


Figure 3-124: 500-Millibar Weather Chart for October 18, 2021

3.9 GENERALIZED ADDITIVE MODEL ANALYSIS

The EPA guidance identifies the use of statistical regression models as an example of a Tier 3 analysis to show that wildfire emissions caused an ozone exceedance “because regression equations are developed with several years of data, they represent the relationship between air quality and meteorology under typical emission patterns” (U.S. EPA, 2016a). Therefore, days that the regression model cannot explain can be thought of as exceptional days.

There are many ways to investigate the impacts of meteorology on ozone concentrations. Camalier *et al.* (2007) developed a model using Generalized Linear Models (GLM) to predict ozone from meteorological variables. Jaffe *et al.* (2004) used statistical models to quantify the amount of ozone due to wildfire. The Generalized Additive Model (GAM) is a statistical method used for modeling data as a function of many predictor variables (Woods 2017). Alvarado *et al.* (2015) used GAMs to see the relationship between ozone and meteorological variables using six Texas urban areas. Gong, *et al.* (2017) applied the GAM method to estimate the wildfire contributions to MDA8 zone for 2015 fires burning in the Pacific Northwest. The Louisiana Department of Environmental Quality (2018) also used GAM to show the 2017 Northwest wildfire contribution to ozone. The TCEQ submitted GAM results as supplemental material (Jaffe, 2017) in its 2016 exceptional event demonstration for El Paso, Texas (TCEQ, 2016) and DFW, Texas (TCEQ, 2021).

The GAM is a statistical method used for modeling data as a function of many predictor variables (Woods 2017). An example equation for a GAM for this report can be written as:

$$g(Y_i) = f_1(X1_i) + f_2(X2_i) + f_3(X3_i) + \dots + \text{residual}_i$$

Where f_1 , f_2 , f_3 , etc. are link functions obtained from spline fits to the observations, $X1$, $X2$, etc. are the predictor variables and the “ i ” refers to each daily observation. The “R” (2023) software program with an add-on package “mgcv” (2023) was used for GAM analysis. Here, we used 10 predictor variables for the GAM analysis.

Gong, *et al.* (2017) applied GAM to identify impacts in ozone in different urban areas due to wildfires. Houston was the one of the cities used in the study. The meteorological variables used in the study were able to explain 77% ($R^2 = 0.77$) of variability in ozone in Houston. The TCEQ also closely followed the methodology of this study and used the same type of variables for GAM. The daily meteorological variables used in this study are wind speed, wind direction, temperature, relative humidity, and solar radiation. Some variables were derived from meteorological parameters for modeling purposes. Table 3-8: *Meteorological Parameters Used for Houston Bayland Park GAMs*, shows the meteorological variables used in the process of model building and data sources. Bayland Park monitoring data was obtained from the EPA’s site <https://www.epa.gov/outdoor-air-quality-data/air-data-concentration-plot>. Only the months May through October from 2015 through 2022 were used in this demonstration. Data from 2015 through 2021 were used for model development and training and data from 2022 were used for test case. As EPA guidance suggests, the TCEQ used a train and test approach for this demonstration’s statistical GAM.

The TCEQ's GAM used 10 variables from Table 3-8: *Meteorological Parameters Used for Houston Bayland Park GAMs*. Penalized cubic regression splines (CRS) were used for the smoothing functions to allow a nonlinear response between MDA8 ozone and each meteorological parameter except variable number 10 in Table 3-8.

Table 3-8: Meteorological Parameters Used for Houston Bayland Park GAMs

Variable Number	Variables	Description
1	YEAR	Year
2	DOY	Day of Year
3	VAVG	Daily averaged(24-hour) wind V vector (mph)
4	TAVGPM	Afternoon (1-4 pm LST) average temperature (°F)
5	TDELTA	Diurnal temperature change (max-min, °F)
6	H500	Morning (12:00 UTC) height of 500 mb surface (m)
7	RHAVG	Average daily (24-hour) relative humidity (%)
8	TrajQ	Endpoint quadrant after 12 hours of transport for a back trajectory initialized at 2 pm LST
9	TrajD	Endpoint distance (point to point) after 12 hours of transport for a back trajectory initialized at 2 pm LST
10	SRAVGPM	Afternoon (1-4 pm LST) average solar radiation (Langley/minute)

Data for variables YEAR and DOY were derived using calculations, while variables DAVG, TAVGPM, TDELTA, and SRAVGM were obtained from the TCEQ's Texas Air Monitoring Information System (TAMIS) and Leading Environmental Analysis and Display System (LEADS). Data for variable H500 was obtained from [NOAA radiosonde - archive](https://www.ncei.noaa.gov/data/integrated-global-radiosonde-archive/access/data-por/) (https://www.ncei.noaa.gov/data/integrated-global-radiosonde-archive/access/data-por/). Data for RHAVG was obtained from [NOAA land -based integrated -surface -database](https://www.ncei.noaa.gov/products/land-based-station/integrated-surface-database) (https://www.ncei.noaa.gov/products/land-based-station/integrated-surface-database), and trajectories data was derived using HYSPLIT.

Table 3-9: *Houston Bayland Park Ozone GAM Performance* characteristics describes this model. The ability of the model to predict daily maximum eight-hour average ozone is shown graphically in Figure 3-125: *Training Model Results Compared to Observed Ozone* and Figure 3-126: *2022 Model Predictions Compared to Observed Ozone*. The results for days of interest are plotted in red. A more direct comparison of GAM performance is shown in Figure 3-127: *Comparison of 2022 Predictions with Results from Training Model*. The figure shows that 2022 validation data are unbiased throughout the range of concentration.

The difference between observed and predicted values are residuals. A residuals check is another way of testing model performance. Figure 3-128: *GAM Residuals for Training and Validation Dataset* shows the overlapped plot of training residuals and the 2022

validation residuals. Both sets of residuals show no clear pattern or bias in one or other way around zero line. This unbiased relationship throughout the range of predicted ozone values shows that the GAM used to predict daily maximum ozone averages performs well.

Table 3-9: Houston Bayland Park Ozone GAM Performance

Statistic	Training dataset (2015-2021)	Validation dataset (2022)
N	1142	156
R ²	0.71	0.63
Residual Mean	0	0.16

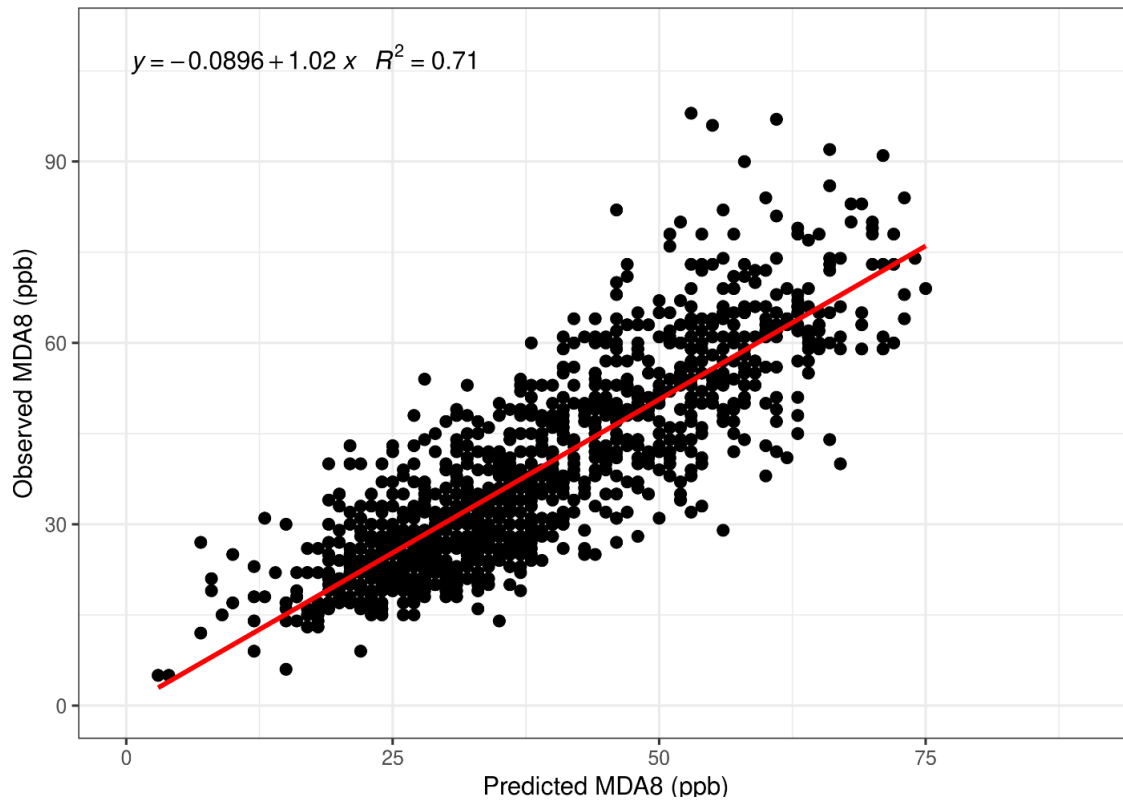


Figure 3-125: Training Model Results Compared to Observed Ozone

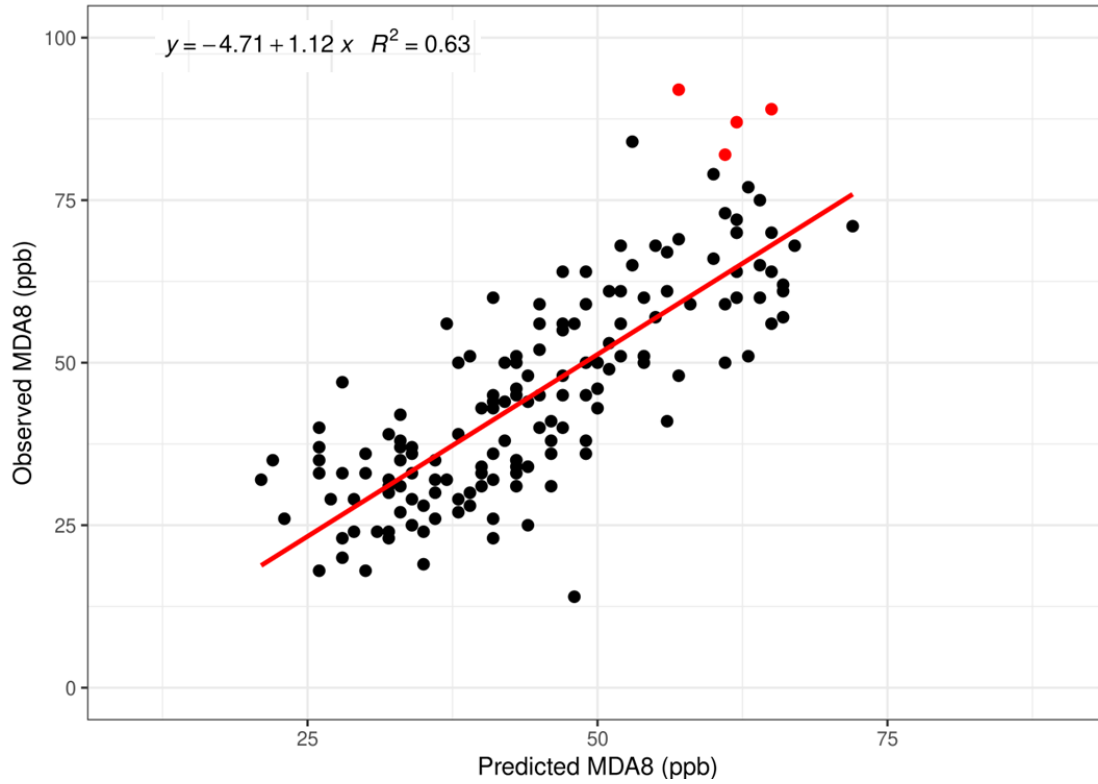


Figure 3-126: 2022 Model Predictions Compared to Observed Ozone

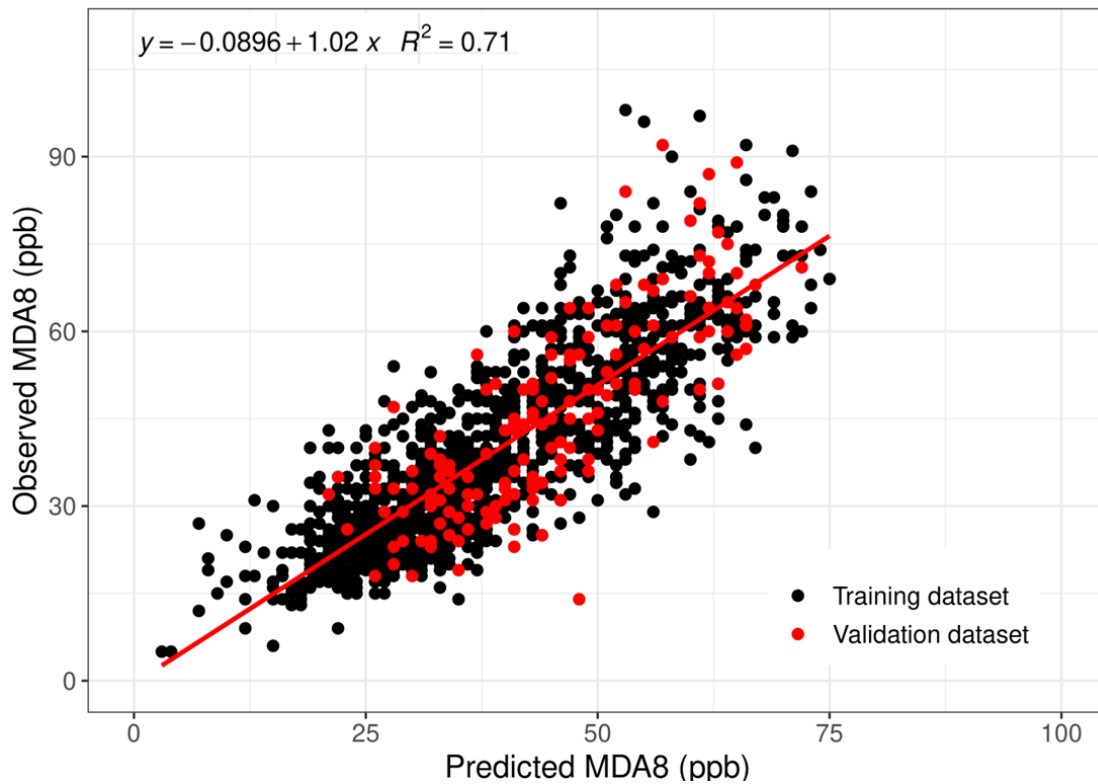


Figure 3-127: Comparison of 2022 Predictions with Results from Training Model

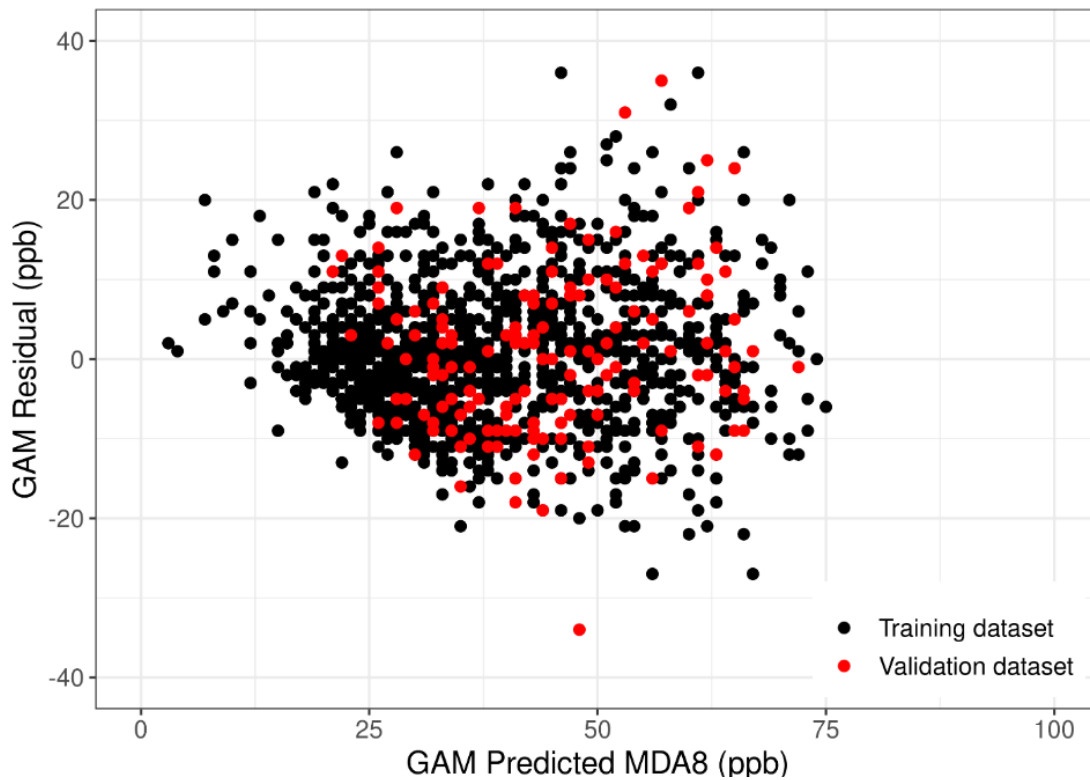


Figure 3-128: GAM Residuals for Training and Validation Dataset

Figure 3-129: *Time Series of Observed and Predicted Maximum Daily Ozone for June 2022*, Figure 3-130: *Time Series of Observed and Predicted Maximum Daily Ozone for September 2022*, and Figure 3-131: *Time Series of Observed and Predicted Maximum Daily Ozone for October 2022* show the model has performed satisfactorily.

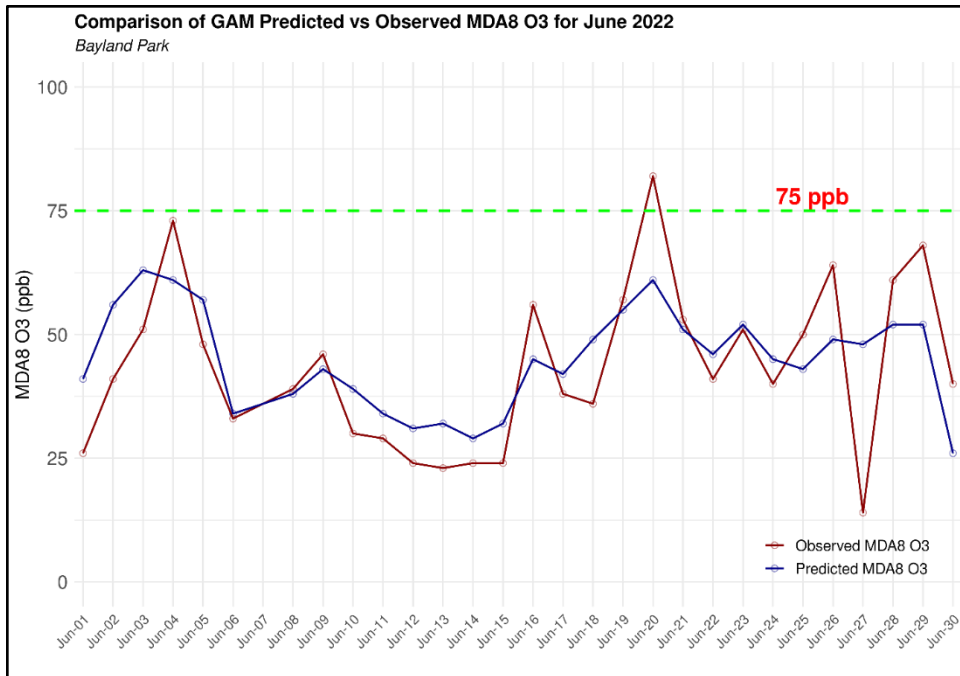


Figure 3-129: Time Series of Observed and Predicted Maximum Daily Ozone for June 2022

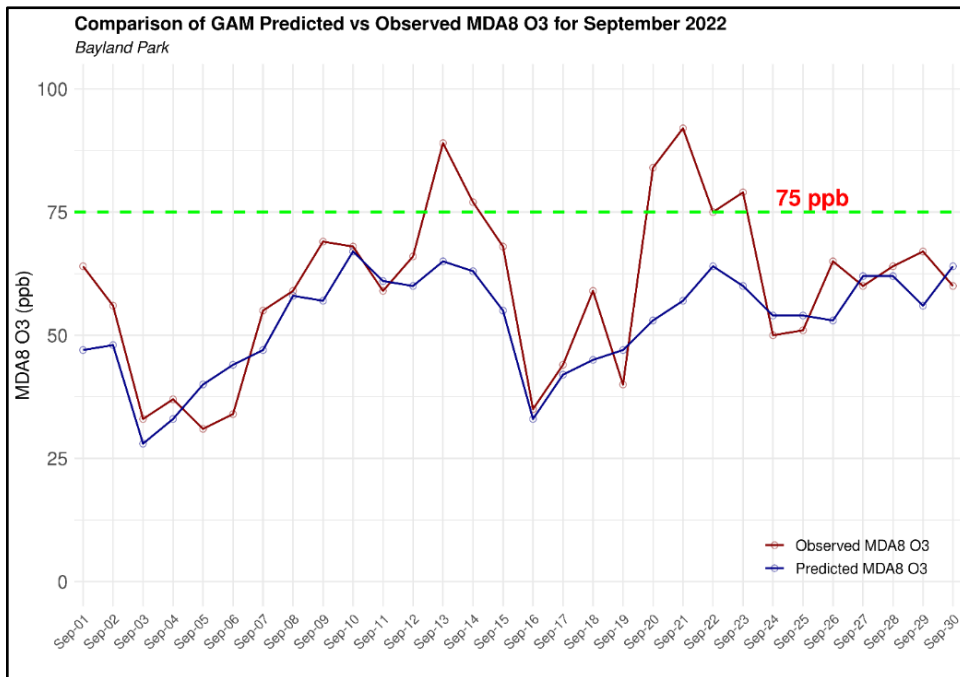


Figure 3-130: Time Series of Observed and Predicted Maximum Daily Ozone for September 2022

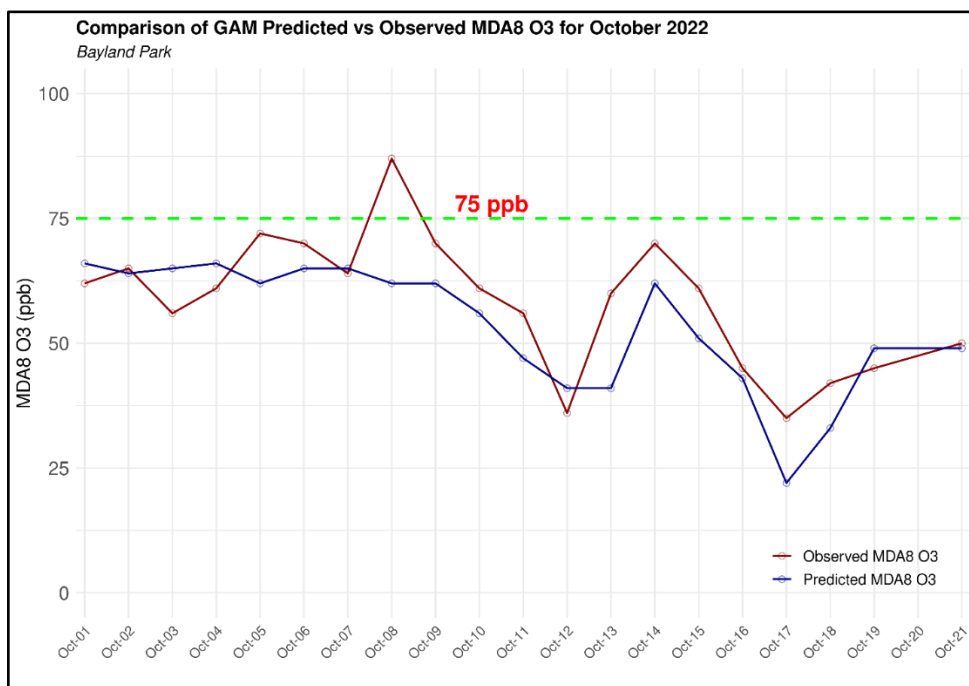


Figure 3-131: Time Series of Observed and Predicted Maximum Daily Ozone for October 2022

Table 3-10: *GAM Results for 2022 Ozone Exceedance Days at Houston Bayland Park* shows a wildfire impact on ozone of between 21 to 35 ppb, with GAM predicted values well below the 75 ppb 2008 NAAQS for all analysis days. Residuals are the difference between observed values and predicted values. When the model predicts a value less than the observed value then the residual is positive. Analysis of all of the positive residuals from model training and the validation dataset provides an explanation for those positive residuals based on model parameters. The percentile rank of positive residuals from 2015 through 2022 shows the ranking of exceedance days positive residual differences were at the 95th percentile or above. This indicates only 1% to 5% chance that the ozone levels on exceptional event days would be produced or explained under normal meteorological conditions in the HGB area. The 95th percentile of the positive differences is a very high number, conservative, and rare to compare against, given other study results (Arizona June 20, 2015; Clark County, Nevada June 19-20, 2018; Clark County, Nevada June 26, 2020). This strongly suggests that other emission sources, in this case wildfire, contributed to the ozone exceedance on those days.

Table 3-10: GAM Results for 2022 Ozone Exceedance Days at Houston Bayland Park

Days	Observed MDA8 Ozone (ppb)	GAM Predicted MDA8 Ozone (ppb)	GAM Residual (ppb)	Percentile Rank of Positive Residual
Jun 20, 2022	82	61	21	95th
Sep 13, 2022	89	65	24	97th

Days	Observed MDA8 Ozone (ppb)	GAM Predicted MDA8 Ozone (ppb)	GAM Residual (ppb)	Percentile Rank of Positive Residual
Sep 21, 2022	92	57	35	99th
Oct 08, 2022	87	62	25	98th

When evaluating model results for June 20, September 13, September 21, and October 8, 2022, the TCEQ used EPA guidance (2016, p. 28) in assigning potential wildfire contributions to maximum ozone that day. The guidance states that a State may use the difference between a particular day’s residual and the 95th percentile of positive predicted residuals as the wildfire contribution to maximum ozone on that day. Table 3-11: *Determination of Wildfire Contribution to Ozone at Houston Bayland Park in 2022* shows the details of this approach. This approach is shown graphically in Figure 3-132: *Predicted and Observed Ozone with 95th Percentile of Positive Residuals*. Using this approach, the TCEQ concludes that there was a wildfire contribution in daily maximum eight-hour ozone at the Houston Bayland Park monitor on June 20, September 13, September 21, and October 8, 2022. Despite the limitations of regression models and the strict standard set by the 95th percentile value of positive residuals (explained in the Arizona June 20, 2015; Clark County, Nevada June 19-20, 2018; and Clark County, Nevada June 26, 2020 demonstrations), the GAM results show a 1 to 15 ppb ozone contribution from fire on June 20, September 13, September 21, and October 8, 2022 at the Houston Bayland Park monitor.

Table 3-11: Determination of Wildfire Contribution to Ozone at Houston Bayland Park in 2022

GAM Results	June 20, 2022	September 13, 2022	September 21, 2022	October 8, 2022
Observed MDA8 (ppb)	82	89	92	87
GAM Prediction (ppb)	61	65	57	62
GAM Residual (ppb)	21	24	35	25
GAM residual 95th percentile (positive difference only)	20	20	20	20
GAM Prediction + 95th percentile	81	85	77	82
Estimated Wildfire Contribution	1	4	15	5

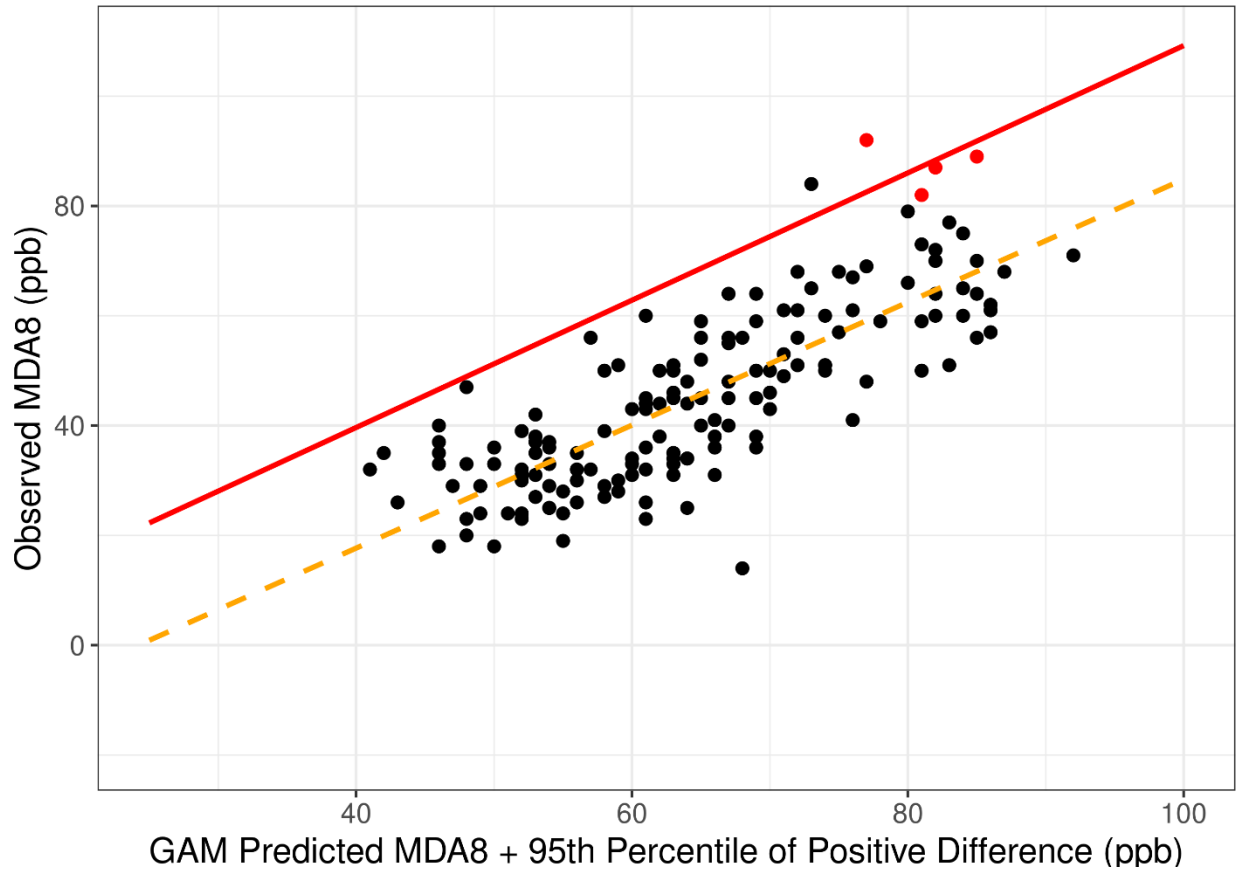


Figure 3-132: Predicted and Observed Ozone with 95th Percentile of Positive Residuals

3.10 CAUSAL RELATIONSHIP CONCLUSION

The analyses provided in this chapter demonstrate that air quality in the HGB area was affected by wildfires on June 20, September 13, September 21, and October 8, 2022. These wildfires generated ozone and/or its precursors that resulted in elevated ozone concentrations at the Houston Bayland Park and Houston Harvard Street monitors. The monitored MDA8 ozone concentrations of 82, 89, 92, and 87 ppb at the Bayland Park monitor, and 97 and 88 ppb at the Harvard Street monitor exceeded the 99th percentile for MDA8 ozone over 2018 through 2022 on an annual basis. Meteorological conditions transported ozone and its precursors from wildfires in Texas and other states, including Louisiana, Mississippi, and Alabama, to the Bayland Park and Harvard Street monitors indicating that a clear causal relationship exists between the specific wildfire events and the monitored exceedances on June 20, September 13, September 21, and October 8, 2022.

CHAPTER 4: PUBLIC COMMENT

In following the requirements listed in Title 40 of the Code of Federal Regulations (CFR) §50.14(c)(3), the Texas Commission on Environmental Quality (TCEQ) is posting this Exceptional Events Demonstration Package on its website for public comment from May 24 through June 24, 2023. All comments received during the comment period will be included in Appendix A: *Public Comments*. The final demonstration may be revised to incorporate changes made in response to comments received.

CHAPTER 5: REFERENCES

- Alvarado, Matthew, Chantelle Lonsdale, Marikate Mountain, and Jennifer Hegarty. 2015. "Investigating the Impact of Meteorology on O3 and PM2.5 Trends, Background Levels, and NAAQS Exceedances." Work Order No. 582-15-54118-01. TCEQ Contract No. 582-15-50415. Atmospheric and Environmental Research (AER) Inc. <https://www.tceq.texas.gov/assets/public/implementation/air/am/contracts/reports/da/5821554118FY1501-20150831-aer-MeteorologyAndO3PMTrends.pdf>.
- Arizona Department of Environmental Quality. 2016. State of Arizona exceptional event documentation for wildfire-caused ozone exceedances on June 20, 2015 in the Maricopa nonattainment area. Final report, Available at https://static.azdeq.gov/pn/1609_ee_report.pdf.
- Camalier, Louise, William Cox, and Pat Dolwick. 2007. "The Effects of Meteorology on Ozone in Urban Areas and Their Use in Assessing Ozone Trends." *Atmospheric Environment* 41 (33): 7127-37. <https://doi.org/10.1016/j.atmosenv.2007.04.061>.
- Clark County Department of Environment and Sustainability .2021. Exceptional Event Demonstration for Ozone Exceedances in Clark County, Nevada-June 19-20, 2018. Available at https://files.clarkcountynv.gov/clarknv/Environmental%20Sustainability/Exceptional%20Events/20180619-20_ClarkCounty_Wildfire_EE.pdf?t=1672898665584&t=1672898665584
- Clark County Department of Environment and Sustainability .2021. Exceptional Event Demonstration for Ozone Exceedances in Clark County, Nevada-June 26, 2020. Available at https://files.clarkcountynv.gov/clarknv/Environmental%20Sustainability/Exceptional%20Events/20200626_ClarkCounty_Wildfire_EE.pdf?t=1672898665584&t=1672898665584
- Flynn, James, Rebecca J. Sheesley, and Sascha Usenko. "Black and Brown Carbon (BC)2 Monitoring in Houston and El Paso in 2020." Final Grant Activity Report. University of Houston, Baylor University, July 12, 2021. <https://www.tceq.texas.gov/downloads/air-quality/research/reports/data-analysis/5822012102011-20210712-uh-bc2-2020-monitoring.pdf>.
- Gong, Xi, Aaron Kaulfus, Udaysankar Nair, and Daniel A. Jaffe. 2017. "Quantifying O3 Impacts in Urban Areas Due to Wildfires Using a Generalized Additive Model." *Environmental Science & Technology* 51 (22): 13216-23. <https://doi.org/10.1021/acs.est.7b03130>.
- Jaffe, Dan. "O3 Formation in Urban Areas from Fire Emissions." PowerPoint presented at the 8-Hour Coalition, Internet, September 21, 2021.
- Jaffe, Daniel A., Susan M. O'Neill, Narasimhan K. Larkin, Amara L. Holder, David L. Peterson, Jessica E. Halofsky and Ana G. Rappold (2020). "Wildfire and prescribed burning impacts on air quality in the United States." *Journal of the*

- Air & Waste Management 70 (6): 583–615.
<https://doi.org/10.1080/10962247.2020.1749731>
- Jaffe, Dan. 2017. “Wildfire Impacts on Ozone on June 21, 2015 at the El Paso UTEP Monitoring Site.” Consulting Report. <https://www.tceq.texas.gov/assets/public/airquality/airmod/docs/ozoneExceptionalEvent/2017.05.17-wildfireImpacts-Jaffe.pdf>.
- Jaffe, Daniel A., and Nicole L. Wigder. 2012. “Ozone Production from Wildfires: A Critical Review.” *Atmospheric Environment* 51 (May): 1–10.
<https://doi.org/10.1016/j.atmosenv.2011.11.063>.
- Jaffe, Dan, Isaac Bertschi, Lyatt Jaeglé, Paul Novelli, Jeffrey S. Reid, Hiroshi Tanimoto, Roxanne Vingarzan, and Douglas L. Westphal. 2004. “Long-Range Transport of Siberian Biomass Burning Emissions and Impact on Surface Ozone in Western North America.” *Geophysical Research Letters* 31 (16).
<https://doi.org/10.1029/2004GL020093>.
- Laing, James R., Daniel A. Jaffe, Abbigale P. Slavens, Wenting Li, and Wenxi Wang. 2017. “Can $\Delta\text{PM}_{2.5}/\Delta\text{CO}$ and $\Delta\text{NO}_y/\Delta\text{CO}$ Enhancement Ratios Be Used to Characterize the Influence of Wildfire Smoke in Urban Areas?” *Aerosol and Air Quality Research* 17 (10): 2413–23. <https://doi.org/10.4209/aaqr.2017.02.0069>.
- Louisiana Department of Environmental Quality. 2018. “Louisiana Exceptional Event of September 14, 2017: Analysis of Atmospheric Processes Associated with the Ozone Exceedance and Supporting Data.” Exceptional Event Demonstration. Baton Rouge, Louisiana: Louisiana Department of Environmental Quality.
https://www.epa.gov/sites/production/files/2018-08/documents/ldeq_ee_demonstration_final_w_appendices.pdf.
- Permar, Wade, Qian Wang, Vanessa Selimovic, Catherine Wielgasz, Robert J. Yokelson, Rebecca S. Hornbrook, Alan J. Hills, et al. “Emissions of Trace Organic Gases From Western U.S. Wildfires Based on WE-CAN Aircraft Measurements.” *Journal of Geophysical Research: Atmospheres* 126, no. 11 (2021): e2020JD033838.
<https://doi.org/10.1029/2020JD033838>.
- National Aeronautics and Space Administration. 2020. “NASA Worldview.” Government Agency. NASA Worldview. November 15, 2020.
<https://worldview.earthdata.nasa.gov/>.
- National Oceanic and Atmospheric Administration, Air Resources Laboratory. 2020. *HYSPLIT* (version 5.0.0). Windows. Fortran; Tcl/Tk. College Park, Maryland.
<https://www.arl.noaa.gov/hysplit/hysplit/>.
- National Oceanic and Atmospheric Administration, National Center for Environmental Prediction. 2003. “Daily Weather Map.” Government Agency. National Center for Environmental Prediction. January 2003.
<https://www.wpc.ncep.noaa.gov/dailywxmap/index.html>.

- National Oceanic and Atmospheric Administration Office of Satellite and Product Operations. 2003. "Hazard Mapping System Fire and Smoke Product." Government Agency. Office of Satellite and Product Operations. June 13, 2003. <https://www.ospo.noaa.gov/Products/land/hms.html#maps>.
- R Core Team. 2021. *R: A Language and Environment for Statistical Computing* (version 4.0.4). C, C++, Fortran. Vienna, Austria: R Foundation for Statistical Computing. <https://www.R-project.org>.
- Sullivan, David W., and Dan Jaffe. "Final Report: Oxygenated Volatile Organic Compound (OVOC) Sampling for Biomass Burning Tracers Project." Final Contract Report. Austin, TX: University of Texas at Austin, July 31, 2022.
- Stein, A. F., R. R. Draxler, G. D. Rolph, B. J. B. Stunder, M. D. Cohen, and F. Ngan. 2015. "NOAA's HYSPLIT Atmospheric Transport and Dispersion Modeling System." *Bulletin of the American Meteorological Society* 96 (12): 2059–77. <https://doi.org/10.1175/BAMS-D-14-00110.1>.
- Sullivan, David W., and Dan Jaffe. "Final Report: Oxygenated Volatile Organic Compound (OVOC) Sampling for Biomass Burning Tracers Project." Final Contract Report. Austin, TX: University of Texas at Austin, July 31, 2022.
- Sutron Company. 2013. *Leading Environmental Analysis and Display System (LEADS)*. Sutron. Internal.
- Texas Commission on Environmental Quality. 2016. "El Paso UTEP (CAMS 12) Monitoring Site June 21, 2015, Exceptional Event Demonstration Package for the El Paso County Maintenance Area." Texas Commission on Environmental Quality. <https://www.tceq.texas.gov/airquality/airmod/docs/ozone-data-exceptional-event-flag-demonstrations>.
- Texas Commission on Environmental Quality .2021. Dallas-Fort Worth area exceptional event demonstration for ozone on August 16, 17, and 21, 2020. Available at <https://www.tceq.texas.gov/assets/public/airquality/airmod/docs/ozoneExceptionalEvent/2020-DFW-EE-Ozone.pdf>.
- United States Census Bureau. 2020. "Metropolitan and Micropolitan Statistical Areas Population Totals and Components of Change: 2010-2019." Government Agency. United States Census Bureau. June 18, 2020. <https://www.census.gov/data/tables/time-series/demo/popest/2010s-total-metro-and-micro-statistical-areas.html>.
- United States Environmental Protection Agency. 2016a. "Guidance on the Preparation of Exceptional Events Demonstrations for Wildfire Events That May Influence Ozone Concentrations." United States Environmental Protection Agency. https://www.epa.gov/sites/production/files/2018-10/documents/exceptional_events_guidance_9-16-16_final.pdf.
- United States Environmental Protection Agency. 2016b. "Treatment of Data Influenced by Exceptional Events." *Federal Register* 81 (191): 68216–82.

- United States Environmental Protection Agency. 2020. “2016 Revisions to the Exceptional Events Rule: Update to Frequently Asked Questions.” United States Environmental Protection Agency.
https://www.epa.gov/sites/production/files/2019-07/documents/updated_faqs_for_exceptional_events_final_2019_july_23.pdf.
- United States Environmental Protection Agency. 2021. “Air Data: Air Quality Data Collected at Outdoor Monitors Across the US.” Government Agency. United States Environmental Protection Agency. January 2021.
<https://www.epa.gov/outdoor-air-quality-data>.
- United States Navy Naval Research Laboratory. 2010. “Navy Aerosol Analysis and Prediction System.” Military. NRL Monterey Aerosol Page. April 17, 2010.
<https://www.nrlmry.navy.mil/aerosol/>.
- Wiedinmyer, Christine, and Robert Yokelson. n.d. “Fire INventory from NCAR (FINN): A Daily Fire Emissions Product for Atmospheric Chemistry Models.” Research Organization. National Center for Atmospheric Research: Atmospheric Chemistry Observations & Modeling (ACOM). Accessed February 9, 2021.
<https://www2.acom.ucar.edu/modeling/finn-fire-inventory-ncar>.
- Wood, Simon. 2017. *Generalized Additive Models: An Introduction with R*. 2nd ed. Chapman & Hall/CRC Texts in Statistical Science. Boca Raton: Chapman and Hall/CRC.
- Wood, Simon. 2021. *mgcv: Mixed GAM Computation Vehicle with Automatic Smoothness Estimation* (version 1.8-34). Edinburgh, United Kingdom. <https://CRAN.R-project.org/package=mgcv>.
- Zhang, Zhou, Yanli Zhang, Xinming Wang, Sujun Lü, Zhonghui Huang, Xinyu Huang, Weiqiang Yang, Yuesi Wang, and Qiang Zhang. “Spatiotemporal Patterns and Source Implications of Aromatic Hydrocarbons at Six Rural Sites across China’s Developed Coastal Regions.” *Journal of Geophysical Research: Atmospheres* 121, no. 11 (2016): 6669–87. <https://doi.org/10.1002/2016JD025115>.

APPENDIX A: PUBLIC COMMENTS

Note to reviewers:

All public comments received will be placed here for submission to the Environmental Protection Agency.

